INVESTIGATING THE ROLE OF AUTOPHAGY IN HERPES SIMPLEX ENCEPHALITIS

by

NUR LIYANA HAJI AHMAD

Presented to the Department of Medicine
Imperial College London

In Fulfilment of the Requirement
For the Degree of

DOCTOR OF PHILOSOPHY

Imperial College London
London, United Kingdom
March 2018

Declaration of Originality

I declare that the content of this thesis is entirely of my own work. Parts that are not original to this work have been appropriately acknowledged and referenced. This thesis is submitted to Imperial College London for the degree of Doctor of Philosophy. The data and findings that are presented in this thesis have not been previously submitted in any form for any other qualifications at Imperial College London or other institutions. The research work leading up to the production of this thesis was undertaken at Virology and Paediatrics Departments at Imperial College London, and was co-supervised by Dr. Vanessa Sancho-Shimizu and Professor Peter O'Hare.

Copyright Declaration

The copyright of this thesis rests with the author and is made available under a Creative Commons Attribution Non-Commercial No Derivatives licence. Researchers are free to copy, distribute or transmit the thesis on the condition that they attribute it, that they do not use it for commercial purposes and that they do not alter, transform or build upon it. For any reuse or redistribution, researchers must make clear to others the licence terms of this work.

Acknowledgements

I would like to take this opportunity to express my sincerest gratitude and appreciation to Dr. Vanessa Sancho-Shimizu for her supervision, help, support and the opportunities she has given me throughout my time in her lab at Imperial College London. I am truly grateful for her encouragement and constant guidance which have enabled me to grow as a scientist. Her enthusiasm, kindness and patience have been the source of my motivation and inspiration. Additionally, I would like to thank Professor Peter O'Hare for his supervision, valuable advice and insights.

I would like to express my deepest gratitude to Dr. Bayarchimeg Mashbat for her constant moral support and help in the laboratory. I would like to thank Dr. Serge Mostowy and Sina Krowkowski for providing me with access to their microscope and for their guidance and valuable advice. Also, I would like to express my appreciation to Dr. Avinash Shenoy, Julia Sanchez-Garrido and Dr. Axel Freischmidt for their technical help, advice and provision. I thank Axol Bioscience for their training, guidance and help in the laboratory. I would also like to thank the members of Virology and Paediatrics Departments who have provided moral support throughout my work.

I would like to express my deepest gratitude to my parents, Haji Ahmad bin Jumaat and Sauyah binti Hashim, for their warm support and constant encouragement throughout my journey here. I am also grateful to my family and friends, who in one way or another shared their moral support for me. Last but not least, my gratitude extends to the Brunei Government and Universiti Brunei Darussalam, for sponsoring my education and giving me this opportunity to learn and grow.

Abstract

The role of autophagy in innate immunity has recently garnered attention from molecular biologists and pathologists alike. A growing number of reports suggest its anti-viral role in various infections, including Herpes simplex virus 1 (HSV1) which is the causative pathogen for herpes simplex encephalitis (HSE). Whilst studies have shown the non-redundant role of Toll-like receptor 3 (TLR3)-interferon (IFN) signalling pathway in HSV1 defence, the role of autophagy in HSV1 infection and HSE pathogenesis remains elusive. In this study, we characterised autophagy phenotypes in response to rapamycin, poly(I:C), c-di-GMP and HSV1 dsDNA stimulations as well as HSV1 infection, of human dermal fibroblasts derived from HSE patients harbouring mutations in components of the TLR3-IFN pathway – *UNC93B1* (c.103del4), *TLR3* (p.R867Q)*, TRIF* (p.R141X)*, TRAF3* (p.R118W) and *TBK1* (p.D50A and p.G159A). By using the autophagy marker LC3B, we established the HSV1-induced formation of two distinct autophagy phenotypes: cytoplasmic and perinuclear LC3B phenotypes. We correlated the former with the host protective autophagy response triggered early in HSV1 infection, which is TBK1-dependent but TLR3- and IFN-independent, and can be induced in neighbouring non-infected cells. Fibroblasts carrying the G159A mutation in *TBK1* failed to induce LC3BII:I and reduce the autophagy adaptor p62 protein levels, suggesting a defect in autophagy response upon HSV1 infection. This impairment is reproducible by inhibiting TBK1 function using TBK1 inhibitor BX795 and depleting endogenous TBK1 in control fibroblasts. Furthermore, we demonstrated the cytoprotective nature of autophagy in HSV1 infection, whereby prior upregulation of autophagy by rapamycin in fibroblasts, led to enhanced cell viability following HSV1 infection.

Table of Contents

Declaration of Originality ..... **iii**

Copyright Declaration ..... **iv**

Acknowledgements ..... **v**

Abstract ..... **vi**

Table of Contents ..... **vii**

Publication ..... **xii**

List of Figures ..... **xiii**

List of Tables ..... **xvii**

List of Abbreviations ..... **xviii**

Chapter 1 ..... **1**

1. General introduction **2**

1.1. Autophagy 2

1.1.1. Autophagy 2

1.1.2. Autophagy machinery 2

1.1.3. Autophagy in immunity 4

1.1.4. Autophagy in controlling inflammation 9

1.1.5. Autophagy promotes cell survival in the CNS during infection 10

1.2. Herpes Simplex Virus-1 12

1.2.1. Herpes Simplex Virus-1 (HSV1) and HSV1 primary infection 12

1.2.2. Herpes simplex encephalitis (HSE) 15

1.2.3. Mendelian predisposition to HSE 18

1.2.4. HSV1 and autophagy 21

1.3. TBK1 is a multifaceted kinase in innate immunity 26

1.3.1. TBK1 molecular composition and function 26
1.3.2. TBK1 in innate immunity 27
1.3.3. TBK1 in autophagy 29
1.3.4. TBK1 in human neuropathologies 33
1.4 Aims of this study 36

Chapter 2 38

2. Materials and Methods 39

2.1. Cell maintenance and culture 39
2.2. Viral strains and propagation 39
2.3. Plaque assay 40
2.4. Cell viability assay 41
2.5. Stimulation, treatment and infection 42
2.6. Plasmids and transient transfection 42
2.7. Site-directed mutagenesis 45
2.8. Depleting endogenous TBK1 using transient siRNA transfection 46
2.9. Transduction and generation of stably TBK1-depleted HEK293T cell line (HEK293T/miRTBK1) 47
2.9.1. Designing targeting shRNA sequence and cloning 48
2.9.2. Production of lentiviral pseudoparticles for miRTBK1 56
2.9.3. Transducing HEK293T cells with pseudoparticles carrying miRTBK1 and clone selection and expansion 57
2.10. Sodium dodecyl sulphate polyacrylamide gel electrophoresis (SDS-PAGE) and Western blotting 58
2.11. Immunofluorescence, image acquisition and puncta quantification 59
2.12. Cytokine measurement using enzyme-linked immunosorbent assay (ELISA) 61
2.13. Nuclease and heat treatments for conditioned media 61
2.14. Neural stem cells culture and differentiation into pure neuronal culture 62

2.15. Statistical analysis and software 63

Chapter 3 64

3. Autophagy phenotypes of HSE patient-derived fibroblasts with defective TLR3-IFN pathway 65

3.1. General introduction 65

3.2. Rapamycin-induced autophagy 66

3.3. Poly(I:C)-induced autophagy 73

3.4. IFN-induced autophagy 79

3.5. C-di-GMP-induced autophagy 84

3.6. HSV1-induced autophagy in HSE patients' fibroblasts 87

3.6.1. HSV1 infection induces LC3B and reduces p62 protein levels in control dermal fibroblasts 87

3.6.2. WT HSV1 triggers cytoplasmic and perinuclear LC3B phenotypes 89

3.6.3. Impairment of HSV1-induced autophagy in TBK1$^{+/-}$ (p.G159A) fibroblasts 90

3.6.3.1. TBK1$^{+/-}$ (p.G159A) failed to induce LC3BII:I and reduce p62 proteins following HSV1 infection. 90

3.6.3.2. UNC93B$^{-/-}$ and TBK1$^{+/-}$ (p.G159A) fibroblasts showed impairment in cytoplasmic LC3B formation following HSV1 infection 92

3.7. HSV1 dsDNA-induced autophagy 96

3.8. Discussion 99

Chapter 4 106

4. TBK1 plays a role in HSV1-induced autophagy in human dermal fibroblasts 107

4.1. General introduction 107

4.2. Cytoplasmic and perinuclear LC3B phenotypes are formed during early and late in HSV1 infection respectively 108

4.3. Infection with ICP34.5-mutant HSV1 enhances HSV1-induced autophagy phenotypes 110

4.4. Perinuclear LC3B structures co-localised with LC3A and Golgi bodies during late HSV1 infection 113
4.5. Depletion or inhibition of TBK1 impairs HSV1-induced autophagy 117
4.5.1. Depletion of endogenous TBK1 abrogated HSV1-induced autophagy in control fibroblasts 117
4.5.2. Inhibition of TBK1 using BX795 reduced the cytoplasmic LC3B phenotype and did not affect the perinuclear LC3B phenotype 120
4.6. Autophagy promotes cell viability without altering HSV1 replication 123
4.7. Paracrine autophagy induction is mediated by infected cell-derived nucleic acid . 129
4.8. Discussion 132

Chapter 5 137

5. Dissecting the role of TBK1 in HSV1-induced autophagy 138

5.1. General introduction 138
5.2. HEK293T/miRTBK1 cells as a system to study TBK1 function in HSV1-induced autophagy 140
5.2.1. HEK293T/miRTBK1 cells showed reduced endogenous TBK1 and were more susceptible to HSV1 infection than HEK293T 140
5.2.2. HEK293T/miRTBK1 cells overexpressing TBK1 mutants showed enhanced HSV1 replication 142
5.3. Kinase-dead TBK1 mutants impaired LC3B puncta formation 145
5.4. HSV1-induced autophagy requires another component in addition to TBK1 148
5.5. Discussion 150

Chapter 6 154

6. Discussion and Future Directions 155

6.1. General discussion 155
6.1.1. Poly(I:C) and HSV1 dsDNA induce autophagy in human dermal fibroblasts .. 156
6.1.2. Dynamics of autophagy during HSV1 infection 160

6.1.3. TBK1 is a crucial component of autophagy that mediates protection against HSV1 163

6.2. Future directions 165

6.2.1. Purpose and mechanism of HSV1-induced paracrine autophagy 165

6.2.2. HSV1-induced autophagy involves TBK1 and selective autophagy adaptors. 167

6.2.3. Autophagy suppresses inflammation in the CNS 170

Bibliography 173

Appendix 209

Publication

Ahmad, L. et al., 2016. Human TBK1: A Gatekeeper of Neuroinflammation. *Trends in Molecular Medicine*, 22(6), pp.511–527.

List of Figures

Chapter 1

Figure 1.1 Schematic diagram illustrating the autophagy process and its machinery……... 4

Figure 1.2 Selective autophagy can be achieved by recruiting selective adaptors……..… 6

Figure 1.3 HSV1 replication cycle…… 14

Figure 1.4 HSV1 interaction with host autophagy…… 23

Figure 1.5 Schematic illustration of the TBK1 protein……. 27

Figure 1.6 TBK1 is a crossroad component of inflammatory pathway and autophagy…… 29

Chapter 2

Figure 2.1 Sequence chromatogram of TBK1 subjected to mutagenesis 46

Figure 2.2 shRNA structure and the plasmid map of lentiviral pMX CMV YFP miR30E plasmid……. 50

Figure 2.3 Addition of EcoRI and XhoI restriction site to dsDNA insert… 53

Figure 2.4 pMX CMV YFP miR30E vector map carrying shRNA sequence that targets 3' UTR of endogenous human TBK1 (miRTBK1) …….. 54

Figure 2.5 Confirmation of successful cloning of miRNA targeting TBK1 in control human dermal fibroblasts……..… 55

Chapter 3

Figure 3.1 Rapamycin induces autophagy in human dermal fibroblasts.. 67

Figure 3.2 Rapamycin-induced autophagy in HSE patient-derived

dermal fibroblasts……... 69
Figure 3.3 Rapamycin-induced autophagy in HSE patient-derived dermal fibroblasts……... 73
Figure 3.4 Poly(I:C)-induced autophagy in control dermal fibroblasts….. 74
Figure 3.5 Poly(I:C)-induced autophagy in HSE patient-derived dermal fibroblasts…… 76
Figure 3.6 Poly(I:C)-induced autophagy in HSE patient-derived dermal fibroblasts…… 79
Figure 3.7 IFNα-2a induced autophagy in control dermal fibroblasts….. 80
Figure 3.8 IFNα-2a-induced autophagy of patient-derived fibroblasts…. 84
Figure 3.9 c-di-GMP-induced autophagy is TBK1-dependent……..…. 86
Figure 3.10 HSV1 infection triggers autophagy response in human dermal fibroblasts……. 88
Figure 3.11 HSV1 infection triggers cytoplasmic and perinuclear LC3B phenotypes in control fibroblasts…… 89
Figure 3.12 UNC93B$^{-/-}$ and TBK1$^{+/-}$ (p.G159A) fibroblasts showed aberrant HSV1-induced autophagy…… 92
Figure 3.13 Cytoplasmic and perinuclear LC3B formation in HSV1-infected patient-derived fibroblasts……. 95
Figure 3.14 HSV1 dsDNA-induced autophagy in human fibroblasts…….. 98

Chapter 4

Figure 4.1 HSV1-induced cytoplasmic and perinuclear LC3B phenotypes in human dermal fibroblasts are induced early and late in infection respectively…….. 110
Figure 4.2 Infection of human dermal fibroblasts with ΔICP34.5 HSV1

enhanced autophagy phenotypes……. 112

Figure 4.3 HSV1-induced perinuclear LC3B structure also stains for LC3A and Golgi bodies……. 116

Figure 4.4 TBK1-depleted control fibroblasts showed impaired HSV1-induced autophagy……. 119

Figure 4.5 Functionally inhibiting endogenous TBK1 using BX795 reduces formation of HSV1-induced cytoplasmic LC3B early in infection without affecting formation of perinuclear LC3B later in infection…….. 122

Figure 4.6 Enhancing autophagy in human dermal fibroblasts prior to HSV1 infection does not affect viral replication……. 125

Figure 4.7 Enhancing autophagy in human dermal fibroblasts prior to HSV1 infection enhances cell viability……. 126

Figure 4.8 Rapamycin-induced autophagy promotes protection in HSV1 infection…… 127

Figure 4.9 Conditioned medium from infected control fibroblasts triggers autophagy in control fibroblasts……..…. 131

Chapter 5

Figure 5.1 Location of TBK1 mutants associated with HSE and ALS with respect to TBK1 protein domains……. 139

Figure 5.2 Stable depletion of TBK1 and susceptibility to HSV1 of HEK293T/miRTBK1 cell line……. 141

Figure 5.3 Effect of various TBK1 mutations on HSV1 replication in HEK293T/miRTBK1 cells…….. 143

Figure 5.4 Effect of various TBK1 mutations on cell susceptibility to

HSV1 infection……. 144

Figure 5.5 Effect of TBK1 mutant overexpression in HEK293T/miRTBK1 cells…….. 147

Figure 5.6 HEK293T and HEK293T/miRTBK1 cell line was incapable of inducing cytoplasmic LC3B phenotype following HSV1 infection……. 149

Figure 5.7 Endogenous expression of STING in various cell lines…… 150

Appendix

Appendix 1 Optimisation of autophagy assays on neurons derived from NS cells……. 210

List of Tables

Chapter 1

Table 1.1 Pattern recognition receptors or innate immune sensors can trigger autophagy…….. 7

Table 1.2 List of HSE-associated mutations found in components of the TLR3-IFN pathway……..…….. 19

Table 1.3 TBK1 mediates autophagy through autophagy adaptors…… 32

Chapter 2

Table 2.1 List of plasmids used in this study…….. 44

Table 2.2 Sequences of mutagenic primers used to create p.G159A and p.D50A point mutations……. 45

Table 2.3 Commercial siRNAs used to target endogenous human TBK1 or for negative control…… 47

Table 2.4 TBK1-targeting 22 bp oligos that specifically targets 3' UTR of human TBK1……..…… 48

Table 2.5 Primer sequences used to add XhoI and EcoRI restriction sites onto targeting shRNA sequence……..…. 52

Table 2.6 Antibodies and dilution conditions used for Western blotting. 59

Table 2.7 Antibodies and dilution conditions used for immunofluorescence staining…….……..…… 60

Chapter 5

Table 5.1 List of selected HSE- or ALS-associated TBK1 mutants and their in vitro functionality……..…. 139

List of Abbreviations

AD	Autosomal dominance
ALS	Amyotrophic lateral sclerosis
AR	Autosomal recessive
ATG	Autophagy
a.u.	Arbitrary unit
Bcl-2	B cell lymphoma-2
BMDCs	Bone marrow-derived dendritic cells
BMMs	Bone marrow-derived macrophages
bp	Base pair
cas9	CRISPR-associated protein 9
CCD1	Coiled-coiled domain 1
CCD2	Coiled-coiled domain 2
c-di-GMP	Cyclic di-guanosine monophosphate
cDNA	Complementary DNA
cGAMP	Cyclic guanosine monophosphate–adenosine monophosphate
cGAS	cGAMP synthase
CMV	Cytomegalovirus
CNS	Central nervous system
CRISPR	Clustered regularly interspaced short palindromic repeats
CSF	Cerebrospinal fluid
DAMPs	Damage-associated molecular pattern molecules
DAPI	4',6-diamidino-2-phenylindole

DMEM	Dulbecco's Modified Eagle's Medium
DNA	Deoxyribonucleic acid
dNTPs	Deoxyribonucleotide triphosphates
dsDNA	Double-stranded DNA
dsRNA	Double-stranded RNA
EGF	Epidermal growth factor
ELISA	Enzyme-linked immunosorbent assay
EM	Electron microscope
ER	Endoplasmic reticulum
FBS	Foetal bovine serum
FDA	United States Food and Drug Administration
FGF2	Fibroblast growth factor 2
FTD	Frontotemporal dementia
GAGs	Glucosaminoglycans
GAPDH	Glyceraldehyde 3-phosphate dehydrogenase
GFP	Green fluorescent protein
GoF	Gain of function
HBS	HEPES-buffered saline
HFFF2	Human feotal foreskin fibroblast
h.p.i	Hour post-infection
HSE	Herpes simplex encephalitis
HSV1	Herpes simplex virus-1
HVEM	Herpes virus entry mediator
ICP34.5	Infected cell protein 34.5
ICP4	Infected cell protein 4

IFN	Interferon
IKKϵ	IkB kinase ϵ
IL	Interleukin
iPS	induced pluripotent stem
IRF	Interferon regulatory transcription factor
ISGs	Interferon-stimulated genes
LATs	Latent associated transcripts
LIR	LC3-interacting region
LoF	Loss of function
LPS	Lipopolysaccharides
MDA5	Melanoma differentiation-associated gene 5
MDMs	Monocyte-derived macrophages
MDP	Muramyl dipeptide
MEFs	Mouse embryonic fibroblasts
MHC	Major histocompatibility complex
miRNA	Micro RNA
MOI	Multiplicity of infection
mRNA	Messenger RNA
mTOR	Mammalian target of rapamycin
NAK	NF-kB-activating kinase
NAP1	NAK-associated protein 1
NBR1	Neighbour of BRCA1 gene 1
NDP52	Nuclear dot protein 52
NEDA	Nuclear envelope-derived autophagy
NLRs	Nucleotide-binding oligomerisation domain (NOD)-like receptors

NS	Neural stem
NTG	Normal tension glaucoma
OPTN	Optineurin
PAMPs	Pathogen-associated molecular patterns
PBS	Phosphate-buffered saline
PCR	Polymerase chain reaction
PE	Phosphatidylethanolamine
PFU	Plaque forming unit
PI(3)K	Phosphatidylinositol 3-kinase
PI(3)P	Phosphatidylinositol 3-phosphate
PKC	Protein kinase C
PKR	Protein kinase R
PNS	Peripheral nervous system
Poly(I:C)	Polyinosinic-polycytidylic acid
PRRs	Pattern recognition receptors
PVDF	Polyvinylidene difluoride
RIG-I	Retinoic acid-inducible protein 1
RLRs	RIG-I-like receptors
RNA	Ribonucleic acid
SCID	Severe combined immune deficiency
SD	Standard deviation
SDD	Scaffold dimerisation domain
SDS-PAGE	Sodium dodecyl sulphate polyacrylamide gel electrophoresis
SEM	Standard error of mean
shRNA	Short hairpin RNA

SINTBAD	Similar to NAP1 TBK1 adaptor
SIV	Simian immunodeficiency virus
SLE	Systemic lupus erythematosus
SLIC	Sequence and ligation-independent cloning
SLR	Sequestosome 1 (SQSTM1)/p62-like receptor
ssRNA	Single-stranded RNA
STING	Stimulator of interferon genes
SV40	Simian virus 40
TANK	TRAF family member-associated NF-kappa-B activator
TBK1	TANK-binding kinase 1
TBS	Tris-buffered saline
$TCID_{50}$	50% tissue culture infective dose
TRAF	Tumour necrosis factor receptor-associated factor
TRIF	Toll/interleukin-1 receptor (TIR)-domain-containing adapter-inducing interferon-β
TLR	Toll-like receptor
TNFRSF14	Tumour necrosis factor receptor superfamily member 14
TNFα	Tumour necrosis factor α
T2K	TRAF2-associated kinase
Ub	Ubiquitin
UBD	Ubiquitin-binding domain
ULD	Ubiquitin-like domain
ULK1	Unc-51 like autophagy activating kinase
UTR	Untranslated region
UV	Ultraviolet

WT	Wild-type
YFP	Yellow fluorescent protein

Chapter 1

1. General introduction

1.1. Autophagy

1.1.1. Autophagy

Autophagy is a primitive, highly conserved cellular process that isolates cellular materials in double-membrane vesicles for downstream lysosomal degradation. It is evolutionary conserved across eukaryotes. Autophagy, which literally means 'self-eating', is a highly orchestrated process involving various autophagy-related (ATG) proteins, which facilitate the engulfment, lysosomal targeting, and eventually degradation of the cargo. Its homeostatic and quality control roles come from its ability to sense and respond to various stresses such as nutrient deprivation and thermal stress as well as defective organelles. Hence, it is traditionally known to be a general non-specific method of bulk elimination and recycling. However, there is a growing appreciation for its role in innate immunity in which it recognises invading pathogens in the cytoplasm and eliminates them via the help of selective autophagy adaptors, a process termed 'xenophagy' (Mizushima, Yoshimori & Ohsumi, 2011).

1.1.2. Autophagy machinery

Autophagy is a complex membrane trafficking event that regulates a variety of cellular substrates such as protein aggregates that do not go through proteasomal degradation system, or defective or redundant organelles such as mitochondria. It also responds to environmental cues such as stress, starvation, and immune signals.

Its fundamental role as a catabolic and homeostatic process has been exemplified in numerous human conditions such as neurodegenerative diseases, cancers, ageing, as well as immunity (Rubinsztein, Mariño & Kroemer, 2011; Jiang & Mizushima, 2014).

Autophagy generally is a process of isolating cytoplasmic contents in double-membrane vesicle with the purpose of degrading them. It is coordinated by an ensemble of 36 ATG proteins, which facilitate the formation, elongation, and maturation of autophagosomes and their eventual fusion with acidifying lysosomes. During autophagy, induction is initiated by the unc-51-like kinase 1 (ULK1) complex, followed by the initial formation of the phagophore membrane (depicted as a crescent-shaped membrane) which is mediated by class III phosphatidylinositol 3-kinase (PI(3)K)) complex consisting of PI(3)K VPS34, VPS15 and Beclin-1 (Figure 1.1). PI(3)K complex is important for the generation of phosphatidylinositol 3-phosphate (PI(3)P) proteins that are present in the growing autophagosomal membrane. The source of the membrane is rather unclear but reports have shown that it may be derived from the endoplasmic reticulum (ER) (Tooze & Yoshimori, 2010) and endosomes (Puri *et al.*, 2013). Subsequent elongation and completion of the autophagosomal structure involve two ubiquitin-like conjugation system: 1) formation of ATG12-ATG5-ATG16L1 complex which is incorporated into the outer membrane, and 2) lipidation of LC3BI into LC3BII via phosphatidylethanolamine (PE) conjugation, which is incorporated into the outer and inner membranes of the vesicle (Glick, Barth & Macleod, 2010). Increase in LC3BII has been widely used as a marker of autophagosomal formation and hence increase in autophagy activity (Klionsky *et al.*, 2016). Once the formation of autophagosome is completed, it then

fuses with proximal lysosomes, which contain hydrolases, effectively acidifying the vesicle and leading to the degradation of contents. Autophagosome-associated LC3BII proteins are then recycled back into the cytosol as LC3BI (Mizushima, Yoshimori & Ohsumi, 2011) (Figure 1.1).

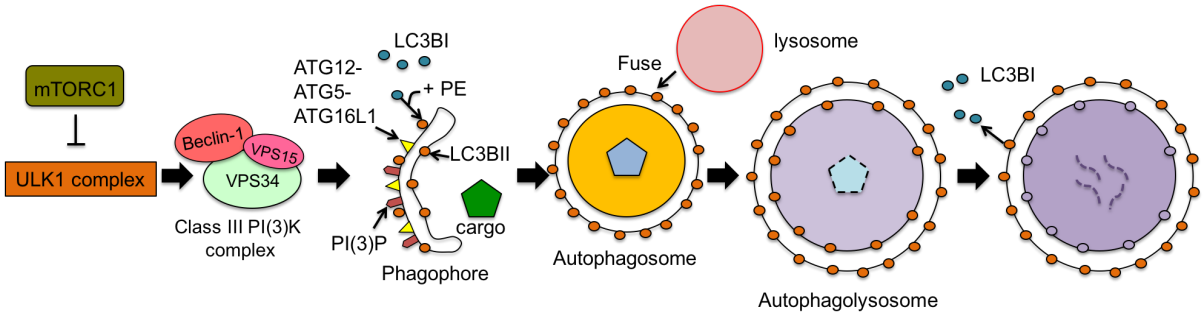


Figure 1.1 Schematic diagram illustrating the autophagy process and its machinery. Autophagy is facilitated by an ensemble of ATG-related proteins (ATGs), which drives the process through from initiation of phagophore formation and its completion into an autophagosome, assembly of autophagosome components, and to its eventual downstream fusion with autolysosomes. Figure is adapted from Glick, Barth & Macleod, 2010.

1.1.3. Autophagy in immunity

Although traditionally known as the disposal bin for bulk cellular waste, it has come to light that autophagy can also exert protective effects against infection by selectively targeting invasive pathogens, establishing it as another arm of the protective innate immune response, termed xenophagy (Stolz, Ernst & Dikic, 2014). Human cells utilise the ubiquitin (ub) conjugation system to tag invading microbes in the cytosol for autophagy recognition via autophagy receptors. This discovery led to the identification of selective autophagy adaptors of the sequestosome 1-like receptor (SLR) family, which carry two important functional domains on each end of

the protein: ub-binding domain (UBD) and LC3-interacting region motif (LIR motif). The role of UBD is to bind to molecular tags such as ub on protein aggregates and microbes, and glycans, which is an infection-induced damage response molecule found on the membrane. The LIR motif pulls the adaptor-cargo complex and bridges it to the LC3B protein on nascent autophagosomes, effectively facilitating the uptake of selected cargo into the autophagy machinery. Autophagy adaptors, such as p62, are degraded along with their associated cargo downstream of autophagy and hence they can also be used as an autophagy marker (Klionsky *et al.*, 2016). Members of the SLR family include p62, neighbour of BRCA1 gene 1 (NBR1), NDP52 and OPTN (Kirkin *et al.*, 2009; Thurston *et al.*, 2009; Mostowy *et al.*, 2011; Wild *et al.*, 2011; von Muhlinen *et al.*, 2012; Korac *et al.*, 2013; Stolz, Ernst & Dikic, 2014). Specifically, NBR1 and OPTN have been shown to participate in recognition and targeting of ub-coated protein aggregates (aggrephagy) (Korac *et al.*, 2013; Kirkin *et al.*, 2009). On the other hand, p62 and NDP52 mediate the recruitment of *Shigella* and *Listeria* to degradative autophagosomes (xenophagy) (Mostowy *et al.*, 2011). In *Salmonella* infection, NDP52 and OPTN have been shown to target bacteria to autophagosomes (Thurston *et al.*, 2009; Wild *et al.*, 2011; von Muhlinen *et al.*, 2012). In addition to aggrephagy, OPTN is also involved in the disposal of damaged ubiquitin-tagged mitochondria (mitophagy) (Heo *et al.*, 2015; Richter *et al.*, 2016) (Figure 1.2).

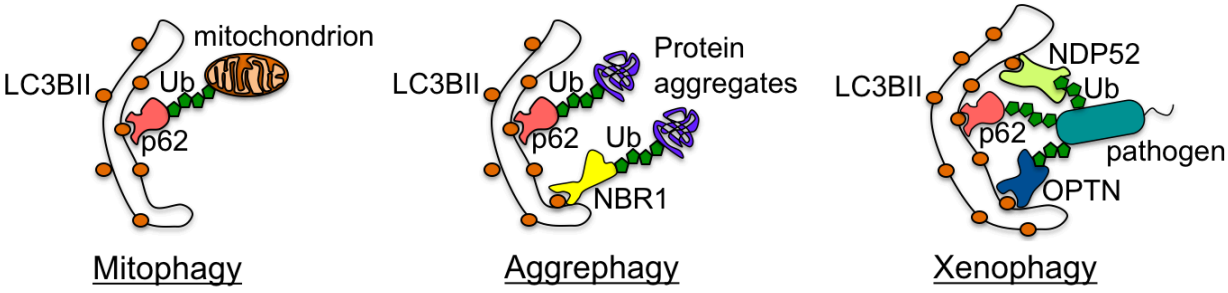


Figure 1.2 Selective autophagy can be achieved by recruiting selective adaptors. Autophagy can recognise polyubiquitinated substrates (mitochondria in mitophagy, protein aggregates in aggrephagy, pathogen in xenophagy) through selective adaptors (p62, NBR1, NDP52, optineurin) that have the ubiquitin-binding domain, which recognises ubiquitin tags on cargo, and leucine-rich motif, which bridges it and its associated cargo to a growing autophagosome. Figure adapted from Stolz, Ernst & Dikic (2014).

Apart from using ubiquitin as a cue, autophagy induction can also be achieved via pattern-recognition receptors (PRRs) recognition of cognate bacterial or viral pathogen-associated molecular patterns (PAMPs) (Table 1.1). Mycobacterial infection has been shown to induce NDP52-mediated autophagy downstream dsDNA recognition in a stimulator of IFN genes (STING)-dependent manner (Watson, Manzanillo & Cox, 2012; Watson *et al.*, 2015). Recognition of bacterial PAMPs by cytosolic Nod-like-receptors (NLRs) such as NOD1/2 and NLRP4 can also induce autophagy. In human HeLa cells infected with *Shigella* flexneri, NOD1 and NOD2 recruit ATG16L1 to the site of bacterial entry on the plasma membrane and invading bacteria are subsequently captured in autophagosomes (Travassos *et al.*, 2010). Furthermore, human epithelial and dendritic cells induce autophagy following NOD2 stimulation with its ligand muramyl dipeptide (MDP) – a bacterial cell wall component – which exerts an anti-bacterial effect on *Salmonella enterica* (Cooney *et al.*, 2010; Homer *et al.*, 2010). NLRP4 was found to associate with

Beclin-1, which it transiently detaches from to induce autophagy, following *Streptococcus pyogenes* infection in human HeLa cells (Jounai *et al.*, 2011). Viral dsRNA-induced PKR can regulate autophagy induction through eIF2α signalling pathway (Tallóczy *et al.*, 2002). Similar to mycobacterial DNA, viral dsDNA can also induce autophagy in a STING-dependent manner (Rasmussen *et al.*, 2011; McFarlane *et al.*, 2011). In addition, stimulation of TLR4, TLR3 and TLR7 with their cognate ligands LPS, poly(I:C) and single-stranded RNA (ssRNA) has been shown to activate autophagy (Xu *et al.*, 2007; Delgado *et al.*, 2008; Shi & Kehrl, 2008).

Table 1.1 Pattern recognition receptors or innate immune sensors can trigger autophagy. Innate immune components (receptors or sensors) that mount inflammatory responses are also associated with autophagy induction. n.d., not determined; n.a., not applicable.

PAMP or ligand	PRR or sensor	Pathogen	Reference
MDP	NOD1, NOD2	*S. flexneri,* *S. enterica*	Travassos *et al.,* 2010; Cooney *et al.,* 2010; Homer *et al.,* 2010
n.d.	NLRP4	*S. pyogenes*	Jounai *et al.,* 2011
dsRNA	PKR	HSV1	Tallóczy *et al.,* 2002
dsDNA	STING	HSV1, *Mycobacterium tuberculosis*	Rasmussen *et al.,* 2011; Watson, Manzanillo & Cox, 2012; Watson *et al.*, 2015
LPS	TLR4	n.a.	Xu *et al.,* 2007; Delgado *et al.,* 2008; Shi & Kehrl, 2008
Poly(I:C)	TLR3	n.a.	Delgado *et al.,* 2008; Shi &

			Kehrl, 2008
ssRNA	TLR7	n.a.	Delgado *et al.,* 2008; Shi & Kehrl, 2008

Furthermore, the production of pro-inflammatory cytokines downstream of these PRRs can amplify autophagy responses, creating a positive feedback loop. In murine macrophages infected with *M. tuberculosis,* interleukin (IL)-1β and IFNγ have been shown to promote engulfment and killing of mycobacteria in autophagosomal compartments (Gutierrez *et al.*, 2004; Pilli *et al.*, 2012). Moreover, tumour necrosis factor α (TNFα) has been shown to stimulate p62-mediated autophagy during *S. flexneri* infection which helped bacterial killing (Mostowy *et al.*, 2011). By integrating autophagy into the PRR signalling pathways, the degradative function of autophagy is made selective and rapid. The synergy between autophagy and PRR signalling can also facilitate the whole process of pathogen elimination.

In adaptive immunity, autophagy has an anti- and pro-inflammatory role. It is critical for ensuring proper development of the immune system, by preventing the generation of autoreactive T cell repertoire that can cause multi-organ inflammation. It does so by ensuring delivery of self-antigens and their presentation on MHC class-II during thymic negative selection (Nedjic *et al.*, 2008). It also plays a role in maintaining homeostasis of the immune system, particularly in lymphocyte survival and counts (Virgin & Levine, 2009; Mortensen *et al.*, 2010). On the other hand, it can promote inflammation by helping prime immune cells of the adaptive system by processing and presenting endogenous antigens on MHC class II, as well as cross-presenting antigens on MHC class I (Paludan *et al.*, 2005). Its role in regulating MHC

class II presentation has been demonstrated to be important in both anti-bacterial and anti-viral infections (Münz, 2010).

1.1.4. Autophagy in controlling inflammation

Given the intricate integration of autophagy in immunity and its role in the regulation of inflammation, it is not surprising that aberrant autophagy can increase the risk for certain diseases. The role of autophagy in controlling inflammation is reflected by multiple human diseases that are associated with defects in autophagy genes. Examples include chronic inflammatory Crohn's disease and autoimmune systemic lupus erythematosus (SLE). Risk mutations associated with Crohn's disease have been identified, among which are autophagy protein-encoding genes *ATG16L1, IRGM,* and *NOD2* (Barrett *et al.*, 2008). Crohn's disease, which is characterised by uncontrolled inflammation in the gut, is caused by altered mucosal barrier function and uncontrolled inflammatory cytokine production, in particular IL-1β and IL-18. The pathogenic mechanism underlying Crohn's disease is thought to be defective autophagy-induced antigen presentation, which leads to reduced recognition of invading commensals in the gut and hence priming of immune cells (Barrett *et al.*, 2008). Genetic variants of *ATG5* are associated with SLE. This multi-organ inflammatory disease is characterised by dysregulated inflammatory cytokine production as well as reduced clearance of cell corpses, which creates a conducive environment for tissue inflammation (Zhou, Cheng & Zhang, 2015).

The homeostatic role of autophagy has also been implicated in pathologies involving mitophagy including neurodegenerative diseases such as ALS and Parkinson's

disease (Rodolfo, Campello & Cecconi, 2017). The depolarised mitochondrion is normally selectively tagged by polyubiquitination on the outer mitochondrial membrane, which attracts ubiquitin-binding OPTN, NDP52, and p62 adaptors. These adaptors are subsequently activated by TBK1-mediated phosphorylation, allowing them to facilitate the formation of the engulfing autophagosome (Matsumoto *et al.*, 2015; Heo *et al.*, 2015; Lazarou *et al.*, 2015). Mutations in *OPTN* and *TBK1* that are associated with ALS have been shown to stall and impair autophagosome formation leading to reduced clearance of damaged mitochondria (Moore & Holzbaur, 2016; Ahmad *et al.*, 2016). Prompt disposal of damaged mitochondria is important in preventing dysregulated inflammation as depolarised mitochondria can introduce danger-associated molecular patterns (DAMPs) such as reactive oxygen species that can activate inflammatory pathways (Zhou *et al.*, 2011). The role of autophagy in clearing pathogenic proteins such as aggregate-prone proteins or polyubiquitinated protein aggregates is also equally important in neurodegenerative diseases such as Huntington's (Huntingtin aggregates), Alzheimer's (neurofibrillary tangles) and Parkinson's (Lewy bodies) diseases (Komatsu *et al.*, 2006; Zatloukal *et al.*, 2002; Sarkar *et al.*, 2007). Impaired clearance of proteins can accelerate neuronal death, which is a hallmark of these diseases.

1.1.5. Autophagy promotes cell survival in the central nervous system (CNS) during infection

As mentioned earlier, autophagy is a homeostatic process that can sense and respond to stress cues including infection. The presence of an intracellular pathogen usually accompanies depletion of available nutrients due to competition and would,

therefore, trigger autophagy in attempt to replete the resources to maintain cell survival. Additionally, its overt cytoprotective role has been illustrated in various viral infections in the central nervous system (CNS) where its role in preventing apoptosis is critical in ensuring the survival of non-renewable CNS-resident cells such as neurons (Yordy *et al.*, 2012).

In neuronal cells infected with simian immunodeficiency virus (SIV), impairment of autophagy has been correlated with enhanced neuronal death and rapamycin-induced autophagy could reduce SIV-induced neurodegenerative effects (Moreau, Luo & Rubinsztein, 2010). Rapamycin-induced autophagy was shown to improve mitochondrial clearance and prevent accumulation of mitochondrial-derived pro-apoptotic cues such as cytochrome c, and hence promoting cell survival (Ravikumar *et al.*, 2006). The importance of autophagy-mediated cell survival is further highlighted by the role of Beclin-1 in Sindbis viral infection in neurons. By binding to anti-apoptotic protein B-cell lymphoma-2 (Bcl-2) during Sindbis infection, Beclin-1 prevents apoptosis during infection (Liang *et al.*, 1998). Whilst autophagy has been found to promote the survival and clearance of viral proteins and p62 aggregates in neuronal cells, it did not have an impact on Sindbis viral replication in these neurons (Orvedahl *et al.*, 2010).

The protective nature of autophagy also extends beyond the CNS. In human pregnancy, maternal trophoblastic cells were shown to be able to resist viral infections, including HSV1, by upregulating autophagy (Delorme-Axford *et al.*, 2013). This resistance was also found to be transferrable to non-trophoblastic cells, which is thought to represent a protective mechanism for the growing foetus (Delorme-Axford

et al., 2013). These studies illustrate the importance and versatility of autophagy in controlling inflammation in sensitive tissues such as the CNS, and in protecting cells in the periphery.

1.2. Herpes Simplex Virus-1

1.2.1. Herpes Simplex Virus-1 (HSV1) and HSV1 primary infection

Herpes simplex virus-1 (HSV1) is a member of the alphaherpesvirinae family that is neurotropic. It persists in infected human host for life owing to its ability to stay latent in neurons. Its 150 kilobase pairs (kbps) genomic double-stranded deoxyribonucleic acid (dsDNA) is encapsulated in a capsid enveloped in lipid bilayer that is studded with tegument protein (Whitley & Roizman, 2001). HSV1 is prevalent in the human population, with an estimate of 67% of global population under 50 years old is seropositive for it (Looker *et al.*, 2015). It primarily infects individuals during early childhood and stays latent throughout the host's life (Abel *et al.*, 2010).

Primary infection is often asymptomatic or benign and self-limiting. Recurrent infection may include facial or oral cold sores, keratitis, and herpetic whitlow. HSV1 is transmitted through intimate contact with individuals shedding virus and its productive infection is supported by epithelial cells and keratinocytes. Once HSV1 establishes its first contact with mucocutaneous keratinocytes or epithelial cells, it attaches and activates a membrane fusion event. By utilising its glycoproteins gB and gC, the HSV1 virion attaches to the glycosaminoglycans (GAGs) on the host cell membrane. Following this attachment, gD engages with one of three HSV1 host

receptors: the herpesvirus entry mediator (HVEM)/tumor necrosis factor receptor superfamily member 14 (TNFRSF14), the nectins (nectin-1 or nectin-2) or 3-O-sulphated heparan sulphate. Subsequently, gD recruits membrane fusion factors gB, gH and gL to initiate virion fusion with the host cell membrane. The nucleocapsid is released into the cell following fusion completion, which then travels to the nuclear membrane using microtubules. Through nuclear pores, HSV1 DNA in the nucleocapsid is injected into the nucleus to initiate viral DNA transcription and synthesis. HSV1 proteins are expressed in a temporal fashion with respect to its replication cycle: immediate early (α), early (β), and late proteins (γ). Newly synthesised DNA and regulatory and structural proteins assemble into a new virion which then buds out of the infected cell, lysing it in the process and infects adjacent cells for further viral propagation, effectively establishing a productive lytic infection (Figure 1.3) (Campadelli-Fiume & Menotti, 2007).

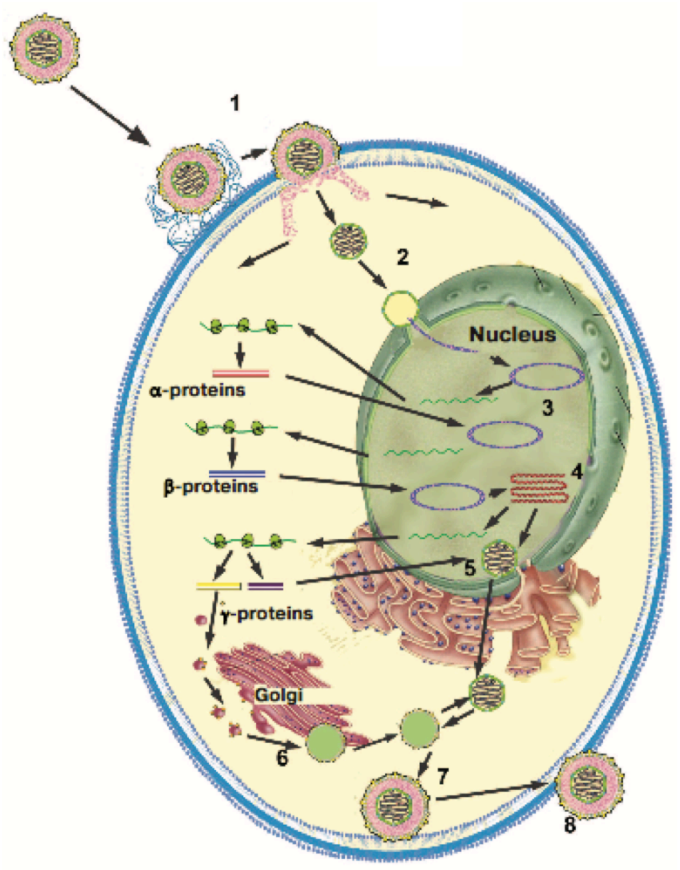


Figure 1.3 HSV1 replication cycle. 1) HSV1 virion attaches onto host cell via cell surface receptors. Viral nucleocapsid is released into host cell following fusion and 2) travels to the nucleus into which it 3) injects its genome. 4) Viral protein expression occurs in temporal cascades (immediate early (α), early (β) and late (γ)) followed with 5) nucleocapsid and 6) capsid assembly to create new virions. 7) Virions travel towards host cell membrane which releases them out via exocytosis. 8) Virions egress to infect other cells. Figure adapted from Kukhanova *et al.,* 2014.

As it spreads to the neurons of the peripheral nervous system (PNS) neighbouring the primary infection site (mainly trigeminal or dorsal root ganglia), it may proceed with a lytic infection that destroys them, or take refuge in them to permanently dwell in and establish a latent infection phase (Smith, 2012). In the latent phase, HSV1 circularises its DNA to halt its replication and gene expression. The only viral ribonucleic acid (RNA) expressed in the infected nuclei during this phase is latent-

associated transcripts (LATs) whose role is to establish and maintain HSV1 latency in the host (Kent *et al.*, 2003). Latent HSV1 may reactivate following reactivation cues such as immunosuppression, ultraviolet (UV) exposure, hormonal changes, stress or withdrawal of anti-viral treatments. As it reactivates, HSV1 reinitiates its lytic infection cycle in the peripheral tissues by shuttling virions from the resident neurons to innervated mucocutaneous tissues to promote its own shedding to another host. Primary infection or reactivated infection may infect neurons (neuroinvasion) of the CNS where it may cause more severe life-threatening encephalitis (Smith, 2012).

1.2.2. Herpes simplex encephalitis (HSE)

HSV1 was first identified as the causative pathogen of herpes simplex encephalitis (HSE) in 1941 following its isolation from a fatal encephalitis case (Smith, Lennette & Reames, 1941). A small portion of the human population, notably 2 to 4 in a million individuals, sporadically develops life-threatening HSE every year as a result of complication with HSV1 infection in the CNS. HSE is the most common form of viral encephalitis in the Western world and has poor outcomes with high morbidity amongst patients (Whitley & Roizman, 2001; Sabah, Mulcahy & Zeman, 2012). HSE follows a bimodal incidence curve, where it predominantly affects children of 3 months to 6 years old and elderly of over 50 years old. Whereas HSE occurrence in the elderly is often associated with viral reactivation, childhood HSE coincides with primary infection with HSV1 (Abel *et al.*, 2010; Whitley & Gnann, 2002; Whitley & Kimberlin, 2005). The clinical features of HSE caused by primary infection or reactivation are indistinguishable. Diagnosis of HSE is normally done by

HSV1 detection in cerebrospinal fluid (CSF) via polymerase chain reaction (PCR) method and clinical presentations (Gnann & Whitley, 2017). HSE patients tend to exhibit confusion, seizures, epilepsy, psychomotor disability, altered consciousness and cognitive impairment (Whitley & Kimberlin, 2005).

Without intensive treatment, HSE can be fatal with a mortality rate as high as 70% (Whitley & Kimberlin, 2005). The only Food and Drug Administration (FDA)-approved drug for HSE is acyclovir which stifles HSV1 replication by inhibiting viral DNA polymerase (Elion *et al.*, 1977). HSE survivors can now persist with the help of acyclovir, although neurological impairment is unacceptably prominent, with over 50% of patients, particularly children, never returning to normal neurologic function (Abel *et al.*, 2010). Sequelae include impairment in language comprehension, memory loss, altered motor function, behavioural changes, impaired cognitive function, and seizures. In addition to this, significant emotional and financial burden also exist amongst survivors as HSE relapses throughout lifetime due to reactivation of latent virus (Whitley & Kimberlin, 2005). Furthermore, because acyclovir can only target HSV1 replication, eradication of HSV1 is not yet possible. There is also a growing concern over the emergence of acyclovir-resistant HSV1 strains, highlighting the need for new therapeutics for this debilitating neurological disease (Jiang *et al.*, 2016).

During the acute phase of HSE, patients exhibit neuroinflammation in the CNS. HSE patients' B and T cells were reportedly showing normal responses towards HSV1 infection (Zhang *et al.*, 2007; Guo *et al.*, 2011; Abel *et al.*, 2010; Herman *et al.*, 2012; Sancho-Shimizu *et al.*, 2011b; Pérez de Diego *et al.*, 2010; Zhang *et al.*, 2013).

Moreover, severe combined immunodeficiency which condition is defined by the lack of B and T cells does not increase the risk for HSE (Buckley, 2004; Sancho-Shimizu *et al.*, 2007). This suggests that HSE has a CNS-restricted immune response and pathogenesis and given that HSE incidence peaks during childhood, cell-intrinsic control of HSV1 infection by CNS resident cells is therefore particularly important, especially during the course of primary infection in childhood (Sancho-Shimizu *et al.*, 2007). Neuroinvasion by HSV1 leads to neuroinflammatory manifestations in the cortical lobes of the brain. The lytic infection causes disseminated necrotising cell death of neurons, astrocytes, and oligodendrocytes, which is histopathologically evident by the formation of focal lesions in the temporal and frontal lobes. Disease progression manifests as haemorrhage in inflamed and necrotising areas (Whitley & Kimberlin, 2005). Immune-driven pathologies are also involved in HSE, where cytotoxic T cells infiltrate and increase focal lesions by killing infected CNS cells. Whilst inflammatory response is crucial in the early stage of infection in combating HSV1 infection, prolonged inflammation can aggravate pathological effects (Wang *et al.*, 2012).

Current efforts are focusing on developing improved anti-viral drugs and anti-inflammatory drugs that can help manage pathologies and improve prognosis. Various murine studies have been testing a combination of anti-viral and immunomodulatory drugs, but none has been done in humans (Prichard *et al.*, 2011). Studies that linked HSE pathogenesis to impaired interferon (IFN) production in selected HSE patients suggested the benefit of exogenous IFNα/β treatment for these patients in addition to current acyclovir therapy (Zhang *et al.*, 2013). Additionally, the anti-inflammatory effect of autophagy-inducer rapamycin in

combination with anti-viral valacyclovir has been explored where it helped reduce the inflammatory cytokine level in the CNS and encouraged the survival of mice with encephalitis (Canivet *et al.*, 2015). This, however, has not been tested in humans.

1.2.3. Mendelian predisposition to HSE

Seroprevalence data have associated childhood HSE with impairment in controlling HSV1 during primary acquisition of the virus (Abel *et al.*, 2010). Why childhood HSE only occurs in a minority of children remained a mystery until the first genetic etiology of HSE was discovered in 2006 which subsequently led to extensive genetic screening of components of the Toll-like receptor (TLR)3-IFN signalling pathway in HSE patients. Cumulative studies revealed this IFN pathway to be crucial particularly for protection against HSV1, as a subset of these HSE patients who were born with mutations in components of TLR3-IFN pathway namely *UNC93B, TLR3, TRIF, TRAF3, TBK1,* and *IRF3,* were otherwise healthy without showing susceptibility to other common viruses (Table 1.2) (Casrouge *et al.*, 2006; Zhang *et al.*, 2007; Pérez de Diego *et al.*, 2010; Guo *et al.*, 2011; Sancho-Shimizu *et al.*, 2011b; Herman *et al.*, 2012; Lim *et al.*, 2014; Andersen *et al.*, 2015; Zhang *et al.*, 2013; Sancho-Shimizu *et al.*, 2011a).

Table 1.2. List of HSE-associated mutations found in components of the TLR3-IFN pathway. Patient-derived fibroblasts used in this study are denoted with *. AD, autosomal dominant; AR, autosomal recessive.

Gene	Mutations	Inheritance mode	Deficiency	Mechanism	No. of cases	Reference
TLR3	p. P554S	AD	Partial	Dominant negative	2	Zhang *et al.,* 2007
TLR3	p. P554S/ E746X	AR	Complete	Compound heterozygous	1	Zhang *et al.,* 2007; Guo *et al.,* 2011
TLR3	p. G743D+R811I	AD	Partial	Haploinsufficiency	1	Lim *et al.,* 2014
TLR3	p. L360P	AD	Partial	Negative dominance	1	Lim *et al.,* 2014
TLR3*	p. R867Q	AR	Partial	Homozygous	1	Lim *et al.,* 2014
UNC93B1*	c. 1034del4	AR	Complete	Homozygous	1	Casrouge *et al.,* 2006
UNC93B1	c. 781 G>A	AR	Complete	Homozygous	1	Casrouge *et al.,* 2006
TRIF*	p. R141X	AR	Complete	Homozygous	1	Sancho-Shimizu *et al.,* 2011
TRIF	p. S186L	AD	Partial	Dominant negative	1	Sancho-Shimizu *et al.,* 2011
TRAF3*	p. R118W	AD	Partial	Dominant negative	1	Pérez de Diego *et al.,* 2010
TBK1*	p. G159A	AD	Partial	Dominant negative	1	Herman *et al.,* 2012
TBK1*	p. D50A	AD	Partial	Haploinsufficiency	1	Herman *et al.,* 2012
IRF3	p. R285Q	AD	Complete	Haploinsufficiency	1	Andersen *et al.,* 2015

HSV1 infection has been shown to produce dsRNA intermediates during replication that arise from self-annealing complementary viral mRNA transcripts (Jacquemont & Roizman, 1975). Infecting dermal fibroblasts derived from these HSE patients with HSV1 or stimulating them with dsRNA synthetic analogue polyinosinic-polycytidylic acid (poly(I:C)) (agonist of TLR3) revealed an impairment in producing IFNs (both IFNβ and IFNγ). These studies suggest the importance of TLR3-IFN signalling in detecting and responding to HSV1-derived dsRNA intermediates during infection by producing anti-viral IFNs. This impairment, therefore, leads to enhanced viral replication and high cell mortality. This susceptibility can be rescued by supplementing the fibroblasts with exogenous IFN (Casrouge *et al.*, 2006; Zhang *et al.*, 2007; Guo *et al.*, 2011; Lim *et al.*, 2014; Sancho-Shimizu *et al.*, 2011b; Pérez de Diego *et al.*, 2010; Herman *et al.*, 2012; Andersen *et al.*, 2015).

Although data derived from these simian virus 40 (SV40)-transformed fibroblasts reflect that of the clinical phenotype, it remained a question, whether these patients' CNS cells display a similar dependence on the TLR3-IFN pathway. Lafaille and colleagues pursued this question by deriving neurons, astrocytes, and oligodendrocytes from induced pluripotent stem (iPS) cells generated from UNC93B- and TLR3-deficient HSE patient-derived fibroblasts. UNC93B$^{-/-}$ neurons and oligodendrocytes, and TLR3$^{-/-}$ neurons, in particular, showed heightened susceptibility to HSV1 infection. This seminal study also demonstrated that this phenotype could be rescued by exogenous treatment of IFNα or IFNβ, linking the TLR3-IFN pathway to CNS-specific immunity against HSV1 infection (Lafaille *et al.*, 2012).

Despite this exciting finding on the non-redundant role of the TLR3-IFN pathway for protection against HSV1 in fibroblasts and CNS cells, it can only explain the pathogenesis in a small traceable fraction of HSE patients. This suggests the existence of yet another HSV1- and CNS-specific pathway(s) that may play an equally important role in host protection against HSV1.

1.2.4. HSV1 and autophagy

Although most viruses subvert autophagy, some viruses actually harness this conserved process to promote and reinforce their replication (Cavignac & Esclatine, 2010). In the case of HSV1, this neurotropic virus evidently antagonises this process by encoding proteins that directly target host autophagic machinery and this inhibition of autophagy is key to its neurovirulence. The first association between HSV1 and autophagy was made when electron microscope (EM) images revealed the presence of HSV1 virions in lysosomal bodies (Smith & de Harven, 1978; Tallóczy, Virgin & Levine, 2006).

As an obligate intracellular pathogen, the success of HSV1 is determined by its ability to seize host transcription and translation machinery and to sustain it, while at the same time repressing host anti-viral mechanisms such as IFN production and autophagy (Figure 1.4). Infection with HSV1 was shown to trigger dsRNA-binding host protein kinase R (PKR), which arrests translation and activates autophagy. To circumvent this blockade, HSV1 expresses infected cell protein 34.5 (ICP34.5) early in infection, which binds to PKR and Beclin-1, resulting in the inhibition of PKR-eIF2α-mediated translational arrest and Beclin-1-mediated autophagy induction,

respectively (Chou & Roizman, 1994; He, Gross & Roizman, 1997). Its interaction with PKR and Beclin-1 has proven to be important in HSV1 neurovirulence as the HSV1 strain with ICP34.5 lacking Beclin-1-binding was neuroattenuated in mice (Orvedahl *et al.*, 2007). Similarly, the HSV1 ICP34.5-deleted strain sustained similar virulence as wild-type in PKR-deficient mice (Leib *et al.*, 2000). ICP34.5 also targets TBK1 to downregulate IFN production and facilitate neuroinvasion. HSV1 with defective TBK1-binding ICP34.5 induced higher anti-viral responses and showed less spread to the brain and trigeminal ganglia *in vivo* (Ma *et al.*, 2012). Interestingly, a recent finding has implicated a role for TBK1 in facilitating p62-mediated HSV1-induced autophagy in human HEK293T cells (Sparrer *et al.*, 2017). Taken together, these studies illustrate the involvement of ICP34.5 in promoting HSV1 neurovirulence and spread *in vivo* by modulating autophagy protein Beclin-1 and TBK1. Although TBK1 has been mainly implicated in bacterial autophagy, solving the conundrum of autophagy versus HSV1 by addressing TBK1 autophagic control during HSV1 infection will undoubtedly help provide clues into the mechanism and role of HSV1-induced autophagy.

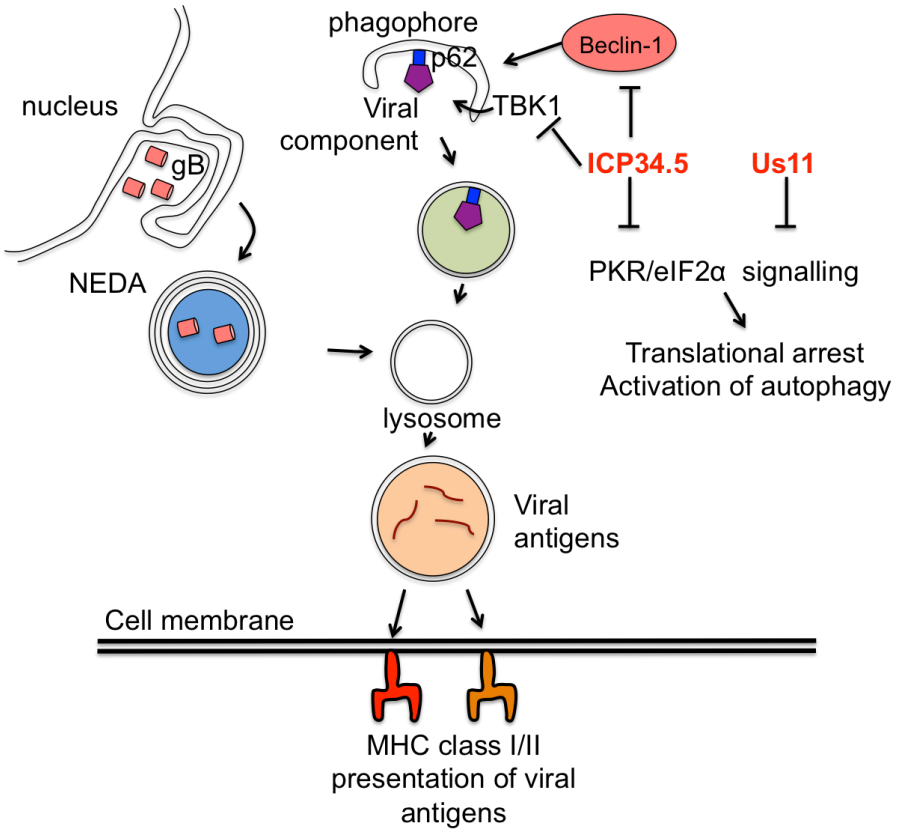


Figure 1.4 HSV1 interaction with host autophagy. HSV1 triggers autophagy following infection, which it counteracts by expressing ICP34.5 early in infection, and Us11 late in infection. Expression of ICP34.5 is aimed to seize host translational control and inhibit autophagy induction by binding to Beclin-1. ICP34.5 has also been shown to directly bind to TBK1 which kinase activity is required for p62-mediated HSV1-induced autophagy. Late in infection, HSV1 induces nuclear envelope-derived autophagy (NEDA), which is shown to be involved in the processing of HSV1 gB protein and in stimulating T cell activation by promoting MHC class I/II presentation of the processed antigen. Image adapted from O'Connell & Liang (2016).

Additionally, late in infection, HSV1 expresses Us11, which also regulates PKR/eIF2α signalling to alleviate host translational arrest (Poppers *et al.*, 2000). Further investigation of this protein revealed its anti-autophagic role, which it exerts

by directly binding to PKR. Overexpression of Us11 in fibroblasts was shown to cause defective autophagosome formation (Lussignol *et al.*, 2013).

Autophagy can also prevent the spread of HSV1 infection by promoting humoral immunity. It mediates the processing of viral peptides and their subsequent loading onto major histocompatibility complex (MHC) class I and II molecules. Antigen presentation by both MHC molecules is important for the priming of $CD8^+$ and $CD4^+$ immune cells during HSV1 infection (English *et al.*, 2009; Leib *et al.*, 2009; Lee *et al.*, 2010). Late in infection of murine macrophages, HSV1 triggers the formation of a 4-layered perinuclear LC3-positive structure termed nuclear envelope-derived autophagy (NEDA), where it is thought to be involved in the degradation of HSV1 glycoprotein gB and its processing for MHC class I presentation (English, Chemali & Desjardins, 2009; English *et al.*, 2009) (Figure 1.4). Further investigation following this report revealed the dependency of NEDA induction on ICP34.5 modulation on host translational arrest and on late viral protein production, suggesting a host counter-response induced by HSV1 antagonism on host translational arrest. Why HSV1 seems to promote NEDA in this scenario is not clearly understood (Radtke *et al.*, 2013). The role of autophagy in anti-HSV1 adaptive immunity was further underscored by the finding that HSV1 Beclin-1-binding deficient ICP34.5 strain was able to restore its neurovirulence in mice that lacked functional T and B cells (Leib *et al.*, 2009).

Despite the evidence of autophagy being a target of HSV1, a better understanding is still required to fully appreciate the role of autophagy in HSV1 pathogenesis. HSV1 mutant ICP34.5 strain showed similar growth rate to its wild-type counterpart strain

despite inducing higher autophagy, suggesting that autophagy does not have an impact on HSV1 replication (Alexander *et al.*, 2007). Given that the primary goal of HSV1 is to persist and establish lifelong latency in the host and the present findings implicating the role of autophagy in HSV1 progression to the CNS, it is tempting to speculate a tissue-specific role of autophagy. Indeed, Yordy and colleagues have demonstrated this facet of host defence. Upon comparison between post-mitotic cells and post-mitotic neurons, neurons preferentially utilised autophagy, more than IFN for protection against HSV1 infection due to its cytoprotective nature. Post-mitotic cells, on the other hand, mount an IFN response and do not require autophagy to control HSV1 infection (Yordy *et al.*, 2012; Yordy & Iwasaki, 2013).

Nonetheless, anti-viral IFN signalling in CNS is still required for host protection. Various experimental mice models have illustrated the significance of IFN in controlling HSV1 infection *in vivo* (Sancho-Shimizu *et al.*, 2007; Zhang *et al.*, 2013; Kollias *et al.*, 2015). Impaired IFN production by iPS cell-derived neuronal cells was associated with an enhanced HSV1 load in selected HSE patients (Lafaille *et al.*, 2012). In fact, IFN and autophagy have been shown to work in parallel in controlling HSV1 infection in neurons (Yordy *et al.*, 2012).

The cooperative role of IFN in neuronal autophagy has also been demonstrated in the CNS. Paracrine IFN signalling is required during HSV1 infection for inducing non-canonical autophagic clusters, which are decorated with autophagy proteins LC3 and p62, exclusively in HSV1 genome-positive antigen-negative neurons. Because this event is dependent on intact IFN signalling, the report postulated an anti-viral role of this autophagy response. Notably, antigen-positive neurons did not exhibit these

autophagic clusters. How these autophagic clusters prevent the establishment of lytic infection and cause HSV1 to switch to latency remains to be investigated (Katzenell & Leib, 2016).

Although the role of IFN has taken centre stage, emerging data have shown a rather exclusive role of autophagy in the CNS. Future studies are required in order to fully dissect how autophagy regulates HSV1 infection in the CNS, and additionally the establishment of latency (Katzenell & Leib, 2016).

1.3. TBK1 is a multifaceted kinase in innate immunity

1.3.1. TBK1 molecular composition and function

TBK1 (TANK-binding kinase 1; also known as NF-kB-activating kinase (NAK) and TRAF2-associated kinase (T2K)) is a serine/threonine kinase that participates in various signalling pathways, including inflammatory pathways and autophagy (discussed later, see Figure 1.6). It is an 84-kDa protein that is encoded by 729 amino acids and is divided into four functional domains – a kinase domain, ubiquitin-like domain (ULD), coiled-coiled domain 1 (CCD1) and CCD2 (Figure 1.5). The kinase domain lies in the N terminus and consists of an activation loop and an active site that mediates phosphorylation of TBK1 substrates. Following dimerisation, TBK1 autophosphorylates at its activation loop, specifically at Serine 172 (Ser172), resulting in the change of its conformation and allowing its substrate to bind to its active site and become phosphorylated (Larabi *et al.*, 2013). The function of ULD is thought to be important for the kinase activity of the protein and the protein's

interaction with ubiquitinated proteins and organelles (Li *et al.*, 2012). CCD1 (also known as scaffold dimerisation domain (SDD)) is rather less described but has been shown to be crucial for TBK1 dimerisation process which precedes its activation (Tu *et al.*, 2013). CCD2, on the other hand, determines the specificity of TBK1, in terms of the pathway it participates in, by binding to specific TBK1 adaptor proteins. To date, there are three known TBK1 adaptors – TRAF family member-associated NF-kB activator (TANK), NAK-associated protein 1 (NAP1) and similar to NAP1 TBK1 adaptor (SINTBAD), which occupy different spaces in the cells. TANK, found in the perinuclear area, binds to TBK1 CCD2 to mediate TBK1 role in IFN signalling pathway. In contrast, NAP1 and SINTBAD, which are found diffuse in the cytoplasm, bind to CCD2 to regulate TBK1 function in autophagy (Goncalves *et al.*, 2011; Thurston *et al.*, 2009).

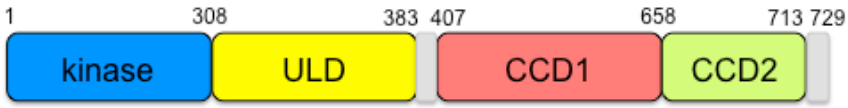


Figure 1.5 Schematic illustration of the TBK1 protein. TBK1 is a 729-amino acid long protein and is made of four domains – serine/threonine kinase, ubiquitin-like domain (ULD), coiled-coiled domain 1 (CCD1) and CCD2. Each domain has its own role in promoting the activation, phosphorylation function and pathway specificity of theTBK1 protein.

1.3.2. TBK1 in innate immunity

The role of TBK1 in the inflammatory pathway is well established. it has been found to primarily control phosphorylation of interferon regulatory transcription factor (IRF) proteins downstream of TLRs and RIG-I-like receptors (RLRs) that lead to

type-I and type-III IFNs (IFNα, IFNβ, and IFNγ) transcription. Following TLR3 and TLR4 activation via dsRNA and lipopolysaccharide (LPS) binding respectively, TBK1 is recruited to phosphorylate the transcription factor IRF3, resulting in its homodimerisation and nuclear translocation. In the nucleus, IRF3 subsequently activates the transcription of proinflammatory IFN genes (Yamamoto *et al.*, 2003; Sharma *et al.*, 2003; Fitzgerald *et al.*, 2003). Similarly, TBK1 is recruited downstream of RLRs such as retinoic acid-inducible gene I (RIG-I), melanoma differentiation-associated protein 5 (MDA5), and the DNA sensor cyclic GMP-AMP (cGAMP) synthase (cGAS) following the engagement of their ligands RNA and dsDNA to induce IRF3 phosphorylation (Figure 1.6) (Sun *et al.*, 2013; Paz *et al.*, 2006; Ishii *et al.*, 2006; Loo & Gale, 2011). Apart from IRF3, TBK1 also binds to DDX3X. DDX3X is a cytoplasmic RNA helicase which, following activation by TBK1, travels to the nucleus to bind to IFN promoter and activate IFN gene transcription directly (Gu *et al.*, 2013; Soulat *et al.*, 2008).

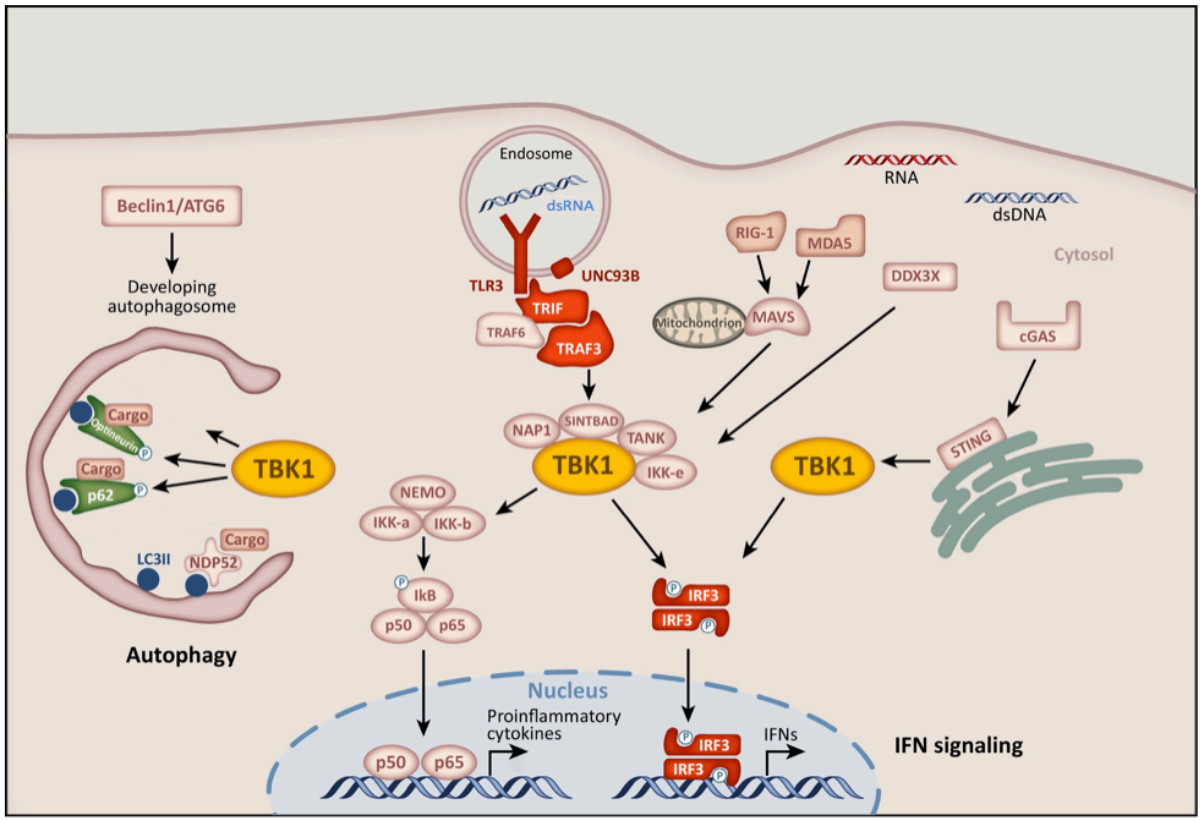


Figure 1.6 TBK1 is a crossroad component of inflammatory pathway and autophagy. TBK1 is involved in IRF3-mediated IFN type I and III transcription downstream of multiple inflammatory pathways including TLR3, RIG-I, MDA5 and cGAS pathways which can detect endosomal dsRNA, and cytosolic dsRNA and dsDNA. TBK1 function is regulated by its interaction with adaptor proteins NAP1, SINTBAD, and TANK. On the other hand, TBK1 is also involved in regulating autophagy where it helps enhance the tethering function of autophagy adaptor p62, OPTN and NDP52 to autophagosomal protein LC3B. Figure is adapted from Ahmad *et al.,* 2016.

1.3.3. TBK1 in autophagy

In the context of autophagy, TBK1 has been shown to play at least two roles, which are dependent on its catalytic activity and independent of its IRF3 substrate: 1) enhancing binding of autophagy adaptors to cargo and LC3B, and 2) promoting

autophagosomal formation and maturation (Table 1.3). In xenophagy (autophagic degradation of pathogen), TBK1 participates upstream of autophagy, by controlling the recruitment of ATG18 orthologue WIPI2 to the forming anti-bacterial autophagosome as shown in *Salmonella typhimurium* infection (Thurston *et al.*, 2016). Although the substrate that TBK1 phosphorylates in this context is still unknown, its localisation to the vicinity of the target bacterium has been shown to be important for WIPI2 recruitment and the subsequent nucleation of autophagosomes (Thurston *et al.*, 2016). TBK1 also helps enhance the engulfment of ubiquitinated *S. typhimurium* into the autophagosome, by interacting with the ubiquitin (ub)-binding autophagy adaptor nuclear dot protein 52 kDa (NDP52) through its adaptor proteins NAP1 and/or SINTBAD. Together, this TBK1-NAP1-SINTBAD-NDP52 complex bridges the ub-coated *S. typhimurium* to autophagosomes and promotes the autophagic clearance of the bacteria. Although the exact role of TBK1 in this context is yet to be explored, its function has been shown to be crucial as TBK1-depleted human HeLa cells showed enhanced *S. typhimurium* proliferation (Thurston *et al.*, 2009). In addition, TBK1 is required in *Salmonella* infection, particularly for its kinase role. Autophagy adaptor optineurin (OPTN) binds to the ubiquitinated *Salmonella* and brings them into autophagosomes through its LC3B-binding domain. The activity of OPTN is then augmented by TBK1 through its phosphorylation at serine-177 (Ser177) residue (Wild *et al.*, 2011). Therefore, one can envisage that NDP52-mediated autophagic capture of *S. typhimurium* also most likely requires the phosphorylation of NDP52 by TBK1. Apart from autophagy, TBK1 has also been shown to be necessary for maintaining membrane integrity of vacuoles that contain *Salmonella* and preventing them from escaping into and proliferating in the cytosol (Radtke *et al.*, 2007).

In *Mycobacterium tuberculosis* infection, TBK1 is crucial for the maturation of mycobacteria-containing autophagosome into bactericidal compartments. It does so by delivering bactericidal cathepsin D enzyme to these autophagosomes. In addition, *M. tuberculosis*-induced autophagy is p62-mediated, where TBK1 also functions to phosphorylate p62 at serine-403 (Ser403) residue (Pilli *et al.*, 2012). Although this report did not further dissect the role of this p62 phosphorylation in the clearance of *Mycobacteria*, another study has shown that phosphorylation of p62 at Ser403 enhances its autophagic role by improving its ub-binding function and its recruitment to degradative autophagosomes (Matsumoto *et al.*, 2011).

The role of TBK1 in anti-viral autophagy is rather limited. Recently, one report has shown that HSV1 induced p62-mediated autophagy in infected human HEK293T cells and that TBK1 was required for phosphorylating p62 at Ser403 residue (Sparrer *et al.*, 2017). The specific cargo to which p62 binds to and whether this cargo-p62 interaction is ub-dependent remain unknown. The TBK1-enhanced binding of autophagy adaptors also extends beyond xenophagy. In aggrephagy (autophagic degradation of protein aggregates) and mitophagy (autophagic degradation of mitochondria), TBK1 was found to mediate the autophagic activity of OPTN that is bound to protein aggregates (Korac *et al.*, 2013) and damaged mitochondria (Richter *et al.*, 2016) by phosphorylating this adaptor at its serine-177 (Ser177) residue.

The region in TBK1 that autophagy adaptors interact with has been mapped to the CCD2 domain. OPTN directly binds to the C-terminus region of TBK1 that extends from residue 601-729 (Morton *et al.*, 2008). NDP52, on the other hand, was found to

indirectly bind TBK1 through CCD2-binding NAP1 and/or SINTBAD adaptor proteins (Thurston *et al.*, 2009). Therefore, it can be assumed that mutations in the CCD2 domain of TBK1 may affect the role of TBK1 in autophagy by abrogating its interaction with autophagy adaptors.

Table 1.3 TBK1 mediates autophagy through autophagy adaptors. TBK1 facilitates the uptake and clearance of selectively targeted cargo by binding to autophagy adaptors (to enhance their binding to autophagosome-associated LC3B, or to promote maturation of autophagosomes).

Type of autophagy	TBK1-interacting autophagy adaptor	Target cargo	Reference
Xenophagy	NDP52, OPTN	*Salmonella typhimurium*	Thurston *et al.,* 2009; Wild *et al.,* 2011
	p62	Mycobacteria	Pilli *et al.,* 2012
	p62	HSV1 infection (cargo unknown)	Sparrer *et al.,* 2017
Mitophagy	OPTN, NDP52	Mitochondria	Heo *et al.,* 2015; Richter *et al.,* 2016
Aggrephagy	OPTN	Protein aggregates	Korac *et al.,* 2013

1.3.4. TBK1 in human neuropathologies

TBK1 is ubiquitously expressed in human tissues, with some cell types showing much higher expression than others, such as the cortical and hippocampal neurons (Uhlén *et al.*, 2015) (https://www.proteinatlas.org/ENSG00000183735-TBK1/tissue). Not surprisingly, the impact of TBK1 deficiency is more pronounced in CNS tissues, as demonstrated by multiple human neuropathologies that have been linked to mutations in *TBK1*. A total of 96 human TBK1 variants have been reported in human pathologies – 2 in HSE, 85 in amyotrophic lateral sclerosis (ALS)/ALS-frontotemporal dementia (FTD) and 9 in normal tension glaucoma (NTG) (Pozzi *et al.*, 2017; Herman *et al.*, 2012; Freischmidt *et al.*, 2015; Gijselinck *et al.*, 2015; Pottier *et al.*, 2015; Cirulli *et al.*, 2015; Le Ber *et al.*, 2015; Fingert *et al.*, 2011; Kawase *et al.*, 2012; Ritch *et al.*, 2014; Ahmad *et al.*, 2016).

Two heterozygous loss-of-function (LoF) mutations in *TBK1* have been associated with HSE (Herman *et al.*, 2012). Two unrelated HSE patients carried heterozygous missense mutations p.G159A and p.D50A located in the kinase domain of TBK1. G159A patient was diagnosed with HSE at 7 years old and has since suffered from epilepsy and motor dysfunction. The patient carrying the D50A mutation developed HSE at 11 months old and has since suffered from cognitive and motor impairments. The G159A allele is dominant negative and results in a kinase-dead protein as it failed to phosphorylate IRF3 or induce IFN production following poly(I:C)-TLR3 stimulation. The D50A mutation, on the other hand, results in poor expression of TBK1 at both the messenger RNA (mRNA) and protein levels. It, therefore, causes LoF by haploinsufficiency. Fibroblasts from both HSE patients could not control

HSV1 infection and this phenotype has been attributed to their inability to produce IFN downstream of the TLR3 signalling pathway (Herman *et al.*, 2012). Autophagy function in these patients has never been tested. To date, the involvement of TBK1 has been described in regulating p62-mediated autophagy in HSV1-infected human HEK293T cells (Sparrer *et al.*, 2017). Although G159A and D50A are not located in the CCD2 domain where autophagy adaptors dock on, these dominant mutations can presumably affect HSV1-induced autophagy as they both alter overall TBK1 function.

While HSE is mainly caused by a complication of HSV1 primary infection which occurs during childhood, ALS is an adult late-onset neurodegenerative disease affecting people of 50-60 years of age with an incidence rate of 1-2 per 100, 000 individuals. ALS is largely sporadic and is characterised by muscle weakening (atrophy) and paralysis which eventually lead to fatality mainly due to respiratory failure (Shaw, 2005). Up to 15% of ALS cases are concurrent with FTD (ALS-FTD), a disorder characterised by cognitive dysfunction (Lomen-Hoerth, Anderson & Miller, 2002). Hallmarks of ALS include extensive deterioration of motor neurons in the spinal cord and brain and the presence of insoluble cytoplasmic protein aggregates, and mitochondrial dysfunction in the affected neurons as well as neuroinflammation. ALS-associated protein aggregates have been shown to be associated with p62, indicating the involvement of autophagy in ALS pathogenesis (Peters, Ghasemi & Brown, 2015).

Similar to HSE, ALS and ALS-FTD have been linked to LoF variants in *TBK1*. 85 *TBK1* variants have been found in ALS/ALS-FTD cases and they are scattered

across the protein. To date, 13 out of these variants have been demonstrated to be disease-causing *in vitro* (Freischmidt *et al.*, 2015; Gijselinck *et al.*, 2015; Pottier *et al.*, 2015; Cirulli *et al.*, 2015; Le Ber *et al.*, 2015; Pozzi *et al.*, 2017; Ahmad *et al.*, 2016). In particular, p.690-713del and p.E696K variants that are located in the autophagy adaptor-binding CCD2 domain both showed impairment in OPTN-binding. p.T320QfsX40, p.I450KfsX15, and p.V479EfsX4 mutations occur upstream of the CCD2 domain and they cause premature stop codon that results in TBK1 that lacks CCD2 domain. As a result, these three mutations also showed impairment in OPTN-binding (Freischmidt *et al.*, 2015). This suggests a possibility for mutations residing outside of CCD2 to affect autophagy function of TBK1. TBK1 is thought to exert its autophagic role in ALS and/or ALS-FTD in mitophagy by recruiting and augmenting the binding of autophagy adaptors (p62 and OPTN) to LC3B by phosphorylating them. Mutations in the CCD2 domain or mutations that abrogate CCD2 by truncating TBK1 can hinder TBK1 binding to autophagy adaptors, resulting in reduced phosphorylation of these adaptors. TBK1 harbouring E696K mutation in the CCD2 domain failed to bind to OPTN, and as a result, could not be recruited to damaged mitochondria (Moore & Holzbaur, 2016). Moreover, mutations in TBK1 kinase domain may affect phosphorylation of autophagy adaptors that is subjected to TBK1 regulation, resulting in an inefficient aggrephagy or mitophagy. Impairment of clearance of protein aggregates and damaged mitochondria has been linked to exacerbated neuroinflammation (Komine & Yamanaka, 2015), highlighting the importance of autophagy-mediated control of inflammation.

In contrast to HSE and ALS/FTD/ALS-FTD, NTG has been associated with gain-of-function (GoF) TBK1 mutations. It is a late-onset irreversible blindness that affects

adults over 40 years of age. This neurodegenerative disease affects the ganglion cells of the retinal optical nerve (Quigley, 2011). Gene duplications on chromosome 12, which stretch to include *TBK1*, have been found in NTG patients. They resulted in an elevated level of TBK1 mRNA in NTG patient-derived dermal fibroblasts, suggesting that GoF may underlie NTG pathology (Fingert *et al.*, 2011; Kawase *et al.*, 2012; Ritch *et al.*, 2014).

Collectively, multiple human neuroinflammatory diseases, particularly those involving the CNS, have described a role for TBK1 in autophagy. Additionally, defects in TBK1 caused by disease-causing mutations can underlie aberrant autophagy, which is important in dampening down the inflammation that is causing progressive irreversible loss of CNS tissues.

1.4 Aims of this study

Evidence has demonstrated the contribution of autophagy to cell intrinsic immunity against HSV1 infection. However, the mechanism and purpose of autophagy induction following HSV1 infection remained long unclear and is an active subject of investigation in the field. To date, there has only been one report that has implicated the requirement of TBK1 in regulating p62 adaptor protein during HSV1 infection (Sparrer *et al.*, 2017). Furthermore, the intricate interplay between autophagy and IFN signalling opens up a question on the relative contribution and roles of these two distinct processes. Elaborate studies on a subset of HSE patients have revealed a non-redundant role for the TLR3-IFN signalling in mediating HSV1 defence in human fibroblasts. Given the involvement of several components of the

TLR3-IFN pathway in autophagy, and that autophagy exhibits a CNS-specific role in neuropathologies including HSE, studying autophagy responses in fibroblasts and neuronal cells of these HSE patients, who may exhibit autophagy impairment following HSV1 infection, would provide useful insights into the understanding of the complex host-HSV1 evolutionary battle and may offer clues into the development of therapeutics for this debilitating disease.

The aims of this study :

1. To characterise autophagy phenotypes of HSE patient-derived fibroblasts following different stimuli – rapamycin, poly(I:C), c-di-GMP, HSV1 dsDNA (60mer) and HSV1 infection
2. To assess the involvement of TBK1 in HSV1-induced autophagy phenotypes by knocking down or inhibiting TBK1 in fibroblasts
3. To assess the role of autophagy in HSV1 infection of fibroblasts
4. To investigate the effect of TBK1 mutations on autophagy in HSV1 infection

This study was also originally set out to carry out autophagy phenotyping of neuronal cells derived from TBK1 patient carrying p.G159A mutation. Unfortunately, I did not manage to accomplish this aim due to several limitations which will be discussed in Chapter 6, along with its relevance.

Chapter 2

2. Materials and Methods

2.1. Cell maintenance and culture

Control, UNC93B$^{-/-}$, TLR3$^{-/-}$, TRIF$^{-/-}$, TRAF3$^{+/-}$, TBK1$^{+/-}$ (p.D50A) and TBK1$^{+/-}$ (p.G159A) dermal fibroblasts derived from upper arm biopsies of healthy individual or HSE patients have been described elsewhere (Sancho-Shimizu *et al.*, 2011a; Zhang *et al.*, 2013), and were maintained in Dulbecco Modified Eagle Medium (DMEM) (Invitrogen) supplemented with 10% foetal bovine serum (FBS) (Invitrogen). HEK293T and Vero (African green monkey kidney) cell lines were maintained similarly in DMEM supplemented with 10% FBS. HEK293T/miRTBK1 stable cell line was maintained in DMEM containing 10% FBS and 2 μg/mL of puromycin for the selection and maintenance of the microRNA (miRNA) construct. All cell lines were grown in a humidified incubator at 37 ^{o}C supplied with 5% CO_2. For seeding, cells were counted using trypan blue exclusion method. Method of cell layer detachment was via trypsinisation.

2.2. Viral strains and propagation

HSV1-GFP (KOS) strain carries green fluorescent protein (GFP) tag on its capsid protein VP26 (Desai & Person, 1998). ΔICP34.5 HSV1 (17termA) is a mutant strain carrying the deletion of ICP34.5 gene. WT HSV1 is its marker-rescued strain (17termAR). Both of these strains are a kind gift from Peter O'hare (Imperial College London, United Kingdom). All strains were propagated by inoculating Vero cell

monolayers. Briefly, Vero cells were grown to confluency in a T75 cm^2 culture flask and subsequently infected with HSV1. Once the monolayer was morphologically showing cytopathic effect (rounding up), the flask was frozen at -80 ^oC and thawed. The culture medium was then harvested and spun at 2, 000 rpm for 5 minutes at 4 ^oC. Supernatants containing HSV1 was then collected and passed through 0.45 µm filter to clean up the infectious viral stock from cell debris. Titre (multiplicity of infection, MOI) of viral stocks was determined by titrating on control dermal fibroblasts using 50% tissue culture infective dose ($TCID_{50}$) Reed and Muench method. HSV1-GFP viral replication was monitored based on GFP fluorescence visualised by the Axiovert 135 TV inverted fluorescence microscope (Zeiss). Phase-contrast and fluorescence images were acquired using Image-Pro Plus software version 7.0 that controlled the microscope (Media Cybernetics).

2.3. Plaque assay

To determine viral titers harvested from experiments, a plaque assay using a lawn of confluent Vero cells was performed. Vero cells were seeded in 12-well plates at a density of 0.25 X 10^6 cells/well and grown overnight. The following day, viral inoculum was prepared by serially diluting it by 1:10 in DMEM supplemented with 2% FBS (i.e. dilutions of 10^0/neat-10^{-12}). 1 mL of inoculum was added per well in duplicates and incubated on Vero monolayers for 2 hours for adsorption before the medium was refreshed with DMEM supplemented with 2% FBS and 1% human serum. Cells were left in 37 ^oC incubator for a week. Once viral plaques have established, the culture medium was removed from wells. The wells were then rinsed once with 1X phosphate-buffered saline (PBS). 400 µL of PBS containing 4%

paraformaldehyde was added in each well to fix cell layers and incubated for 15 minutes at room temperature. The fixative was then removed and 400 µL of PBS supplemented with 0.1% crystal violet was added per well to stain the cell layer which is further incubated for 5 minutes at room temperature. Once stained, wells were washed once with water to remove excess stain and then left to dry. The number of plaques was enumerated and the number of plaque forming unit (PFU) per mL was determined by using the following formula:

$$\text{PFU/mL} = \frac{\text{Average number of plaques}}{\text{dilution factor} \times \text{inoculum volume}}$$

2.4. Cell viability assay

Following infection, the culture medium was removed and cells were rinsed once with 1X PBS. Cells were then incubated with dual dye mix (Invitrogen, catalogue no. L3224) at 37 ^{o}C for 30 minutes. Dual dye mix was prepared in 1X PBS which is composed of calcein AM (live stain, green fluorescence) diluted by 1:2500 and ethidium heterodimer-1 (dead stain, red fluorescence) diluted by 1:1000. Fluorescence was visualised using Axiovert 135 TV inverted fluorescence microscope (Zeiss). Phase-contrast and fluorescence images were acquired using Image-Pro Plus software version 7.0 (Media Cybernetics). The number of cells showing green and red fluorescence was counted using ImageJ software. The viability of cells was determined as the number of dead cells over the total number of live cells and normalised against control non-infected or non-stimulated cells.

2.5. Stimulation, treatment and infection

Unless otherwise stated, stimulations and treatments were done as follows in DMEM supplemented with 2% FBS: 25 µg/mL of poly(I:C) (dsRNA synthetic and ligand of TLR3) (GE Healthcare), 10 nM of rapamycin (Calbiochem), 1 µM of BX795 (Sigma), 10^5 IU/mL of IFNα-2a (PBL Assay Science). Lipofectamine 2000 (Invitrogen) was used to deliver 8 µg/mL of c-di-GMP (Invivogen) or c-di-GMP control (Invivogen), and HSV dsDNA 60mer (Integrated DNA Technology). HSV dsDNA 60mer has been described elsewhere (Rasmussen *et al.*, 2011; Unterholzner *et al.*, 2010) and carries the following nucleotide sequence:

5′-TAAGACACGATGCGATAAAATCTGTTTGT

AAAATTTATTAAGGGTACAAATTGCCCTAGC-3′.

For HSV1 infection, the length of infection and viral dosage (MOI) are as indicated in figure legends. Following initial two hours of adsorption, viral inoculum prepared in DMEM supplemented with 2% FBS was removed and culture medium was replenished with DMEM supplemented with 2% FBS.

2.6. Plasmids and transient transfection

Plasmids used in this study are listed in Table 2.1 below. pEF BOS plasmids carrying wild-type (WT), p.E696K, p.R47H and p.M559R TBK1 mutants which are N-terminally tagged with FLAG were a generous gift of Dr. Axel Freischmidt from Universitätsklinikum Ulm, Germany. pEF BOS FLAG-tagged p.G159A and p.D50A

were generated by creating point mutation on pEF BOS FLAG-tagged WT TBK1 plasmid using site-directed mutagenesis (see section 2.7). For transient transfection, 100 ng of pEF BOS TBK1-FLAG plasmid and 400 ng of empty vector was delivered using Lipofectamine L2000 (Invitrogen) to cells that have been seeded at a density of 0.2 X 10^6 cells/well in a 24-well plate and left to grow overnight. pEF BOS empty vector was used to make up total DNA amount to 500 ng. Transfected cells were incubated overnight before performing assays on them. pMX CMV YFP miR30E was a kind gift from Dr. Avinash Shenoy (Imperial College London, United Kingdom). This plasmid was used to construct pMX CMV YFP miRTBK1 lentiviral plasmid for the generation of HEK293T/miRTBK1 cell line, which will be described later in this chapter (see section 2.9). All plasmid stocks were expanded by transforming competent DH5α *Escherichia coli* and selecting for ampicillin resistance. Stocks were then prepared by using HiSpeed Plasmid Maxi Kit (Qiagen).

Table 2.1. List of plasmids used in this study. Abbreviation, YFP; yellow fluorescent protein.

Plasmid	Description	Antibiotics selection	Expression tag	Source
pEF BOS Empty	Used to control for transfection efficiency	Ampicillin	-	Addgene
pEF BOS FLAG WT TBK1	Flag-tagged (N-terminus) human wild-type TBK1	Ampicillin	N-terminal FLAG	Freischmidt *et al.,* 2012
PEF BOS FLAG G159A TBK1	Flag-tagged (N-terminus) human c.G476C/p.G159A TBK1 variant	Ampicillin	N-terminal FLAG	This study
pEF BOS FLAG D50A TBK1	Flag-tagged (N-terminus) human c.A149C/p.D50A TBK1 variant	Ampicillin	N-terminal FLAG	This study
pEF BOS FLAG E696K TBK1	Flag-tagged (N-terminus) human c.G2086A/p.E696K TBK1 variant	Ampicillin	N-terminal FLAG	Freischmidt *et al.,* 2012
pEF BOS FLAG R47H TBK1	Flag-tagged (N-terminus) human c.G140A/p.R47H TBK1 variant	Ampicillin	N-terminal FLAG	Freischmidt *et al.,* 2012
pEF BOS FLAG M559R TBK1	Flag-tagged (N-terminus) human c.T1676G/p.M559R TBK1 variant	Ampicillin	N-terminal FLAG	Freischmidt *et al.,* 2012
pMX CMV YFP miR30E	Lentiviral microRNA (miR30E) plasmid as described by Fellmann *et al.* (2013)	Ampicillin	YFP	Dr. Avinash Shenoy
pMx CMV YFP miRTBK1	Lentiviral plasmid carrying human TBK1-targeting miRNA expression	Ampicillin	YFP	This study

2.7. Site-directed mutagenesis

To generate pEF BOS carrying FLAG-tagged p.G159A and p.D50A TBK1 mutants, point mutations c.G476C/p.G159A and c.A149C/p.D50A were introduced by site-directed mutagenesis using QuickChange II Site-Directed Mutagenesis kit (Agilent Technologies) on pEF BOS FLAG-tagged WT TBK1 plasmid. Pairs of mutagenic primers were designed (Table 2.2) using an online tool at http://www.genomics.agilent.com/primerDesignProgram.jsp. Successful mutagenesis was confirmed by Sanger DNA sequencing (Genewiz, United Kingdom) of the mutagenesis region using TBK1 complementary DNA (cDNA) primer with the sequence 5'-ACTCCAGATATTGCACCAGA-3' (Figure 2.1).

Table 2.2. Sequences of mutagenic primers used to create p.G159A and p.D50A point mutations.

Point mutation	Primer sequence
c.G476C/p.G159A	3’-cttctaattctctagctgcagcaaaatctgtgagtttgtaca-5’
	3’-tgtacaaactcacagattttgctgcagctagagaattagaag-5’
c.A149C/p.D50A	3’-aattctctcatttgaacagccactggacgaaggaagc-5’
	3’-gcttccttcgtccagtggctgttcaaatgagagaatt-5’

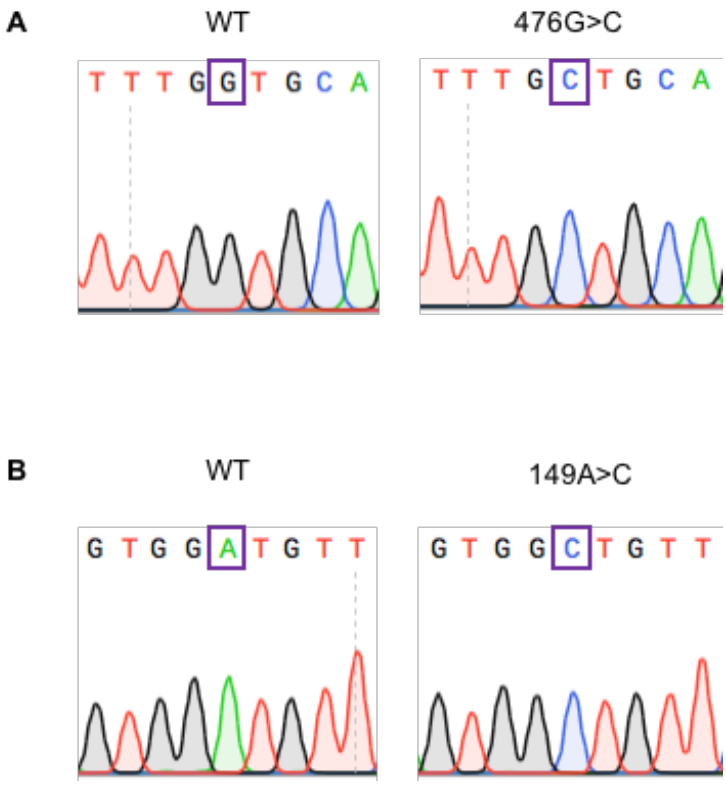


Figure 2.1. Sequence chromatogram of *TBK1* regions subjected to mutagenesis. Mutagenesis was performed on pEF BOS WT *TBK1* plasmid to create (A) 476G>C and (B) 149A>C mutation which were confirmed by Sanger sequencing.

2.8. Depleting endogenous TBK1 using transient siRNA transfection

Cells were seeded in 24-well plate at a density of 0.05 X10^6 cells/well overnight. The following day, cells were transfected with three pooled 15 nM of small interfering RNAs (siRNAs) that target TBK1 (siTBK1) (Ambion) by using Lipofectamine RNAiMAX reagent (Invitrogen) (Table 2.3). Non-targeting siRNA (siNegative) (Ambion) was used to control for transfection control and siRNA specificity. Culture medium was refreshed 24 hours later with DMEM supplemented with 2% FBS. Cells were left incubated for further 24 hours before performing subsequent experiments.

Table 2.3. Commercial siRNAs used to target endogenous human TBK1 or for negative control.

siRNA	Ambion® siRNA ID no.	Ambion® catalogue no.
TBK1	134003	AM16708
TBK1	134002	AM16708
TBK1	899	AM51331
Negative	-	AM4613

2.9. Transduction and generation of stably TBK1-depleted HEK293T cell line (HEK293T/miRTBK1)

HEK293T stably expressing miRNA that targets endogenous *TBK1* was generated by transducing HEK293T cell line with a lentiviral construct (to ensure genome-integrated and stable expression) carrying miRNA sequence that targets 3' untranslated region (UTR) of *TBK1* and puromycin resistance. Because this miRNA only targets 3' UTR of *TBK1*, *TBK1* exogenous cDNA overexpression (plasmid transfection) could be used to complement the cells without itself being targeted. I thank Julia Sanchez-Garrido from Dr. Avinash Shenoy's Lab (Imperial College London, United Kingdom) for their help with the protocol used to generate this cell line. The protocol leading up to the creation of this cell line is as follows.

2.9.1. Designing targeting shRNA sequence and cloning

TBK1 3' UTR cDNA sequence was obtained from ensembl.org website. Twenty-two base pair (bp) TBK1-targeting shRNA sequences were generated using the online iScore Designer tool (http:/www.med.nagoya-u.ac.jp/neurogenetics/i_Score/i_score.html). Potent short hairpin RNA (shRNA) sequence was selected from based on the following criteria as described by Fellmann *et al.* (2013, 2011): thermodynamically asymmetrical, global low GC% content, and guide sense oligo that follows these rules: position 1 is U, position 2, 10, 13 and 14 are A or U, position 20 is G and preferably not an A, and position 21 is G (Table 2.4).

Table 2.4. TBK1-targeting 22 bp oligos that specifically targets the 3' UTR of human *TBK1*. The sequence of oligo was selected by matching with criteria described by Fellmann *et al.,* 2013 to achieve potency.

Oligo	Sequence
Sense	5'-CAAGTGGTATTATTTTATTTTA-3'
Antisense	5'-TAAAATAAAATAATACCACTTT-3'

The TBK1-targeting shRNA sequence was then placed in a string of 118 bp sequence that will generate a stem-loop-stem miR30E shRNA structure (Figure 2.2A). The resulting 118 bp sequence is as follows, where bases in uppercase letters indicate 22 bp oligos that specifically target TBK1:

5’-tcgagaaggtatattgctgttgacagtgagcgCAAGTGGTATTATTTTATTTTAtagtgaagccac
agatgtaTAAAATAAAATAATACCACTTTtgcctactgcctcggacttcaag-3’

The shRNA oligos were subsequently cloned into lentiviral miR30E vector (pMX CMV YFP miR30E plasmid (Figure 2.2B) through four main steps: cutting open the destination vector miR30E using XhoI and EcoRI restriction enzymes, converting the single-stranded oligos into dsDNA insert format, adding XhoI and EcoRI on ends of the dsDNA, and ligating the dsDNA into cut open miR30E backbone using Sequence and Ligation-independent cloning (SLIC) method (Jeong *et al.*, 2012).

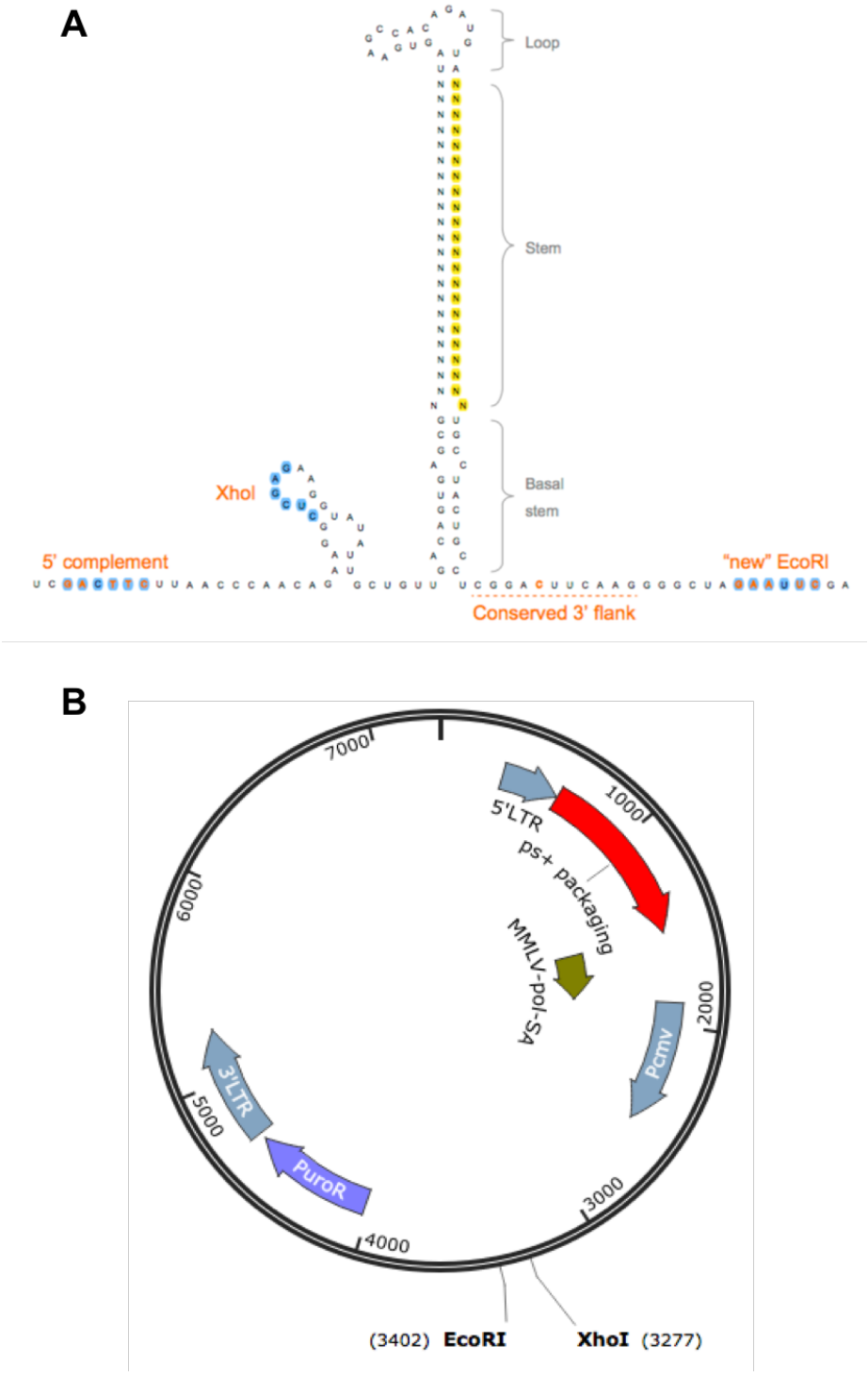


Figure 2.2. shRNA structure and the plasmid map of lentiviral pMX CMV YFP miR30E plasmid. (A) shRNAmiRE sequence designed allows formation of stem-loop-stem secondary structure. Stem indicated by yellow highlighted Ns is where TBK1 targeting sequence is located. Image is adapted from Fellmann *et al.* (2013). **(B)** Lentiviral pMX

CMVYFP miR30E is used as a destination vector with XhoI and EcoRI sites indicated. shRNA sequence can be recombined with this miR30E vector via XhoI and EcoRI sites.

Briefly, miR30E destination vector was cut open by digesting it with XhoI and EcoRI restriction enzymes. The oligos were made into a dsDNA format using the following quick amplification PCR:

PCR Mix:		Thermocycling conditions:	
RNAse-free water	18 µL	1. 98 ^{o}C	2 minutes
Phusion HF buffer (5x)	5 µL	2. 98 ^{o}C	30 seconds
Deoxyribonucleotide		3. 58 ^{o}C	30 seconds
triphosphates (dNTPs)	0.5 µL	4. 72 ^{o}C	5 seconds
(10mM)		Cycle step 2-4 for 16 times	
Forward oligo (10 µM)	1.25 µL	5. 98 ^{o}C	30 seconds
Reverse oligo (10 µM)	1.25 µL	6. 52 ^{o}C	30 seconds
Phusion polymerase	0.25 µL	7. 72 ^{o}C	5 seconds
Total volume	25 µL	Cycle step 5-7 for 15 times	
		8. 72 ^{o}C	1 minute

Restriction sites EcoRI and XhoI (ligation sites for destination miR30E backbone) were then added onto the ends of the dsDNA insert by PCR amplifying the DNA using complementary primers carrying the restriction site sequences (Table 2.5). PCR reaction was done as follows:

PCR mix:		Thermocycling conditions:	
Water	17.5 µL	1. 98 ^{o}C	2 minutes
Phusion HF buffer (5x)	5 µL	2. 98 ^{o}C	30 seconds
dNTPs (10mM)	0.5 µL	3. 58 ^{o}C	30 seconds
XhoI primer (10 µM)	1.25 µL	4. 72 ^{o}C	10 seconds
EcoRI primer (10 µM)	1.25 µL	Cycle step 2-4 for 16 times	
dsDNA insert from first PCR	0.5 µL	5. 98 ^{o}C	30 seconds
Phusion polymerase	0.25 µL	6. 52 ^{o}C	30 seconds
Total volume	25 µL	7. 72 ^{o}C	10 seconds
		Cycle step 5-7 for 15 times	
		8. 72 ^{o}C	1 minute

Table 2.5. Primer sequences used to add XhoI and EcoRI restriction sites onto targeting shRNA sequence. Uppercase letters are bases that are complementary to shRNA sequence. Underlined bases indicate XhoI and EcoRI restrictions sites.

XhoI primer: primer sequence with XhoI restriction site: 5'-tgtacaagtccggactcagatgatcgacttcttaacccaacagaaggcTCGAGAAGGTATATTGCTG-3'
EcoRI primer: primer with EcoRI restriction site: 5'-gcggccgcggcgcgccggccgaattctagcccCTTGAAGTCCGAGGCAGTAGG-3'

PCR products derived from first and second PCR (restriction sites added) were electrophoresed on 2% agarose gel at 100 V for 1 hour in 1X TAE running buffer. Addition of restriction sites was confirmed by the size shift of the band from 118 bp (first PCR) to 198 bp (second PCR) (Figure 2.3). The PCR reaction from second PCR was then directly purified using QIAquick PCR Purification Kit (Qiagen).

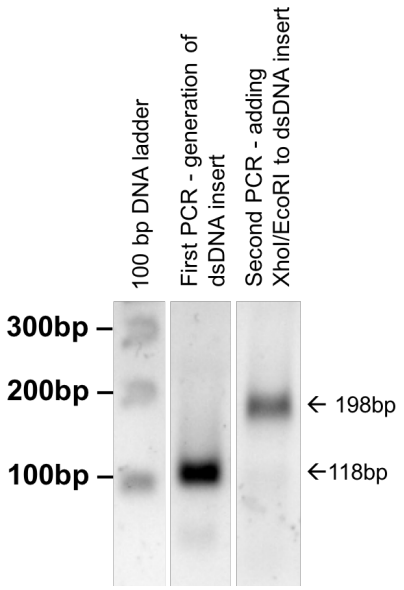


Figure 2.3. Addition of EcoRI and XhoI restriction site to dsDNA insert. Confirmation of EcoRI and XhoI restriction sites was determined by size shift from 118 bp to 198 bp.

Purified dsDNA insert with EcoRI/XhoI ends were then recombined with EcoRI/XhoI digested destination vector miR30E using SLIC protocol (Jeong *et al.*, 2012). Briefly, a ligation mix was prepared as follows and incubated at room temperature for 2.5 minutes and subsequently transferred on ice for minimum 10 minutes.

Digested destination vector miR30E	100 ng
Insert (1:4 molar ratio, vector:insert*)	11.28 ng
T4 DNA ligase buffer (10x)	1 µL
T4 DNA ligase	0.5 µL
Total volume	10 µL

* vector:insert molar ratio was calculated by using online tool NEBioCalculator™ (http://nebiocalculator.neb.com/#!/ligation).

The SLIC ligation product was then transformed into One Shot® TOP10 Chemically Competent *E. coli* (Invitrogen). Briefly, 2 µL of the ligation product was incubated with 50 µL of competent *E. coli* for 30 minutes on ice. The competent bacteria were then heat-shocked at 42 ^{o}C for 30 seconds and immediately chilled on ice for 2 minutes afterward. 50 µL of pre-warmed (37 ^{o}C) S.O.C medium (Invitrogen) was added to the bacteria, which were then incubated on a shaker (225 rpm) for 1 hour at 37 ^{o}C. 100 µL of the bacterial transformant was then spread on LB agar plate supplemented with selective antibiotic (100 µg/mL of ampicillin) to select for successful transformant. The plate was placed in 37 ^{o}C incubator overnight to let successful clones grow. The following day, few candidate colonies were picked on pipette tips and placed in 250 mL liquid LB broth supplemented with 100 µg/mL ampicillin antibiotics to expand them further overnight, in a shaker (225 rpm) at 37 ^{o}C. The following day, bacteria were collected and spun down into a pellet at 15, 000 rpm for 15 minutes at 4 ^{o}C. Lentiviral miR30E pMX cytomegalovirus (CMV) YFP plasmid carrying TBK1-targeting shRNA (miRTBK1) sequence was extracted and purified from bacterial pellets using HiSpeed Plasmid Maxi Kit (Qiagen) (Figure 2.4).

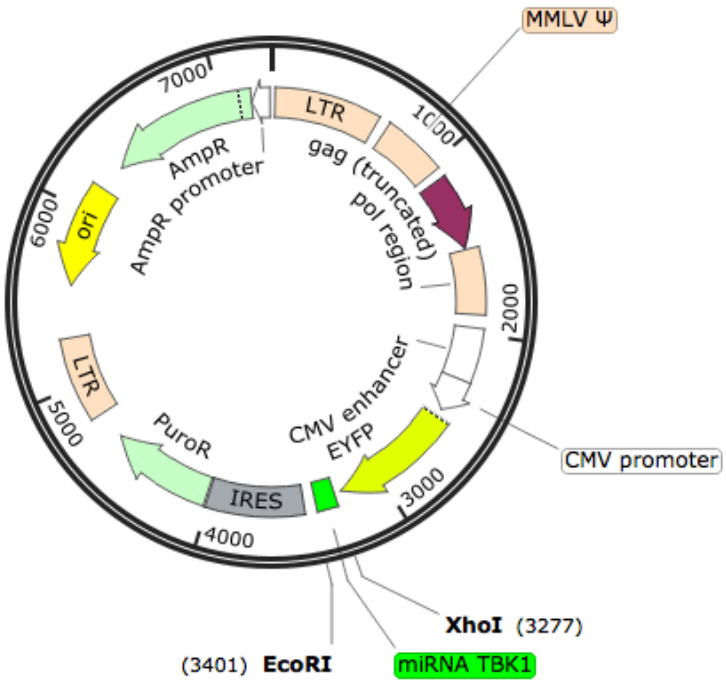


Figure 2.4. pMX CMV YFP miR30E vector map carrying shRNA sequence that targets 3' UTR of endogenous human TBK1 (miRTBK1). Recombining miRTBK1 with pMX CMV YFP vector via XhoI/EcoRI sites creates a 7294 bp plasmid driven by CMV promoter and with a puromycin resistance cassette.

To assess the success of the cloning, the resultant pMX CMV YFP miRTBK1 plasmids derived from few candidate colonies were transiently transfected in control dermal fibroblasts by using Lipofectamine LTX reagent to deliver 100 ng of the plasmid per well of cells in a 24-well plate. 24 hours post-transfection, the expression of plasmid was assessed based on YFP indicative of expression of miRTBK1 driven by shared CMV promoter. From the transfection with one of the candidate plasmids, approximately 30% of cells were YFP-positive 24 hours post-transfection (Figure 2.5A). Visualisation and image acquisition was done using Axiovert 135 TV microscope (Zeiss) attached to the acquisition software Image Pro Plus (Media Cybernetics). Subsequent experiments including the derivation of the stable cell line were done using this plasmid. Cells were then subjected to 24-hour incubation with 2 µg/mL of puromycin selection for positive cells before whole-cell lysates were harvested. Protein samples were electrophoresed and immunoblots were probed for TBK1 expression. As confirmed by immunoblots, the amount of endogenous TBK1 is reduced in the cells following transfection with the miRTBK1 plasmid (Figure 2.5B).

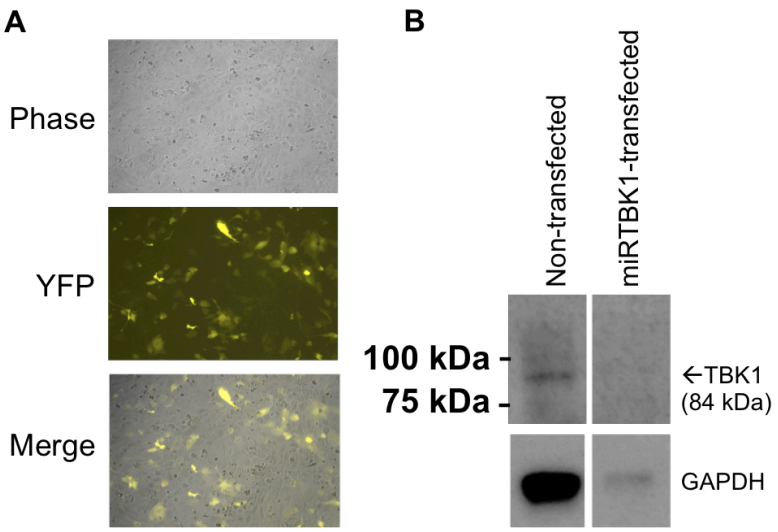


Figure 2.5. Confirmation of successful cloning of miRNA targeting TBK1 in control human dermal fibroblasts. (A) Cells were transiently transfected with 100 ng of pMX CMV YFP vector carrying miRNA targeting 3' UTR of human TBK1 (miRTBK1) for 24 hours, before visualising the expression of miRTBK1 based on YFP expression (with which it shares the same CMV promoter). **(B)**

Following 24 hours after transfection, cells were treated with 2 µg/mL of puromycin* to select for transfected cells for further 24 hours before lysis. Whole cell lysates were subjected to immunoblotting and probed for TBK1 expression. Glyceraldehyde 3-phosphate dehydrogenase (GAPDH) was used as a loading control. *Puromycin titration (kill curve) was done on control human dermal fibroblasts beforehand to determine the minimum puromycin concentration that gives 100% killing within 48 hours.

2.9.2. Production of lentiviral pseudoparticles for miRTBK1

Following confirmation of lentiviral construct, infectious lentivirus pseudoparticles were generated by transfecting HEK293T cells with the lentiviral miRTBK1 construct together with pCMV-VSVg and pGag-pol using calcium phosphate ($CaPO_4$) transfection kit (Sigma). 0.3 $X10^6$ cells/mL of HEK293T cells were seeded in 6-well plate overnight. $CaPO_4$ transfection mix was prepared in a polypropylene tube as follows:

2M CaCl2	7.2 µL
pGAG-pol	0.4 µg
pCMV-VSVg	1.4 µg
Lentiviral construct	2 µg
Water	x
Total volume	30 µL

In a polypropylene tube, 30 µL of 2 x Hepes-buffered saline (HBS) solution was aerated while 30 µL of DNA mix was dripped into it. The transfection mix (total 60 µL) was incubated for 30 minutes at room temperature before adding it to HEK293T

cell monolayer in a drop-wise manner. Cells were incubated overnight at 37 ^{o}C. Culture medium was refreshed with DMEM supplemented with 10% FBS. 48 hours post-transfection, culture medium containing lentivirus pseudoparticles was harvested and passed through a 0.45 µm filter to remove cell debris. HEPES solution (4-(2-hydroxyethyl)-1-piperazineethanesulfonic acid (Sigma)) was added to the viral stock to final concentration of 20 mM before the harvest was stored at -80 ^{o}C until use. Culture medium was replenished with fresh DMEM supplemented with 10% FBS and cells were incubated for further 24 hours. 72 hours post-transfection, similar harvesting method was performed.

2.9.3. Transducing HEK293T cells with pseudoparticles carrying miRTBK1 and clone selection and expansion

HEK293T cells were seeded at a density of 0.3 X 10^6 cells/mL in a 6-well plate in three wells. Using 72-hour pseudoparticle harvest, two wells of the cells were infected with either 500 µL or 250 µL of the lentivirus pseudoparticles which were prepared in DMEM supplemented with 2% FBS and 4 µg/mL of polybrene (hexadimethrine dibromide (Sigma)). 6 hours post-transduction, the culture medium was refreshed with DMEM supplemented with 10% FBS. 24 hours post-transduction, the culture medium was replaced with DMEM supplemented with 10% FBS and 2 µg/mL of puromycin, including that of the non-transduced well. Puromycin titration (kill curve) was performed beforehand on HEK293T cell line to get a minimum concentration of puromycin that kills 100% of cells within 48 hours. Culture medium was refreshed every other day with 2 µg/mL puromycin to maintain selection for cell clones that carry the miRTBK1 expression. Following clonal expansion, the first

generation of cell stock was generated before whole-cell lysates were obtained and assayed for TBK1 expression using immunoblotting.

2.10. Sodium dodecyl sulphate polyacrylamide gel electrophoresis (SDS-PAGE) and Western blotting

For LC3B immunoblotting, bafilomycin A1 (Sigma) was added to the culture medium at a final concentration of 10 ng/mL 6 hours before the end of experiment, to inhibit degradation of autophagosomes and hence allowing us to capture the accumulation of LC3BII protein (Klionsky *et al.*, 2016). At the end of experiment, whole-cell lysis was done by incubating cells with 1X Laemmli buffer supplemented with protease inhibitor cocktail (Roche), 10% β-mercaptoethanol and 0.1% benzonase nuclease for 5 minutes on ice. Collected lysates were then boiled at 95 ^{o}C for 10 minutes and electrophoresed on 12% tris-glycine or 10% bis-tris gels (Biorad) at constant 120 V for approximately 90 minutes until optimum protein separation is achieved. Precision Plus Protein^{TM} dual colour ladder (Biorad) was used as the protein ladder. Proteins were then transferred onto polyvinylidene difluoride (PVDF) membrane using semi-dry transfer system (iBlot transfer stack, Invitrogen) at constant 20 V for 7 minutes (iBlot transfer machine, Invitrogen). Blocking was done by incubating blots with 1X tris-buffered saline (TBS) solution supplemented with 0.1% Tween20 and 5% milk for 1 hour at room temperature. Blots were washed thrice 5 minutes each with 1x TBS containing 0.1% Tween20 before incubating with primary antibody and before incubating with secondary antibody. All antibodies and their dilutions and diluents used for immunoblotting in this study are listed in Table 2.6 below.

Table 2.6. Antibodies and dilution conditions used for Western blotting.

Antibodies	Dilution	Diluent	Company and catalogue number
LC3B	1:1000	1XTBS 0.1% Tween20 5% milk	Sigma (L7543)
P62 (SQSTM1)	1:1000	1XTBS 0.1% Tween20 3% milk	MBL Intl (PM045)
GAPDH-HRP	1:500	1XTBS 0.1% Tween20 5% milk	Santa Cruz Biotech (sc25778)
NDP52 (CALCOCO2)	1:1000	1XTBS 0.1% Tween20 5% milk	Abcam (68588)
TBK1 (NAK)	1:1000	1XTBS 0.1% Tween20 5% milk	Cell Signaling Technology (3013)
HRP	1: 10, 000	1XTBS 0.1% Tween20 5% milk	GE Healthcare (NA934)

2.11. Immunofluorescence, image acquisition and puncta quantification

Cells that were grown on a glass coverslip were washed once with 1X PBS before being fixed using -20 ^{o}C-cold 100% methanol on ice for 15 minutes. Following fixation, cells were rinsed with 1X PBS three times. Cells were permeabilised with 0.1% Triton-X for 4 minutes at room temperature before rinsing them with 1X PBS. They were then blocked with 1X PBS supplemented with 10% FBS for 10 minutes at

room temperature. Incubation with primary antibody and subsequently secondary antibody was done for 45 minutes each at room temperature in a dark humidified chamber with a wash with 1X PBS in between. Fluorescence was visualised by using wide-field fluorescence Cell Observer microscope (Zeiss). Fluorescence images were captured with 63X oil-immersion lens using Zen Pro image acquisition software (Zeiss). The number of cells positive for LC3B puncta was quantified on a minimum number of >100 cells in each experiment. The antibodies used, antibody dilutions and diluents are shown in the table below (Table 2.7):

Table 2.7. Antibodies and dilution conditions used for immunofluorescence staining.

Antibodies	Dilution	Diluent	Company and catalogue number
Rabbit anti-LC3B	1:500	10% FBS-PBS	Abcam (48394)
Mouse anti-ICP4	1:500	1% BSA-PBS	Virusys (H1A021)
Rabbit anti-LC3A	1:100	10% FBS-PBS	Abgent (AP1805a)
Mouse anti-giantin (Golgi marker)	1:200	1% BSA-PBS	Abcam (ab37266)
Mouse anti-DDK (FLAG)	1:1000	1% BSA-PBS	Origene (TA50011)
Alexa anti-rabbit 488 conjugated	1:750	10% FBS-PBS	Thermofisher (35552)
Alexa anti-mouse 594 conjugated	1:1000	1% BSA-PBS	Thermofisher (A11020)

2.12. Cytokine measurement using enzyme-linked immunosorbent assay (ELISA)

IFNβ and IL-6 cytokines in culture supernatants were measured by using VeriKine-HS^{TM} human IFNβ serum ELISA kit (protocol A) (PBL Assay Science) and PeliPair human IL-6 ELISA kit (Sanquin) respectively. ELISA was performed as per manufacturers' instructions. Absorbance data were acquired by using VersaMax microplate reader (Molecular Devices) at 450 nm.

2.13. Nuclease and heat treatments for conditioned media

Condtioned media were harvested from control or TBK1$^{+/-}$ (p.G159A) fibroblasts that were not-infected or infected with HSV1-AR. Briefly, MOI 10 of HSV1-AR was prepared in serum-free DMEM and added to fibroblasts. 2 hours post-infection, medium was replaced with fresh serum-free DMEM. At the end of 3-hour infection, media were collected, passed through a 0.22 μm pore size sterile filter, UV-irradiated and either left untreated or treated with benzonase nuclease (1:1000) or with heat at 95 ^{o}C for 10 minutes. Human serum was added to the treated media to a final concentration of 1% before adding them onto control fibroblasts (that had been cultured overnight on coverslips in a 24-well plate at the seeding density of 0.06 X 10^6 cells/mL). The conditioned media were left to incubate on the fibroblasts for 8 hours at 37 ^{o}C before the fibroblasts were fixed with absolute methanol. Immunostaining was done as described in section 2.11.

2.14. Neural stem cells culture and differentiation into pure neuronal culture

iPS cell-derived neural stem (NS) cells (from a healthy donor, catalogue no. ax0016) were purchased from Axol Bioscience (Cambridge, United Kingdom) and cultured according to the company's guidelines. Briefly, NS cells were seeded at a density of 75, 000 cells/cm^2 on a feeder-free culture area that had been coated with Geltrex coating matrix (Invitrogen), grown and maintained in neural expansion medium supplemented with 20 ng/mL of epidermal growth factor (EGF) and fibroblast growth factor 2 (FGF2) (Axol Bioscience). For passaging, cells were lifted by incubating with accutase reagent (Life Technologies), for 5 minutes at 37 ^oC and were collected by centrifuging the cell suspension at 200 X g for 5 minutes.

To start the differentiation of NS cells into pure cortical neurons, the culture medium of NS cells was replaced with neural differentiation medium (Axol Bioscience, catalogue no. ax0034) upon reaching 60-70% confluency. After the pure population of neurons was achieved approximately 7 days later, the culture medium is replaced with neural maintenance medium (Axol Bioscience, catalogue no. ax0032). Cortical neurons were maintained in this medium for up to 7 days before performing stimulation or infection on them.

2.15. Statistical analysis and software

Nucleotide sequence, plasmid mapping, and sequence chromatogram analyses were done using SnapGene Viewer software version 4.0.2 (GSL Biotech). Densitometric analysis of immunoblots and quantification of fluorescent cells were done by using ImageJ software 1.49v (Schneider, Rasband & Eliceiri, 2012). Immunofluorescence images were processed and analysed by using Icy imaging software version 1.8.6.0 (BioImage Analysis). ELISA absorbance data were analysed by using SoftMax Pro 5 software (Molecular Devices). Statistical analyses (Student's t-test and two-way ANOVA) were done by using Prism software (GraphPad).

Chapter 3

3. Autophagy phenotypes of HSE patient-derived fibroblasts with defective TLR3-IFN pathway

3.1. General introduction

Inborn mutations in components of the TLR3-IFN pathway found in selected HSE patients have been associated with HSE pathogenesis – *UNC93B*, *TLR3*, *TRIF*, *TRAF3*, *TBK1* and *IRF3*. Further studies using these patients' dermal fibroblasts revealed a narrow HSV1-specific defect in anti-viral IFN production (Casrouge *et al.*, 2006; Zhang *et al.*, 2007; Pérez de Diego *et al.*, 2010; Guo *et al.*, 2011; Sancho-Shimizu *et al.*, 2011b; Lim *et al.*, 2014; Herman *et al.*, 2012; Andersen *et al.*, 2015; Zhang *et al.*, 2013; Sancho-Shimizu *et al.*, 2011a). Whilst the TLR3-IFN pathway is evidently important in HSE pathogenesis, the involvement of other anti-viral pathways cannot be ruled out.

One such pathway is autophagy, a cell-autonomous recycling and waste disposal system that runs homeostatically. Although its role has been emphasised in the elimination of invading bacteria, its role in HSV1 infection is still unclear. Few components of the TLR3-IFN pathway have been implicated in autophagy – TLR3, Toll/interleukin-1 receptor (TIR)-domain-containing adapter-inducing interferon-β (TRIF) and TBK1 (Gorbea *et al.*, 2010; Shi & Kehrl, 2008; Pilli *et al.*, 2012). However, involvement of these components in HSV1-induced autophagy is unclear. Herein, the characterisation of autophagy phenotypes during HSV1 infection as well as other stimuli poly(I:C), cyclic di-guanosine monophosphate (c-di-GMP) and HSV1 dsDNA

was performed by using fibroblasts derived from the HSE patients carrying various mutations in the TLR3-IFN pathway.

3.2. Rapamycin-induced autophagy

In order to assess functionality of basal autophagy of fibroblasts, I treated the fibroblasts with rapamycin, a classic inducer of autophagy. Rapamycin is a macrolide that inhibits protein kinase mTOR (mammalian target of rapamycin), which regulates cellular growth in response to cues such as nutrients. Inhibiting mTOR using rapamycin mimics a starvation cue, resulting in the induction of autophagy (Mizushima, Yoshimori & Levine, 2010).

Control fibroblasts were treated with various concentrations of rapamycin and were subsequently probed for LC3B and p62, both of which are markers of autophagy. Induction of LC3B was measured by its relative ratio II to I level, as the conversion of LC3BI to LC3BII is an indicator of an increased autophagy flux. Reduction of p62 is also monitored which also is a marker of increased autophagy flux as it gets degraded downstream of the autophagy process (Klionsky *et al.*, 2016). As seen on immunoblots, rapamycin treatment induced LC3BII:I in fibroblasts, with the highest level seen at 10 nM (Figure 3.1A). Using 10 nM concentration, treatment was further optimised by performing different lengths of treatment. The level of LC3BII:I increased in a time-dependent manner, which peaked at 24 hours (Figure 3.1B). p62 levels however were not reduced following rapamycin treatment across time (Figure 3.1B). To further study the induction of LC3B in the cells, immunofluorescence was employed to visualise the LC3B response. At basal levels, control fibroblasts showed

diffuse distribution of LC3B in the cytosol. However, following 24 hours of treatment with 10 nM rapamycin, accumulation of LC3B puncta in the cytoplasm of control fibroblasts was observed (Figure 3.1C).

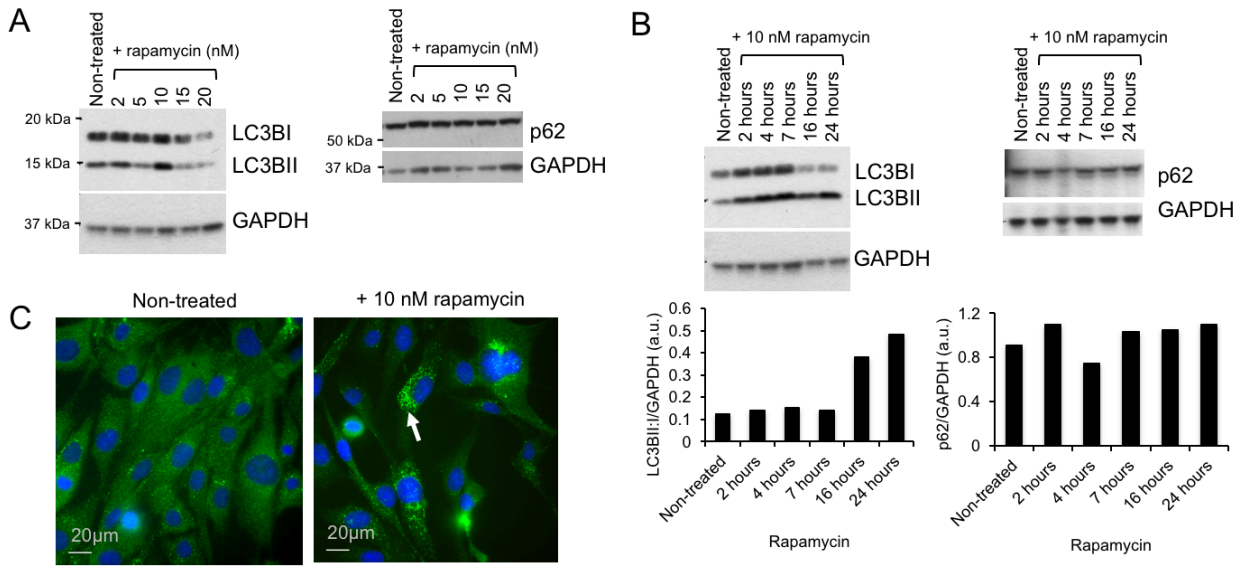


Figure 3.1. Rapamycin induces autophagy in human dermal fibroblasts. (A) Control fibroblasts were treated with various concentration of rapamycin for 2 hours before subjected to whole-cell lysis, (*n* = 1). **(B)** Control fibroblasts were treated with 10 nM of rapamycin for various period of time before subjected to whole-cell lysis. Lysates were electrophoresed and probed for LC3B and p62 expression. GAPDH was used as a loading control, (*n* = 1) (upper panel). Immunoblots from (B) were subjected to densitometric analyses (lower panel). **(C)** Control fibroblasts grown on coverslips were treated with 10 nM of rapamycin for 24 hours, fixed and stained for endogenous LC3B (green). 4',6-diamidino-2-phenylindole (DAPI) was used to stain nuclei (blue). Immunofluorescence images are representative of three independent experiments (*n* = 3). White arrow indicates LC3B puncta. Scale bar, 20 μm; a.u., arbitrary unit.

Next, I used treatment with 10 nM of rapamycin for 24 hours to test autophagy function in UNC93B$^{-/-}$, TLR3$^{-/-}$, TRIF$^{-/-}$, TRAF3$^{+/-}$, TBK1$^{+/-}$ (p.D50A) and TBK1$^{+/-}$

(p.G159A) fibroblasts, and probed their lysates for LC3B expression using immunoblotting. Rapamycin treatment triggered the increase of LC3BII:I in control fibroblasts by 2-fold although statistical analysis did not determine it to be significant (Figure 3.2). Similarly, UNC93B$^{-/-}$, TLR3$^{-/-}$, TRAF3$^{+/-}$, TBK1$^{+/-}$ (p.D50A) and TBK1$^{+/-}$ (p.G159A) fibroblasts were able to induce LC3BII:I levels by 1.6-, 1.5-, 1.5-, 1.8- and 2.5-fold respectively. By immunoblotting, TRIF$^{-/-}$ fibroblasts did not show induction of LC3BII:I. Consistent with the previous observation in control fibroblasts, rapamycin did not trigger the reduction of p62 in all patients' fibroblasts but rather upregulated it (Figure 3.2). Rapamycin has been reported to upregulate the expression of p62 in at least three human cell lines: fibroblasts, MG63 osteosarcoma cell line and macrophages. Rapamycin-induced p62 was shown to participate in regulating cellular oxidative stress and apoptosis in response to mitochondrial damage (Ko *et al.*, 2017; Lerner *et al.*, 2013; Xie, Xie & Dong, 2013). Whether rapamycin-induced p62 observed in this study is to perform similar function as in these cell lines remains to be investigated.

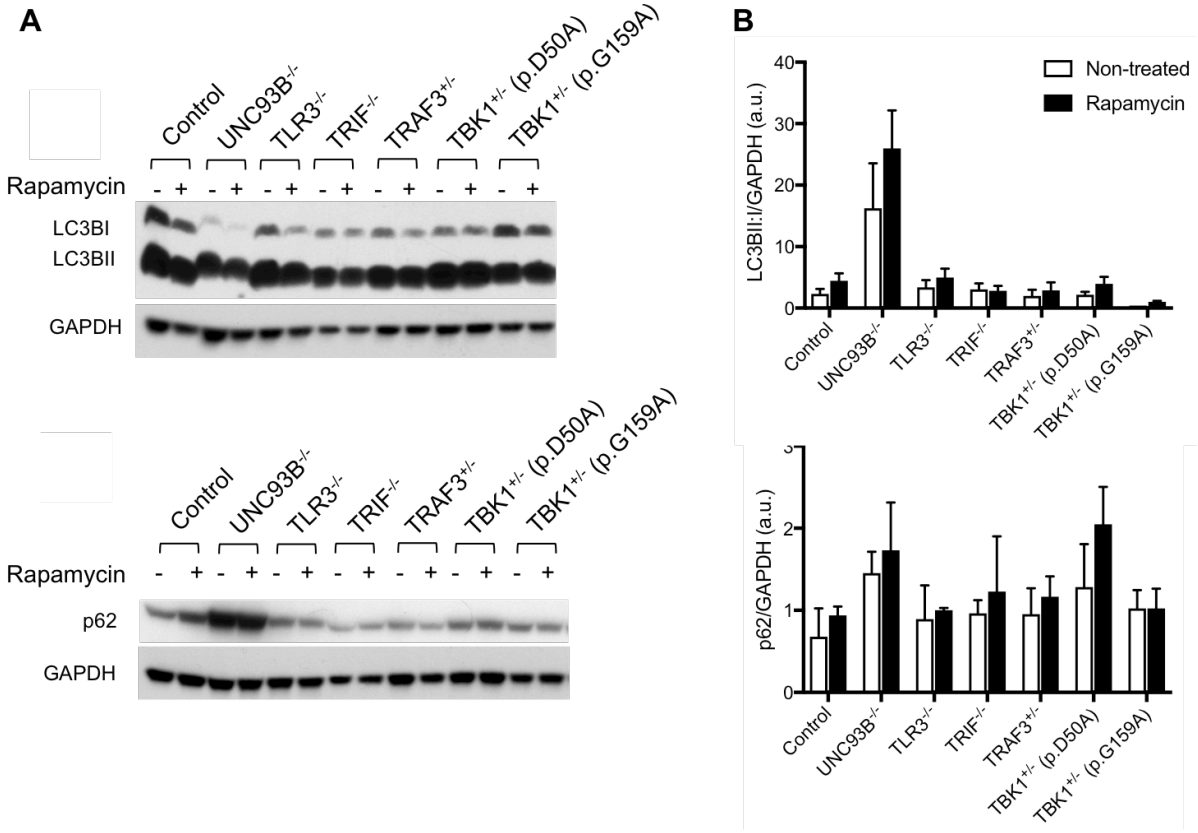
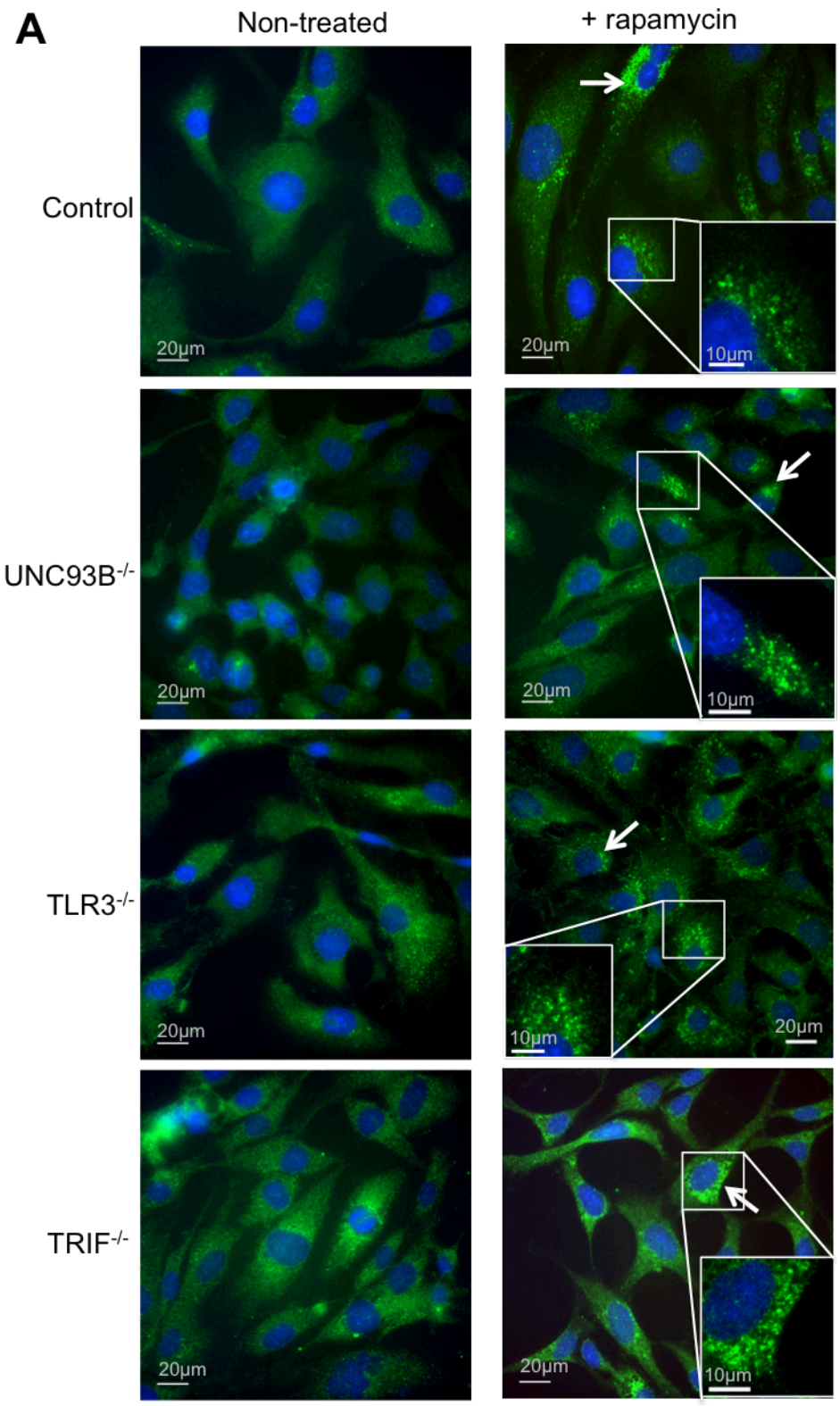
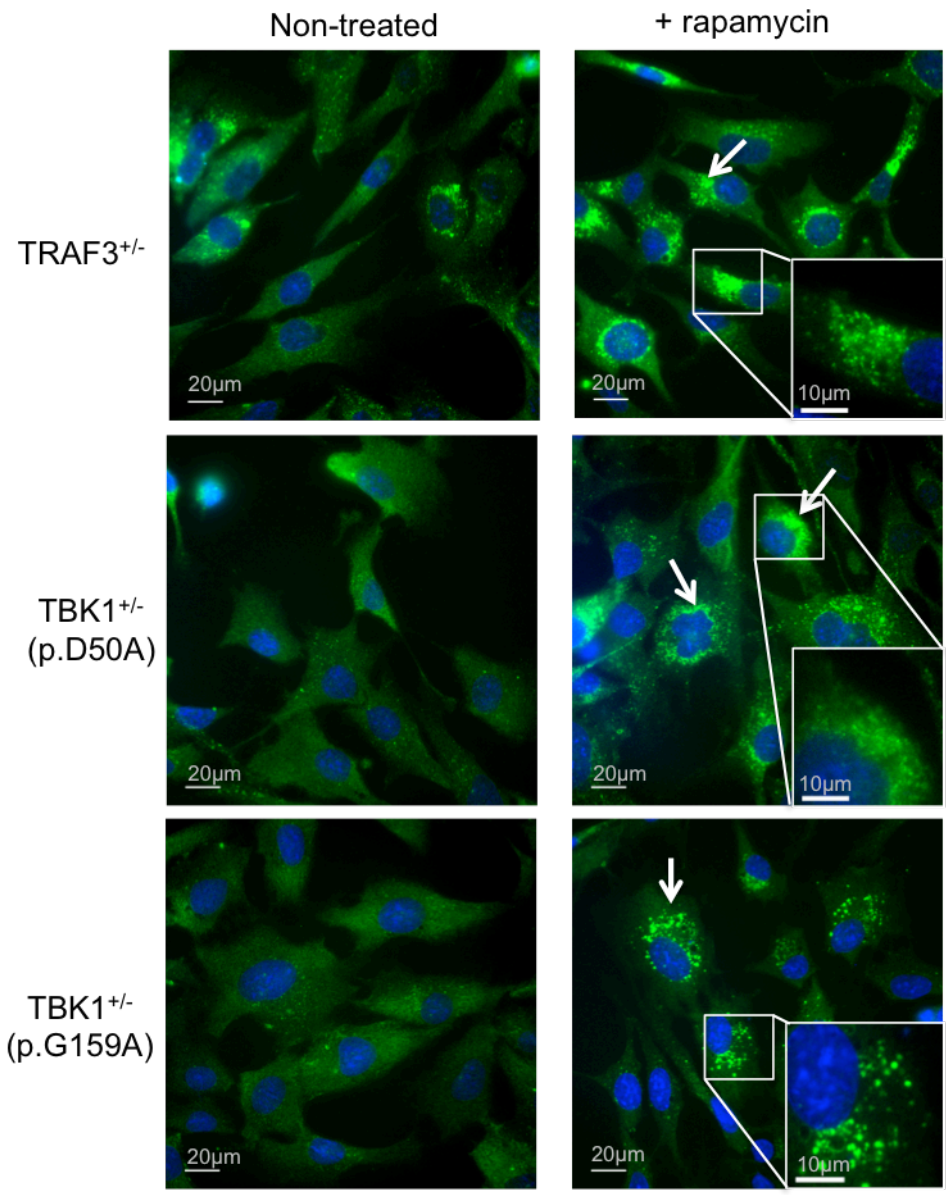


Figure 3.2. Rapamycin-induced autophagy in HSE patient-derived dermal fibroblasts. Fibroblasts were treated with 10 nM of rapamycin for 24 hours before subjected to whole-cell lysis. **(A)** Lysates were separated by electrophoresis, immunoblotted and probed for LC3B (upper panel) and p62 (lower panel) protein expression. GAPDH was used as a loading control. **(B)** Immunoblots from (A) were subjected to densitometric analyses. Immunoblots are representative of three independent experiments (*n* = 3). Data are represented as mean ± standard error of mean (SEM) and were analysed by two-way ANOVA. a.u., arbitrary unit.

I extended my observation by using immunofluorescence to visualise autophagy induction. Immunofluorescence images confirmed the phenotypes seen on immunoblots (Figure 3.3A). Control fibroblasts showed a marked increase of LC3B puncta formation by 3.6-fold following rapamycin treatment. Similarly UNC93B$^{-/-}$, TLR3$^{-/-}$, TRIF$^{-/-}$, TRAF3$^{+/-}$, TBK1$^{+/-}$ (p.G159A) and TBK1$^{+/-}$ (p.D50A) induced LC3B puncta formation by 3.1-, 2.3-, 3.2-, 2.0-, 5.5- and 2.4-fold respectively (Figure 3.3B).

In contrast to the observations made by immunoblotting, immunofluorescence revealed significant induction of autophagy in UNC93B$^{-/-}$ and TRIF$^{-/-}$ fibroblasts following rapamycin treatment. This discrepancy could be due to the technical difference between these two techniques. Whilst immunoblotting assesses a whole-population response, immunofluorescence allows the visualisation of single-cell response, which gives a more accurate assessment in this context. Collectively, these data suggest that these patient-derived fibroblasts have functional basal autophagy machinery and rules out a general autophagy deficit.


A
Non-treated
+ rapamycin
Control
UNC93B-/-
TLR3-/-
TRIF-/-
20μm
10μm


Non-treated
+ rapamycin
TRAF3+/-
TBK1+/-
(p.D50A)
TBK1+/-
(p.G159A)
20μm
10μm

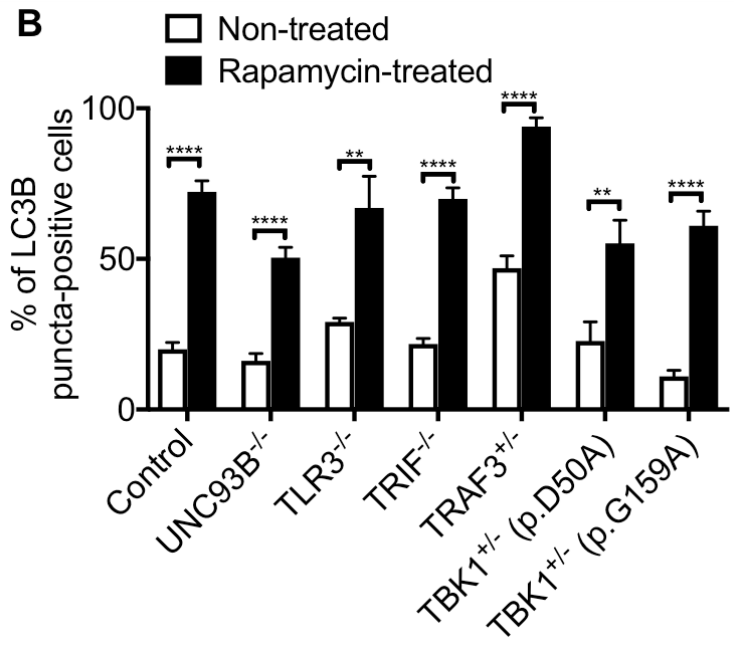


Figure 3.3. Rapamycin-induced autophagy in HSE patient-derived dermal fibroblasts. **(A)** Fibroblasts grown on coverslips were treated with 10 nM of rapamycin for 24 hours before being fixed and stained for endogenous LC3B protein (green). DAPI was used to stain nuclei. White arrows indicate LC3B puncta, scale bar, 20 μm. Inset is magnified view of area marked with a box in each image, scale bar 10 μm. **(B)** Number of cells positive for LC3B puncta were counted. Experiments were repeated independently for at least three times (*n* = 3). Data are represented as mean ± SEM and analysed by Student's t-test; ***P* <0.01 and *****P* <0.0001.

3.3. Poly(I:C)-induced autophagy

HSV1 produces dsRNA intermediates during its active replication which can be detected by TLR3, a receptor which is non-redundant in anti-HSV1 defence (Zhang *et al.*, 2007, 2013). I sought to assess whether components of the TLR3-IFN pathway may have a dual role – promoting autophagy in addition to inducing IFN production – by stimulating TLR3 receptor using the dsRNA agonist poly(I:C).

Following stimulation with poly(I:C), control fibroblasts showed an increase in LC3BII:I level after 16 hours (Figure 3.4A). Moreover, p62 levels did not decrease following poly(I:C) stimulation (Figure 3.4A). Immunofluorescence images of poly(I:C)-stimulated fibroblasts further confirmed autophagy induction as shown by significant LC3B puncta formation (Figure 3.4B).

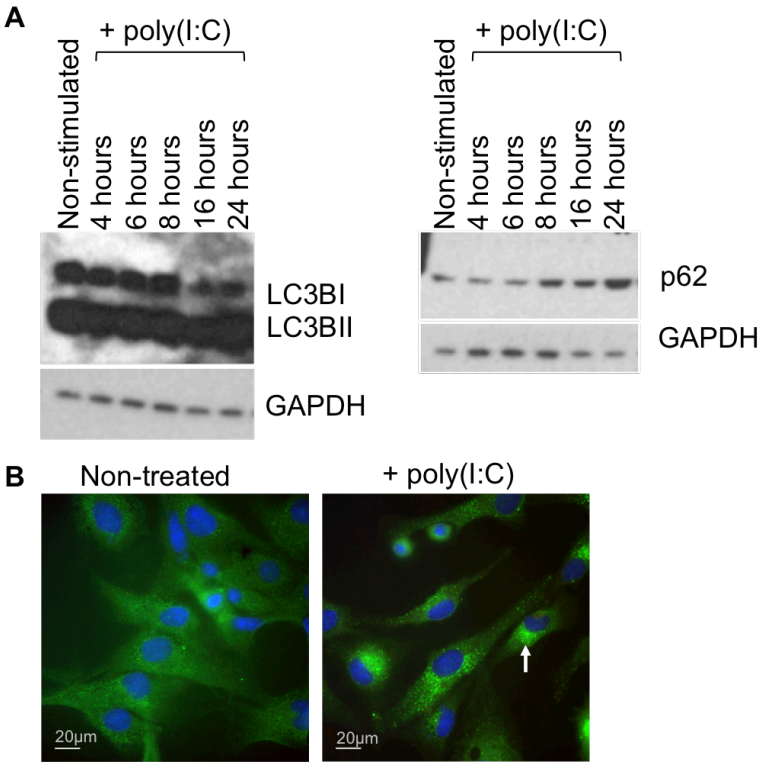


Figure 3.4. Poly(I:C)-induced autophagy in control dermal fibroblasts. (A) Control fibroblasts were stimulated with 25 μg/mL of poly(I:C) for indicated length of time before subjected to whole-cell lysis. Whole-cell lysates were electrophoresed and probed for LC3B and p62 protein expression. GAPDH was used as loading control, (*n* = 1) **(B)** Control fibroblasts grown on coverslips were stimulated with 25 μg/mL of poly(I:C) for 24 hours before being fixed and stained for endogenous LC3B protein (green). DAPI was used to stain nuclei. White arrow indicates LC3B puncta. *n* = 3; scale bar, 20 μm.

Subsequently, I performed 24 hour stimulation with 25 μg/mL of poly(I:C) on HSE patients' fibroblasts. Immunoblots revealed an impairment in LC3BII:I induction following poly(I:C) stimulation in UNC93B$^{-/-}$, TLR3$^{-/-}$ and TRIF$^{-/-}$ fibroblasts (Figure 3.5A). Consistently, immunofluorescence images revealed lack of cytoplasmic LC3B puncta formation in UNC93B$^{-/-}$, TLR3$^{-/-}$ and TRIF$^{-/-}$ fibroblasts following poly(I:C) stimulation, confirming my observation on immunoblots (Figure 3.6A & 3.6B). TRAF3$^{+/-}$, TBK1$^{+/-}$ (p.G159A) and TBK1$^{+/-}$ (p.D50A) were able to induce LC3BII:I levels in response to poly(I:C) similar to control fibroblasts as demonstrated by immunoblots, and showed elevated presence of LC3B puncta by 1.9-, 3.9- and 4.2-fold respectively (Figure 3.5A, 3.6A & 3.6B).

Across all fibroblasts, p62 was not reduced following poly(I:C) treatment, but was rather upregulated (except for TLR3 and TBK1$^{+/-}$ (p.D50A)) (Figure 3.5B). Little is known about the relevance of p62 in poly(I:C)-induced autophagy. A recent study has shown similar observation where poly(I:C) treatment on mice cardiomyocytes triggered the upregulation of both LC3B and p62 levels (Gao *et al.*, 2018). However, this study did not further dissect the underlying signalling that p62 participates in in poly(I:C)-induced autophagy.

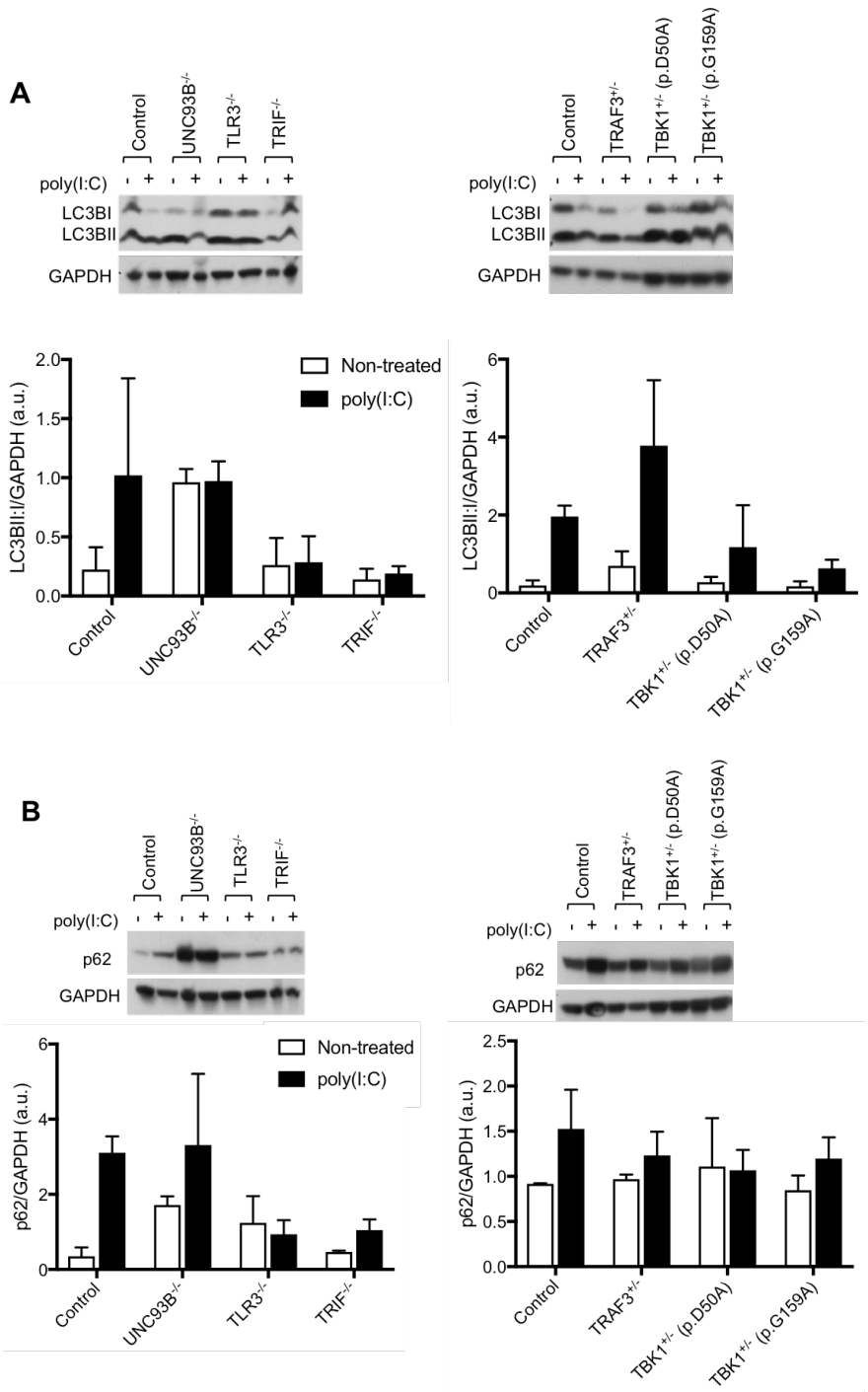
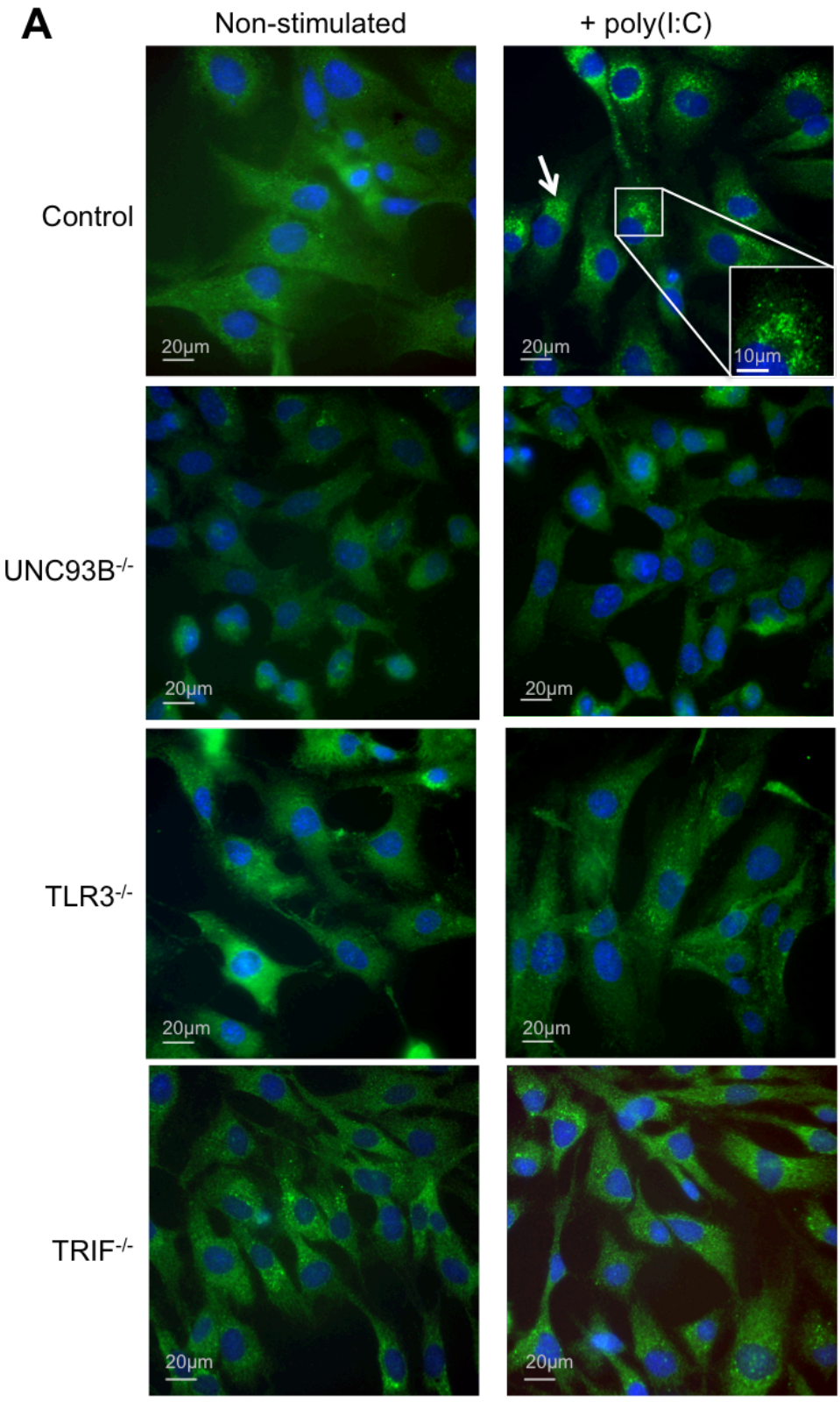
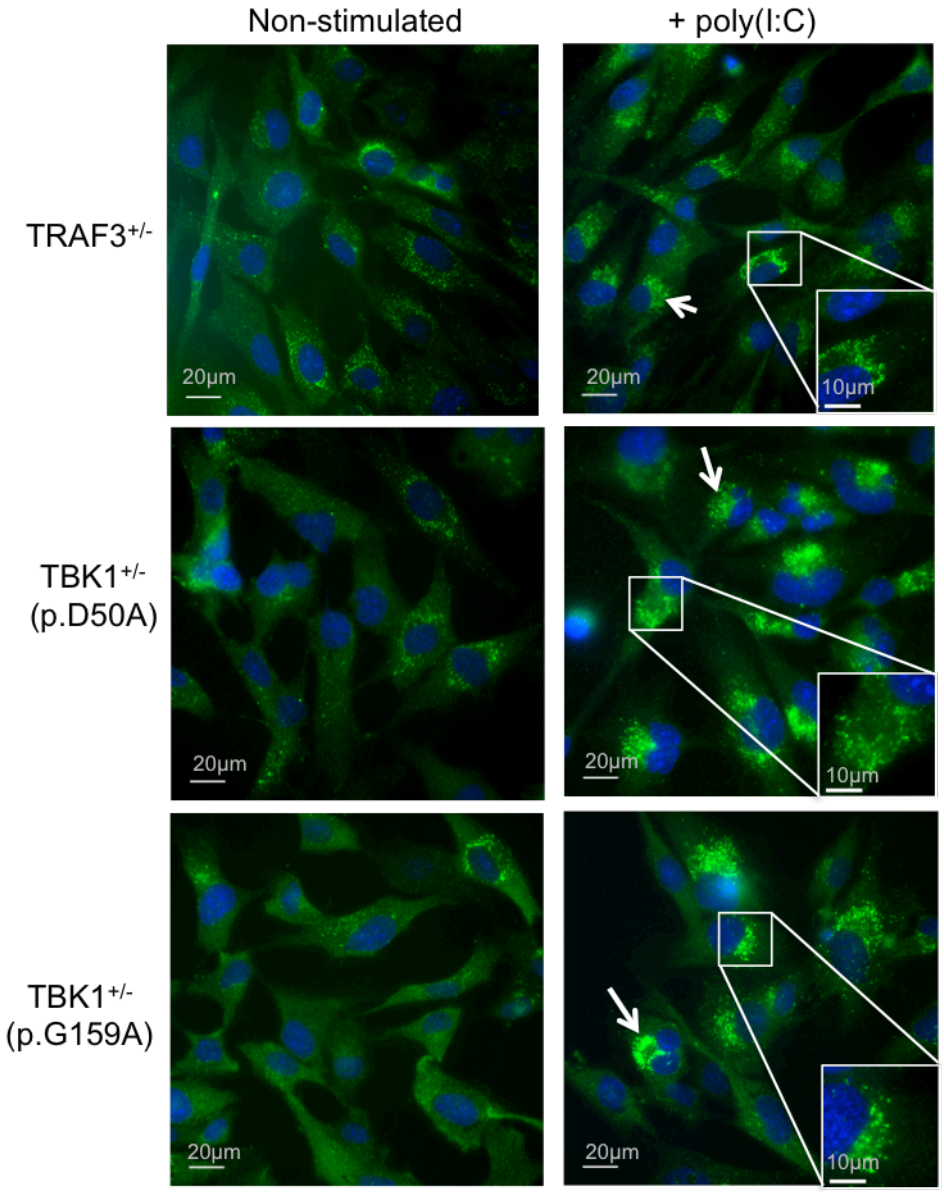


Figure 3.5. poly(I:C)-induced autophagy in HSE patient-derived dermal fibroblasts. Fibroblasts were treated with 25 µg/mL of poly(I:C) for 24 hours before being lysed and probed for endogenous **(A)** LC3B and **(B)** p62 proteins. GAPDH was used as a loading control. Immunoblots are representative of two independent experiments (*n* = 2) Data are represented as mean ± SEM and were analysed by two-way ANOVA. a.u., arbitrary units.


A
Non-stimulated
+ poly(I:C)
Control
UNC93B-/-
TLR3-/-
TRIF-/-
20μm
10μm


Non-stimulated
+ poly(I:C)
TRAF3+/-
TBK1+/- (p.D50A)
TBK1+/- (p.G159A)
20μm
10μm

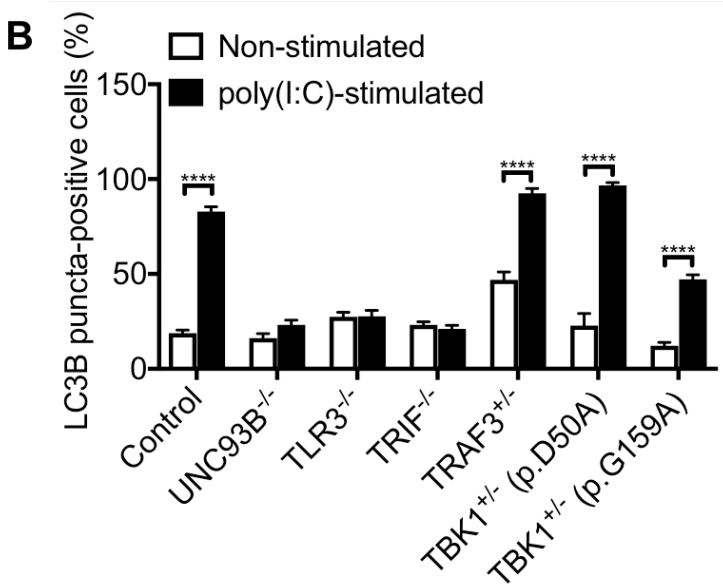

B
Non-stimulated
poly(I:C)-stimulated
LC3B puncta-positive cells (%)
150
100
50
0
****
Control
UNC93B-/-
TLR3-/-
TRIF-/-
TRAF3+/-
TBK1+/- (p.D50A)
TBK1+/- (p.G159A)

Figure 3.6. Poly(I:C)-induced autophagy in HSE patient-derived dermal fibroblasts. (A) Fibroblasts grown on coverslips were treated with 25 μg/mL of poly(I:C) for 24 hours before being fixed and stained for endogenous LC3B protein (green). DAPI was used to stain nuclei. White arrows indicate LC3B puncta. Insets are expanded view of areas marked with white box within each image. Scale bar, 20 μm, scale bar of inset, 10 μm. **(B)** Number of cells showing positive for LC3B puncta was counted. Images are representative of three independent experiments (*n* = 3). Data are represented as mean ± SEM and were analysed by Student's t-test; ****P <0.0001.

3.4. IFN-induced autophagy

As previously mentioned, UNC93B$^{-/-}$, TLR3$^{-/-}$, TRIF$^{-/-}$, TRAF3$^{+/-}$, TBK1$^{+/-}$ (p.G159A) and TBK1$^{+/-}$ (p.D50A) fibroblasts have impairment in IFN production following TLR3 stimulation with poly(I:C). However, supplementing the cells with exogenous IFNα-2a rescued the cells during HSV1 infection. This suggests that whilst IFN production itself is impaired, IFN signalling pathway through STAT1 is still functional as they are able to mount downstream interferon-stimulated genes (ISGs) production that provides global anti-viral protection (Casrouge *et al.*, 2006; Zhang *et al.*, 2007; Pérez de Diego *et al.*, 2010; Guo *et al.*, 2011; Sancho-Shimizu *et al.*, 2011b; Lim *et al.*, 2014; Herman *et al.*, 2012).

In contrast to autophagy, which is a continuous process, IFN production is rather delayed following HSV1 infection. IFN therefore most likely does not have a role in inducing autophagy during early HSV1 infection but may support amplification of autophagy response in a positive feedback loop later on. I sought to assess whether

IFN could indeed trigger autophagy and whether or not components of the TLR3-IFN pathway are involved in this autophagy.

Firstly, control fibroblasts were treated with 10^5 IU/mL of IFNα-2a for various time periods. Immunoblots revealed an increase of LC3BII:I level as early as 8 hours post treatment (Figure 3.7A & 3.7B). The level of p62 protein did not show any significant decrease despite the increase of LC3BII:I level, suggesting a non-selective mode of autophagy (Figure 3.7A & 3.7B). Furthermore, 24 hours treatment of control fibroblasts with IFNα-2a revealed enhanced formation of LC3B puncta in cytoplasm (Figure 3.7C).

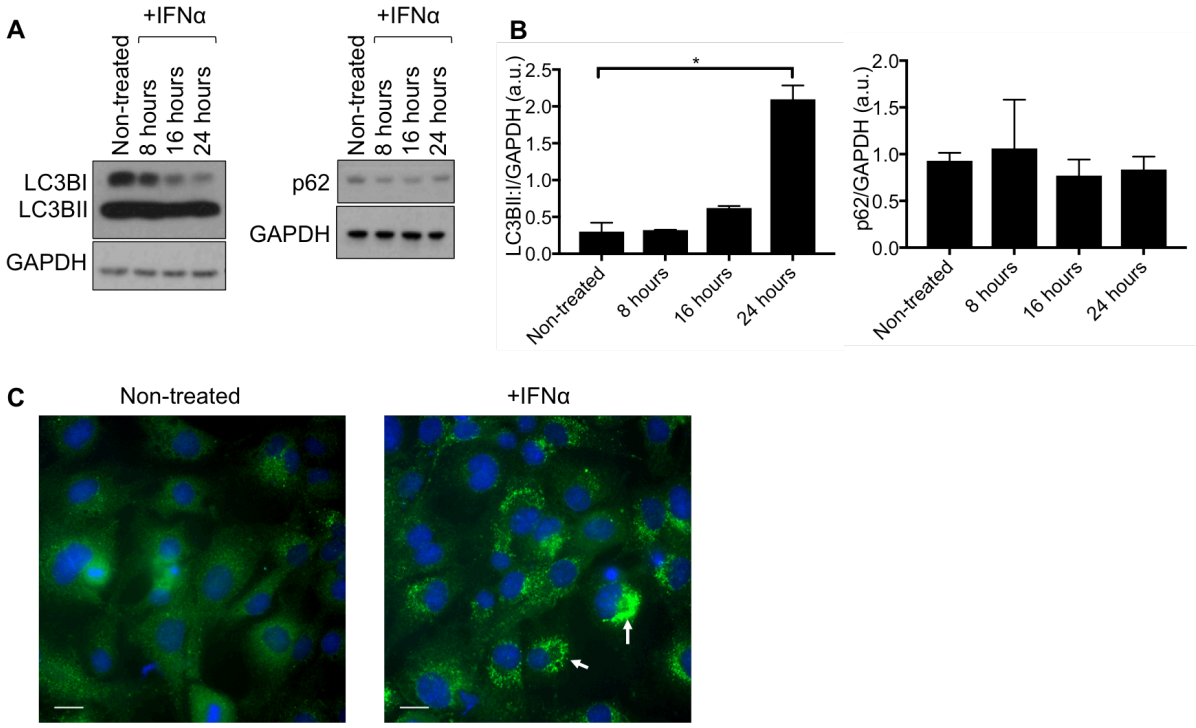
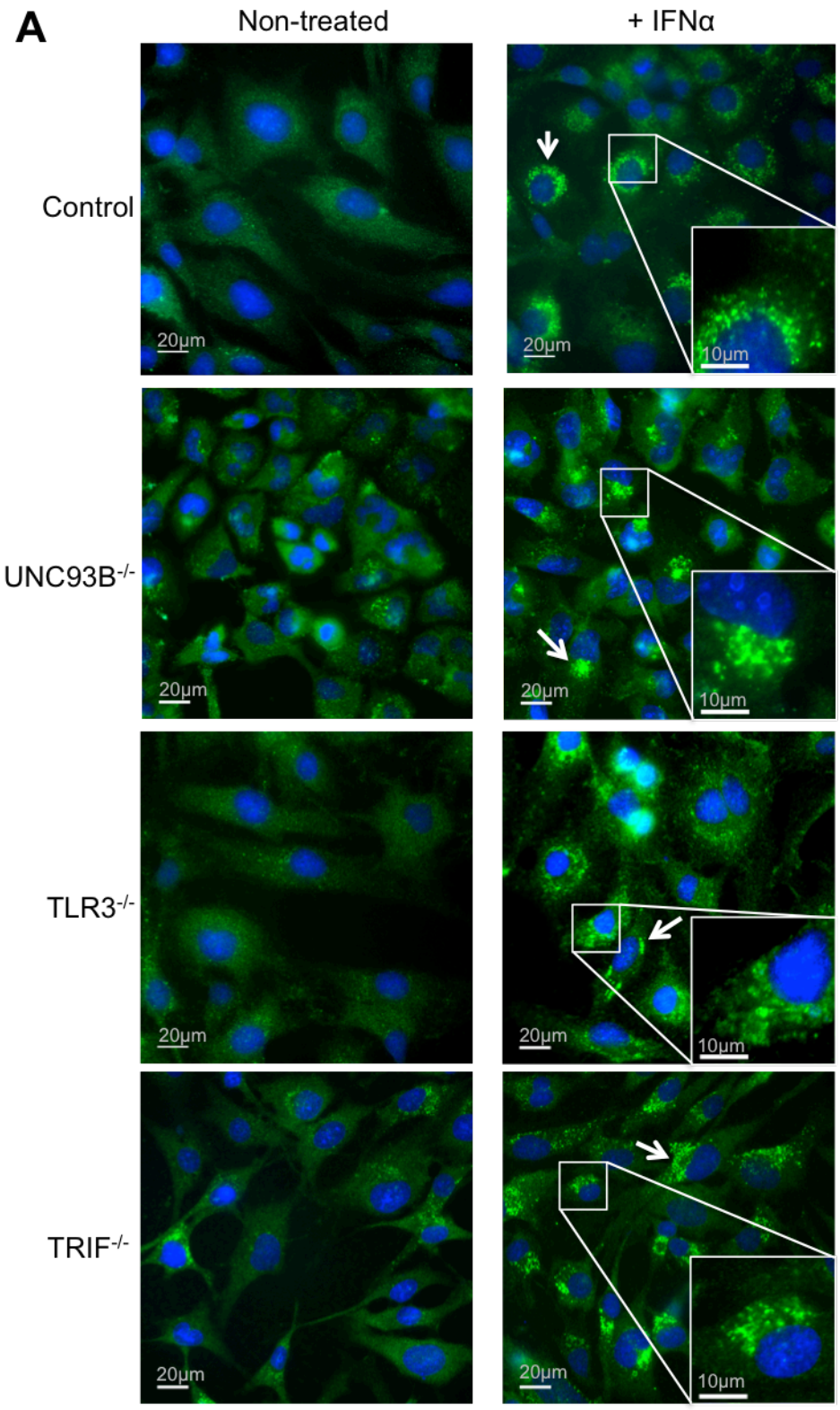
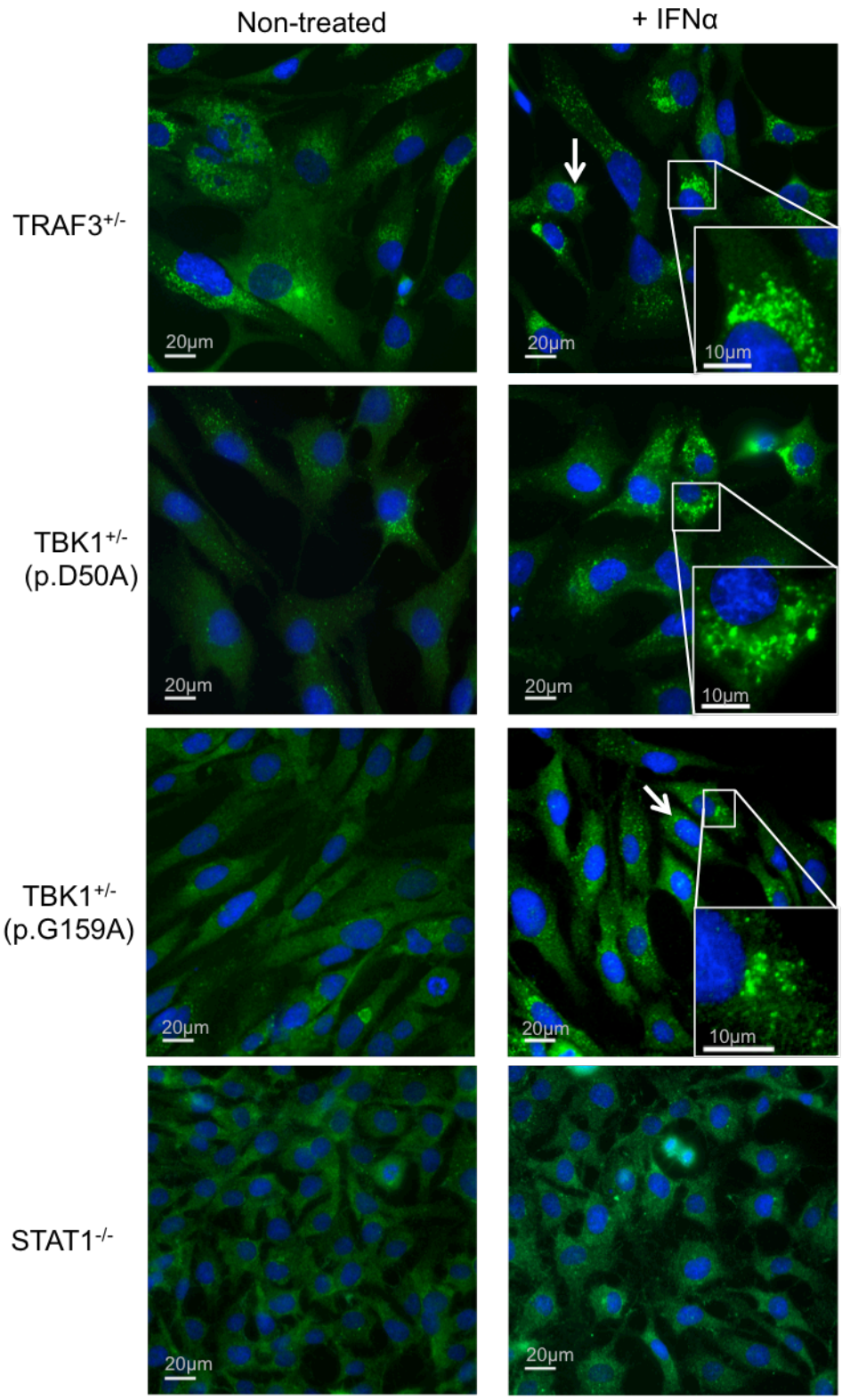


Figure 3.7. IFNα-2a induced autophagy in control dermal fibroblasts. (A) Control fibroblasts were treated with 10^5 IU/mL of IFNα-2a for indicated lengths of time before collecting whole-cell lysates, which were then electrophoresed and probed for LC3B and p62 proteins. GAPDH was used a loading control. Immunoblots are from a single experiment (*n* = 2) **(B)** Immunoblots from (A) were subjected to densitometric analysis; a.u., arbitrary units.

Data are represented as mean ± standard deviation (SD) and were analysed by Student's t-test where *P<0.05. **(C)** Control fibroblasts were seeded on coverslips, treated with 10^5 IU/mL of IFNα-2a for 24 hours before being fixed and stained for LC3B protein (green). DAPI (blue) was used as a nuclear stain. White arrows indicate LC3B induction in treated cells. Images are representative of three independent experiments (n = 3), scale bar, 20 μm.

Next, patient-derived fibroblasts were given similar treatment of IFNα-2a for 24 hours. Immunofluorescence images revealed positive induction of LC3B puncta across all patient fibroblasts following treatment (Figure 3.8A). Control, UNC93B$^{-/-}$, TLR3$^{-/-}$, TRIF$^{-/-}$, TRAF3$^{+/-}$, TBK1$^{+/-}$ (p.G159A) and TBK1$^{+/-}$ (p.D50A) were able to increase LC3B puncta formation by 4.6-, 3.7-, 2.1-, 2.7-, 2.6-, 2.5- and 1.5-fold respectively (Figure 3.8B). Meanwhile, STAT1$^{-/-}$ fibrosarcoma cells, used as a negative control cells that do not have functional response to IFN due to lack of STAT1 signalling pathway (Dupuis *et al.*, 2003), showed no induction of LC3B puncta (Figure 3.8A & 3.8B). One can postulate that IFN produced during HSV1 infection could induce autophagy in dermal fibroblasts and that this IFN-induced autophagy requires functional STAT1 signalling pathway.


A
Non-treated
+ IFNα
Control
UNC93B-/-
TLR3-/-
TRIF-/-
20μm
10μm


Non-treated
+ IFNα
TRAF3+/-
TBK1+/-
(p.D50A)
TBK1+/-
(p.G159A)
STAT1-/-
20μm
10μm

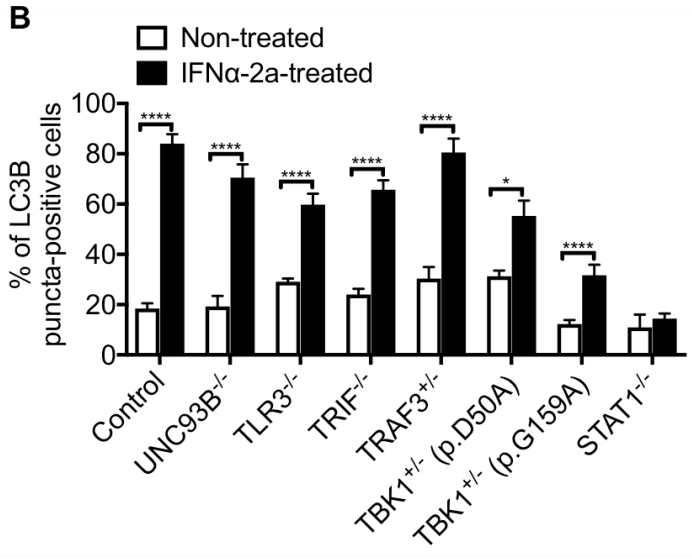


Figure 3.8. IFNα-2a-induced autophagy of patient-derived fibroblasts. (A) Fibroblasts were seeded on coverslips, treated with 10^5 IU/mL of IFNα-2a for 24 hours before being fixed and stained for LC3B protein (green). DAPI (blue) was used as a nuclear stain. White arrows indicate LC3B induction in treated cells. Scale bar, 20 μm. Inset is magnified view of area marked in box within each image, scale bar 10 μm. **(B)** Number of cells positive for LC3B puncta was counted. Images are representative of two independent experiments (*n* = 2). Data are represented as mean ± SEM and were analysed by Student's t-test; ****P <0.0001; *P <0.05.

3.5. C-di-GMP-induced autophagy

In addition to the TLR3-IFN pathway, TBK1 is a kinase responsible for inducing IFN production downstream of STING (also known as MITA or TMEM173), a scaffold protein through which dsDNA sensors signal through and can be stimulated with c-di-GMP ligand (Tanaka & Chen, 2012; Zhong *et al.*, 2008). Moreover, the STING-TBK1 pathway is also involved in activating autophagy during *Mycobacterium tuberculosis* infection (Watson, Manzanillo & Cox, 2012; Watson *et al.*, 2015). HSV1 infection has also been shown to activate autophagy in a STING-dependent manner,

but the involvement of TBK1 in this has yet to be unravelled (Rasmussen *et al.*, 2011). In addition to this, a study has shown that TRIF may also take part in this pathway (Wang *et al.*, 2016). Given the heavy implication of STING in both IFN production and anti-microbial autophagy, I sought to assess contribution of STING-TBK1 pathway to autophagy by stimulating STING with its ligand c-di-GMP.

In control fibroblasts, mock Lipofectamine stimulation did not show significant increase in cytoplasmic LC3B puncta compared with non-stimulated (Figure 3.9A). However, when control cells were stimulated with 8 µg/mL of c-di-GMP for 2 hours, I observed marked increase of cytoplasmic LC3B puncta by 2-fold compared with c-di-GMP control stimulated cells. Similarly, $TRIF^{-/-}$ fibroblasts were able to induce significant accumulation of cytoplasmic LC3B puncta by 1.7-fold (Figure 3.9A & 3.9B). In contrast, $TBK1^{+/-}$ (p.G159A) fibroblasts did not induce significant cytoplasmic LC3B puncta suggesting that STING-induced autophagy is a TBK1-dependent but TRIF-independent process (Figure 3.9A & 3.9B).

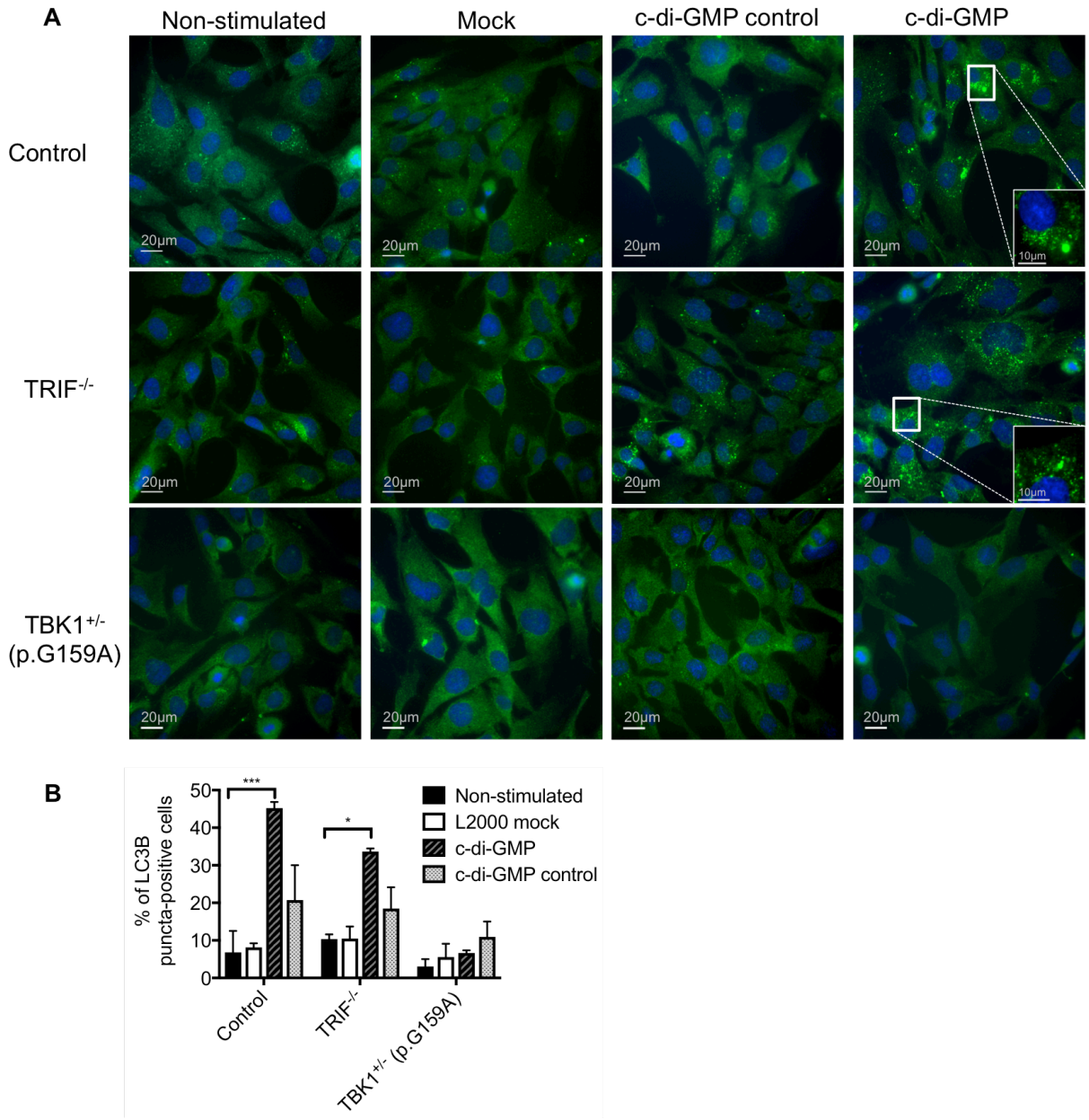


Figure 3.9. c-di-GMP-induced autophagy is TBK1-dependent. (A) Fibroblasts were seeded on coverslips, transfected using Lipofectamine 2000 (L2000) with 8 μg/mL of c-di-GMP or c-di-GMP control, or L2000 alone (mock) for 2 hours before being fixed and stained for LC3B protein (green). DAPI (blue) was used as a nuclear stain. White arrows indicate LC3B induction in treated cells. Scale bar, 20 μm. Insets are magnified view of area marked with white box within each image and have scale bar of 10 μm **(B)** Number of cells positive for LC3B puncta was counted. Images are representative of three independent experiments (n = 3). Data are represented as mean ± SEM and were analysed by two-way ANOVA; ***P <0.001; *P <0.05.

3.6. HSV1-induced autophagy in HSE patients' fibroblasts

HSV1 has been shown to activate autophagy in fibroblasts and neurons *in vitro* (Tallóczy, Virgin & Levine, 2006; Tallóczy *et al.*, 2002; McFarlane *et al.*, 2011; Katzenell & Leib, 2016; Alexander *et al.*, 2007; Radtke *et al.*, 2013; English *et al.*, 2009). In mouse embryonic fibroblasts (MEFs), late HSV1 infection triggers formation of perinuclear autophagosomes consisting of coiling of the inner and outer membrane of the nucleus – a phenomenon termed as nuclear enveloped-derived autophagy (NEDA) (English *et al.*, 2009; Radtke *et al.*, 2013). Human foetal foreskin fibroblast-2 (HFFF2) cells induced LC3BII:I following infection with HSV1 (McFarlane *et al.*, 2011). To my knowledge, autophagy response towards HSV1 infection in human dermal fibroblasts has not been described before. Herein, I characterised autophagy phenotypes of human dermal fibroblasts infected with HSV1 by looking at endogenous LC3B and p62 proteins as markers of autophagy.

3.6.1. HSV1 infection induces LC3B and reduces p62 protein levels in control dermal fibroblasts

To assess autophagy response to HSV1 infection, control fibroblasts were infected with HSV1 at various doses (multiplicity of infections (MOIs)) and for various periods of infection. Positive for autophagy activation in response to HSV1 infection, the level of LC3BII:I was increased in a time-dependent and dose-dependent manner following infection (Figure 3.10A & 3.10B). Simultaneously, levels of p62 protein were also decreasing suggesting a role for autophagy adaptor in HSV1-induced autophagy in human dermal fibroblasts and effectively classifying this type

of autophagy as selective (Figure 3.10A & 3.10B). This is in agreement with a study that found similar trend in human HEK293T cells infected with HSV1 whereby HSV1 infection prompted the induction of LC3B and reduction of p62 proteins (Sparrer *et al.*, 2017). 48-hour infection with HSV1 led to an almost complete absence of LC3BI as seen in the representative blot Figure 3.10A. Although this makes the interpretation of LC3BII:I level difficult, it indicates a complete conversion of LC3BI to II, which is characteristic of autophagy induction.

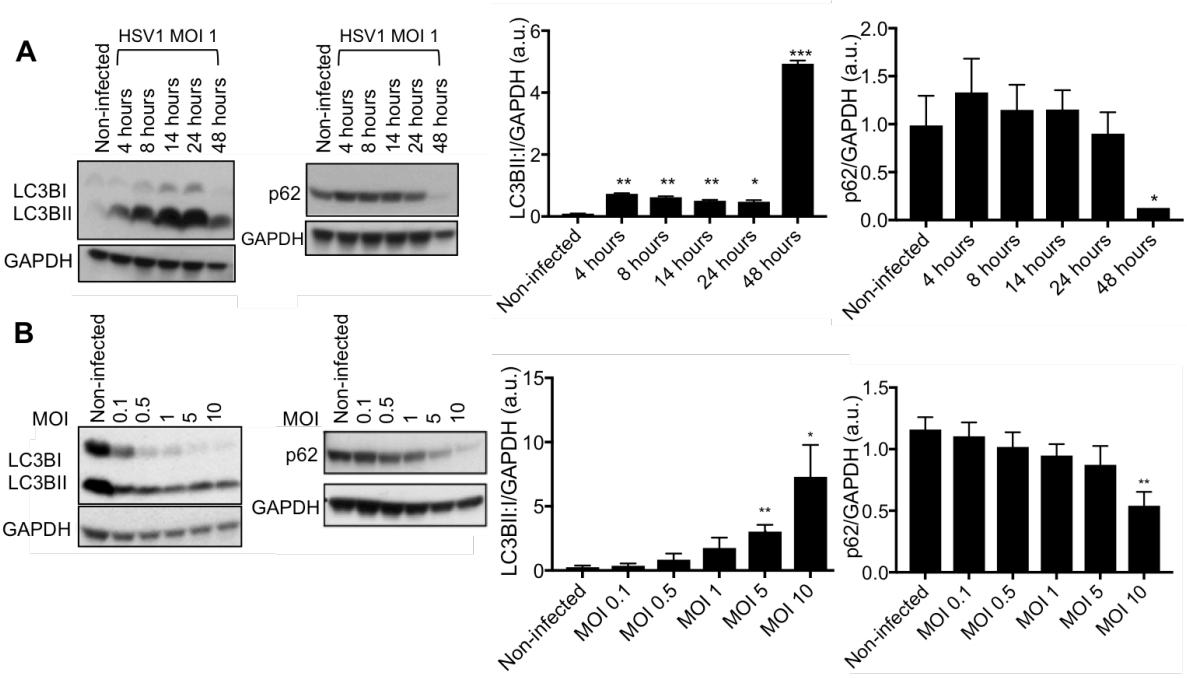


Figure 3.10. HSV1 infection triggers autophagy response in human dermal fibroblasts. Control fibroblasts were infected with **(A)** HSV1 at MOI 1 for various lengths of time, or **(B)** various MOIs of HSV1 for 48 hours, before cell lysates were harvested. Whole-cell lysates were subjected to electrophoresis and probed for LC3B and p62 proteins. GAPDH was used a loading control. Immunoblots were analysed by densitometry (right panel). Experiments were repeated three times (n = 3), and representative blots are shown. Data were analysed by Student's t-test by comparing non-infected to infected, and are represented as mean ± SEM, *P <0.05, **P< 0.01, ***P< 0.001. a.u., arbitrary units.

3.6.2. WT HSV1 triggers cytoplasmic and perinuclear LC3B phenotypes

To visualise autophagy response towards a progressing infection, I performed a low dose infection with MOI 0.001 for 24 hours in the presence of 1% human serum containing neutralising HSV1 antibodies to allow the establishment of viral plaques (clusters of infected cells resulting from a single infected cell from which the virus spreads by cell-to-cell contact) surrounded by non-infected cells. I used infected cell protein 4 (ICP4), an immediate early HSV1 protein, to identify infection and observed autophagy response by studying endogenous LC3B protein. After 24 hours, I found infected control fibroblasts that were ICP4-positive to form dense LC3B localised in the perinuclear area (Figure 3.11, indicated by yellow arrow).

Interestingly, neighbouring non-infected ICP4-negative cells showed formation of cytoplasmic LC3B puncta suggestive of autophagy upregulation in response to the presence of neighbouring infection (Figure 3.11, indicated by white arrow).

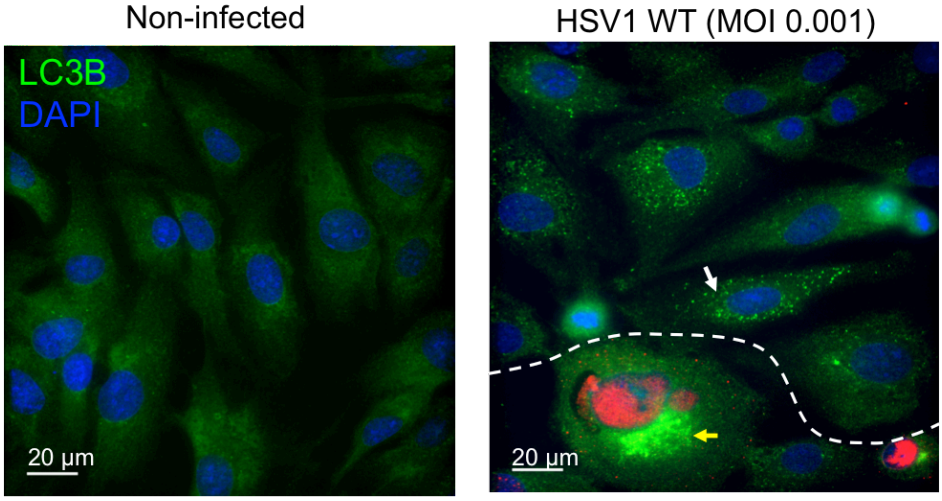


Figure 3.11. HSV1 infection triggers cytoplasmic and perinuclear LC3B phenotypes in control fibroblasts. Control fibroblasts were infected with MOI 0.001 of HSV1 WT for 24 hours in the presence of 1% human serum. Cells were subsequently fixed and stained for

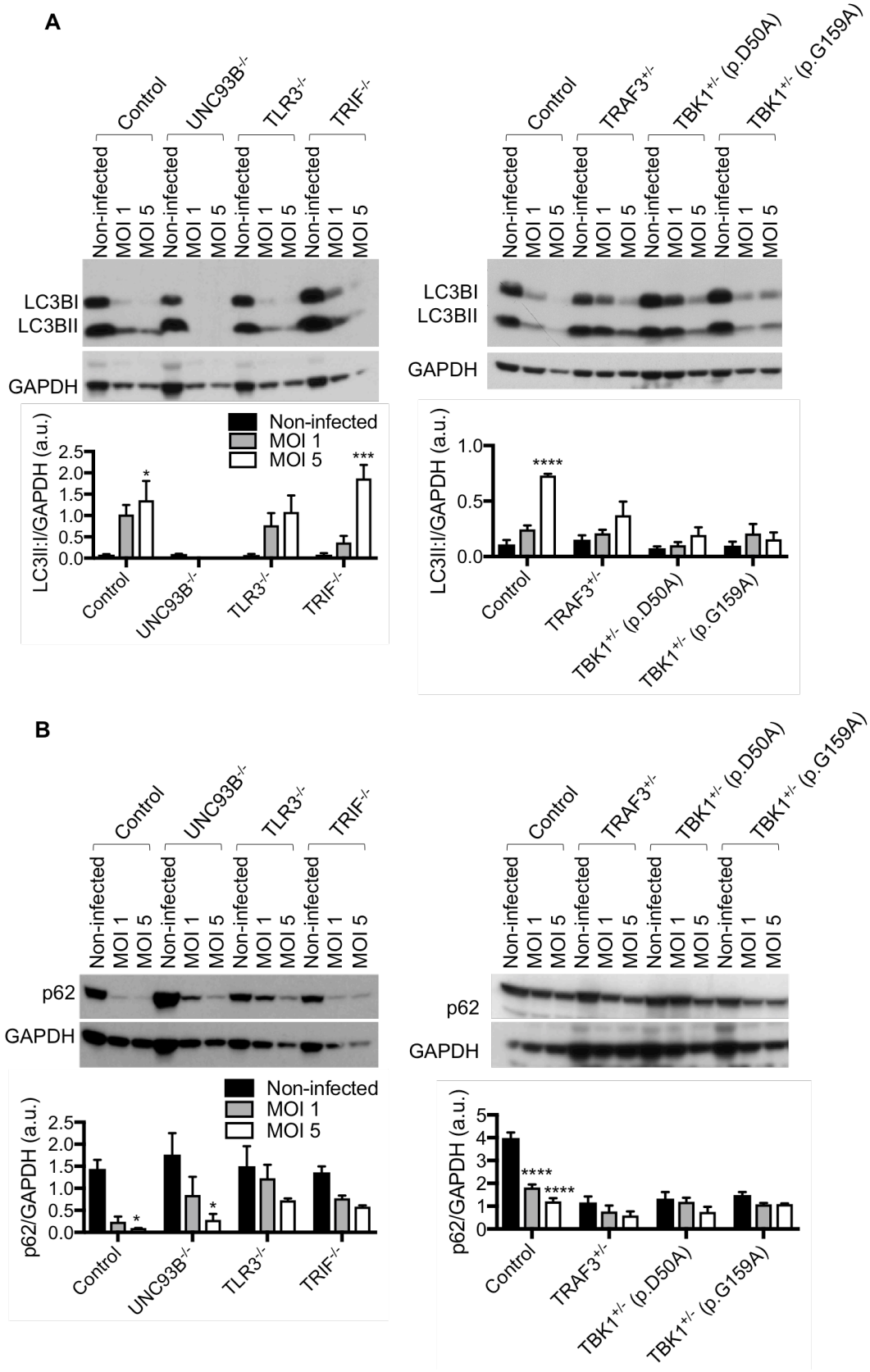
endogenous LC3B (green), HSV1 ICP4 (red) and DAPI (blue nuclear stain). White arrow indicates cytoplasmic LC3B and yellow arrow indicates perinuclear LC3B formation. Dashed line marks boundary of viral plaque. Images are representative of three independent experiments (*n* = 3); scale bar, 20 μm.

3.6.3. Impairment of HSV1-induced autophagy in TBK1$^{+/-}$ (p.G159A) fibroblasts

3.6.3.1. TBK1$^{+/-}$ (p.G159A) failed to induce LC3BII:I and reduce p62 proteins following HSV1 infection.

Autophagic responses in HSE patients' fibroblasts infected with WT HSV1 at MOI 1 and 5 were then assessed. Control fibroblasts showed increase of LC3BII:I and reduction in p62 protein levels following infection. Similarly, TLR3$^{-/-}$, TRIF$^{-/-}$, TRAF3$^{+/-}$, TBK1$^{+/-}$ (p.D50A) fibroblasts were able to induce LC3BII:I and reduce p62 protein levels. Immunoblots of HSV1-infected UNC93B$^{-/-}$ fibroblasts revealed lack of LC3B induction. However, UNC93B$^{-/-}$ fibroblasts showed reduction of p62, suggesting an induction of autophagy in response to the infection. Following HSV1 infection, TBK1$^{+/-}$ (p.G159A) cells were not able to induce LC3BII:I and reduce p62 protein levels, suggesting a complete impairment in HSV1-induced autophagy (Figure 3.12A & 3.12B). In addition to p62, I also tested the cells for their ability to deplete NDP52, another autophagy adaptor that participates in selective autophagy and has been previously shown to be TBK1-dependent in bacterial xenophagy (Thurston *et al.*, 2009; Wild *et al.*, 2011). While control and TRIF$^{-/-}$ fibroblasts were able to clear

NDP52 protein following HSV1 infection, TBK1$^{+/-}$ (p.G159A) fibroblasts failed to do so (Figure 3.12C).



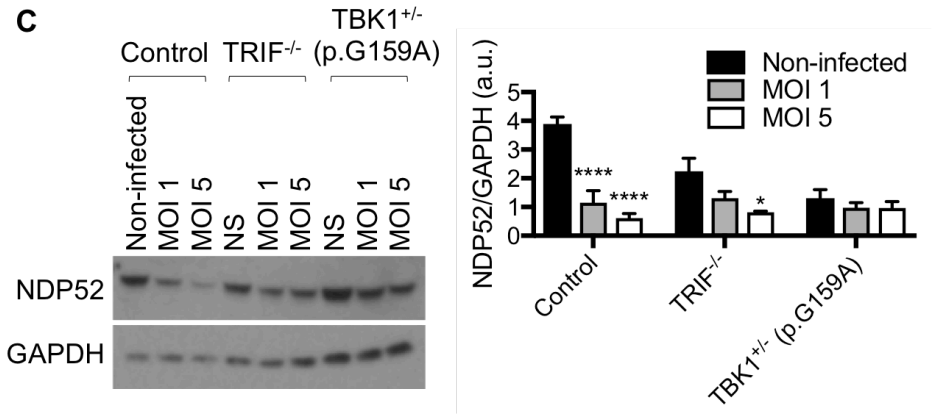
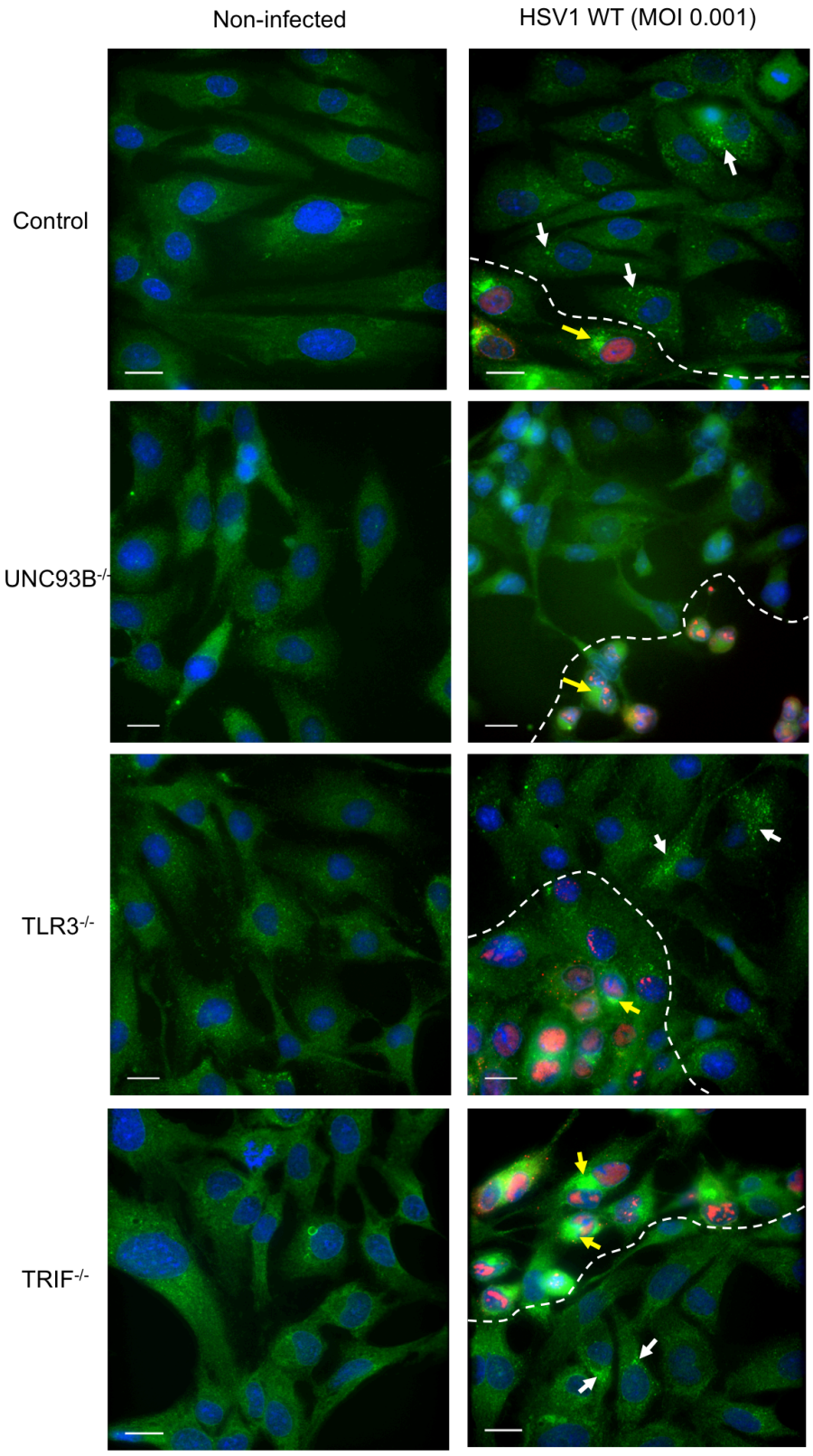


Figure 3.12. UNC93B$^{-/-}$ and TBK1$^{+/-}$ (p.G159A) fibroblasts showed aberrant HSV1-induced autophagy. Fibroblasts were infected with HSV1 at MOI 1 and 5 for 48 hours before subjected to whole-cell lysis. Lysates were electrophoresed and probed for **(A)** LC3B **(B)** p62 and **(C)** NDP52 proteins. GAPDH was used as a loading control. Immunoblots are representative of three independent experiments (*n* = 3) and were analysed by densitometry. Data are represented as mean ± SEM and were analysed by two-way ANOVA to compare between non-infected and infected within each cell line. **P* <0.05, ****P* <0.001 and *****P* <0.0001. a.u., arbitrary units.

3.6.3.2. UNC93B$^{-/-}$ and TBK1$^{+/-}$ (p.G159A) fibroblasts showed impairment in cytoplasmic LC3B formation following HSV1 infection

To further investigate the autophagy responses of these fibroblasts, infection with low dose (MOI 0.001) WT HSV1 infection was visualised. As per validation, control fibroblasts revealed two distinct autophagic LC3B phenotypes 24 hours following infection – cytoplasmic LC3B puncta (indicated by white arrows) in ICP4-negative cells neighbouring a viral plaque, and perinuclear LC3B (indicated by yellow arrows) in ICP4-positive infected cells in the viral plaque (Figure 3.13). TLR3$^{-/-}$, TRIF$^{-/-}$, TRAF3$^{+/-}$ and TBK1$^{+/-}$ (p.D50A) fibroblasts were able to mount both cytoplasmic and perinuclear LC3B phenotypes in ICP4-negative and ICP4-positive cells respectively.

UNC93B$^{-/-}$ and TBK1$^{+/-}$ (p.G159A) fibroblasts however, failed to form cytoplasmic LC3B puncta in ICP4-negative cells neighbouring viral plaques. Despite so, they were able to form perinuclear LC3B phenotype in ICP4-positive cells (Figure 3.13).


Non-infected
HSV1 WT (MOI 0.001)
Control
UNC93B-/-
TLR3-/-
TRIF-/-

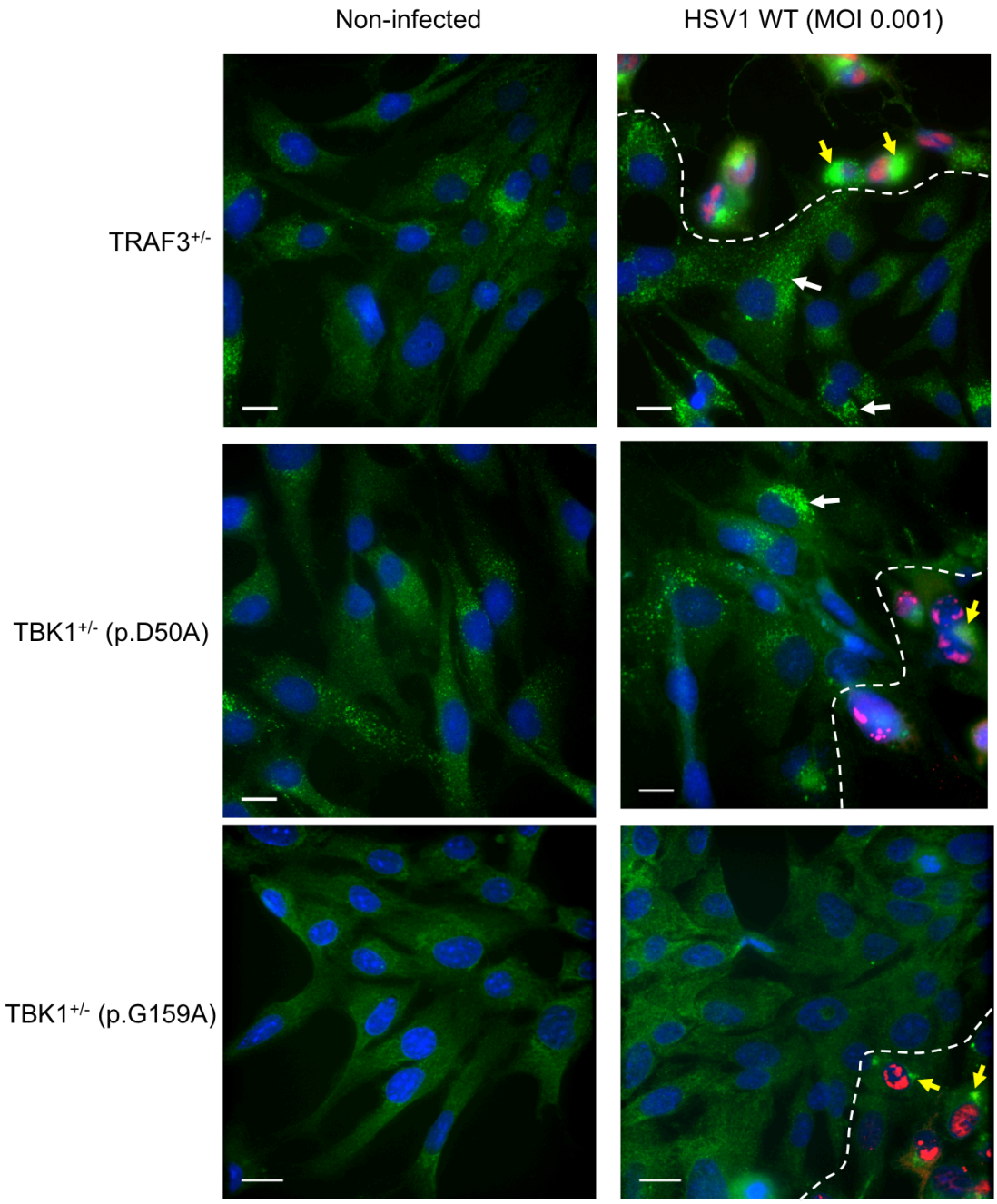
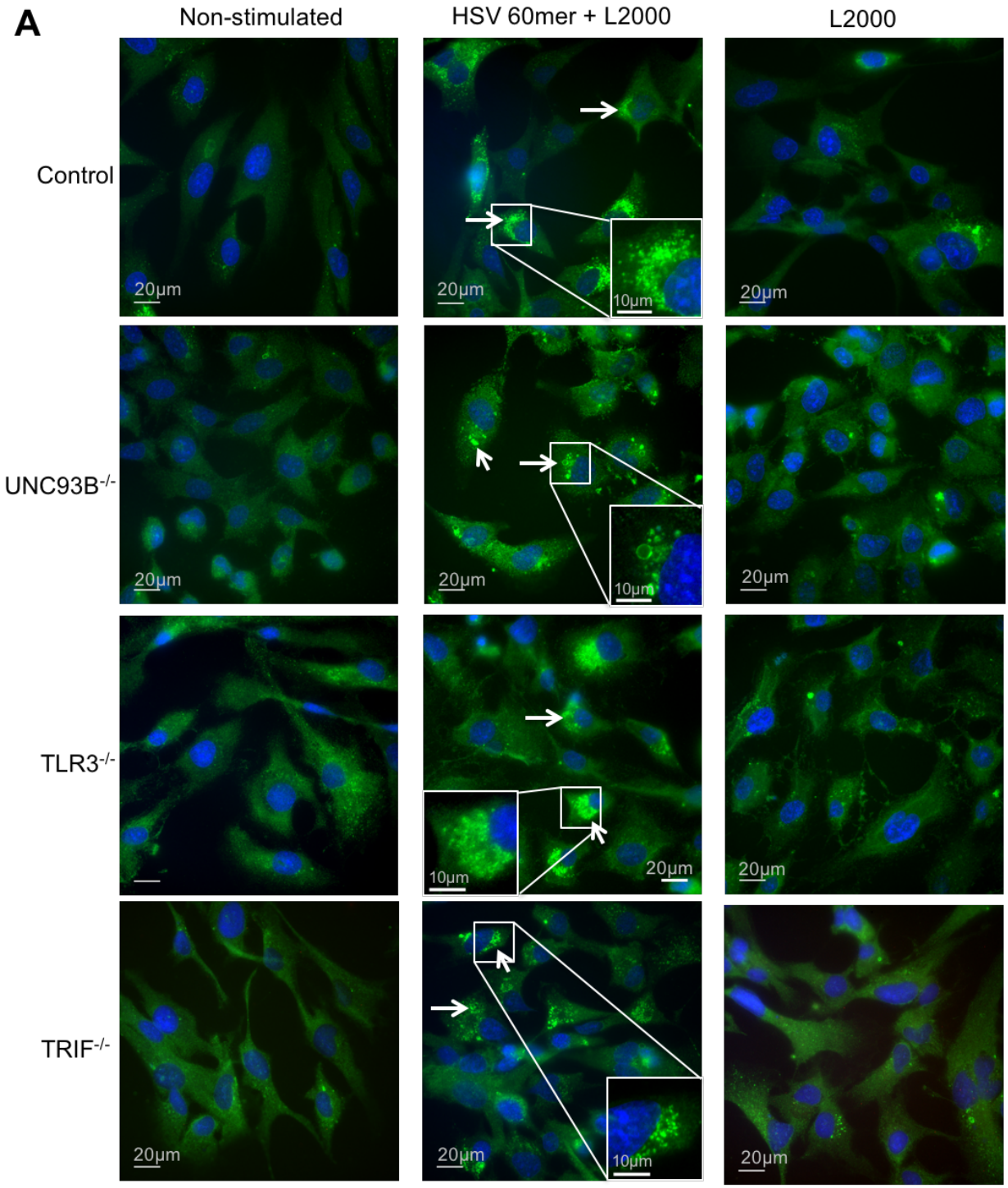


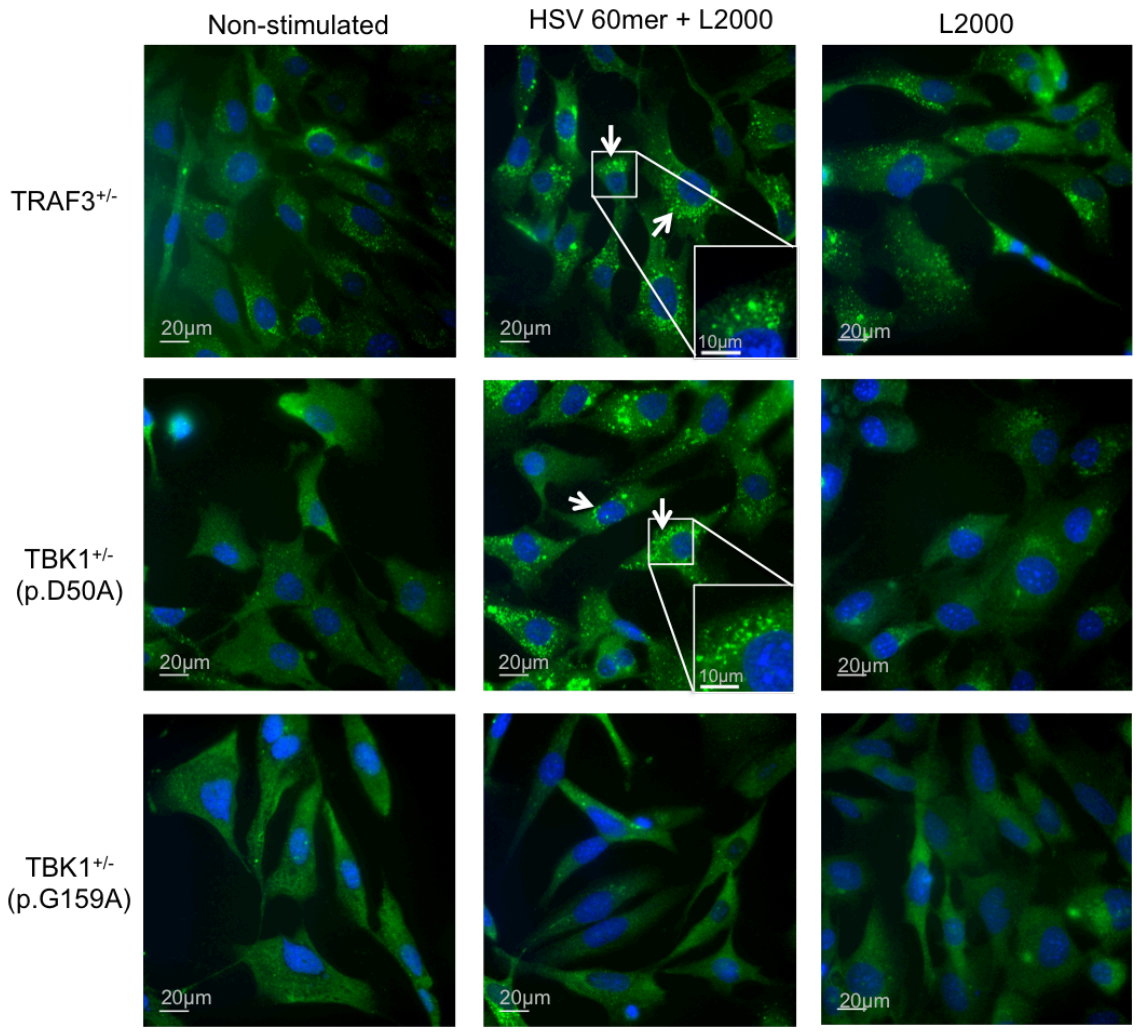
Figure 3.13. Cytoplasmic and perinuclear LC3B formation in HSV1-infected patient-derived fibroblasts. Fibroblasts were grown on coverslips, infected with HSV1 WT at MOI 0.001 for 24 hours in presence of 1% human serum before being fixed and stained for endogenous LC3B (green) and HSV1 ICP4 (red) proteins. White arrows indicate cytoplasmic LC3B puncta, yellow arrows indicate perinuclear LC3B formation. Dashed line marks viral plaque boundary within each representative image. DAPI was used to stain the nuclei. Scale bar, 20 μm. Images are representative of three independent experiments (*n* = 3).

3.7. HSV1 dsDNA-induced autophagy

Several studies have suggested the involvement of HSV1 dsDNA in inducing autophagy in mouse bone marrow-derived dendritic cells (BMDCs) and human HFFF2 cells, which may be dependent on dsDNA sensor STING (Rasmussen *et al.*, 2011; McFarlane *et al.*, 2011). Having demonstrated that TBK1 is involved in c-di-GMP-induced autophagy via STING (presented above), I speculated whether the dsDNA genome of HSV1 would induce autophagy in human fibroblasts and whether components of the TLR3-IFN pathway may be involved in this.

Control fibroblasts were transfected with 2 μg/mL of synthetic 60 bp (60mer) dsDNA oligonucleotide carrying sequence derived from HSV1 genome. Discovery and characterisation of 60mer has been demonstrated elsewhere (Rasmussen *et al.*, 2011; Unterholzner *et al.*, 2010). Mock transfection did not trigger significant LC3B puncta formation in all fibroblasts (Figure 3.14A). However, following 3 hours of dsDNA 60mer stimulation, there was a significant increase in formation of cytoplasmic LC3B puncta by 4.4-fold in control cells compared with non-stimulated cells. UNC93B$^{-/-}$, TLR3$^{-/-}$, TRIF$^{-/-}$, TRAF3$^{+/-}$ and TBK1$^{+/-}$ (p.D50A) were also able to show enhanced cytoplasmic LC3B puncta by more than 2-fold following dsDNA 60mer stimulation (Figure 3.14A & 3.14B). Notably, TBK1$^{+/-}$ (p.G159A) fibroblasts were not able to induce LC3B puncta formation following dsDNA 60mer stimulation (Figure 3.14), providing yet another clue into the mechanism by which dsDNA-induced autophagy works. These data suggest that whilst UNC93B, TLR3, TRIF and TRAF3 are not involved in dsDNA-induced autophagy, TBK1 is critical for this process.


A
Non-stimulated
HSV 60mer + L2000
L2000
Control
UNC93B-/-
TLR3-/-
TRIF-/-
20μm
10μm



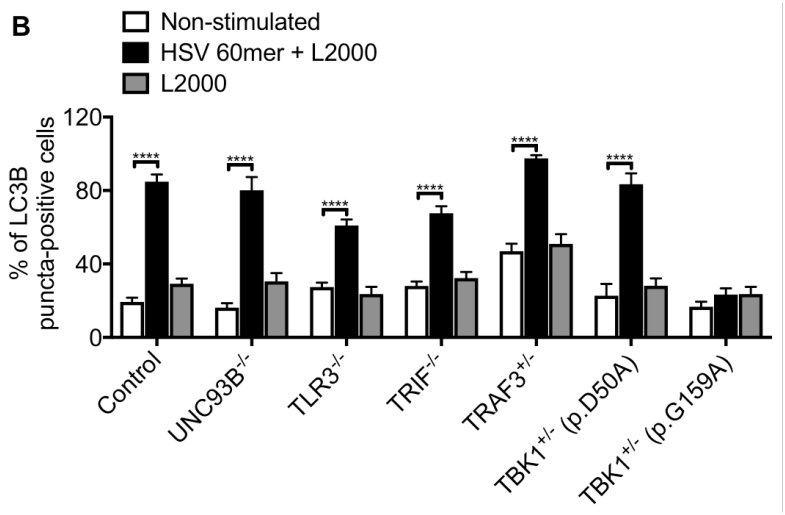


Figure 3.14. HSV1 dsDNA-induced autophagy in human fibroblasts. (A) Fibroblasts were stimulated with 2 μg/mL of 60mer which is delivered using Lipofectamine 2000 (L2000), or with mock L2000 alone for 3 hours before being fixed and stained for LC3B (green). DAPI was used to stain the nuclei. White arrows indicate LC3B puncta. Scale bar,

20 μm. Inset is magnified view of area marked within box in each representative image, scale bar 10 μm **(B)** Number of cells positive for LC3B puncta was counted. Images are representative of two independent experiments (*n* = 2). Data are represented as mean ± SEM and were analysed by Student's t-test; ****P <0.0001.

3.8. Discussion

In this chapter, the prospect of other components released during HSV1 infection that may potentiate autophagy was explored: dsRNA and IFN. As HSV1 produces dsRNA intermediates during its replication (refer to Chapter 1), it is conceivable that HSV1 dsRNA may engage with TLR3 receptor and result in the activation of autophagy in addition to the production of anti-viral IFN. Using dsRNA mimicking molecule poly(I:C) as a stimulant, we showed that dsRNA may indeed contribute to autophagy response in human dermal fibroblasts, suggesting an existence of yet another autophagy inducing pathway that is dependent on at least three upstream components of TLR3-IFN pathway: UNC93B, TLR3 and TRIF, but independent of TBK1. This finding is in contrast to a report that showed that despite showing LC3B puncta formation in response to HSV1 infection, human HFFF2 fibroblasts did not activate autophagy upon poly(I:C) stimulation which may be due to cell type (McFarlane *et al.*, 2011). A couple of other reports are in line with my finding, which demonstrated TLR3-mediated dsRNA-induced autophagy in other cell lines but the relevance and involvement of dsRNA in inducing autophagy during infection is still elusive and not well described (Tormo *et al.*, 2009; Delgado *et al.*, 2008). Also, to what extent this TLR3-dependent dsRNA-induced autophagy contributes to overall host protection is yet to be explored but is most unlikely to underlie HSV1-induced autophagy.

The role of IFN in inducing autophagy is also not well described. Several human cell lines have been shown to induce autophagy following IFN stimulation (Ambjørn *et al.*, 2013; Schmeisser, Bekisz & Zoon, 2014; Schmeisser *et al.*, 2013). My data provide another aspect to the role of autophagy during HSV1 infection, whereby IFN clearly was capable of stimulating autophagy in control and HSE-patient derived fibroblasts. As these patient-derived fibroblasts have impaired HSV1-induced IFN production, it is therefore unlikely that they were able to mount IFN-induced autophagy during HSV1 infection without exogenous supplementation of IFN.

Herein I provide the first characterisation of autophagy phenotypes of human dermal fibroblasts infected with HSV1. HSV1 infection induces two forms of LC3B phenotypes: cytoplasmic LC3B and perinuclear LC3B. Cytoplasmic LC3B puncta is induced in cells that were negative for HSV1 immediate early protein ICP4. Complete absence of HSV1 antigen cannot be ascertained as ICP4 is expressed as early as 2 hours post infection. Further dissection into these two differential autophagy phenotypes will be addressed in the next chapter.

To the best of my knowledge, this is the first description of autophagic upregulation in non-infected plaque-neighbouring cells in response to incoming infection in human dermal fibroblasts. We speculate that this cytoplasmic LC3B phenotype represents a form of a ‘danger’ signal, which may be involved in priming adjacent non-infected cells for autophagic elimination of incoming virus. A similar autophagy phenomenon has been reported in HSV1-infected murine trigeminal neurons where antigen-negative neurons showed formation of LC3B clusters in response to HSV1-induced

IFN production primarily from CNS resident non-neuronal cells (Katzenell & Leib, 2016). This report also demonstrated the requirement for functional IFN pathway in order to form neuronal LC3B clusters, as neurons deficient for IRF3, IFN receptor or STAT1 were not able to induce this clustering feature. My data showed that fibroblasts from the selected HSE patients known to have impaired HSV1-induced IFN production were able to induce cytoplasmic LC3B puncta phenotype (with exception of UNC93B$^{-/-}$ and TBK1$^{+/-}$ (p.G159A)), ruling out the requirement for IFN production in inducing this neighbouring LC3B effect. Difference in cell type may underlie this discrepancy as they may utilise different mechanism in controlling viral spread. Indeed, it has been shown that whereas IFN is crucial for controlling HSV1 in fibroblasts, neuronal cells opt for cytoprotective autophagy as a preferential strategy in fighting HSV1 infection as IFN could induce cell death in these non-renewable cells (Yordy *et al.*, 2012; Yordy & Iwasaki, 2013). My HSE patient-derived fibroblast data neatly showed that despite their ability in mounting cytoplasmic LC3B puncta in response to HSV1 infection, their intrinsic impairment in IFN production remains to be a causal factor leading to widespread HSV1 replication and enhanced cell death. It is therefore of future interest to dissect the involvement of autophagy in HSV1-infected neurons of these HSE patients to better understand this cell type-specific role of autophagy and how HSV1-specific mutations of the TLR3-IFN pathway may play a role in autophagy regulation in the CNS.

In this chapter, I demonstrated the strict requirement for TBK1 in inducing autophagy upon HSV1 infection in fibroblasts. Whereas TBK1 carrying the p.D50A mutation showed positive for autophagy induction and presented both cytoplasmic and perinuclear LC3B autophagy phenotypes, TBK1 with the p.G159A mutation

specifically failed to do both. To my knowledge, these are the only two TBK1 mutations that are associated with HSE and their innate immune responses towards multiple IFN-inducing stimuli and HSV1 infection have been extensively characterised by Herman and colleagues (Herman *et al.*, 2012). Both D50A and G159A mutations are loss-of-function mutations caused by protein instability (haploinsufficiency) and loss of kinase activity (dominant negative) respectively and result in uncontrolled dissemination of HSV1 infection and impaired HSV1-induced IFN production. D50A allele causes poor expression of TBK1 protein leading to impaired poly(I:C)-induced IFN production as shown previously (Herman *et al.*, 2012), but does not impair autophagy responses following HSV1 infection as shown in our study, suggesting that residual TBK1 might be sufficient in inducing these responses. G159A *TBK1* however does not affect expression of TBK1 protein, but renders the kinase catalytically inactive. As a result, poly(I:C)-induced IFN production is impaired (Herman *et al.*, 2012). Given the heavy implication of TBK1 in HSV1 pathogenesis most of which revolves around its kinase activity, it is therefore not surprising that TBK1$^{+/-}$ (p.G159A) fibroblasts failed to induce autophagy following HSV1 infection.

A report has shown a requirement for TBK1 in phosphorylating p62 receptor in HSV1-induced autophagy in human HEK293T cells (Sparrer *et al.*, 2017). TBK1 was found to co-localise with p62 during HSV1 infection in HEK293T cells and this interaction is crucial for the phosphorylation of autophagosomal p62 at serine residue 403 (S403) (Sparrer *et al.*, 2017). Whilst I have shown that HSV1-induced autophagy is also p62-mediated in human dermal fibroblasts, the phosphorylation of p62 at S403 and hence the direct involvement of TBK1 is yet to be demonstrated.

p62 S403 phosphorylation is not HSV1-specific as it has been previously demonstrated in anti-bacterial autophagy (Pilli *et al.*, 2012), nor pathogen-specific as it has also been shown to promote mitophagy (Matsumoto *et al.*, 2015) and protein clearance (Matsumoto *et al.*, 2011). It is therefore likely that fibroblastic HSV1 induced-autophagy employs a similar mechanism. Hence, it will be of future interest to test p62 phosphorylation phenotype of HSV1-infected TBK1$^{+/-}$ (p.G159A) fibroblasts. Furthermore, I observed the involvement of NDP52 autophagy adaptor in mediating HSV1 infection. NDP52 has been previously known to regulate anti-*Salmonella* xenophagy and mitophagy (Thurston *et al.*, 2009; Heo *et al.*, 2015). To date, my finding describes the first demonstration of its involvement in HSV1 infection.

In addition to their failure in mounting HSV1-induced autophagy, TBK1$^{+/-}$ (p.G159A) fibroblasts also showed impairment in HSV1 dsDNA-induced autophagy. I showed that TLR3$^{-/-}$, TRIF$^{-/-}$ and TRAF3$^{+/-}$ fibroblasts were able to induce autophagy upon both HSV1 infection and HSV1 dsDNA stimulation which rules out the involvement of TLR3 pathway in mounting HSV1-induced autophagy. Although all known dsDNA sensors are shown to be TBK1-dependent, TBK1$^{+/-}$ (p.G159A) fibroblast appeared to have normal IFN production following synthetic dsDNA poly dA:dT stimulation which is the ligand of STING-independent dsDNA sensors including RIG-I and DAI (Herman *et al.*, 2012). This conflicting finding could be as a result of partial TBK1 defect. My data suggest that TBK1 is absolutely required for activating HSV1 dsDNA-induced autophagy. An attractive candidate by which TBK1 mediates this autophagy is STING, which functions downstream of dsDNA sensors such as cGAS and strictly utilises TBK1 as its kinase. STING-TBK1 pathway has been receiving

equally heavy implication in its dual role in inducing IFN and autophagy upon microbial infections, including HSV1 (Watson *et al.*, 2015; Dey *et al.*, 2015; Zhong *et al.*, 2008). Indeed, a report by Rasmussen and colleagues showed that STING-deficient mouse BMDCs were incapable of inducing autophagy following stimulation with the same HSV1 dsDNA used in our study (Rasmussen *et al.*, 2011). This HSV1 dsDNA was previously shown to bind IFI16 and trigger IFNβ production (Unterholzner *et al.*, 2010; Rasmussen *et al.*, 2011). Using c-di-GMP stimulation, a ligand of STING, $TBK1^{+/-}$ (p.G159A) fibroblasts additionally showed an aberrant autophagy response, highlighting the role of STING and TBK1 in inducing autophagy upon HSV1 infection.

This study also found that $UNC93B^{-/-}$ fibroblasts failed to mount cytoplasmic LC3B puncta phenotype, despite being able to reduce p62 level as shown by immunoblots. UNC93B is an ER protein known to facilitate the trafficking of TLR receptors to endosomes (Kim *et al.,* 2008). To the best of my knowledge there is no report on the role of UNC93B in autophagy. Future investigation on the mechanism underlying HSV1-induced cytoplasmic LC3B puncta may reveal a link between UNC93B and autophagy.

In this chapter, Western blotting and immunofluorescence microscopy techniques were utilised to assess autophagy phenotypes following different stimuli and HSV1 infection. I found that immunofluorescence microscopy to be invaluable and informative in evaluating and interpreting the data. Western blotting allowed the assessment of LC3BI to LC3BII conversion to measure autophagy induction. However, densitometric analyses of independent experimental repeats often gave

wide variation between data (demonstrated by error bars of representative data). This made it difficult to decipher the data. In comparison, immunofluorescence microscopy was able to provide with similar information in the form of LC3B puncta formation, in addition to allowing the visual identification of two different autophagy phenotypes in HSV1 infection. Hereon, information gathered from immunofluorescence microscopy weighs more in my opinion, and hence mostly utilised in the rest of this study.

Taken together, I have provided several clues into the mechanism of HSV1-induced autophagy. Complimentary to previous report (Sparrer *et al.*, 2017), my data support the role of TBK1 in mediating HSV1-induced autophagy, which I have also found to involve p62 and NDP52. HSV1-induced autophagy seems to be independent of TLR3, and can be stimulated by HSV1 dsDNA alone, suggestive of the involvement of STING dsDNA adaptor which pathway is heavily dependent on TBK1 kinase in HSV1 infection. HSV1 triggers the formation of cytoplasmic LC3B puncta and perinuclear LC3B structures in human dermal fibroblasts whereby the former may have a protective role in HSV1 infection. As TRIF and TBK1 are implicated in autophagy, I pursued further investigation into the dynamics of these two distinct autophagy phenotypes by using $TRIF^{-/-}$ and $TBK1^{+/-}$ (p.G159A) fibroblasts in the next chapter, to better understand the role of autophagy in HSV1 infection. The role of TBK1 in mediating HSV1-induced autophagy will also be investigated in the next chapter.

Chapter 4

4. TBK1 plays a role in HSV1-induced autophagy in human dermal fibroblasts

4.1. General introduction

Components of the TLR3-IFN pathway, specifically TRIF and TBK1, have been implicated in autophagy induction. TRIF is well known for its adaptor role in IFN-inducing pathways downstream of TLR3 and TLR4 receptors. Additionally, it can also interact with Beclin-1 to promote autophagosomal formation (Shi & Kehrl, 2008). TBK1 is a downstream kinase for IFN-inducing pathways including the TLR3-IFN and STING-IFN pathways. In recent years, its role as a kinase has expanded rapidly to include autophagy particularly in facilitating xenophagy, mitophagy and removal of protein aggregates. It promotes autophagy by activating autophagy adaptors and facilitating autophagosomal maturation (Ahmad *et al.*, 2016). For these reasons, I decided to focus my study on HSV1-induced autophagy in $TRIF^{-/-}$ (p.R141X/R141X) and $TBK1^{+/-}$ (p.WT/G159A) patient fibroblasts.

In the previous chapter, I have shown that HSV1 induced two autophagy phenotypes in human dermal fibroblasts – cytoplasmic LC3B and perinuclear LC3B. In this chapter, I further investigated the induction of these two phenotypes spatially and temporally. Following the finding that $TBK1^{+/-}$ (p.G159A) fibroblasts have impaired autophagy responses upon HSV1 infection, I explored the role of TBK1 further by knocking down this protein or inhibiting its function, and subsequently studied the downstream effect on HSV1-induced autophagy. Reports have revealed the

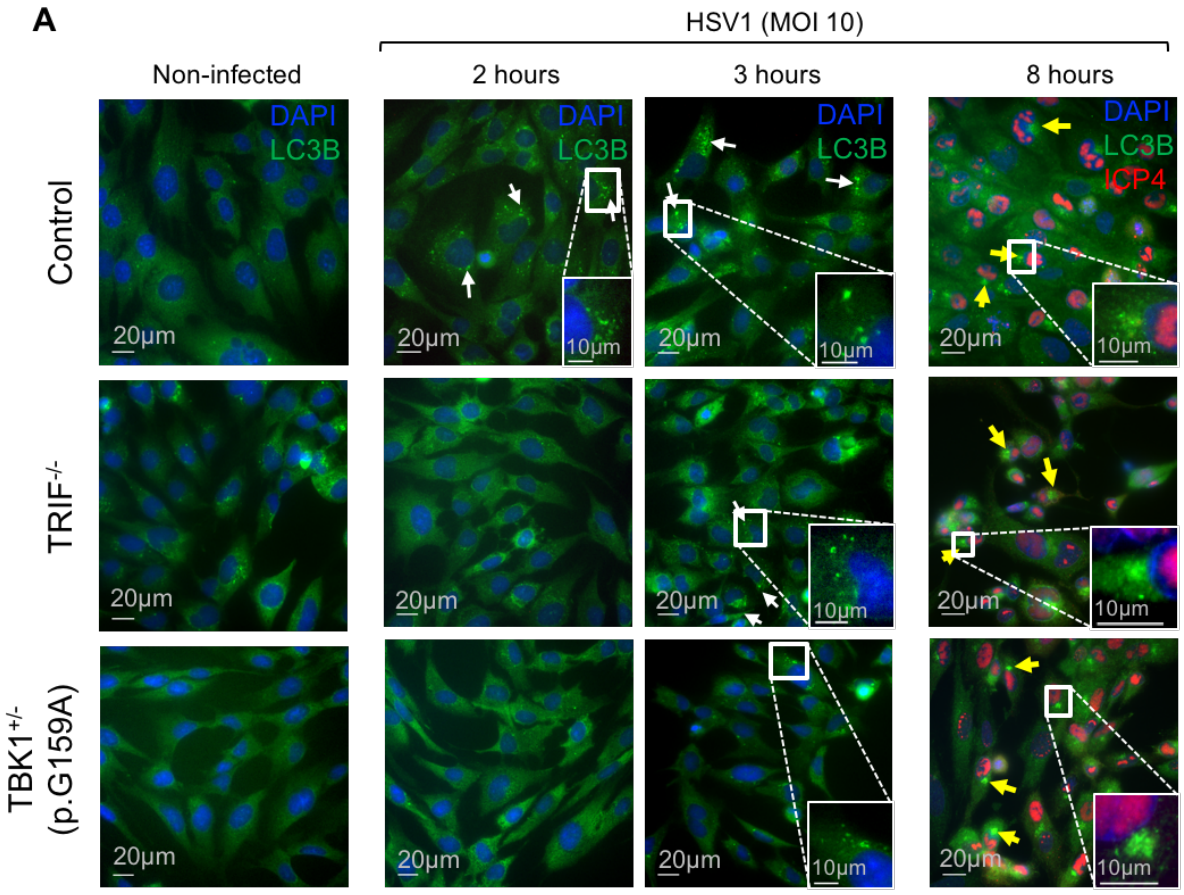
protective effect of enhanced autophagy during viral infections (Delorme-Axford *et al.*, 2013; Zhou *et al.*, 2016; McLean *et al.*, 2011; Orvedahl *et al.*, 2010). I explored this possibility by upregulating autophagy in fibroblasts, prior to HSV1 infection and subsequently measured cell viability and viral load. I also dissected the nature of the 'danger' signal that mediates cytoplasmic LC3B puncta formation in non-infected cells during HSV1 infection.

4.2. Cytoplasmic and perinuclear LC3B phenotypes are formed during early and late in HSV1 infection respectively

In the previous chapter, I described two distinct LC3B autophagy phenotypes induced by HSV1 in human dermal fibroblasts. However, the assay required a low dose of HSV1 and a long period of infection (24 hours) so that I could investigate autophagy response towards a viral spread radiating from viral plaques. It, therefore, did not provide a clue on how these two spatially distinct autophagy phenotypes take place immediately following HSV1 inoculation. Hence, I infected fibroblasts with a higher dose (MOI 10) and studied LC3B protein early in infection (2 and 3 hours) and late in infection (8 hours) when infection has established and viral replication is activated.

Strikingly, the cytoplasmic and perinuclear LC3B phenotypes occurred sequentially in infected control fibroblasts (Figure 4.1A). Cytoplasmic LC3B puncta were induced early in infection in control fibroblasts (2 and 3 hours post-infection (h.p.i.)), showing significant 3-fold induction after 3 hours of infection (Figure 4.1B). On the other hand, perinuclear LC3B was only seen later in infection (8 h.p.i.) in control fibroblasts.

TRIF$^{-/-}$ fibroblasts also induced cytoplasmic LC3B puncta early in infection, although rather delayed by an hour. Cytoplasmic LC3B puncta formation was only significantly induced, reaching 3-fold increase, at 3 h.p.i. in TRIF$^{-/-}$ fibroblasts. TBK1$^{+/-}$ (p.G159A) fibroblasts, on the other hand, failed to induce cytoplasmic LC3B punta early in infection (Figure 4.1A and B). Similar to control fibroblasts, both TRIF$^{-/-}$ and TBK1$^{+/-}$ (p.G159A) fibroblasts were able to form perinuclear LC3B structures late in infection (Figure 4.1A).



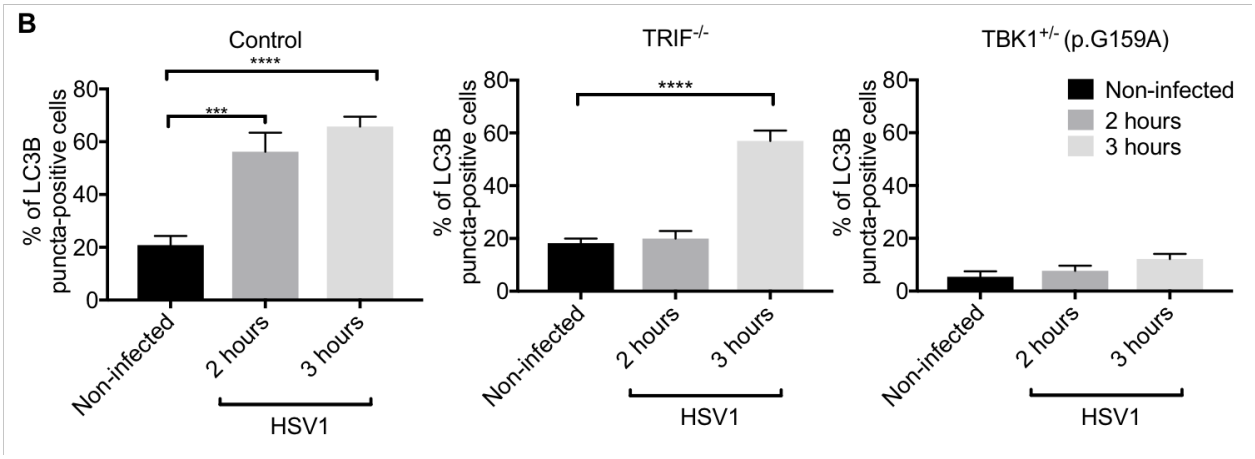
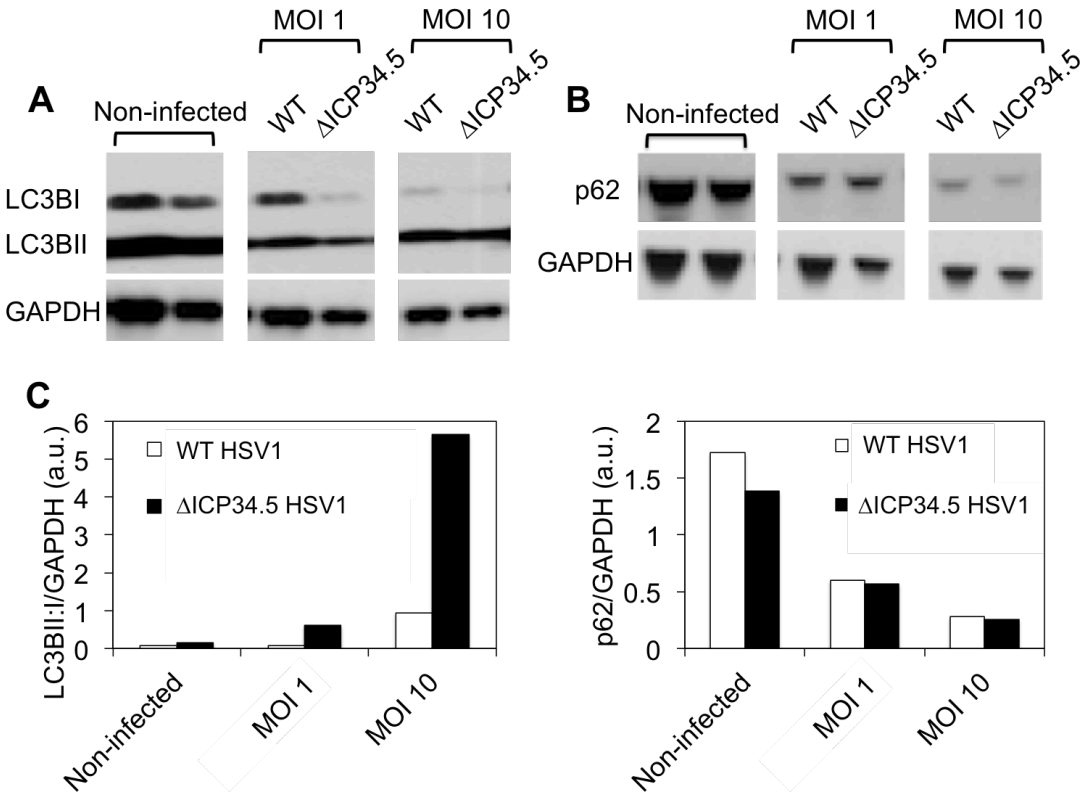


Figure 4.1. HSV1-induced cytoplasmic and perinuclear LC3B phenotypes in human dermal fibroblasts are induced early and late in infection respectively. (A) Control, TRIF$^{-/-}$ and TBK1$^{+/-}$ (p.G159A) fibroblasts were infected with WT HSV1 at MOI 10 for 2, 3 and 8 hours before being fixed and stained for endogenous LC3B (green) and HSV1 ICP4 (red) proteins. DAPI (blue) was used to stain for nuclei. White arrow indicates cytoplasmic LC3B and yellow arrow indicates perinuclear LC3B. Scale bar, 20 μm. Inset is a magnified view of the area marked in the box within each representative image and has scale bar 10 μm. **(B)** The number of LC3B-positive cells in indicated length of infection was counted on a minimum number of 100 cells per experiment. Images and data are representative of three independent experiments (*n* = 3). Data represent mean ± SEM and were analysed by two-way ANOVA; ***P <0.001 and ****P <0.0001.

4.3. Infection with ICP34.5-mutant HSV1 enhances HSV1-induced autophagy phenotypes

HSV1 encodes ICP34.5 as a measure to counteract host autophagy by blocking Beclin-1 autophagy protein and dephosphorylating host eIF2α (Tallóczy, Virgin & Levine, 2006; Tallóczy *et al.*, 2002; Orvedahl *et al.*, 2007). Although shown to exert its effect on host translation machinery in MEFs (Alexander *et al.*, 2007), deletion of

ICP34.5 was shown to impair the ability of HSV1 in regulating host autophagosome formation in human breast carcinoma (MCF7) cells (Orvedahl *et al.*, 2007). To observe the effect of ICP34.5 on HSV1-induced autophagy, I used ΔICP34.5 HSV1 strain and compared the autophagy phenotypes to WT HSV1 infection. In control fibroblasts, I observed a more pronounced induction of LC3BII:I upon ΔICP34.5 HSV1 infection compared with WT HSV1 infection (Figure 4.3A & 4.3C). This observation is consistent with reports on human HeLa and MEF cell lines (Lussignol *et al.*, 2013; Tallóczy *et al.*, 2002). However, I did not see a significant effect on p62 degradation in dermal fibroblasts infected with the HSV1 ΔICP34.5 strain (Figure 4.3B & 4.3C).



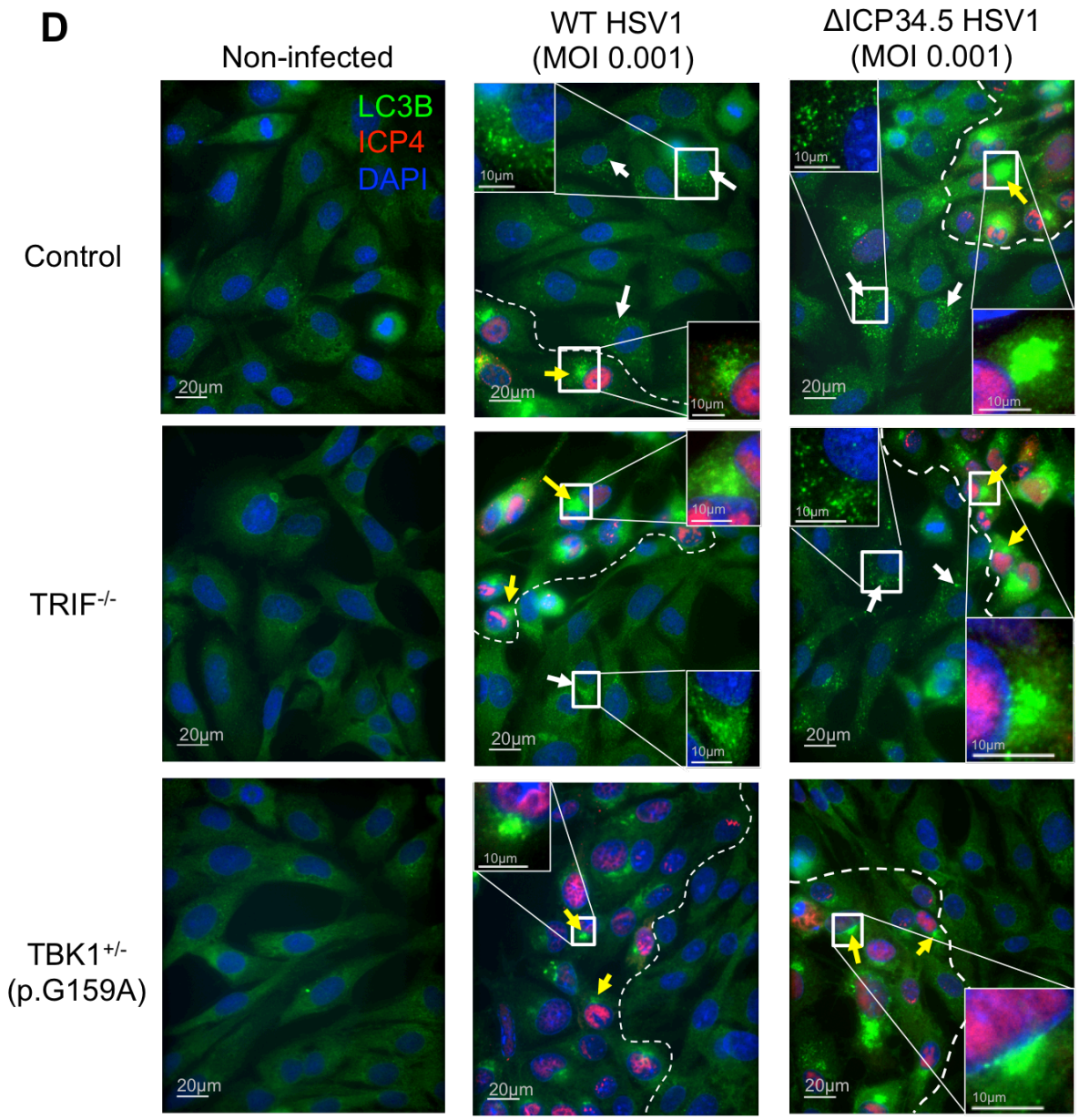


Figure 4.2. Infection of human dermal fibroblasts with ΔICP34.5 HSV1 enhanced autophagy phenotypes. (A-B) Control fibroblasts were infected with WT HSV1 or ΔICP34.5 HSV1 at MOI 1 or 10 for 48 hours before whole-cell lysis and immunoblotting. Endogenous (A) LC3B and (B) p62 proteins were probed. GAPDH was used a loading control. **(C)** Immunoblots from (A) were subjected to densitometry, a.u., arbitrary units **(D)** Control, TRIF$^{-/-}$ and TBK1$^{+/-}$ (p.G159A) fibroblasts were infected with WT HSV1 or ΔICP34.5 HSV1 at MOI 0.001 for 24 hours in presence of 1% human serum before cells were fixed and stained for endogenous LC3B (green) and HSV1 immediate-early protein ICP4 (red). DAPI (blue) was used as a nuclear stain. Dotted line outlines viral plaque boundary, white arrow indicates

cytoplasmic LC3B and yellow arrow indicates perinuclear LC3B. Scale bar, 20 μm. Inset is a magnified view of the area marked in the box within each representative image and has scale bar 10 μm. Images are representative of three independent experiments (*n* = 3).

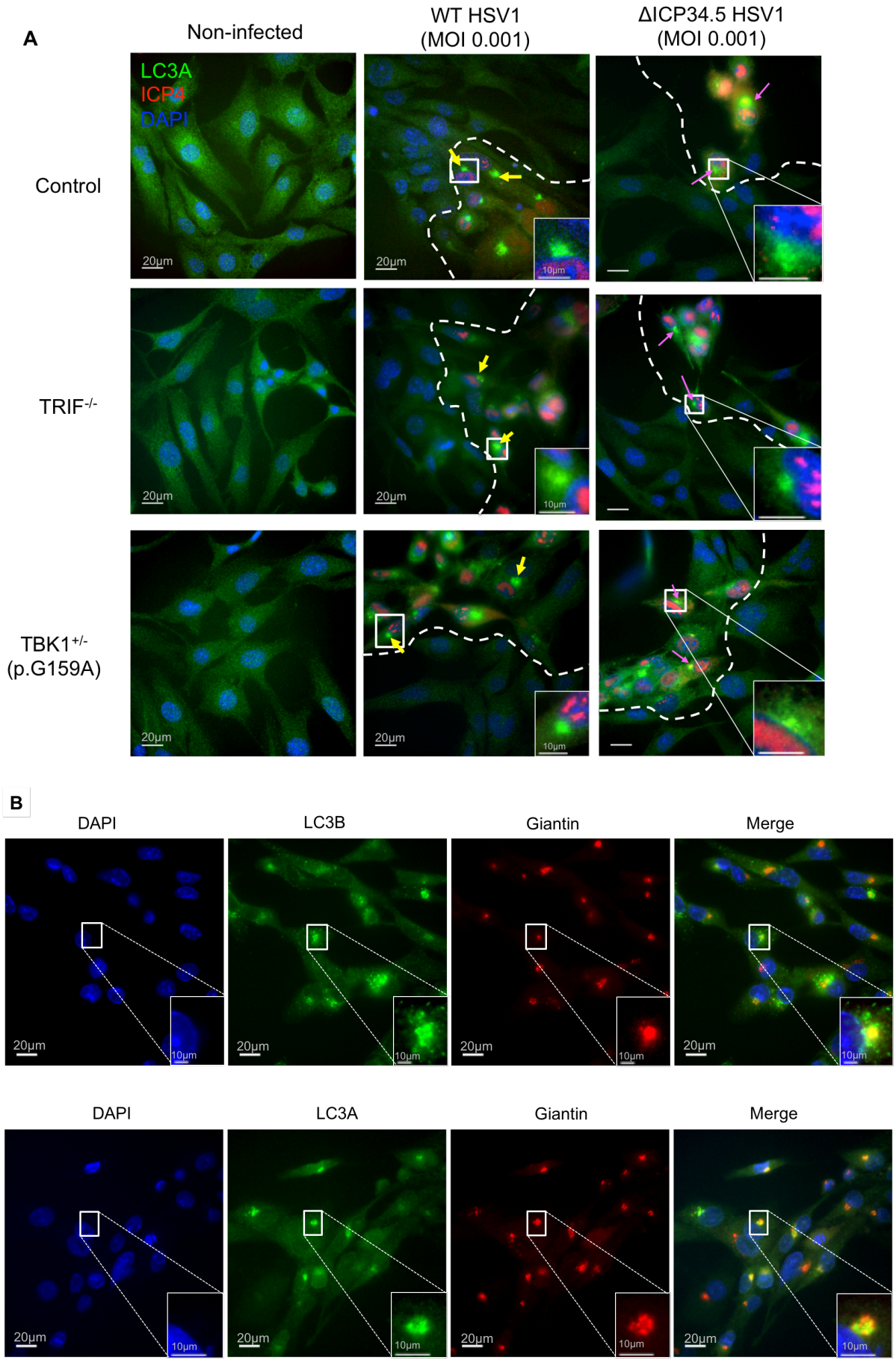
Using immunofluorescence, I further inspected LC3B response to ΔICP34.5 HSV1 infection in control, $TRIF^{-/-}$ and $TBK1^{+/-}$ (p.G159A) fibroblasts. Similar to WT HSV1 infection, ΔICP34.5 HSV1 infection triggered both cytoplasmic and perinuclear LC3B phenotypes in control and $TRIF^{-/-}$ fibroblasts and only cytoplasmic LC3B phenotype in $TBK1^{+/-}$ (p.G159A) fibroblasts. However, cytoplasmic LC3B phenotype was more pronounced in ΔICP34.5 HSV1 infection compared to WT HSV1 infection, as shown by the increased presence of cells positive for cytoplasmic LC3B puncta in control and $TRIF^{-/-}$ fibroblasts (Figure 4.3D). ΔICP34.5 HSV1 infection did not affect the inability of $TBK1^{+/-}$ (p.G159A) fibroblasts to form cytoplasmic LC3B phenotype (Figure 4.3D). This suggests that WT HSV1 exerts some degree of regulation over host autophagy in human dermal fibroblasts, which is mediated by ICP34.5.

4.4. Perinuclear LC3B structures co-localised with LC3A and Golgi bodies during late HSV1 infection

Two reports have documented a novel non-canonical autophagy phenotype in MEFs where infection gave rise to perinuclear dense structures that are enriched with the autophagy protein LC3A. This structure is formed by the coiling of the inner and outer membrane of the nucleus and hence is termed nuclear envelope-derived autophagy (NEDA) (English *et al.*, 2009; Radtke *et al.*, 2013). The HSV1-induced perinuclear LC3B phenotype that was observed in human dermal fibroblasts is

reminiscent of this structure hence I sought to assess whether this perinuclear LC3B structure would also stain with LC3A. Because TBK1$^{+/-}$ (p.G159A) cells could also form this perinuclear LC3B phenotype, I postulate that this is an immunomodulatory action executed by HSV1 and does not constitute a host response.

Similar to NEDA, perinuclear LC3B structures in HSV1-infected human dermal fibroblasts also stained for LC3A. Infection with ΔICP34.5 HSV1 did not affect the formation of perinuclear LC3A phenotype (Figure 4.2A). Notably, I did not observe LC3A cytoplasmic puncta formed in ICP4-negative (or -positive) cells following infection with WT and ΔICP34.5 HSV1, suggesting that it does not share the same role as cytoplasmic LC3B in HSV1-induced autophagy, and is unlikely to underlie HSV1 protective autophagy (Figure 4.2A). The perinuclear LC3B and LC3A structure was also observed to stain with Golgi bodies (Figure 4.2B and 4.2C). Given that this perinuclear LC3B phenotype occurs only in late HSV1 infection in fibroblasts, I postulate that it is a result of HSV1 modulation of the host's immune response to infection rather than a host anti-viral response.


A
Non-infected
WT HSV1
(MOI 0.001)
ΔICP34.5 HSV1
(MOI 0.001)
LC3A
ICP4
DAPI
Control
TRIF-/-
TBK1+/-
(p.G159A)
20μm
10μm
B
DAPI
LC3B
Giantin
Merge
DAPI
LC3A
Giantin
Merge

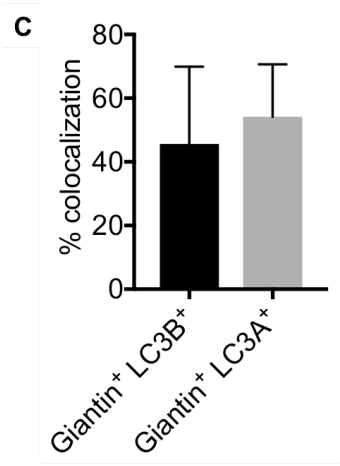


Figure 4.3. HSV1-induced perinuclear LC3B structure also stains for LC3A and Golgi bodies. (A) Control, TRIF$^{-/-}$ and TBK1$^{+/-}$ (p.G159A) fibroblasts were infected with WT HSV1 or ΔICP34.5 HSV1 strains at MOI 0.001 for 24 hours in presence of 1% human serum before being fixed and stained for endogenous LC3A (green) and HSV1 ICP4 (red) proteins. Arrow indicates perinuclear structures. **(B)** Control fibroblasts infected with HSV1 WT at MOI 0.001 for 24 hours in presence of 1% human serum before being fixed and stained for endogenous LC3B (green, upper panel) or LC3A (green, lower panel) and giantin (Golgi marker, red). DAPI (blue) was used to stain for nuclei. Scale bar, 20 μm. Inset is a magnified view of the area marked in the box within each representative image and has scale bar 10 μm. **(C)** The number of cells double-positive for giantin and LC3B (giantin^{+} LC3B^{+}) or for giantin and LC3A (giantin^{+} LC3A^{+}) was counted and expressed as percentage over the total number of cells positive for perinuclear structures. Images and data are representative of three independent experiments (*n* = 3). Data represent mean ± SEM.

4.5. Depletion or inhibition of TBK1 impairs HSV1-induced autophagy

4.5.1. Depletion of endogenous TBK1 abrogated HSV1-induced autophagy in control fibroblasts

Given the impairment in HSV1-induced autophagy seen in TBK1$^{+/-}$ (p.G159A) cells, I further confirmed the role of TBK1 in HSV1-induced autophagy by knocking down endogenous TBK1 in control fibroblasts using siRNA (siTBK1). I first confirmed the efficiency of siTBK1 knockdown delivered using Lipofectamine (Figure 4.4C). Control fibroblasts that were depleted of TBK1 exhibited enhanced viral replication (Figure 4.4A) compared to non-transfected cells. siTBK1 cells also showed more cell death and detachment (see phase image) compared to non-transfected. This is in line with a report that showed that TBK1 is protective in HSV1 infection, likely through inducing IFN production (Herman *et al.*, 2012). Transfecting with siNegative led to significantly less infected cells as seen at 24 h.p.i. GFP images, with more cells exhibiting normal morphology and uninfected (Figure 4.4A). I am not able to deduce whether Lipofectamine used to the deliver the RNA and/or siNegative used was blocking infection as Lipofectamine (mock)-transfected cells was not included in the experiments. Lipofectamine transfection reducing infection efficiency is not uncommon in many cases which has been reported to induce IFN production (Li *et al.*, 1998). Additionally, siRNA have been shown to have an immunostimulatory effect by inducing IFN through PKR and other TLRs (reviewed by Whitehead *et al*., 2011). Therefore, future studies extending from here should take these bystander effects into consideration. Viral load assessed at 48 h.p.i. revealed a significantly higher viral titre in siTBK1 transfected cells, compared to non-transfected cells and

siNegative-transfected cells (Figure 4.4B). However the difference is only by a log-fold. Performing the experiment with a lower viral dose (e.g. MOI 0.1) or harvesting virus at earlier infection time-point for titration (before cell viability becomes a limiting factor) may reveal a less subtle effect of TBK1 knock-down on HSV1 replication. Data derived from performing infection with lower dose should be taken with caution as transfection itself may hamper infection efficiency (and hence it is imperative to include mock transfection). siTBK1-transfected cells also showed impaired LC3BII:I induction and p62 degradation compared to the non-transfected counterpart (Figure 4.4D). In non-transfected control fibroblasts, cells were able to reduce NDP52 level following HSV1 infection. However, in the siTBK1 knockdown cells clearance of NDP52 is impaired after HSV1 infection. These data suggest a specific requirement for TBK1 to facilitate p62- and NDP52-mediated autophagy during HSV1 infection (Figure 4.4D).

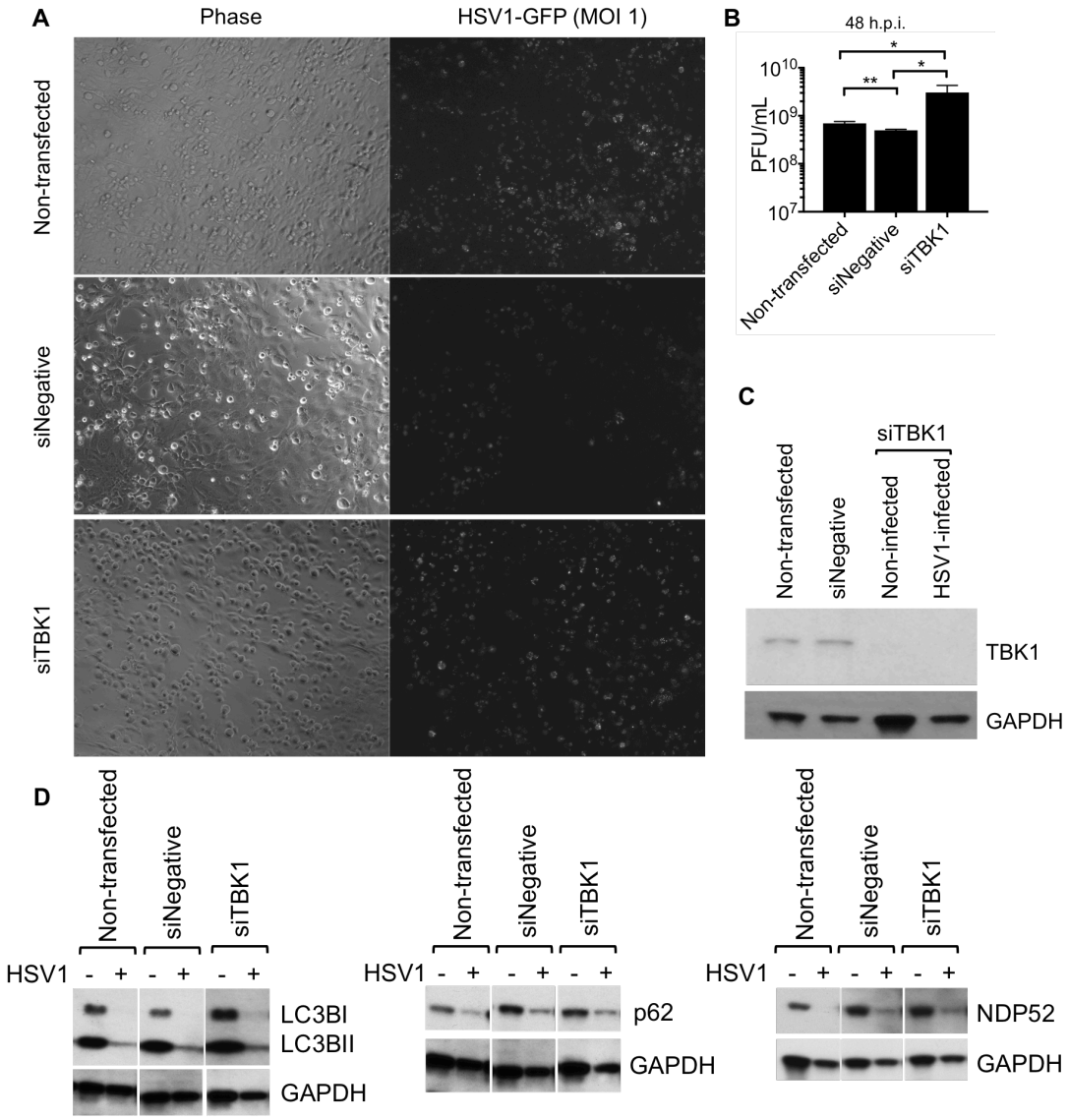


Figure 4.4. TBK1-depleted control fibroblasts showed impaired HSV1-induced autophagy. Control fibroblasts were transfected with siRNA that targets endogenous TBK1 (siTBK1) or with non-specific siRNA (siNegative) for 48 hours before being infected with HSV1-GFP (MOI 1) for further 48 hours and subjected to whole-cell lysis. **(A)** Replication of HSV1-GFP was monitored 24 h.p.i. based on GFP fluorescence. **(B)** HSV1 titre 48 h.p.i was measured by plaque assay **(C)** Efficiency of siTBK1 knockdown was confirmed by immunoblotting whole-cell lysates for TBK1. **(D)** Whole-cell lysates were resolved and probed for LC3B, p62, and NDP52 proteins. For all immunoblots, GAPDH was used as a loading control. Images and data are representative of three independent experiments (*n* =

3). Data represent mean ± SEM and were analysed by two-way ANOVA where *P< 0.05 and **P< 0.01.

4.5.2. Inhibition of TBK1 using BX795 reduced the cytoplasmic LC3B phenotype and did not affect the perinuclear LC3B phenotype

To investigate the role of TBK1 in the formation of cytoplasmic and perinuclear LC3B phenotypes induced by HSV1 infection, I inhibited TBK1 function in control fibroblasts using the TBK1 inhibitor BX795 and infected the cells with HSV1 at MOI 0.001. BX795 is an aminopyrimidine drug that specifically inhibits TBK1 and IkB kinase ϵ (IKKϵ) by preventing their phosphorylation at serine-172 (S172) residue which is essential for their kinase activity (Clark *et al.*, 2009; Kishore *et al.*, 2002). Its kinase activity has been shown to be indispensable in the autophagic elimination of *Salmonella typhimurium* (Thurston *et al.*, 2009, 2016; Radtke *et al.*, 2007).

I observed a reduction by half in the number of BX795-treated control fibroblasts with cytoplasmic LC3B puncta in ICP4-negative cells neighbouring viral plaques (indicated by white arrows), compared to non-treated cells (Figure 4.5A & 4.5B). The presence of perinuclear LC3B phenotype within viral plaques, however, was unaffected with ICP4-positive cells showing dense perinuclear LC3B formation in both BX795-treated and non-treated control cells (Figure 4.5A). TBK1$^{+/-}$ (p.G159A) fibroblasts, on the other hand, showed no induction of cytoplasmic LC3B puncta in plaque-neighbouring ICP4-negative cells and BX795 treatment did not affect this outcome (Figure 4.5A & 4.5B).

To further confirm this finding, I performed high dose of infection (MOI 10) on control fibroblasts that have been treated with BX795 and visualised LC3B protein at early (3 h.p.i.) and late (8 h.p.i.) infection. In BX795-treated HSV1-infected control cells, there was reduction by 2-fold in cytoplasmic LC3B puncta formation (white arrows) at 3 h.p.i. compared to non-treated HSV1-infected cells (Figure 4.5C & 4.5D). Consistently, the formation of perinuclear LC3B phenotype (yellow arrows) late in infection in control fibroblasts is unaffected by BX795 treatment (Figure 4.5C). Confirming previous findings, $TBK1^{+/-}$ (p.G159A) fibroblasts failed to induce cytoplasmic LC3B puncta during early in infection and this outcome is unaffected by BX795 treatment (Figure 4.5C & 4.5D). Similarly, $TBK1^{+/-}$ (p.G159A) could form perinuclear LC3B structures during late in infection in presence or absence of BX795 (Figure 4.5C). These data suggest that TBK1 is involved in the formation of HSV1-induced cytoplasmic LC3B phenotype that is formed during early infection, and that the formation of perinuclear LC3B phenotype later in infection is independent of TBK1.

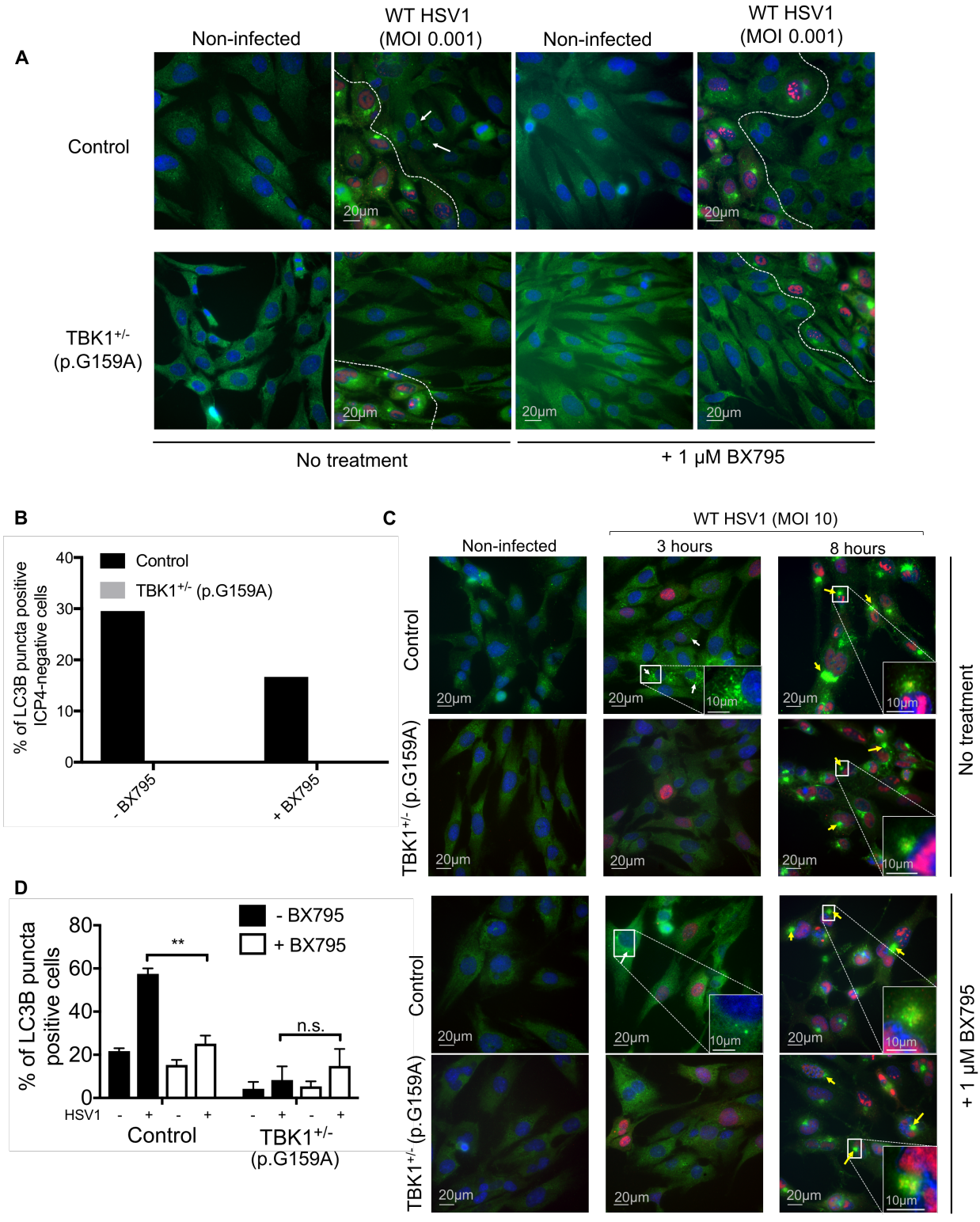


Figure 4.5. Functionally inhibiting endogenous TBK1 using BX795 reduces formation of HSV1-induced cytoplasmic LC3B early in infection without affecting formation of perinuclear LC3B later in infection. (A) Control or TBK1$^{+/-}$ (p.G159A) fibroblasts were pre-treated with 1 μM of BX795 overnight before infecting them with MOI 0.001 of WT HSV1 for

24 hours in presence of 1% human serum. Dotted line indicates boundary of viral plaque. Images and data are derived from a single experiment (*n* = 1) **(C)** Control or TBK1$^{+/-}$ (p.G159A) fibroblasts were pre-treated with 1 μM of BX795 overnight before being infected with MOI 10 of WT HSV1 for 3 hours or 8 hours. For both (A) and (C), cells were fixed and stained for endogenous LC3B (green) and HSV1 ICP4 (red) proteins. DAPI (blue) was used to stain for nuclei. Scale bar of representative images is 20 μm. Inset is the magnified view of the area marked within the box in each representative image and has scale bar of 10 μm. **(B) and (D)** Number of cells positive of cytoplasmic LC3B formation in (A) and (C) was counted respectively. Images and data are representative of three independent experiments (*n* = 3). Data represent mean ± SEM and were analysed by two-way ANOVA; ***P* <0.01; n.s., non-significant.

4.6. Autophagy promotes cell viability without altering HSV1 replication

Autophagy has been shown to promote cell survival in various bacterial and viral infections, where in some cases, increased number of cells made available is utilised by pathogens to foster their replication (McLean *et al.*, 2011; Zhou *et al.*, 2016). On the other hand, autophagy has been shown to protect and promote survival of non-renewable post-mitotic neuronal cells from Sindbis virus without altering viral replication (Orvedahl *et al.*, 2010; Liang *et al.*, 1998). I wondered whether re-establishing autophagy in TBK1$^{+/-}$ (p.G159A) fibroblasts may provide cytoprotection against HSV1 infection and if so, if it would increase viral burden or curtail it. I explored this possibility in fibroblasts by enhancing autophagy using rapamycin or poly(I:C) pre-treatment prior to infection, and subsequently assayed their autophagy phenotypes, cell viability as well as viral replication.

After 24 hours treatment with poly(I:C) or rapamycin, I infected the cells with GFP-tagged HSV1 at MOI 1. HSV1 replication was monitored 24 h.p.i. based on GFP fluorescence and its titre at 48 h.p.i. later was measured by plaque assay. To monitor the effect of ligand treatments on HSV1 infection, cells were infected with MOI 0.001 of WT HSV1 for 24 hours after pre-treatment, and their LC3B expression was visualised afterwards using immunofluorescence imaging. Cell viability was also assayed after pretreatment and infection by phase imaging and live/dead fluorescence staining.

HSV1 replication was significantly reduced in control fibroblasts after poly(I:C) pretreatment (Figure 4.6A & 4.6B) and this protection can be attributed to IFNβ production resulting from poly(I:C)-stimulated TLR3-IFN pathway (Figure 4.6C). This protection conferred by IFNβ is also evident by the absence of viral plaques in poly(I:C)-pretreated control cells which were infected with MOI 0.001 of HSV1 (Figure 4.8A & 4.8C). Both poly(I:C)-treated control and $TBK1^{+/-}$ (p.G159A) fibroblasts showed cytoplasmic LC3B puncta after 24 hours infection. Whilst $TBK1^{+/-}$ (p.G159A) fibroblasts were able to produce detectable IFNβ following poly(I:C) pre-treatment (Figure 4.6C), this level of IFNβ was not sufficient for protection against subsequent infection as $TBK1^{+/-}$ (p.G159A) fibroblasts still developed viral plaques and sustained similar viral load compared to non pretreated cells (Figure 4.6B & 4.8A). $TRIF^{-/-}$ fibroblasts did not induce autophagy or produce IFNβ following poly(I:C) stimulation and therefore could not benefit from protection conferred by poly(:I:C)-induced IFN against HSV1 infection (Figure 4.6 & 4.8). However, I observed cytoplasmic LC3B puncta in poly(I:C)-pretreated $TRIF^{-/-}$ fibroblasts after

being infected with HSV1, suggesting that the formation of HSV1-induced cytoplasmic LC3B puncta phenotype is an IFN-independent process as TRIF$^{-/-}$ fibroblasts have impaired IFN production following poly(I:C) stimulation (Figure 4.8A & 4.8B).

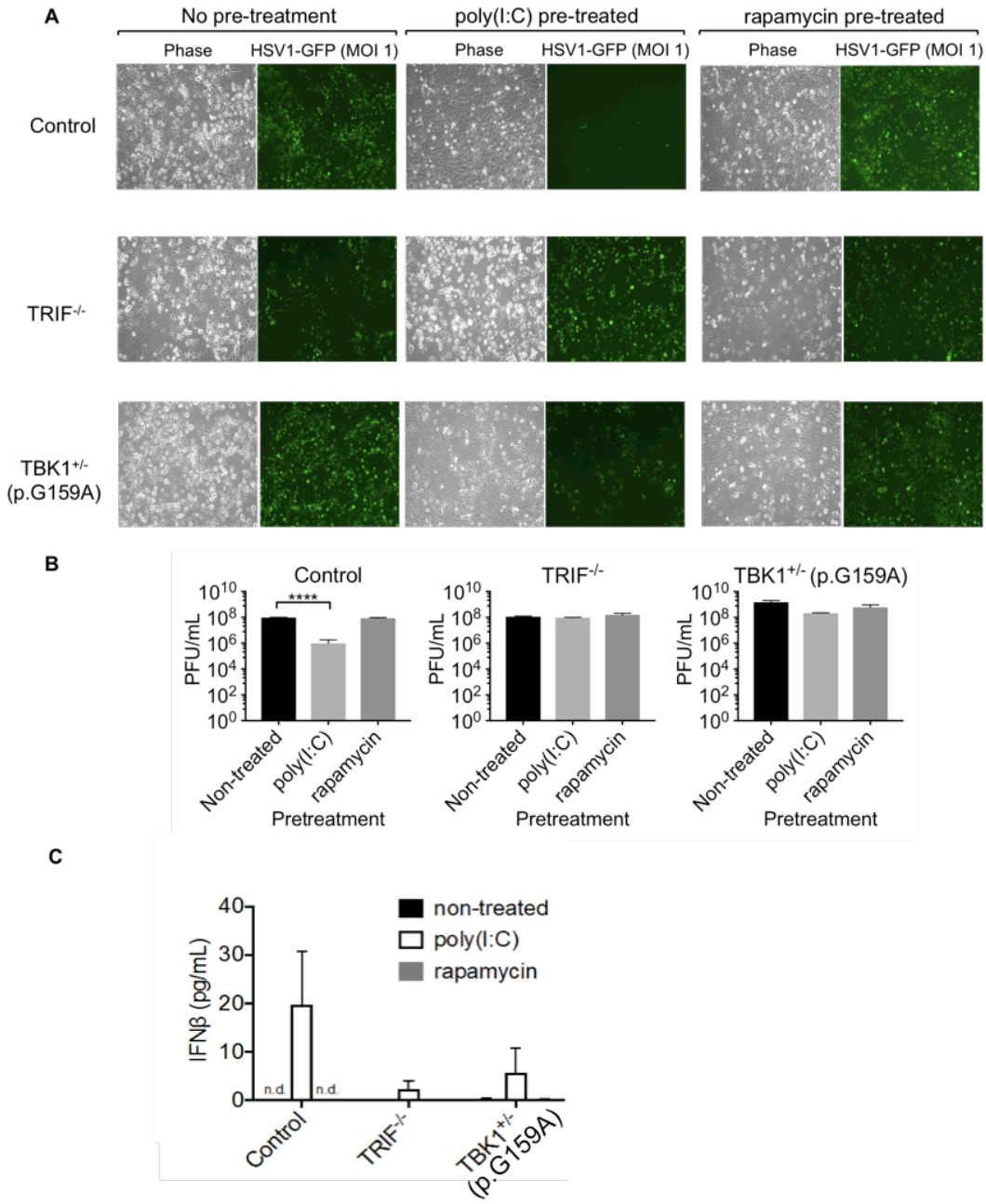


Figure 4.6. Enhancing autophagy in human dermal fibroblasts prior to HSV1 infection does not affect viral replication. Control, TRIF or TBK1$^{+/-}$ (p.G159A) fibroblasts were pre-

treated with 10 nM of rapamycin or 25 µg/mL of poly(I:C) for 24 hours before infecting them with GFP-tagged HSV1 at MOI 0.1 or 1 for 48 hours. **(A)** HSV1 replication in cells infected with MOI 1 was visualised 24 h.p.i. based on GFP fluorescence **(B)** At the end of 48 h.p.i, viral supernatants were harvested and titrated by plaque assay on Vero cells **(C)** Culture medium 24 hours post-treatment with rapamycin or poly(I:C) was harvested and assayed for cytokine IFNβ production. Images and data are representative of three independent experiments (*n* = 3). Data represent mean ± SEM and were analysed by two-way ANOVA; ****P <0.0001; n.d., non-detected.

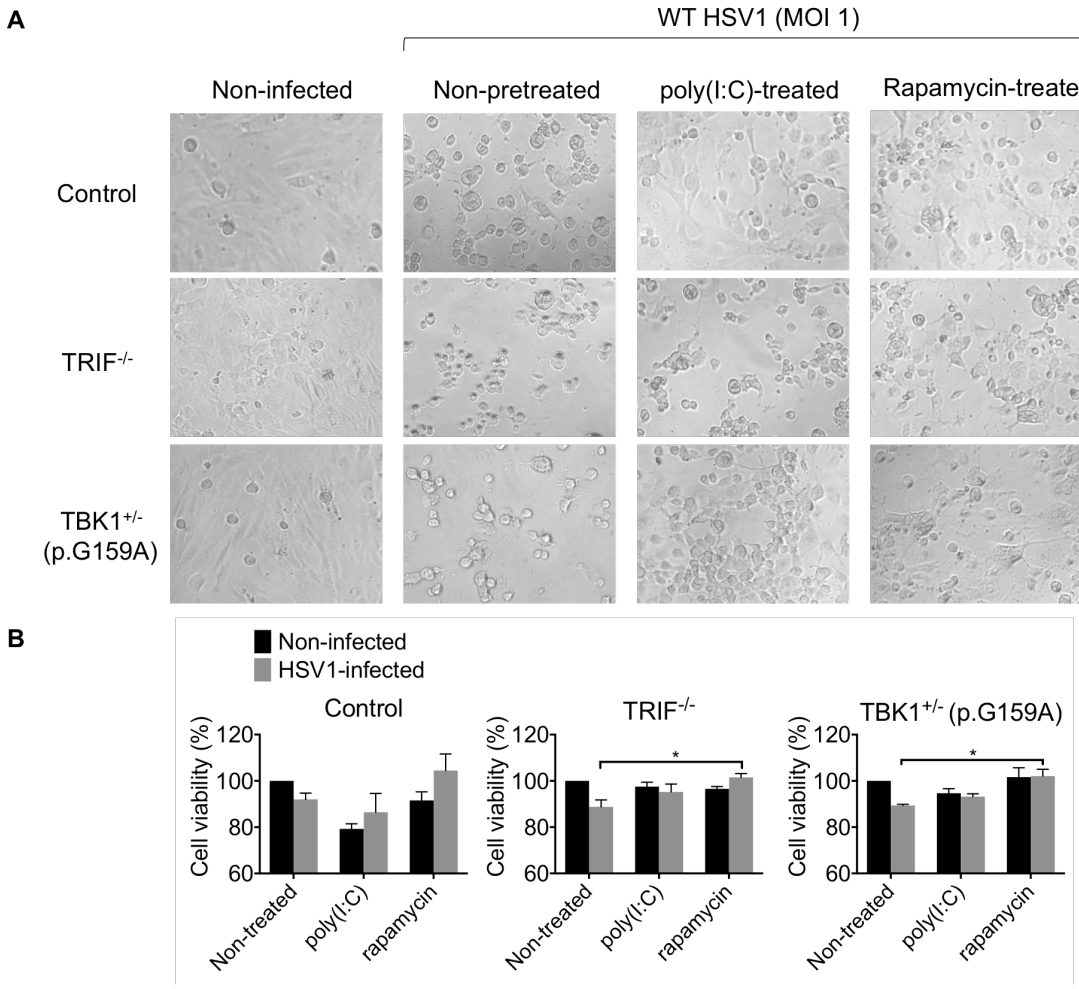


Figure 4.7. Enhancing autophagy in human dermal fibroblasts prior to HSV1 infection enhances cell viability. (A) Phase images of pre-treated or non-pre-treated cells infected with HSV1 (MOI 1) were taken 24 h.p.i. **(B)** Cells were dual stained with calcein AM and

ethidium heterodimer-1 to stain for live and dead cells respectively following 24-hour infection. The number of cells was counted based on fluorescence. Results are representative of three independent experiments (*n* = 3). Data were represented as mean ± SEM and analyzed by two-way ANOVA. Statistical significance indicates **P* <0.05.

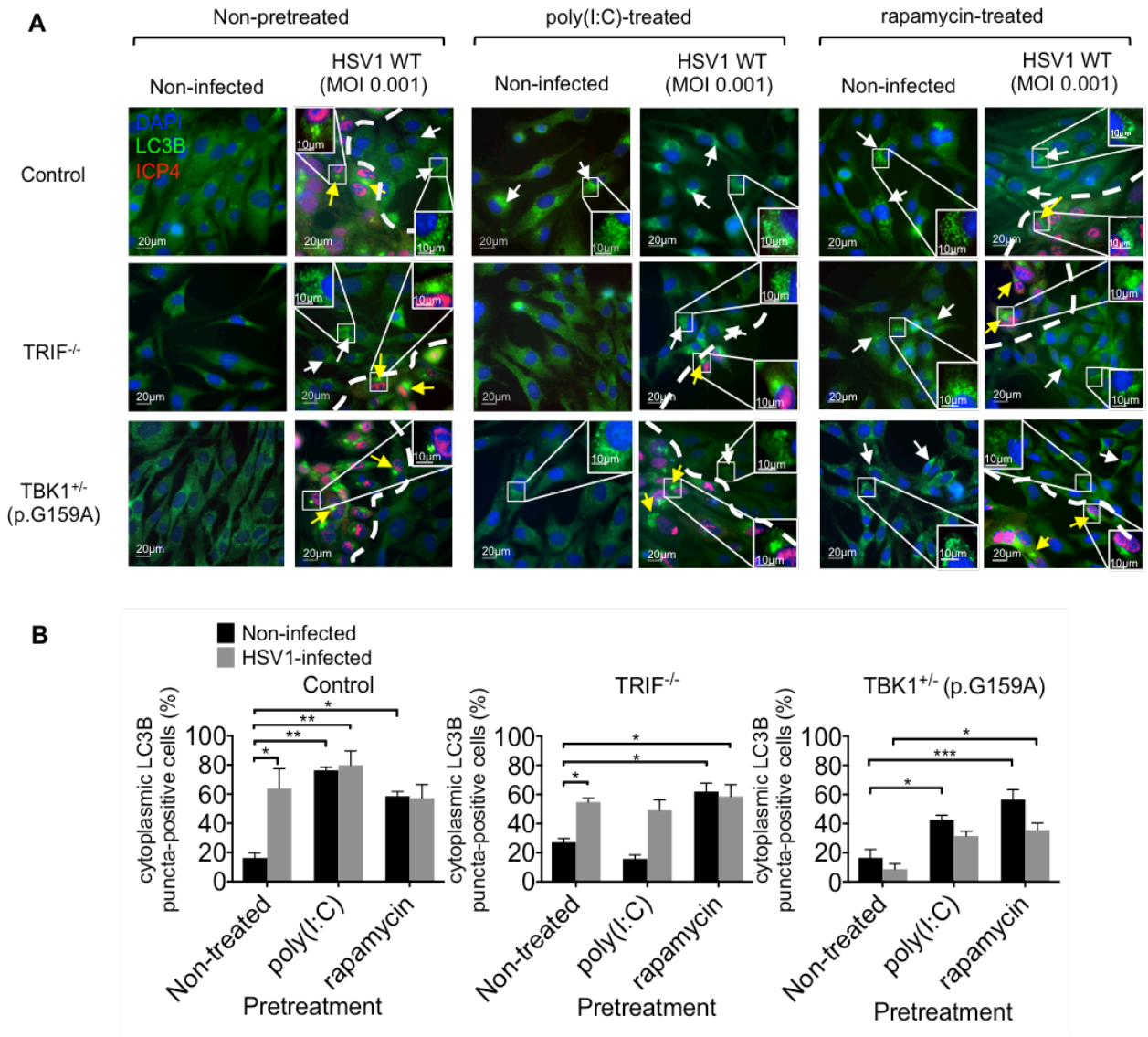


Figure 4.8. Rapamycin-induced autophagy promotes protection in HSV1 infection. (A) Fibroblasts grown on coverslips were pre-treated with 25 μg/mL of poly(I:C) or 10 nM of rapamycin for 24 hours prior to infection with WT HSV1 (MOI 0.001) for another 24 hours. Cells were fixed and stained for LC3B (green) and ICP4 proteins (red). DAPI (blue) was used for nuclear stain. Inset boxes are magnified views of areas marked within each

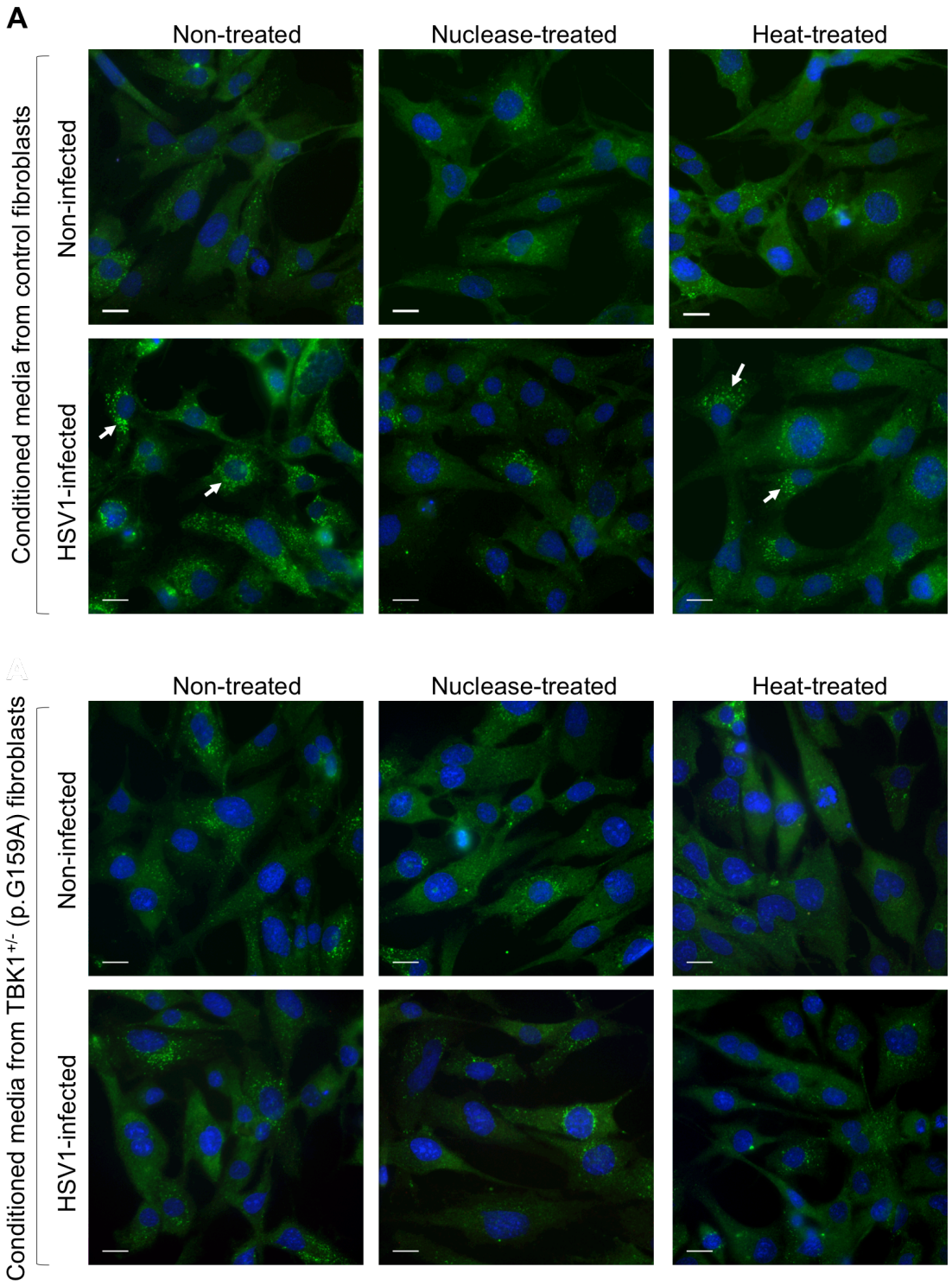
representative image. White arrows indicate cytoplasmic LC3B puncta, yellow arrows indicate perinuclear LC3B. **(B)** Number of cells positive for cytoplasmic LC3B puncta was quantified on a minimum number of 100 cells. Results are representative of three independent experiments (n = 3) where data represent mean ± SEM, data and are analysed by two-way ANOVA; *P <0.05, **P <0.01 and ***P <0.001.

In contrast to poly(I:C) treatment, rapamycin did not induce IFN production (Figure 4.6C) nor alter HSV1 replication (Figure 4.6B) whilst still inducing autophagy in control, TRIF$^{-/-}$ and TBK1$^{+/-}$ (p.G159A) fibroblasts (Figure 4.8A & 4.8B). Notably, rapamycin treatment, despite not inducing IFN production, promoted viability of HSV1-infected control, TRIF$^{-/-}$ and TBK1$^{+/-}$ (p.G159A) fibroblasts (Figure 4.7A & 4.7B). The autophagy phenotype, particularly the formation of HSV1-induced cytoplasmic LC3B puncta in non-infected cells neighbouring viral plaques, was not affected in rapamycin-pretreated control and TRIF$^{-/-}$ fibroblasts. However, TBK1$^{+/-}$ (p.G159A) fibroblasts, showed an elevated presence of cytoplasmic LC3B puncta in non-infected cells neighbouring viral plaques by 4-fold, compared to non-treated cells (Figure 4.8A & 4.8B). Collectively, pre-conditioning TRIF$^{-/-}$ and TBK1$^{+/-}$ (p.G159A) fibroblasts for autophagy using rapamycin prior to infection led to higher cell viability but did not alter HSV1 replication.

4.7. Paracrine autophagy induction is mediated by infected cell-derived nucleic acid

In previous chapter (Chapter 3) and this chapter, I observed cytoplasmic LC3B puncta induction in non-infected cells that were neighbouring infected cells and speculate the existence of 'danger' signal behind the induction. I extended my investigation by assessing this 'danger' signal that was triggering this phenotype. I approached this question by collecting medium from infected fibroblasts (conditioned medium), which was filtered and UV-irradiated (to exclude infectious viral particles), and was either nuclease-treated (to eliminate nucleic acids) or heat-treated at 95 ^{o}C (to denature proteins). The conditioned medium was then added to control fibroblasts, which were then assayed for their autophagy response.

Conditioned medium taken from infected control fibroblasts induced a significant formation of cytoplasmic LC3B puncta in the recipient control fibroblasts by 3-fold (Figure 4.9A top panel & 4.9B left panel). This suggests that this 'danger' signal operates in a paracrine manner. Likewise, heat-treated conditioned media harvested from infected control fibroblasts significantly induced cytoplasmic LC3B puncta formation in recipient control fibroblasts by 2-fold. Strikingly, nuclease-treated conditioned medium derived from infected control fibroblasts showed significantly less induction of cytoplasmic LC3B compared to the non-nuclease-treated counterpart and showed no significant difference compared to nuclease-treated conditioned medium derived from non-infected control fibroblasts. This indicates that the 'danger' signal seen in non-infected cells may take the form of nucleic acid rather than protein (Figure 4.9A top panel & 4.9B left panel).


A
Non-treated
Nuclease-treated
Heat-treated
Conditioned media from control fibroblasts
Non-infected
HSV1-infected
Conditioned media from TBK1+/- (p.G159A) fibroblasts

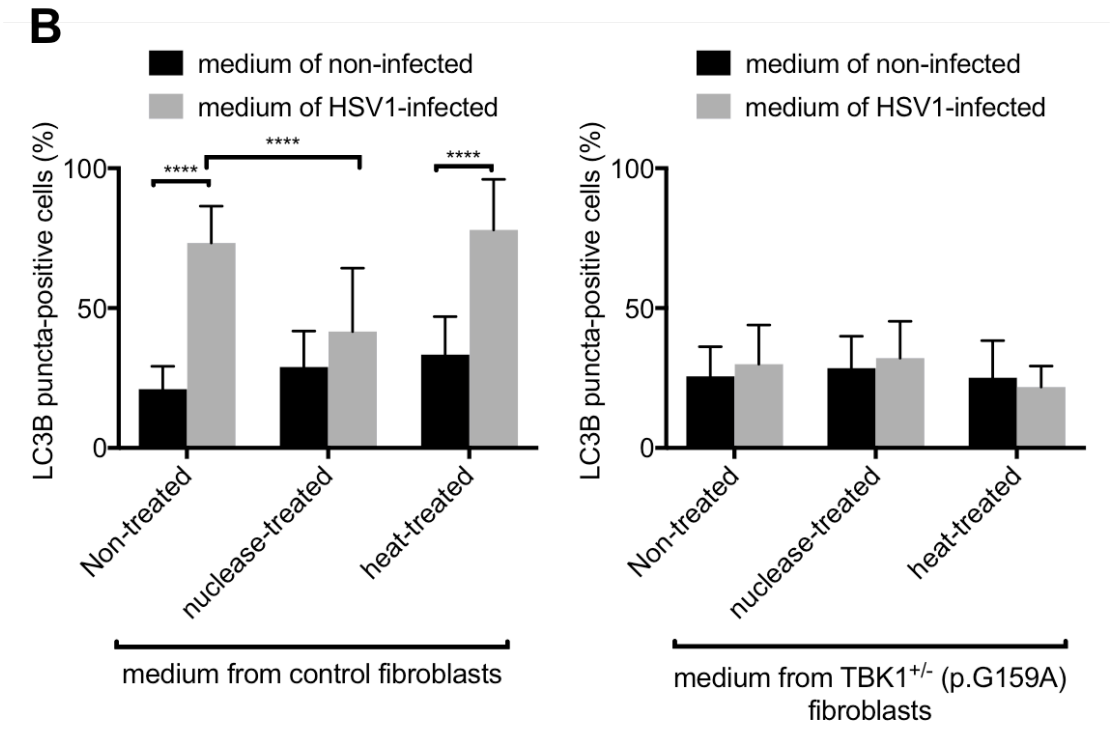


Figure 4.9. Conditioned medium from infected control fibroblasts triggers autophagy in control fibroblasts. (A) Control or TBK1$^{+/-}$ (p.G159A) fibroblasts were infected with WT HSV1 for 3 hours at MOI 10 in serum-free DMEM. Culture media were subsequently collected, filtered and UV-irradiated to clear infectious viral particles. The media were then either treated with nuclease or heat or left untreated, before being added onto control fibroblasts that were grown on coverslips. After 8 hours of incubation with conditioned media, cells were fixed and stained for endogenous LC3B (green) and ICP4 (red). DAPI (blue) was used as a nuclear stain. White arrow indicates cytoplasmic LC3B. Representative images have scale bar of 20 μm. **(B)** The number of cells positive for cytoplasmic LC3B puncta was quantified on a minimum number of 100 cells. Results are from a single experiment (n = 1) where data represent mean ± SD and were analysed by paired Student's t-test. Statistical significance indicates ****P <0.0001.

On the other hand, conditioned media from infected TBK1$^{+/-}$ (p.G159A) fibroblasts failed to induce significant cytoplasmic LC3B puncta in recipient control fibroblasts. Nuclease or heat treatments did not affect this outcome, as all treatments did not induce significant cytoplasmic LC3B puncta in recipient control fibroblasts (Figure 4.9A bottom panel & 4.9B right panel). This implies that TBK1-deficient fibroblasts were not able to produce this 'danger' signal.

4.8. Discussion

Here I report that HSV1 upregulates autophagy in HSV1 antigen-negative non-infected fibroblast cells neighbouring infected ones, evidently by inducing cytoplasmic LC3B puncta in IFN-independent manner. A similar observation has been documented in mice neuronal cells, where autophagic clusters were seen in neighbouring HSV1 antigen-negative neurons although their formation was shown to be IFN-dependent (Katzenell & Leib, 2016). This report has also shown that neuronal LC3B clusters are induced by neurotropic alphaherpesviruses – HSV1, HSV2 and pseudorabies virus. Whether or not cytoplasmic LC3B phenotype response that we observed in fibroblasts is exclusive to HSV1 infection is yet to be tested. This unique paracrine 'danger' signalling mechanism mediated by autophagy expands the scope of the role of autophagy in immunity, which does not only degrade pathogens but also has the ability to alert other cells of the presence of infection.

Additional experimentation suggests a role for nucleic acid in mediating this paracrine autophagy induction, and TBK1 is required for producing this mediator.

How TBK1 or which TBK1-mediated pathway is involved in the production and/or secretion of this 'danger' signal is unknown and warrants further investigation. dsDNA and HSV1 infection in MEFs were shown to activate STING and TBK1 co-translocation from ER compartments into LC3B-positive endosomes by the help of autophagy Atg9 protein (Ishikawa, Ma & Barber, 2009; Saitoh *et al.*, 2009). Further investigation revealed the presence of Sec5 protein in these STING-TBK1 endosomes which directly binds to TBK1 to facilitate its kinase function and promote IFN production (Ishikawa, Ma & Barber, 2009; Chien *et al.*, 2006). Sec5 exists in a complex called exocyst which plays a role in endosomal trafficking and exocytosis (secretion of intracellular secretory vesicles into extracellular space) (Brooks *et al.*, 2012). It is plausible that Sec5/exocyst may promote the secretion of these dsDNA-bound STING-TBK1 vesicles into the extracellular space. Secretion of STING-containing exosomes (a type of extracellular vesicles) by HSV1-infected cells have been reported previously where they help prime IFN response in non-infected neighbouring cells (Kalamvoki & Deschamps, 2016; Kalamvoki, Du & Roizman, 2014). Additionally, dsDNA- and HSV1-induced autophagy occurs in STING-dependent manner in mouse BMDCs (Rasmussen *et al.*, 2011). Furthermore, how TBK1 may mediate Sec5/exocyst function in exocytosis is unclear.

In this study, I extended the role of TBK1 in anti-microbial autophagy, where it is required for HSV1-induced autophagy, particularly in inducing cytoplasmic LC3B puncta early in infection. My study also demonstrated the requirement for TBK1 in facilitating p62- and NDP52-mediated autophagy. Reports have demonstrated the role of TBK1 in anti-bacterial autophagy, where it is recruited into growing autophagosomes and is imperative for phosphorylating autophagy receptors in the

vicinity, such as NDP52, optineurin and p62 (Pilli *et al.*, 2012; Wild *et al.*, 2011; Thurston *et al.*, 2009), which leads to autophagosomal maturation and lysis of the contained pathogen (Pilli *et al.*, 2012). I showed that TBK1 is required for p62 and NDP52 degradation, but whether these two autophagy receptors are present in HSV1-induced cytoplasmic LC3B puncta structures or their activation is required for the formation of cytoplasmic LC3B puncta structures is an attractive hypothesis. I further confirmed the reliance of HSV1-induced autophagy on functional TBK1 by knocking down or inhibiting endogenous TBK1 in fibroblasts.

Amongst multitude proteins encoded by HSV1 during its lytic infection, two have been known to antagonise autophagy – ICP34.5 and Us11. Both proteins exert their anti-autophagic activity by inhibiting Beclin-1, an important upstream component that activates autophagy (Furuya *et al.*, 2005). Here, I showed that cytoplasmic LC3B phenotype induced by HSV1 infection is not regulated by ICP34.5 as HSV1 lacking this protein could still induce this cytoplasmic LC3B puncta phenotype. This is in line with a report that showed the primary function of this ICP34.5 is to alleviate host translational arrest in response to infection (Alexander *et al.*, 2007). As HSV1-induced cytoplasmic LC3B phenotype is formed early in infection, Us11 is unlikely to regulate this phenotype, as Us11 is not expressed early in infection (Lussignol *et al.*, 2013).

HSV1 infection triggers both autophagy and IFN response, but their relative contribution towards immunity is still not clear. In this study, I showed that formation of this cytoplasmic LC3B phenotype does not require IFN, as $TRIF^{-/-}$ fibroblasts which have impaired poly(I:C)-induced IFN signalling pathway, were able to form

cytoplasmic LC3B puncta following HSV1 infection. This is in contrast to HSV1-induced neuronal LC3 cluster formation, which has been shown to be dependent on an intact IFN-signalling pathway (Katzenell & Leib, 2016). This contrasting requirement can be attributed to the difference in cell type and in utilisation of autophagy. In neurons, these HSV1-induced IFN-inducible LC3B cluster formation is thought to be part of the effector function of anti-viral responses down the IFN signalling pathway that tips the lytic-latency balance in neuronal cells (Katzenell & Leib, 2016).

Formed late in infection, HSV1-induced perinuclear LC3B phenotype is found dense in structure rather than in puncta formation and takes place on the perinuclear area of the cell. Its formation is independent of TBK1 and TRIF and is also not regulated by HSV1 ICP34.5 protein. As it is formed late in infection and appears to occupy the perinuclear area, this led me to speculate that it may be an immunomodulatory activity mediated by HSV1. Indeed, this perinuclear LC3B structure colocalised with Golgi bodies. HSV1 is known to hijack Golgi bodies during its productive infection to promote its replication and egress (Leuzinger *et al.*, 2005). This distinct perinuclear LC3B structure is similar to that found in HSV1-infected mouse BMMs described by two reports which they termed as nuclear envelope-derived autophagy (NEDA) (English *et al.*, 2009; Radtke *et al.*, 2013). I therefore tested and confirmed that the perinuclear LC3B structures induced in HSV1-infected fibroblasts, also stained for LC3A protein. This suggests that mouse BMMs and human dermal fibroblasts may partially share similar autophagy response towards HSV1 infection, although only these two studies have documented such phenomenon so far. However, further investigation of this perinuclear LC3B structure using electron microscopy is

necessary to confirm their similarity. This also warrants future investigation of whether mouse BMMs also able to induce cytoplasmic LC3B puncta as human dermal fibroblasts.

There is yet a report demonstrating the direct protective role of TBK1 in viral autophagy. Sindbis virus infection in mice neurons revealed a protective effect of autophagy which functions to clear p62 aggregates, targets viral capsid for autophagic degradation and promotes the viability of neurons without altering viral replication. However, the involvement of TBK1 in this context is unknown (Orvedahl *et al.*, 2010). Similar to this, I showed that autophagy is cytoprotective without affecting HSV1 replication in human dermal fibroblasts.

Taken together, this study has provided insights into the involvement of TBK1 in inducing IFN-independent protective autophagy early in HSV1 infection and may help control inflammation by promoting cell survival. It has also described the ability of non-infected cells to induce autophagy in response to paracrine nucleic acid that is produced by neighbouring infected cells and this production is dependent on TBK1.

Chapter 5

5. Dissecting the role of TBK1 in HSV1-induced autophagy

5.1. General introduction

The role of TBK1 in mediating autophagy is a subject of active investigation in the field. Whilst its role in anti-bacterial autophagy has been established (Thurston *et al.*, 2009; Wild *et al.*, 2011; Pilli *et al.*, 2012; Thurston *et al.*, 2016), little has been demonstrated in anti-viral autophagy. Herein, I developed a HEK293T cell line that carries a stable miRNA-targeted knockdown of endogenous TBK1 (HEK293T/miRTBK1), as a tool to dissect the functional effect of various *TBK1* mutants in HSV1 infection.

In the previous chapters, I demonstrated impairment of HSV1-induced autophagy in HSE patient-derived fibroblasts carrying p.G159A TBK1 mutation. On the other hand, TBK1 has also been linked to the pathogenesis of ALS, another neurodegenerative disease that is associated with autophagy dysregulation (Ahmad *et al.*, 2016). In this chapter, I aimed to understand the function of TBK1 in HSV1–induced autophagy by utilising *TBK1* mutations that have been linked to HSE (p.G159A and p.D50A) (Herman *et al.*, 2012) and ALS (p.E696K, p.R47H, and p.M559R) (Freischmidt *et al.*, 2015). Although the function of G159A and D50A mutants in IFN induction has been characterised, their autophagy function has not been elucidated; and whether autophagy plays a role in HSE pathogenesis remains an open question (Table

5.1) (Herman *et al.*, 2012). The IFN induction and autophagy functions of ALS-linked E696K (impaired OPTN-binding), R47H (impaired IFN-inducing) and M559R (impaired both OPTN-binding and IFN-inducing) mutants have been functionally characterised, but only E696K has been determined to be disease-causing for ALS (Table 5.1) (Freischmidt *et al.*, 2015). Three of these mutations are located in the kinase domain of the TBK1 protein (R47H, D50A, and G159A). M559R mutation is located in the ULD-CCD1 junction. E696K, on the other hand, is found in the CCD2 domain (Figure 5.1).

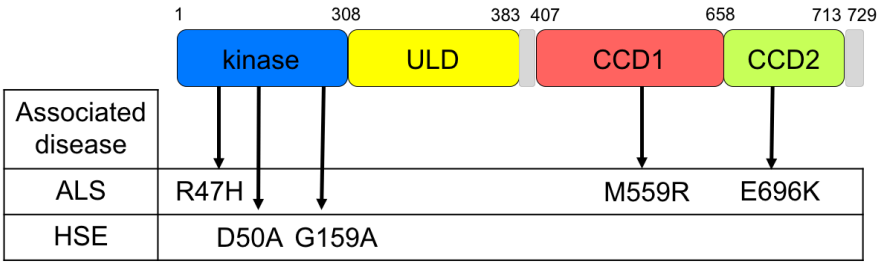


Figure 5.1. Location of TBK1 mutants used in this study that are associated with HSE and ALS with respect to TBK1 protein domains. Protein domains are not drawn to scale.

Table 5.1. List of selected HSE- or ALS-associated TBK1 mutants used in this study and their *in vitro* functionality. HSE-associated mutants were assessed for their IFN-inducing function by the ability of TBK1$^{+/-}$ (p.G159A) and TBK1$^{+/-}$ (p.D50A) fibroblasts to phosphorylate IRF3 substrate and/or produce IFNβ/λ following poly(I:C) stimulation. IFN-inducing function of ALS-associated mutants were assessed by their ability to bind and phosphorylate IRF3 substrate, and activate IFNβ promoter following their overexpression in HEK293T cells. Their ability to bind to OPTN was determined by immunoprecipitation. n.d., not determined.

TBK1 mutation	Disease	Functionality		Reference
		IFN-inducing	OPTN-binding	
R47H	ALS	No	Yes	Freischmidt *et al.,* 2012
D50A	HSE	No	n.d.	Herman *et al.,* 2012
G159A	HSE	No	n.d.	Herman *et al.,* 2012
M559R	ALS	No	No	Freischmidt *et al.,* 2012
E696K	ALS	Yes	No	Freischmidt *et al.,* 2012

5.2. HEK293T/miRTBK1 cells as a system to study TBK1 function in HSV1-induced autophagy

5.2.1. HEK293T/miRTBK1 cells showed reduced endogenous TBK1 and were more susceptible to HSV1 infection than HEK293T

Since TBK1 is required for HSV1-induced autophagy, I generated a stable TBK1-depleted HEK293T cell line (HEK293T/miRTBK1) by transducing HEK293T cells with a lentiviral miRNA that targets the 3' UTR of endogenous *TBK1* (miRTBK1), which was maintained under puromycin selection (Chapter 2). miRNA plays a homeostatic role in regulating cellular protein levels by identifying and binding target mRNAs, leading to their recognition by Dicer ribonuclease enzyme which eventually cuts and degrades them, and therefore preventing their translation (see review by Bartel *et al.,* 2004). The efficiency of stable miRTBK1 knockdown was confirmed using Western blot (Figure 5.2A). I also assessed the effect of TBK1 knockdown in this cell line upon infection with GFP-tagged HSV1 and observed a significant increase in viral

replication compared with HEK293T cell line. This susceptibility could be rescued by restoring wild-type (WT) TBK1 in HEK293T/miRTBK1 cells (Figure 5.2B).

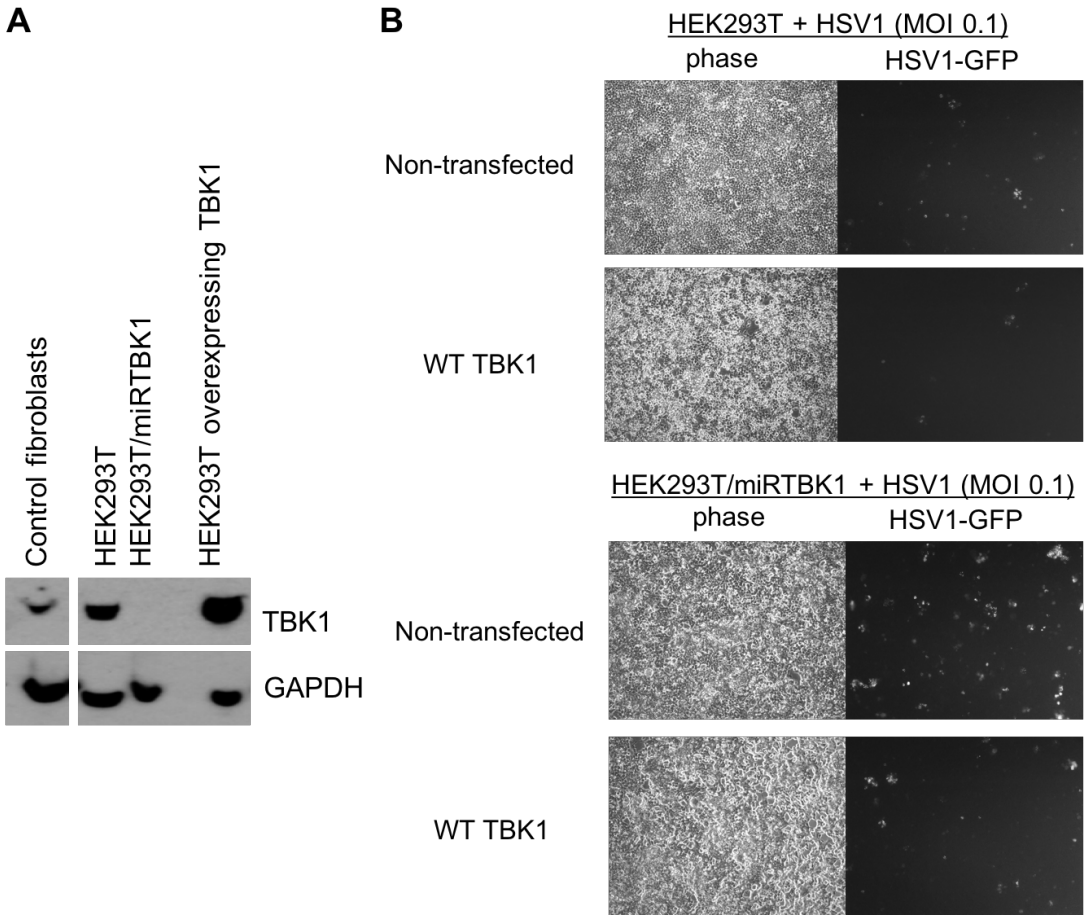


Figure 5.2. Stable depletion of TBK1 and susceptibility to HSV1 of HEK293T/miRTBK1 cell line. (A) Whole-cell lysates were collected from cell culture and electrophoresed and subsequently immunoblotted for TBK1 expression. GAPDH was used as a loading control. Blots are representative of two independent experiments. **(B)** HEK293T and HEK293T/miRTBK1 cells were either non-transfected or transfected with WT TBK1 prior to infection with HSV1-GFP at MOI 0.1. Replication of HSV1 based on GFP fluorescence was visualized 24 hours post infection. Images are representative of two independent experiments (n = 2).

5.2.2. HEK293T/miRTBK1 cells overexpressing TBK1 mutants showed enhanced HSV1 replication

Having confirmed the depletion of endogenous TBK1, I used this HEK293T/miRTBK1 cell line to examine the effect of TBK1 carrying HSE-associated mutations G159A and D50A, and ALS-associated mutations E696K, R47H and M559R on HSV1 replication. As the target of miRTBK1 is the 3' UTR of endogenous TBK1, supplementing HEK293T/miRTBK1 cells with exogenous TBK1 becomes feasible as it lacks 3' UTR and hence permitting its expression in the cells without being targeted by miRNA degradation. This makes this cell line a suitable TBK1-deficient system to study TBK1.

Following 24 hour infection with GFP-tagged HSV1 at dose MOI 0.1, I observed enhanced viral replication in HEK293T/miRTBK1 cells that were expressing TBK1 mutant G159A, E696K, R47H and M559R compared with cells that were transfected with empty vector, based on GFP fluorescence (Figure 5.3). Infecting the cells at higher MOI (MOI 1) revealed more cell death 24 hours post infection in cells that were expressing G159A, E696K, R47H and M559R TBK1 compared to WT TBK1-transfected cells as seen in phase images (Figure 5.4).

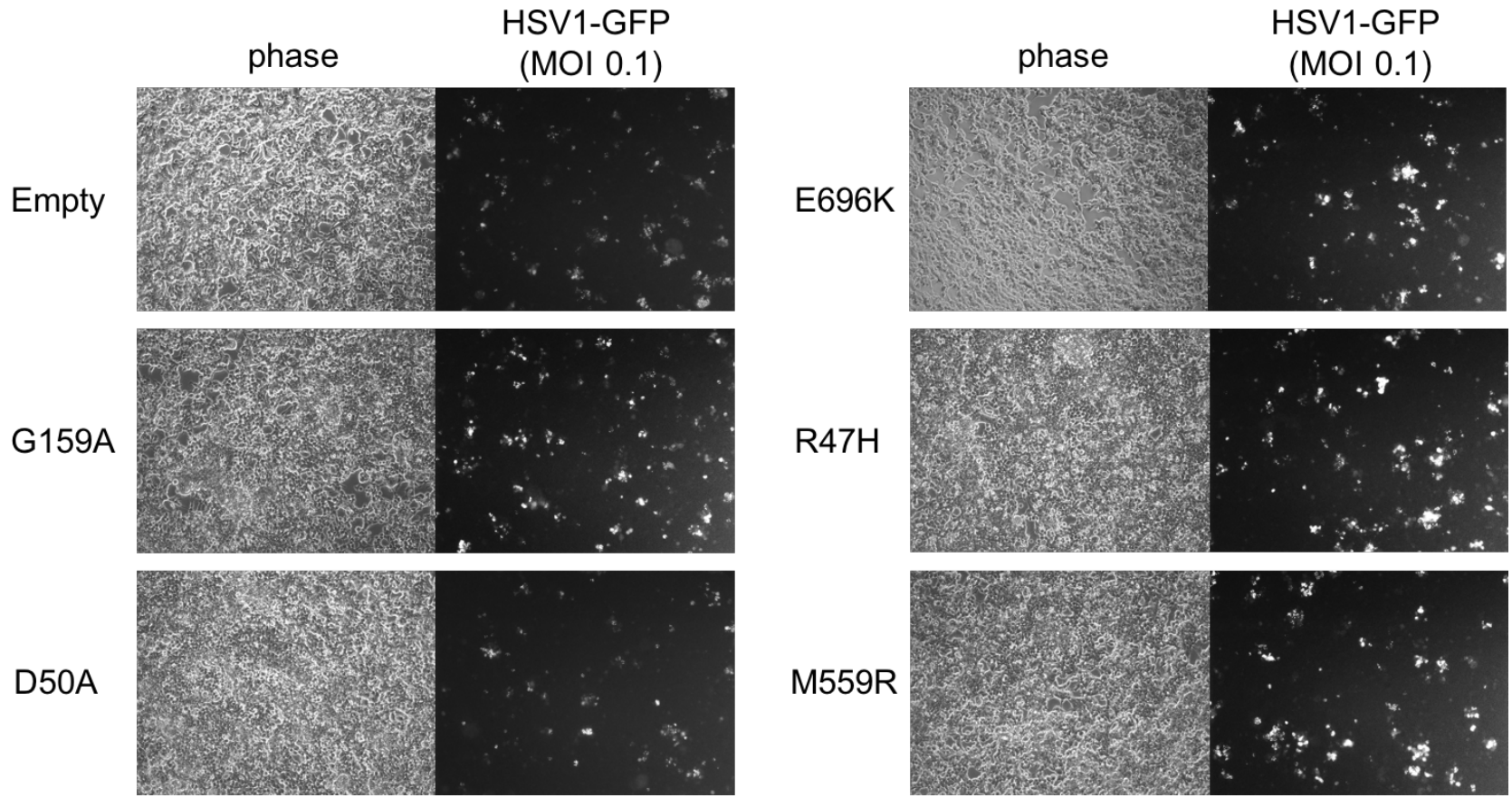


Figure 5.3. Effect of various TBK1 mutations on HSV1 replication in HEK293T/miRTBK1 cells. HEK293T/miRTBK1 cells were transfected with 100 ng of TBK1 or empty vector and subsequently infected with HSV1-GFP at MOI 0.1. Replication of HSV1 was visualized 24 hours later based on GFP fluorescence. Experiment was done once (*n* = 1).

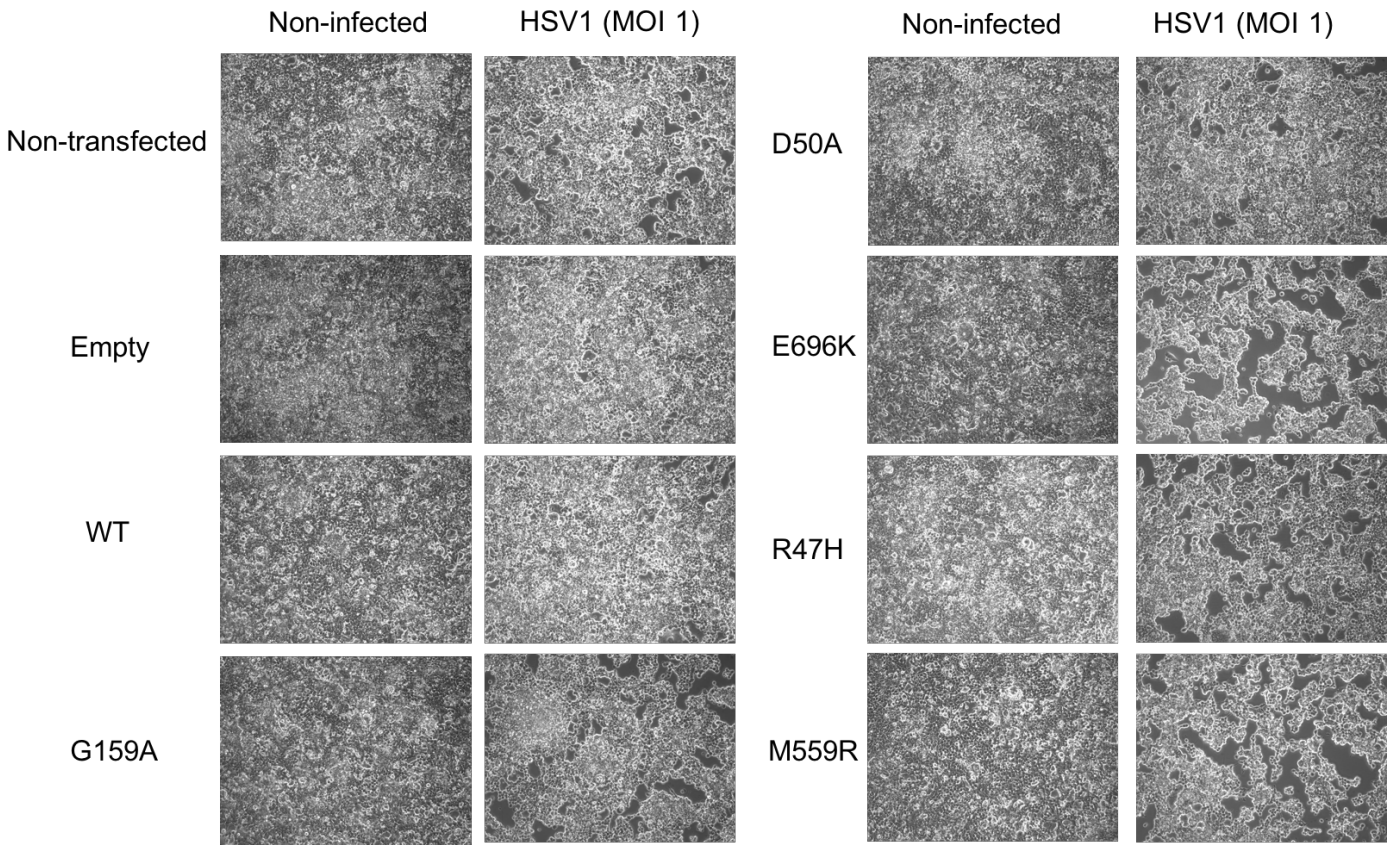


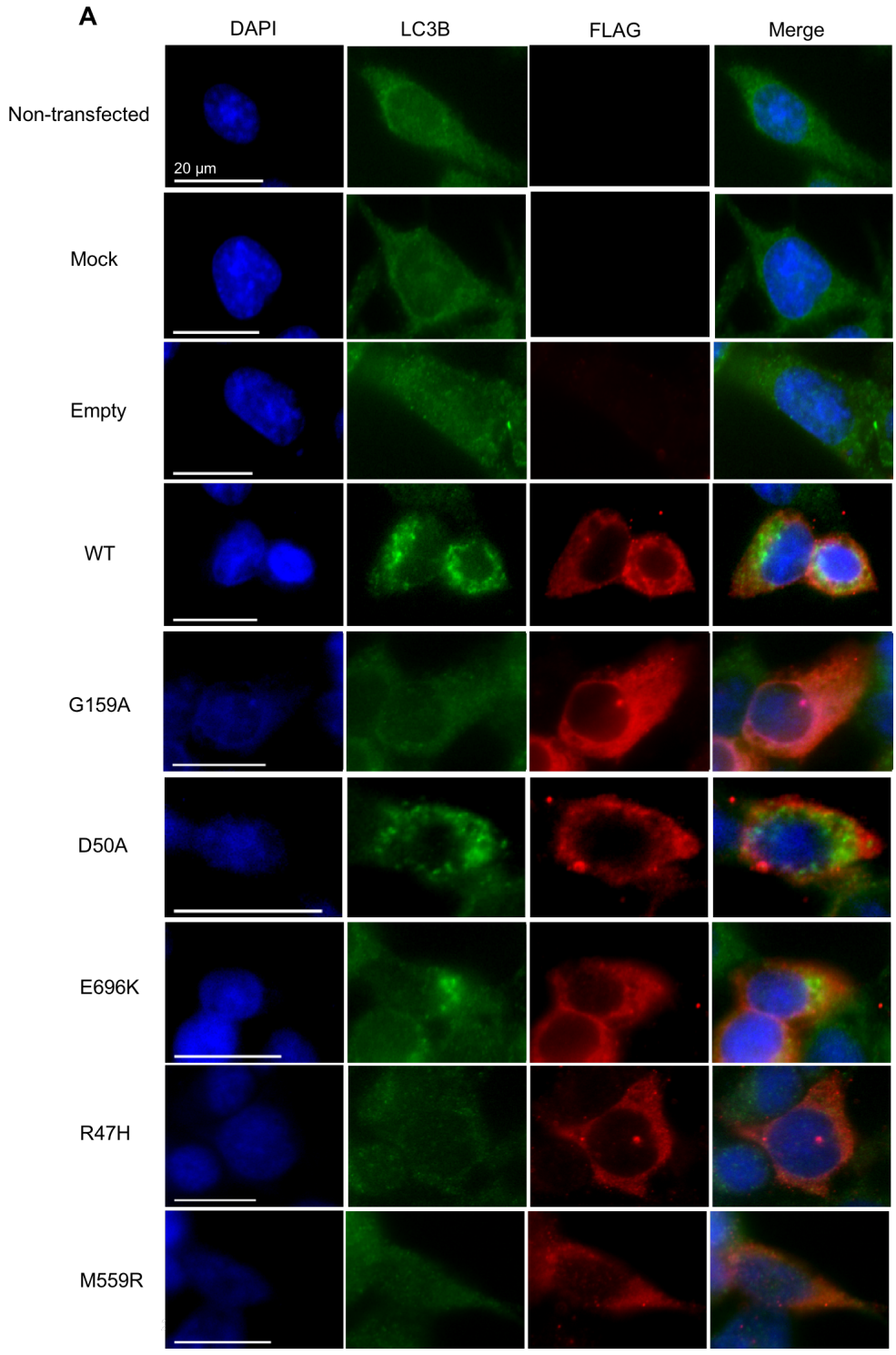
Figure 5.4. Effect of various TBK1 mutations on cell susceptibility to HSV1 infection. HEK293T/miRTBK1 cells were transfected with various TBK1 mutants or WT TBK1 and subsequently infected with HSV1 of MOI 1 for 24 hours before phase images of cells were taken. Experiment was done once (*n* = 1).

5.3. Kinase-dead TBK1 mutants impaired LC3B puncta formation

To better understand the role of TBK1 in HSV1-induced autophagy, I first assessed TBK1 localisation in HEK293T/miRTBK1 cells by reconstituting the cells with WT TBK1 by transfection with FLAG-tagged WT TBK1 and examining the subcellular distribution of TBK1 by immunofluorescence imaging. Overexpressed WT TBK1 appeared diffuse throughout the cytoplasm of HEK293T/miRTBK1 cells and did not co-localise with LC3B structures (Figure 5.5A). This could be attributed to the nature of HEK293 cell line that has heightened protein expression (Thomas & Smart, 2005) resulting in atypical localisation of TBK1 when overexpressed. This unfortunately made this system less informative for assessing TBK1 localisation and/or interaction with LC3B. This is in contrast with other cells lines such as human HeLa and A549 epithelial cells, which express TBK1 in puncta structures when transiently overexpressed, allowing the assessment of TBK1 intracellular localisation and activity (Goncalves *et al.*, 2011; Thurston *et al.*, 2009; Sparrer *et al.*, 2017; Newman *et al.*, 2012). Future selection of cell line for microscopy with the interest of assessing TBK1 localisation should take this factor into consideration. HeLa cell line is extensively utilised in various research areas including autophagy, which makes it a more appropriate cell line for the purpose of this experiment.

Strikingly, I observed a formation of LC3B puncta in cells that were overexpressing WT TBK1 compared to mock-, empty-, or non-transfected cells, in the absence of autophagy inducer, revealing a role for TBK1 in autophagosome formation (Figure 5.5A). The number of WT TBK1-positive cells that were LC3B puncta-positive was half of the total of WT TBK1-positive cells (Figure 5.5B). However, I suspect that this

effect on autophagosome formation would be more pronounced with the stimulation of autophagy by using inducers such as rapamycin or infection. The role of TBK1 in promoting autophagosome formation and maturation has been illustrated previously, where knockdown or inhibiting the function of TBK1 results in a reduction in LC3B puncta formation (Pilli *et al.*, 2012; Moore & Holzbaur, 2016).



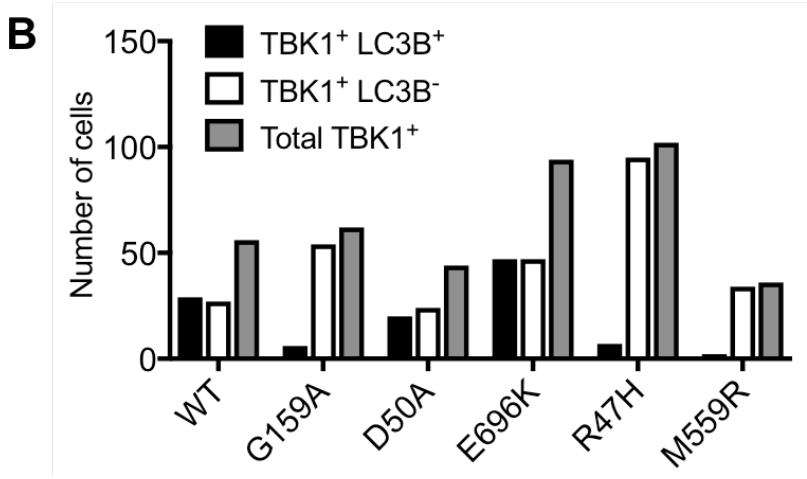


Figure 5.5. Effect of TBK1 mutant overexpression in HEK293T/miRTBK1 cells. (A) HEK293T/miRTBK1 cells were transfected with FLAG-tagged WT or mutant TBK1, empty pEF BOS vector, or mock (L2000), and fixed 24 hours later. Cells were stained for FLAG (red) and endogenous LC3B proteins (green). DAPI (blue) was used to stain the nuclei. Scale bar, 20 μm. **(B)** Number of TBK1-positive cells that were either LC3B puncta-positive ($TBK1^+$ $LC3B^+$) or negative ($TBK1^+$ $LC3B^-$) was counted. Data were derived from a single experiment (*n* = 1).

Having observed the ability of transiently overexpressed WT TBK1 in inducing LC3B puncta in HEK293T/miRTBK1 cells in a non-autophagy-induced condition, I then assessed the effect of G159A, D50A, E696K, R47H and M559R TBK1 mutants on LC3B puncta formation. Similarly, all TBK1 mutants appeared diffuse throughout the cells; hence I was not able to deduce the effect of the mutation on TBK1 localisation with respect to LC3B protein (Figure 5.5A). I found that cells that were overexpressing D50A and E696K TBK1 were able to induce LC3B puncta similar to cells overexpressing WT TBK1. However, cells that were overexpressing G159A, R47H and M559R TBK1 could not form LC3B puncta, suggesting impairment in autophagosome formation (Figure 5.5A). Interestingly, this pattern is correlated to the functionality of their kinases (Table 5.1). E696K mutant TBK1 has been

previously shown to have functional kinase activity as shown by its IFN-inducing ability. In contrast, G159A, R47H, and M559R have in common impaired kinase function (Herman *et al.*, 2012; Freischmidt *et al.*, 2015; Ahmad *et al.*, 2016). Although HEK293T/miRTBK1 cells are not useful for assessing TBK1 localisation we could still infer the effect of TBK1 on autophagy in this system.

5.4. HSV1-induced autophagy requires another component in addition to TBK1

HEK293T/miRTBK1 cell line was further characterised by assessing its autophagy response to HSV1 infection using immunofluorescence. I infected HEK293T and HEK293T/miRTBK1 cells with HSV1 of MOI 0.001 for 24 hours. In both HEK293T and HEK29T/miRTBK1 cell lines, I did not observe the formation of cytoplasmic LC3B phenotype in ICP4-negative cells that I did in control fibroblasts, after 24-hour infection with HSV1. However, both cell lines showed the formation of perinuclear LC3B puncta in ICP4-positive cells (Figure 5.6). Consistently, using high dose infection of MOI 10, I did not observe the formation of cytoplasmic LC3B phenotype after 3 hours of infection in both cell lines as I did in control fibroblasts. In contrast, I observed the occasional formation of perinuclear LC3B at 3 h.p.i., which appeared more uniformly at 8 h.p.i. (Figure 5.6).

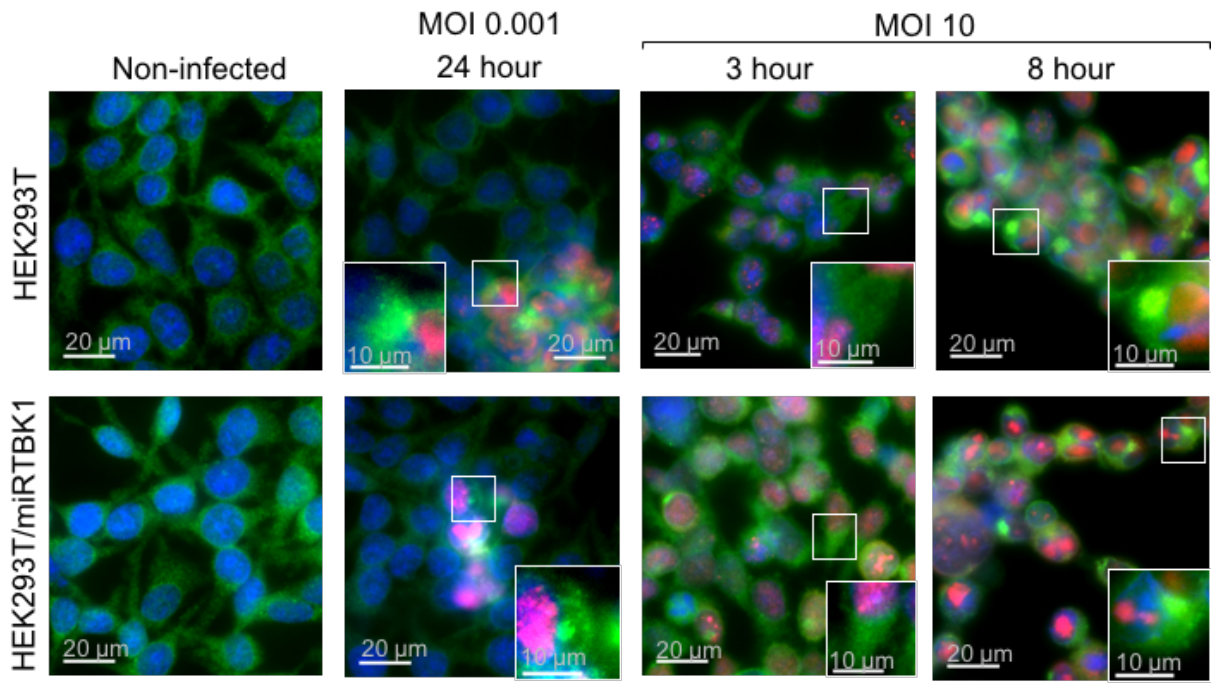


Figure 5.6. HEK293T and HEK293T/miRTBK1 cell lines were incapable of inducing cytoplasmic LC3B phenotype following HSV1 infection. HEK293T and HEK293T/miRTBK1 cells were grown on coverslips, infected with WT HSV1 at dose MOI 10 for 3 or 8 hours, or at dose MOI 0.001 for 24 hours, before being fixed and stained for endogenous LC3B (green) and HSV1 ICP4 (red) proteins. DAPI (blue) was used to stain for nuclei. Inset is magnified view of the area marked in the box of each representative image. Experiment was repeated at least three times. Scale bar, 20 μm, scale bar of insets, 10 μm.

The absence of HSV1-induced cytoplasmic LC3B puncta phenotype in both HEK293T and HEK293T/miRTBK1 cells suggests that these cell lines may not express a protein that is crucial for this phenotype. HSV1 dsDNA-induced autophagy has been shown to be dependent on STING (Rasmussen *et al.*, 2011), a protein adaptor downstream of multiple cytosolic DNA sensing pathways and upstream of TBK1 in these pathways. I assessed the expression of endogenous STING across cell lines: HEK293T, HEK293T/miRTBK1 as well as HSE patient-derived fibroblasts. In contrast to other cell lines, HEK293T and HEK293T/miRTBK1 cell lines did not

express endogenous STING (Figure 5.7). I speculate that STING is another factor that is required for this cytoplasmic LC3B phenotype induction, in addition to TBK1.

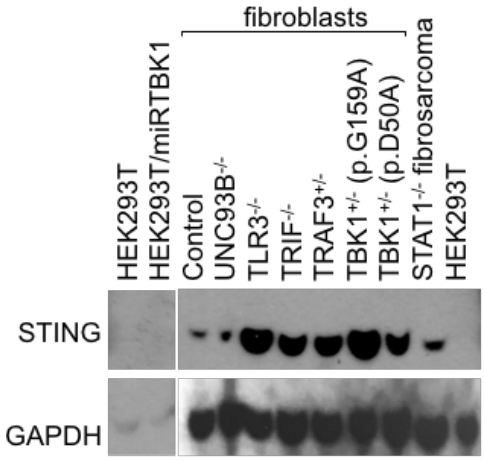


Figure 5.7. Endogenous expression of STING in various cell lines. Whole cell lysates collected from cultured cells were electrophoresed and immunoblotted for endogenous STING protein. GAPDH was used as a loading control. Blots are representative of two independent experiments (*n* = 2).

5.5. Discussion

The impairment of HSE patient-derived fibroblasts carrying p.G159A TBK1 mutation in mounting HSV1- or HSV1 dsDNA-induced autophagy prompted us to investigate the molecular function of TBK1 in HSV1-induced autophagy. I developed a TBK1-negative HEK293T/miRTBK1 cell line to approach this question. Overexpressing G159A, E696K, R47H, and M559R TBK1 mutants led to enhanced replication of HSV1 in the cells, suggesting a general impairment in HSV1 control caused by defective TBK1 in inducing IFN and/or autophagy. Whilst G159A has been previously shown by Herman and colleagues to cause enhanced HSV1 replication (Herman *et al.*, 2012), this is the first demonstration of the effect of ALS-associated E696K, R47H and M559R mutants on HSV1 replication. R47H and

M559R mutants have defective IFN-inducing function, which presumably led to the uncontrolled HSV1 replication. However, E696K TBK1 appeared to be equally susceptible to HSV1 infection despite having intact IFN-inducing function (as tested by TBK1 overexpression-induced IFN reporter assay) (Freischmidt *et al.*, 2015). Whether or not this is a direct cause of its abrogated OPTN-binding ability, impaired anti-viral autophagy function or other unknown defect in anti-viral pathways caused by this mutation is not clear. D50A TBK1 however, did not lead to similar susceptibility to HSV1. Additionally, I did not observe impaired HSV1-induced autophagy in TBK1$^{+/-}$ (p.D50A) fibroblasts. Considering the cell type-specificity of HSV1-induced autophagy, reconstituting D50A mutation in neuronal cells would be more illuminating, where this mutation may exert its effect (Yordy *et al.*, 2012). My preliminary assessment on the effect of TBK1 mutants on HSV1 infection was done qualitatively based on GFP fluorescence tag on the virus from a single experiment, hence the outcome of this experiment must be taken with some reservations.

Immunofluorescence labelling in HEK293T/miRTBK1 revealed a diffuse pattern of overexpressed TBK1. Overexpressed TBK1 was shown to occupy distinct localisation in other cell lines which specifies the pathway it participates in. In mitophagy and xenophagy, TBK1 is recruited to autophagosome by the help of autophagy adaptors OPTN and NDP52 respectively (Goncalves *et al.*, 2011; Thurston *et al.*, 2009; Moore & Holzbaur, 2016). Because overexpression leads to a diffuse rather than distinct localisation of TBK1 in HEK293T/miRTBK1 cells, therefore I was unable to discern the effect of HSV1 infection and/or autophagy on TBK1 distribution.

Nevertheless, this cell line could be used to assess the effect of TBK1 overexpression on autophagy. TBK1 has been shown to be crucial for efficient autophagosome formation (Thurston *et al.*, 2016). In anti-bacterial autophagy, TBK1 kinase activity was demonstrated to be essential for the recruitment of WIPI2, a protein that binds to the PI(3)K-generated autophagosomal protein PI(3)P to promote the formation of anti-bacterial autophagosome (refer to Figure 1.4) (Dooley *et al.*, 2014; Thurston *et al.*, 2016). My finding showed that both M559R and R47H TBK1 overexpression did not induce formation of autophagosomes. Unlike M559R TBK1 whose kinase and OPTN-binding functions are both impaired, R47H TBK1 was previously shown to have defective kinase but was able to bind OPTN (refer to Table 5.1) (Freischmidt *et al.*, 2015; Ahmad *et al.*, 2016). However, given the upstream role of TBK1 kinase activity in regulating autophagosome formation, R47H TBK1 may not be able to mediate efficient autophagy despite being able to bind OPTN. Previous chapters showed that TBK1$^{+/-}$ (p.G159A) fibroblasts have a selective impairment in the formation of cytoplasmic LC3B puncta following HSV1 infection. Whether this HSV1-specific impairment is mediated by its kinase domain function in promoting xenophagic autophagosome formation will make an interesting pursuit of study, which should involve complementing cells with TBK1 kinase-dead mutant and using inhibitors that prevent autophagosome formation. Examples of such inhibitors are wortmannin and 3-methyladenine which block PI(3)K VPS34 from producing PI(3)P proteins, abrogating the recruitment of WIPI2 to autophagosomes and therefore autophagosome formation. By blocking autophagosome formation and by using TBK1 with defective kinase activity during HSV1 infection will help unravel the role of TBK1 in mediating autophagosome formation. Overexpression of E696K TBK1, which has intact kinase function, induced autophagosome formation despite having

faulty OPTN-binding function. This suggests OPTN-binding was not essential for autophagosome formation in this system. Additionally, this overexpression occurred in a non-selective autophagy setting where adaptor-binding function was not required. Performing similar experiment with induction of selective autophagy, such as mitophagy or xenophagy, may reveal the effect of E696K TBK1. Indeed, E696K TBK1 has been shown to impair mitophagy by decreasing autophagosome formation on target mitochondria as OPTN was not able to bind and recruit it the mitochondria (Moore & Holzbaur, 2016). Nonetheless, the observation on the presence of autophagosomes following overexpression of TBK1 in HEK293T cells should be approached with caution as its relevance is still unknown.

In the previous chapters, I demonstrated that HSV1-induced autophagy in human fibroblasts was TBK1-dependent and produced cytoplasmic LC3B puncta phenotype early in HSV1 infection. I could not recapitulate this phenotype in HEK293T/miRTBK1 cells, or in HEK293T cells that endogenously express TBK1. This indicates the requirement for another component, additional to TBK1, to activate HSV1-induced cytoplasmic LC3B puncta phenotype. A report has demonstrated the requirement for STING in triggering HSV1 dsDNA-induced autophagy (Rasmussen *et al.*, 2011). Following immunodetection, both HEK293T and HEK293T/miRTBK1 cell lines did not express endogenous STING, whereas patient-derived fibroblasts that were used for this study including $TBK1^{+/-}$ (p.G159A) fibroblasts, all expressed this protein. I speculate the requirement for both STING and TBK1 in mounting HSV1-induced cytoplasmic LC3B puncta response. Further investigation involving elucidation of STING and TBK1 molecular and functional roles will be required to better illuminate this aspect of HSV1-driven autophagy.

Chapter 6

6. Discussion and Future Directions

6.1. General discussion

Autophagy has been increasingly appreciated in anti-viral innate immunity highlighting its protective effects during viral infection, which it exerts by 1) tagging viral components for subsequent autophagosomal degradation (Orvedahl *et al.*, 2010), 2) bringing in viral components to intracellular TLRs for innate immune activation (Lee *et al.*, 2007), and 3) enhancing antigen presentation on MHC complexes by helping antigen loading (English, Chemali & Desjardins, 2009; English *et al.*, 2009). Whilst the role of TBK1 in autophagy has been described in bacterial infection, protein aggregopathies, and mitophagy (Thurston *et al.*, 2009; Wild *et al.*, 2011; Korac *et al.*, 2013; Pilli *et al.*, 2012; Heo *et al.*, 2015; Richter *et al.*, 2016; Thurston *et al.*, 2016), it has been slowly gaining attention in HSV1 infection. At least four HSV1 proteins (ICP34.5, UL46, ICP27, VP24) have been identified to target this kinase and inhibit its function in inducing anti-viral IFN (Verpooten *et al.*, 2009; Christensen *et al.*, 2016; Zhang, Su & Zheng, 2016; Deschamps & Kalamvoki, 2017). Whilst both IFNs and autophagy are implicated in anti-HSV1 immunity, their relative contribution towards overall immunity is still unclear.

In this present work, I 1) characterised autophagy responses of human dermal skin fibroblasts derived from HSE patients, born with single-gene mutations in *UNC93B, TLR3, TRIF, TRAF3* and *TBK1,* to multiple stimuli (Chapter 3); 2)

characterised HSV1-induced autophagy phenotypes in human dermal fibroblasts (Chapter 4); 3) assessed the involvement of TBK1 in HSV1-induced autophagy (Chapter 4); and 4) demonstrated the cytoprotective role of autophagy in human HSV1 infection (Chapter 4). These studies provide insight into host innate immune response during early HSV1 infection and offer clues into the mechanism by which autophagy is activated following HSV1 infection in human fibroblasts to promote cytoprotection.

6.1.1. Poly(I:C) and HSV1 dsDNA induce autophagy in human dermal fibroblasts

Generally, anti-viral IFNs constitute the first response following infection (Chew, Taylor & Mossman, 2009). Recently, autophagy has also been shown to provide some degree of anti-viral defence, with the field showing a growing interest in identifying factors – host or pathogen – that trigger this cell autonomous pathway as well as mediators that facilitate the selective targeting of virions and viral component (Tallóczy, Virgin & Levine, 2006; Orvedahl *et al.*, 2010).

HSV1 dsRNA produced during infection is thought to engage with the endosomal TLR3 receptor, which triggers the production of downstream IFNs and eventually a plethora of ISGs (Alexopoulou *et al.*, 2001). How HSV1 dsRNA may trigger autophagy is still unclear. A report has shown that intracellular TLR3 is also present in autophagosomes that are decorated with LC3 suggesting that autophagy has the capacity to engulf and deliver

intracellular dsRNAs to endosomes, exposing them to TLR3 (Gorbea *et al.*, 2010). TLR3, among other selected TLRs, has been shown to induce autophagy following stimulation by its ligand poly(I:C) in various cell lines. However, the significance of TLR3-mediated autophagy or its relevance during infection is still not clear (Delgado *et al.*, 2008; Tormo *et al.*, 2009). Apart from the TLR3 receptor, dsRNA can also bind to other dsRNA receptors such as MDA5 and RIG-I as well as PKR (Sen & Peters, 2007). To date, there is no report addressing MDA5- or RIG-I-mediated HSV1-induced autophagy. Reports have shown that naked poly(I:C) is sensed by endosomal TLR3, whereas transfected poly(I:C) is sensed by cytosolic MDA5 or RIG-I receptors (Kato *et al.*, 2008, 2005; Gitlin *et al.*, 2006). My study only applied naked poly(I:C) and did not attempt on transfecting cells with poly(I:C) to asses autophagy induction. Hence I was only able to consider the role of TLR3 signalling in my observation, and not of MDA5 or RIG-I signalling. Furthermore, my observation using poly(I :C) is limited to the TLR3-IFN pathway that is engaged in uninfected setting. It therefore does not address the relative contribution of different innate immune sensors towards dsRNA-induced autophagy during HSV1 infection. Follow-up studies may include using transfected or naked poly(I :C) or viral RNA derived from HSV1 replication, to help dissect the contribution of different dsRNA receptors towards autophagy.

My finding showed that poly(I:C)-induced autophagy is dependent on three upstream components of the TLR3-IFN pathway: UNC93B, TLR3, and TRIF. Therefore, it is tempting to speculate that poly(I:C)-induced autophagy in

fibroblasts occurs via TLR3 recognition which implicates the role of the TLR3-autophagosome platform in inducing dsRNA-activated autophagy as UNC93B, TLR3 and TRIF form a complex on the face of endosome following TLR3 activation (Shi & Kehrl, 2008; Gorbea *et al.*, 2010). It is conceivable that the absence of any of these components would abrogate this autophagy induction as demonstrated by fibroblasts deficient in these proteins. Furthermore, this poly(I:C)-induced autophagy is partially dependent on TBK1, consistent with its partial role in the TLR3 signalling pathway. Although our study suggests that TLR3-mediated autophagy is unlikely to underlie HSE, it has helped provide further insight into this autophagy-inducing pathway which has been implicated in other diseases such as cardiomyopathy and cancers (Harashima *et al.*, 2012; Zhan *et al.*, 2014; Kondo *et al.*, 2005; Gorbea *et al.*, 2010).

My finding showed that HSV1 infection, and particularly its dsDNA, induces autophagy in a TBK1-dependent manner. This is in concordance with two reports that showed that HSV1 non-infectious L-particles (composed of only nucleocapsid and viral genome) and HSV1 dsDNA stimulation trigger autophagy in human HFFF2 fibroblasts and mice BM-DCs respectively (Rasmussen *et al.*, 2011; McFarlane *et al.*, 2011). Although it is generally believed that the HSV1 dsDNA genome delivered in capsids is not liberated until it reaches the nucleus, a study has shown that HSV1 dsDNA can dissociate from its capsid in the cytosol within the first 2-4 hours following infection (Horan *et al.*, 2013; Rasmussen *et al.*, 2011). The main goal of viral dsDNA is to enter the nucleus and initiate viral replication. The fact that it can

also be present in free form in the cytosol this early during infection allowing it to expose viral presence is puzzling. This raises an interesting possibility that this dissociation from capsid may result from host intervention. Indeed, a report by Horan and colleagues showed that the HSV1 capsid is shuttled to the proteasomal degradation system following infection, which degrades and liberates HSV1 dsDNA into the cytosol of primary human monocyte-derived macrophages (MDMs) (Horan *et al.*, 2013). Although I did not determine whether HSV1 capsid is subjected to similar degradation route in human dermal fibroblasts, I speculate that the exposed HSV1 dsDNA may subsequently be detected by a cytosolic dsDNA sensor that can activate autophagy. The dsDNA sensor IFI16 was reported to bind to HSV1 dsDNA, which then co-localises with STING and TBK1 to mediate IFN production (Horan *et al.*, 2013). Furthermore, the dsDNA sensor cGAS holds a dual role in the clearance of *M. tuberculosis* infection in BMDMs where detection of bacterial DNA results in TBK1-dependent autophagy induction as well as IFN production (Watson *et al.*, 2015; Watson, Manzanillo & Cox, 2012). The report further showed that the autophagy induction is independent of the IFN output downstream of the cGAS-STING-TBK1 circuit as *Irf3-/-* BMDMs were able to target *M. tuberculosis* to the autophagosomes (Watson, Manzanillo & Cox, 2012). Given the capacity of dsDNA signalling to activate autophagy, I speculate that HSV1 dsDNA may be detected by any of these two reported dsDNA cytosolic sensors, which function is dependent on TBK1.

6.1.2. Dynamics of autophagy during HSV1 infection

The autophagy-inducing capability of HSV1 is not new and has been extensively documented in various infection systems *in vitro* and *in vivo* (Tallóczy, Virgin & Levine, 2006; Tallóczy *et al.*, 2002; English *et al.*, 2009; Ma *et al.*, 2012). However, there have been only two reports that looked at the kinetics of autophagy response during infection, which hinted at time-dependent induction and anti-viral role of autophagy in murine cells (Katzenell & Leib, 2016; Radtke *et al.*, 2013). Unlike anti-viral IFNs, autophagy is constitutive and hence may play a role during early, rather than late, in infection. My study and a report on murine BM-DCs by Rasmussen *et al.* are in support of this hypothesis where HSV1 infection triggers autophagy during early infection (Rasmussen *et al.*, 2011). In human dermal fibroblasts, this is represented by the formation of host-protective cytoplasmic LC3B puncta, which is TBK1-dependent, but TLR3- and IFN-independent. HSV1 encodes for two autophagy antagonists early protein ICP34.5 and late protein Us11 (Orvedahl *et al.*, 2007; Lussignol *et al.*, 2013). My report showed that the formation of this cytoplasmic LC3B puncta phenotype was not regulated by ICP34.5 as ICP34.5-deficient HSV1 strain was still able to induce this phenotype in fibroblasts (Chapter 4). The involvement of Us11 is also unlikely as this phenotype occurs early in infection.

Additionally, this cytoplasmic LC3B puncta formation can be induced in a paracrine manner in non-infected fibroblasts neighbouring an infected cell where it speculatively represents a ‘danger’ signal. The presence of this

protective autophagy is therefore transient in fibroblasts and may not exert an obvious protective impact on viral replication. Indeed, my finding showed that upregulating autophagy did not alter HSV1 replication in fibroblasts. How this 'danger' signal is delivered and to what extent the resulting autophagy induction contributes towards immunoprotection and/ or confers resistance to infection in non-infected recipient cells warrants further investigation. To date, there is only a single report on paracrine induction of autophagy, which occurs in human pregnancy. Human placental trophoblasts are shown to secrete exosomes that contained C19MC miRNA. Exosomes are evolutionary conserved vesicles that are secreted by both eukaryotes and prokaryotes, into the extracellular space. They can carry proteins, lipids as well as RNAs, and hold various functions including in cell-to-cell communication and infections (Colombo, Raposo & Théry, 2014). Exosomes are derived from endosomes that are produced in intracellular multivesicular bodies, which are directed to the plasma membrane where they fuse with, leading to their secretion as exosomes (Colombo, Raposo & Théry, 2014). These C19MC miRNA-containing exosomes secreted by maternal trophoblasts were shown to confer resistance against multiple viral infections, including HSV1, to non-placental cells by upregulating autophagy in the recipient cells (Delorme-Axford *et al.*, 2013). To the best of my knowledge, there is no direct link associating TBK1 with cellular secretory pathway. Two reports have shown the presence of TBK1 in cytoplasmic LC3B-positive puncta that also stained for STING and dsDNA receptor IFI16, as well as Sec5 following dsDNA stimulation of the cells (Ishikawa, Ma & Barber, 2009; Saitoh *et al.*, 2009; Horan *et al.*, 2013). Similar puncta staining was also observed following HSV1 infection (Ishikawa,

Ma & Barber, 2009; Horan *et al.*, 2013). Sec5 is a component of an exocyst complex that mediates the tethering of endosomes at the plasma membrane that are destined for exocytosis. Whether this Sec5-mediated secretion is the exit route for the 'danger' signal, and whether TBK1 regulates exocyst function in exocytosis are unknown. The function of exocyst is subjected to regulation by kinases including cdk1 and protein kinase C (PKC) (Wu & Guo, 2015). PKC, in particular, phosphorylates Sec5 to mediate continuous endosomal trafficking to the plasma membrane for exocytosis (Chen *et al.*, 2011). While Chien *et al.* showed that Sec5 binds to TBK1 to promote its kinase activity in IFN production (Chien *et al.*, 2006); it begs a question whether Sec5 is also regulated by TBK1 phosphorylation to regulate secretion of this dsDNA-containing endosomes.

Late in infection, HSV1 induced the formation of perinuclear LC3B dense structures in fibroblasts. Unlike cytoplasmic LC3B puncta, this perinuclear LC3B phenotype occurs independent of TBK1. It is also not regulated by HSV1 ICP34.5 and co-localises with Golgi bodies. Similar phenomenon has been observed in murine macrophages infected with HSV1, which is termed NEDA (see Chapter 1). However, the formation of NEDA seemed to depend on the role of ICP34.5 in modulating host translation (Radtke *et al.*, 2013). Whether the perinuclear LC3B phenotype observed in fibroblasts are similar to that of NEDA remains a question. NEDA has been shown to have a four-layered membrane morphology, hence future study could employ electron microscopy to confirm the phenotype observed in this study. The relevance of

this phenotype in the context of viral pathogenesis is still puzzling which prompts future investigation.

6.1.3. TBK1 is a crucial component of autophagy that mediates protection against HSV1

Over the past decades, TBK1 has become known beyond its traditional IFN-inducing function, particularly for its role in mediating various modes of autophagy such as mitophagy and xenophagy (Thurston *et al.*, 2016, 2009; Wild *et al.*, 2011; Pilli *et al.*, 2012; Richter *et al.*, 2016; Heo *et al.*, 2015). Adding onto previous studies that revealed the selective nature of HSV1-induced autophagy (Sparrer *et al.*, 2017; Katzenell & Leib, 2016), my study showed that HSV1-induced autophagy is p62- and NDP52-mediated and that TBK1 may mediate these two autophagy receptors. Therefore, it is not surprising that TBK1 deficiency in HSV1 infection would render autophagy dysfunctional in this study.

I found that cells that have impaired IFN production were able to form cytoplasmic LC3B phenotype following HSV1 infection, which suggests that HSV1-induced autophagy in early infection is independent of IFN. However, it is possible that later in infection, autophagy may regulate a positive feedback towards inflammation by promoting antigen presentation and regulating PRRs (Levine, Mizushima & Virgin, 2011). Indeed, this aspect of HSV1 infection has been explored by Radtke *et al.* and English *et al.* which demonstrated the role of autophagy in facilitating the processing, loading, and presentation of HSV1

antigens on MHC class I to stimulate $CD8^+$ T cell responses (Radtke *et al.*, 2013; English, Chemali & Desjardins, 2009; English *et al.*, 2009). Autophagy may also negatively regulate IFN responses to prevent excessive inflammation later in infection, which is important in preventing tissue damage. It can help clear PAMPs and DAMPs as well as degrade PRRs to dampen down the inflammatory responses (Levine, Mizushima & Virgin, 2011).

Furthermore, I found that the production of the 'danger' signal that mediates paracrine autophagy is TBK1-dependent. This paracrine autophagy phenomenon is astounding as this expands the scope of autophagy, which is traditionally known as a mere recycling bin. Not only can it degrade full virions (Tallóczy, Virgin & Levine, 2006) or viral protein (Orvedahl *et al.*, 2010) as demonstrated by others, I found that it can mediate communication between infected and nearby non-infected cells in the wake of HSV1 infection. Complimentary to a report on neuronal cells (Orvedahl *et al.*, 2010), I found that autophagy upregulation enhanced the survival of fibroblasts during HSV1 infection, without altering viral replication, suggesting a unique mechanism adapted not only by neuronal cells but also fibroblasts.

In addition to the finding of TBK1 having a role in HSV1-driven autophagy, LRBA has also been previously described by Lopez-Hererra *et al.* to play both immunological and autophagy functions. LRBA deficiencies found in patients with autoimmunity were linked to impaired autophagy function, on top of defective B cell proliferation and differentiation into antibody-secreting cells (Lopez-Herrera *et al.*, 2012). LRBA-deficient B cells showed an accumulation

of autophagosomes that would have normally been cleared by their fusion with lysosomes (Lopez-Herrera *et al.*, 2012). The role of LRBA in autophagy is still unclear but is thought to facilitate the autophagosome-lysosome fusion or to involve the lysosomes. This study also showed that the role of LRBA appeared to be restricted to immune cells, as its expression was found to be wide across many human tissues (including the brain) but the clinical phenotype of LRBA-deficient patient was limited to the immune cells (such as B and T cells) (Lopez-Herrera *et al.*, 2012). Given that HSE pathogenesis is restricted to the CNS tissues and HSV1 is strictly a neurotropic virus, the involvement of LRBA in autophagy in the context of HSE pathogenesis is unlikely.

6.2. Future directions

6.2.1. Purpose and mechanism of HSV1-induced paracrine autophagy

The significance of early induction of autophagy towards HSV1 is still unclear. Autophagy-inducing C19MC miRNA packaged in exosomes by placental trophoblasts has been shown to be transferable to non-trophoblast cells, which are otherwise susceptible to a number of viral infections. The autophagy induction resulted in restricted viral replication in these recipient cells, in essence, conferring protection to the developing foetus (Delorme-Axford *et al.*, 2013). It is plausible that fibroblastic induction of autophagy early in infection in neighbouring cells is to transfer protection to cells in the local area, which include innervating neurons – the final destination for HSV1 virus

where it would finally establish latency in the host. A study has shown that HSV1 ICP34.5, which targets TBK1, is particularly crucial for its neuroinvasion to the CNS (Ma *et al.*, 2012). Therefore, it would be of interest to test if the conditioned medium from infected control fibroblasts can induce autophagy in neuronal cells and/or attenuate subsequent HSV1 infection.

It would also be an interesting study to assess if exosomes, known for their versatility in mediating intercellular communication, are the vehicle of this 'danger' signal. An approach for this would involve sonication of nuclease-treated conditioned medium to help disrupt exosomes (as performed by Delorme-Axford *et al*., 2013). My preliminary finding showed that this 'danger' signal is nucleic acid in nature. Exosomal nucleic acids reported so far only include mRNAs and miRNAs (Valadi *et al.*, 2007; Colombo, Raposo & Théry, 2014), which would have also been affected by the nuclease treatment. Although I cannot exclude the possibility of mRNA or miRNA representing this 'danger' signal, my preliminary data suggest the involvement of dsDNA in triggering TBK1-dependent HSV1-induced autophagy. To further investigate this, future work may include isolating exosomes from the conditioned medium and assaying the exosome-enriched samples for the presence of DNA and/or RNA using RNAse or DNAse treatments and/or probing for exosomal markers such as CD9 or CD63 (Colombo, Raposo & Théry, 2014).

6.2.2. HSV1-induced autophagy involves TBK1 and selective autophagy adaptors

The kinase activity of TBK1 has been extensively shown to be crucial in phosphorylating various autophagy adaptors – p62, NDP52, and OPTN (Thurston *et al.*, 2009; Wild *et al.*, 2011; Pilli *et al.*, 2012). While Sparrer *et. al* has recently demonstrated a role for TBK1 in HSV1-induced p62-mediated autophagy (Sparrer *et al.*, 2017), my finding additionally implicates NDP52. This further highlights the role of TBK1 during HSV1 infection. Given non-pathogen specificity of autophagy adaptors, it would be interesting to assess other potential autophagy adaptors that might also be involved and the relative contribution of p62 and NDP52 in HSV1-induced autophagy. Furthermore, my preliminary finding showed that TBK1 may be involved in autophagosome formation which occurs upstream of autophagy. Selected HSE- and ALS-associated TBK1 mutants with impaired IFN-inducing kinase function failed to form autophagosomes in TBK1-depleted human HEK293T cells. A study has demonstrated the role of TBK1 kinase in recruiting WIPI2 phagophore protein, which is required for autophagosome assembly (Thurston *et al.*, 2016). Future study dissecting the role of TBK1 kinase and autophagosome formation using kinase mutant TBK1 and inhibitors of autophagome formation will help illuminate this aspect of autophagy.

Similar to anti-bacterial autophagy, virus infection can lead to the engulfment of the entire virion or viral protein. An electron microscopy (EM) imaging has reported the presence of intact HSV1 virions in autophagosomes in infected

MEFs (Tallóczy, Virgin & Levine, 2006). There has only been one report that demonstrated the involvement of selective autophagy adaptor in targeting viral component. Sindbis virus infection was shown to activate autophagy, which subsequently recruited p62 receptor to target and bring Sindbis viral capsid into autophagosomes for degradation (Orvedahl *et al.*, 2010). Evidently, the role of p62 in autophagy has been demonstrated in neurodegenerative or developmental pathologies, bacterial pathogenesis, and mitophagy, as it is able to recognise various substrates varying from protein aggregates, organelles to microbial components owing to its ubiquitin recognition domain (Matsumoto *et al.*, 2011, 2015; Pilli *et al.*, 2012). Although the interaction between p62 and Sindbis viral capsid has been shown to be ubiquitin-independent, the ability of p62 to recognise particular ubiquitinated HSV1 protein is plausible and may hold similar purpose as in Sindbis viral infection, which is to prevent the death of non-renewable neuronal cells caused by overwhelming viral protein accumulation and aggregation (Orvedahl *et al.*, 2010). To date, a report has shown that HSV1 viral capsid is ubiquitinated in mouse bone marrow-derived macrophages (BMMs) 2 hours following HSV1 infection (Horan *et al.*, 2013). It will be interesting to learn whether HSV1 capsid becomes a target of p62-mediated autophagic degradation.

In this study, I showed that TBK1 is required for producing the ‘danger' signal, as conditioned medium from infected TBK1-deficient fibroblasts was not able to induce autophagy in control fibroblasts. I have not determined whether TBK1 is required for responding to this ‘danger’ signal. To do this, a reciprocal

study involving treatment of TBK1-deficient fibroblasts with conditioned medium from control cells and assaying for their autophagy response would help elucidate this question.

Thus far, the composition of these HSV1-induced cytoplasmic LC3B puncta in fibroblasts and hence its protective mechanism is unknown. Evidence has shown that autophagy can positively and negatively regulate inflammation during infection (Levine, Mizushima & Virgin, 2011). Furthermore, whether they exhibit autophagosomal features or contain selective autophagy adaptors or IFN-inducing components would be an interesting pursuit of study. One can employ electron microscopy to examine autophagosomal features in these HSV1-infected cells, or fluorescence imaging methods such as that of ImageStream® that allows the quantification of fluorescent information, to determine the number of autophagosomes. HSV1 has been shown to induce autophagic clusters that are decorated with p62 in mouse neurons (Katzenell & Leib, 2016). A study also showed that dsDNA or *M. tuberculosis* that are captured in autophagosomes of mouse macrophages and BMDMs respectively, showed colocalisation with cGAS dsDNA sensor, TBK1, and NDP52 in LC3B puncta (Watson *et al.*, 2015; Watson, Manzanillo & Cox, 2012). Whereas the cGAS-TBK1 pathway has been shown to be important for anti-viral IFN production in HSV1 infection, its involvement in mediating HSV1-induced autophagy is unknown (Li *et al.*, 2013; Reinert *et al.*, 2016). IFI16 has also emerged as an important dsDNA sensor that produces anti-viral IFN during HSV1 infection via STING and TBK1 (Li *et al.*, 2013; Reinert *et al.*, 2016; Unterholzner *et al.*, 2010; Horan *et al.*, 2013). HSV1 dsDNA was

identified in IFI16-, STING- and TBK1-positive endosomes in primary human MDMs (Horan *et al.*, 2013). Given the involvement of STING and TBK1 in regulating xenophagy, I speculate that the HSV1-induced cytoplasmic LC3B puncta in fibroblasts may contain STING and TBK1. Future work involving identification of these two proteins and other potential autophagy proteins (such as p62 or NDP52) in these HSV1-induced cytoplasmic LC3B puncta will undoubtedly help reveal the mechanism by which autophagy protects the host and how it is mediated.

6.2.3. Autophagy suppresses inflammation in the CNS

The downside of this study is that it is based on fibroblasts, which limits our observation to autophagy responses in the periphery. Given the 'normal' autophagy phenotypes observed in patients' fibroblasts deficient of TLR3, TRIF, TRAF3 and TBK1 (p.D50A), and the established role of anti-viral IFNs in controlling HSV1 in the periphery, autophagy observations we made are not fully illuminating. Indeed, reports have emphasised a dominant role for autophagy in the CNS, rather than in the periphery, as a defence mechanism against HSV1 (Yordy & Iwasaki, 2013; Yordy *et al.*, 2012). Nonetheless, it has helped us identify TBK1 as a crucial inducer of autophagy during HSV1 infection.

Interestingly, amongst the HSE patients used in this study, the HSE patient carrying p.G159A *TBK1* mutation particularly suffered from a severe neurological deficit, including motor dysfunction, impaired cognitive ability and

epilepsy. This may suggest the importance of TBK1 in CNS defence against HSV1 infection where it may determine the long-term prognosis of HSE. Given the anti-inflammatory nature of autophagy as demonstrated in other various neurodegenerative diseases, it is tempting to hypothesise the relevance of TBK1 in autophagy-mediated control of inflammation, particularly in the CNS, to limit tissue damage and control viral replication during HSV1 infection and/ or reactivation (Ahmad *et al.*, 2016). Therefore, a promising avenue extending from this study is to explore the involvement of TBK1 in neuronal autophagy during infection and the effect of upregulating autophagy in HSV1 infected-neurons on viral replication, spread, and neuronal survival.

Part of the original plan of this study was to apply similar autophagy phenotyping assays on neuronal cells carrying clustered regularly interspaced short palindromic repeats (CRISPR)-CRISPR-associated protein 9 (Cas9)-generated *TBK1* p.G159A mutation. Deriving neurons from iPS cells created from TBK1$^{+/-}$ (p.G159A) patient-derived fibroblasts would be ideal for this study and this technique has been successfully applied to assess the importance of the TLR3-IFN pathway in neurons differentiated from HSE patient fibroblast-derived iPS cells (Lafaille *et al.*, 2012). However, due to ethics restriction, I was not able to do so. To circumvent this, I optimised the assays on a commercial human control fibroblast cell line and derived iPS cells from them through Axol Bioscience company, which specialises in the generation of human iPS and neuronal cells. However, I suffered severe delays after the derivation of iPS cells that resulted in an abnormal karyotype. I only obtained iPS cells with a normal karyotype in the last few months of this

study and due to time restriction, at the time of writing; I am only at the stage of neural stem (NS) cells derivation from these iPS cells. I have also begun optimising autophagy assays on neurons that were differentiated from a commercial NS cell line (see Appendix 1). Nonetheless, having characterised the autophagy phenotype of fibroblasts and hopefully, their corresponding isogenic neurons would be the next step. Thereon, creating CRISPR-Cas9-delivered point mutation p.G159A in *TBK1*, and/or other HSE-associated mutations will undoubtedly help us better understand the role of autophagy in HSV1-infected CNS.

In summary, my study has helped extend and refine the role of autophagy in HSV1 infection. Evasion of autophagy in the CNS by HSV1 and unprecedented finding of paracrine autophagy induced following infection in the periphery portrays an evolutionary battle between the host and HSV1. Future investigation on how autophagy mediates protection and the anti-inflammatory effect will definitely help develop therapeutic compounds that can suppress or alleviate neurological damage caused by HSV1-driven inflammation in HSE.

Bibliography

Abel, L., Plancoulaine, S., Jouanguy, E., Zhang, S.Y., Mahfoufi, N., Nicolas, N., Sancho-Shimizu, V., Alca??s, A., Guo, Y., Cardon, A., Boucherit, S., Obach, D., Clozel, T., Lorenzo, L., Amsallem, D., Berquin, P., Blanc, T., Bost-Bru, C., Chabrier, S., Chabrol, B., Cheuret, E., Dulac, O., Evrard, P., H??ron, B., Lazaro, L., Mancini, J., Pedespan, J.M., Rivier, F., Vall??e, L., Lebon, P., Rozenberg, F., Casanova, J.L., & Tardieu, M. (2010) Age-dependent mendelian predisposition to herpes simplex virus type 1 encephalitis in childhood. *Journal of Pediatrics*. [Online] 157 (4). Available from: doi:10.1016/j.jpeds.2010.04.020.

Ahmad, L., Zhang, S.-Y., Casanova, J.-L., & Sancho-Shimizu, V. (2016) Human TBK1: A Gatekeeper of Neuroinflammation. *Trends in Molecular Medicine*. [Online] 22 (6), 511–527. Available from: doi:10.1016/j.molmed.2016.04.006.

Alexander, D.E., Ward, S.L., Mizushima, N., Levine, B., & Leib, D.A. (2007) Analysis of the Role of Autophagy in Replication of Herpes Simplex Virus in Cell Culture. *Journal of Virology*. [Online] 81 (22), 12128–12134. Available from: doi:10.1128/JVI.01356-07.

Alexopoulou, L., Holt, A.C., Medzhitov, R., & Flavell, R.A. (2001) Recognition of double-stranded RNA and activation of NF-κB by Toll-like receptor 3. *Nature*. [Online] 413 (6857), 732–738. Available from: doi:10.1038/35099560.

Ambjørn, M., Ejlerskov, P., Liu, Y., Lees, M., Jäättelä, M., & Issazadeh-Navikas, S. (2013) IFNB1/interferon-β-induced autophagy in MCF-7 breast cancer cells counteracts its proapoptotic function. *Autophagy*. 9 (3), 287–302.

Andersen, L.L., Mørk, N., Reinert, L.S., Kofod-Olsen, E., Narita, R., Jørgensen, S.E.,

Skipper, K.A., Höning, K., Gad, H.H., Østergaard, L., Ørntoft, T.F., Hornung, V., Paludan, S.R., Mikkelsen, J.G., Fujita, T., Christiansen, M., Hartmann, R., & Mogensen, T.H. (2015) Functional IRF3 deficiency in a patient with herpes simplex encephalitis. *The Journal of Experimental Medicine*. [Online] 212 (9), 1371–1379. Available from: doi:10.1084/jem.20142274.

Barrett, J.C., Hansoul, S., Nicolae, D.L., Cho, J.H., Duerr, R.H., Rioux, J.D., Brant, S. R., Silverberg, M. S., Taylor, K. D., Barmada, M. M., Bitton, A., Dassopoulos, T., Datta, L. W., Green, T., Griffiths, A. M., Kistner, E. O., Murtha, M. T., Regueiro, M. D., Rotter, J. I., Schumm, L. P., Steinhart, A. H., Targan, S. R., Xavier, R. J., Libioulle, C., Sandor, C., Lathrop, M., Belaiche, J., Dewit, O., Gut, I., Heath, S., Laukens, D., Mni, M., Rutgeerts, P., Van Gossum, A., Zelenika, D., Franchimont, D., Hugot, J-P., de Vos, M., Vermeire, S., Louis, E., Cardon, L. R., Anderson, C. A., Drummond, H.,I Nimmo, E., Ahmad, T., Prescott, N. J., Onnie, C. M., Fisher, S. A., Marchini, J., Ghori, J., Bumpstead, S., Gwilliam, R., Tremelling, M., Deloukas, P., Mansfield, J., Jewell, D., Satsangi, J., Mathew, C. G., Parkes, M., Georges, M., Daly, M. J., Parkes, M., Georges, M. & Daly, M.J. (2008) Genome-wide association defines more than 30 distinct susceptibility loci for Crohn's disease. *Nature Genetics*. [Online] 40 (8), 955–962. Available from: doi:10.1038/ng.175.

Le Ber, I., De Septenville, A., Millecamps, S., Camuzat, A., Caroppo, P., Couratier, P., Blanc, F., Lacomblez, L., Sellal, F., Fleury, M.-C., Meininger, V., Cazeneuve, C., Clot, F., Flabeau, O., LeGuern, E., Brice, A., Auriacombe, S., Brice, A., Blanc, F., Couratier, P., Didic, M., Dubois, B., Golfier, V., Hannequin, D., Lacomblez, L., Le Ber, I., Levy, R., Meininger, V., Michel, B.-F., Pasquier, F., Thomas-Anterion, C., Puel, M., Salachas, F., Sellal, F., & Vercelletto, M. (2015)

TBK1 mutation frequencies in French frontotemporal dementia and amyotrophic lateral sclerosis cohorts. *Neurobiology of Aging*. [Online] 36 (11), 3116.e5-3116.e8. Available from: doi:10.1016/j.neurobiolaging.2015.08.009.

Brooks, D.A., Bader, C., Ng, Y.S., Brooks, R.D., Borlace, G.N., & Shandal, T. (2012) At the Intersection of the Pathways for Exocytosis and Autophagy. In: *Crosstalk and Integration of Membrane Trafficking Pathways*. [Online]. p. Available from: doi:10.5772/39111.

Buckley, R.H. (2004) Molecular Defects in Human Severe Combined Immunodeficiency and Approaches to Immune Reconstitution. *Annual Review of Immunology*. [Online] 22 (1), 625–655. Available from: doi:10.1146/annurev.immunol.22.012703.104614.

Campadelli-Fiume, G. & Menotti, L. (2007) *Entry of alphaherpesviruses into the cell*. Cambridge University Press.

Canivet, C., Menasria, R., Rhéaume, C., Piret, J., & Boivin, G. (2015) Valacyclovir combined with artesunate or rapamycin improves the outcome of herpes simplex virus encephalitis in mice compared to antiviral therapy alone. *Antiviral research*. [Online] 123, 105–113. Available from: doi:10.1016/j.antiviral.2015.09.007.

Casrouge, A., Zhang, S.-Y., Eidenschenk, C., Jouanguy, E., Puel, A., Yang, K., Alcais, A., Picard, C., Mahfoufi, N., Nicolas, N., Lorenzo, L., Plancoulaine, S., Senechal, B., Geissmann, F., Tabeta, K., Hoebe, K., Du, X., Miller, R.L., Heron, B., Mignot, C., de Villemeur, T.B., Lebon, P., Dulac, O., Rozenberg, F., Beutler, B., Tardieu, M., Abel, L., & Casanova, J.-L. (2006) Herpes Simplex Virus Encephalitis in Human UNC-93B Deficiency. *Science*. [Online] 314 (5797), 308–312. Available from: doi:10.1126/science.1128346.

Cavignac, Y. & Esclatine, A. (2010) Herpesviruses and Autophagy: Catch Me If You Can! *Viruses*. [Online] 2 (12), 314–333. Available from: doi:10.3390/v2010314.

Chen, X.-W., Leto, D., Xiao, J., Goss, J., Wang, Q., Shavit, J.A., Xiong, T., Yu, G., Ginsburg, D., Toomre, D., Xu, Z., & Saltiel, A.R. (2011) Exocyst function regulated by effector phosphorylation. *Nature Cell Biology*. [Online] 13 (5), 580–588. Available from: doi:10.1038/ncb2226.

Chew, T., Taylor, K., & Mossman, K. (2009) Innate and Adaptive Immune Responses to Herpes Simplex Virus. *Viruses*. [Online] 1 (3), 979–1002. Available from: doi:10.3390/v1030979.

Chien, Y., Kim, S., Bumeister, R., Loo, Y.-M., Kwon, S.W., Johnson, C.L., Balakireva, M.G., Romeo, Y., Kopelovich, L., Gale, M., Yeaman, C., Camonis, J.H., Zhao, Y., & White, M.A. (2006) RalB GTPase-Mediated Activation of the IκB Family Kinase TBK1 Couples Innate Immune Signaling to Tumor Cell Survival. *Cell*. [Online] 127 (1), 157–170. Available from: doi:10.1016/j.cell.2006.08.034.

Chou, J. & Roizman, B. (1994) Herpes simplex virus 1 gamma(1)34.5 gene function, which blocks the host response to infection, maps in the homologous domain of the genes expressed during growth arrest and DNA damage. *Proceedings of the National Academy of Sciences of the United States of America*. 91 (12), 5247–5251.

Christensen, M.H., Jensen, S.B., Miettinen, J.J., Luecke, S., Prabakaran, T., Reinert, L.S., Mettenleiter, T., Chen, Z.J., Knipe, D.M., Sandri-Goldin, R.M., Enquist, L.W., Hartmann, R., Mogensen, T.H., Rice, S.A., Nyman, T.A., Matikainen, S., & Paludan, S.R. (2016) HSV-1 ICP27 targets the TBK1-activated STING signalsome to inhibit virus-induced type I IFN expression. *The EMBO Journal*.

[Online] 35 (13), 1385–1399. Available from: doi:10.15252/embj.201593458.

Cirulli, E.T., Lasseigne, B.N., Petrovski, S., Sapp, P.C., Dion, P.A., Leblond, C.S., Couthouis, J., Lu, Y.-F., Wang, Q., Krueger, B.J., Ren, Z., Keebler, J., Han, Y., Levy, S.E., Boone, B.E., Wimbish, J.R., Waite, L.L., Jones, A.L., Carulli, J.P., Day-Williams, A.G., Staropoli, J.F., Xin, W.W., Chesi, A., Raphael, A.R., McKenna-Yasek, D., Cady, J., De Jong, J.M.B.V., Kenna, K.P., Smith, B.N., Topp, S., Miller, J., Gkazi, A., Al-Chalabi, A., Van Den Berg, L.H., Veldink, J., Silani, V., Ticozzi, N., Shaw, C.E., Baloh, R.H., Appel, S., Simpson, E., Lagier-Tourenne, C., Pulst, S.M., Gibson, S., Trojanowski, J.Q., Elman, L., McCluskey, L., Grossman, M., Shneider, N.A., Chung, W.K., Ravits, J.M., Glass, J.D., Sims, K.B., Van Deerlin, V.M., Maniatis, T., Hayes, S.D., Ordureau, A., Swarup, S., Landers, J., Baas, F., Allen, A.S., Bedlack, R.S., Harper, J.W., Gitler, A.D., Rouleau, G.A., Brown, R., Harms, M.B., Cooper, G.M., Harris, T., Myers, R.M. & Goldstein, D.B. (2015) Exome sequencing in amyotrophic lateral sclerosis identifies risk genes and pathways. *Science*. [Online] 347 (6229), 1436–1441. Available from: doi:10.1126/science.aaa3650.

Clark, K., Plater, L., Peggie, M., & Cohen, P. (2009) Use of the pharmacological inhibitor BX795 to study the regulation and physiological roles of TBK1 and IkappaB kinase epsilon: a distinct upstream kinase mediates Ser-172 phosphorylation and activation. *The Journal of biological chemistry*. [Online] 284 (21), 14136–14146. Available from: doi:10.1074/jbc.M109.000414.

Colombo, M., Raposo, G., & Théry, C. (2014) Biogenesis, Secretion, and Intercellular Interactions of Exosomes and Other Extracellular Vesicles. *Annual Review of Cell and Developmental Biology*. [Online] 30 (1), 255–289. Available from: doi:10.1146/annurev-cellbio-101512-122326.

Cooney, R., Baker, J., Brain, O., Danis, B., Pichulik, T., Allan, P., Ferguson, D.J.P., Campbell, B.J., Jewell, D., & Simmons, A. (2010) NOD2 stimulation induces autophagy in dendritic cells influencing bacterial handling and antigen presentation. *Nature Medicine*. [Online] 16 (1), 90–97. Available from: doi:10.1038/nm.2069.

Delgado, M.A., Elmaoued, R.A., Davis, A.S., Kyei, G., & Deretic, V. (2008) Toll-like receptors control autophagy. *The EMBO journal*. [Online] 27 (7), 1110–1121. Available from: doi:10.1038/emboj.2008.31.

Delorme-Axford, E., Donker, R.B., Mouillet, J.-F., Chu, T., Bayer, A., Ouyang, Y., Wang, T., Stolz, D.B., Sarkar, S.N., Morelli, A.E., Sadovsky, Y., & Coyne, C.B. (2013) Human placental trophoblasts confer viral resistance to recipient cells. *Proceedings of the National Academy of Sciences of the United States of America*. [Online] 110 (29), 12048–12053. Available from: doi:10.1073/pnas.1304718110.

Desai, P. & Person, S. (1998) Incorporation of the green fluorescent protein into the herpes simplex virus type 1 capsid. *Journal of virology*. [Online] 72 (9), 7563–7568. Available from: http://www.ncbi.nlm.nih.gov/pubmed/9696854.

Deschamps, T. & Kalamvoki, M. (2017) Evasion of the STING DNA-Sensing Pathway by VP11/12 of Herpes Simplex Virus 1 Rozanne M. Sandri-Goldin (ed.). *Journal of Virology*. [Online] 91 (16), e00535-17. Available from: doi:10.1128/JVI.00535-17.

Dey, B., Dey, R.J., Cheung, L.S., Pokkali, S., Guo, H., Lee, J.-H., & Bishai, W.R. (2015) A bacterial cyclic dinucleotide activates the cytosolic surveillance pathway and mediates innate resistance to tuberculosis. *Nature Medicine*. [Online] 21 (4), 401–406. Available from: doi:10.1038/nm.3813.

Dooley, H.C., Razi, M., Polson, H.E.J., Girardin, S.E., Wilson, M.I., & Tooze, S.A. (2014) WIPI2 Links LC3 Conjugation with PI3P, Autophagosome Formation, and Pathogen Clearance by Recruiting Atg12–5-16L1. *Molecular Cell*. [Online] 55 (2), 238–252. Available from: doi:10.1016/J.MOLCEL.2014.05.021.

Dupuis, S., Jouanguy, E., Al-Hajjar, S., Fieschi, C., Al-Mohsen, I.Z., Al-Jumaah, S., Yang, K., Chapgier, A., Eidenschenk, C., Eid, P., Ghonaium, A. Al, Tufenkeji, H., Frayha, H., Al-Gazlan, S., Al-Rayes, H., Schreiber, R.D., Gresser, I., & Casanova, J.-L. (2003) Impaired response to interferon-α/β and lethal viral disease in human STAT1 deficiency. *Nature Genetics*. [Online] 33 (3), 388–391. Available from: doi:10.1038/ng1097.

Elion, G.B., Furman, P.A., Fyfe, J.A., de Miranda, P., Beauchamp, L., & Schaeffer, H.J. (1977) Selectivity of action of an antiherpetic agent, 9-(2-hydroxyethoxymethyl) guanine. *Proceedings of the National Academy of Sciences of the United States of America*. [Online] 74 (12), 5716–5720. Available from: http://www.ncbi.nlm.nih.gov/pubmed/202961.

English, L., Chemali, M., & Desjardins, M. (2009) Nuclear membrane-derived autophagy, a novel process that participates in the presentation of endogenous viral antigens during HSV-1 infection. *Autophagy*. 5 (7), 1026–1029.

English, L., Chemali, M., Duron, J., Rondeau, C., Laplante, A., Gingras, D., Alexander, D., Leib, D., Norbury, C., Lippé, R., & Desjardins, M. (2009) Autophagy enhances the presentation of endogenous viral antigens on MHC class I molecules during HSV-1 infection. *Nature Immunology*. [Online] 10 (5), 480–487. Available from: doi:10.1038/ni.1720.

Fellmann, C., Hoffmann, T., Sridhar, V., Hopfgartner, B., Muhar, M., Roth, M., Lai, D.Y., Barbosa, I.A.M., Kwon, J.S., Guan, Y., Sinha, N., & Zuber, J. (2013) An

optimized microRNA backbone for effective single-copy RNAi. *Cell reports*. 5 (6), 1704–1713.

Fellmann, C., Zuber, J., McJunkin, K., Chang, K., Malone, C.D., Dickins, R.A., Xu, Q., Hengartner, M.O., Elledge, S.J., Hannon, G.J., & Lowe, S.W. (2011) Functional identification of optimized RNAi triggers using a massively parallel sensor assay. *Molecular cell*. 41 (6), 733–746.

Fingert, J.H., Robin, A.L., Stone, J.L., Roos, B.R., Davis, L.K., Scheetz, T.E., Bennett, S.R., Wassink, T.H., Kwon, Y.H., Alward, W.L.M., Mullins, R.F., Sheffield, V.C., & Stone, E.M. (2011) Copy number variations on chromosome 12q14 in patients with normal tension glaucoma. *Human Molecular Genetics*. [Online] 20 (12), 2482–2494. Available from: doi:10.1093/hmg/ddr123.

Fitzgerald, K.A., McWhirter, S.M., Faia, K.L., Rowe, D.C., Latz, E., Golenbock, D.T., Coyle, A.J., Liao, S.-M., & Maniatis, T. (2003) IKKε and TBK1 are essential components of the IRF3 signaling pathway. *Nature Immunology*. [Online] 4 (5), 491–496. Available from: doi:10.1038/ni921.

Freischmidt, A., Wieland, T., Richter, B., Ruf, W., Schaeffer, V., Müller, K., Marroquin, N., Nordin, F., Hübers, A., Weydt, P., Pinto, S., Press, R., Millecamps, S., Molko, N., Bernard, E., Desnuelle, C., Soriani, M.-H., Dorst, J., Graf, E., Nordström, U., Feiler, M.S., Putz, S., Boeckers, T.M., Meyer, T., Winkler, A.S., Winkelman, J., de Carvalho, M., Thal, D.R., Otto, M., Brännström, T., Volk, A.E., Kursula, P., Danzer, K.M., Lichtner, P., Dikic, I., Meitinger, T., Ludolph, A.C., Strom, T.M., Andersen, P.M., & Weishaupt, J.H. (2015) Haploinsufficiency of TBK1 causes familial ALS and fronto-temporal dementia. *Nature Neuroscience*. [Online] 18 (5), 631–636. Available from: doi:10.1038/nn.4000.

Furuya, N., Yu, J., Byfield, M., Pattingre, S., & Levine, B. (2005) The evolutionarily conserved domain of Beclin 1 is required for Vps34 binding, autophagy and tumor suppressor function. *Autophagy*. [Online] 1 (1), 46–52. Available from: http://www.ncbi.nlm.nih.gov/pubmed/16874027.

Gao, T., Zhang, S.-P., Wang, J.-F., Liu, L., Wang, Y., Cao, Z.-Y., Hu, Q.-K., Yuan, W.-J., & Lin, L. (2018) TLR3 contributes to persistent autophagy and heart failure in mice after myocardial infarction. *Journal of Cellular and Molecular Medicine*. [Online] 22 (1), 395–408. Available from: doi:10.1111/jcmm.13328.

Gijselinck, I., Van Mossevelde, S., van der Zee, J., Sieben, A., Philtjens, S., Heeman, B., Engelborghs, S., Vandenbulcke, M., De Baets, G., Bäumer, V., Cuijt, I., Van den Broeck, M., Peeters, K., Mattheijssens, M., Rousseau, F., Vandenberghe, R., De Jonghe, P., Cras, P., De Deyn, P.P., Martin, J.-J., Cruts, M., Van Broeckhoven, C., & BELNEU Consortium (2015) Loss of TBK1 is a frequent cause of frontotemporal dementia in a Belgian cohort. *Neurology*. [Online] 85 (24), 2116–2125. Available from: doi:10.1212/WNL.0000000000002220.

Gitlin, L., Barchet, W., Gilfillan, S., Cella, M., Beutler, B., Flavell, R.A., Diamond, M.S., & Colonna, M. (2006) Essential role of mda-5 in type I IFN responses to polyriboinosinic:polyribocytidylic acid and encephalomyocarditis picornavirus. *Proceedings of the National Academy of Sciences*. [Online] 103 (22), 8459–8464. Available from: doi:10.1073/pnas.0603082103.

Glick, D., Barth, S., & Macleod, K.F. (2010) Autophagy: cellular and molecular mechanisms. *The Journal of pathology*. [Online] 221 (1), 3–12. Available from: doi:10.1002/path.2697.

Gnann, J.W. & Whitley, R.J. (2017) Herpes Simplex Encephalitis: an Update.

Current Infectious Disease Reports. [Online] 19 (3), 13. Available from: doi:10.1007/s11908-017-0568-7.

Goncalves, A., Bürckstümmer, T., Dixit, E., Scheicher, R., Górna, M.W., Karayel, E., Sugar, C., Stukalov, A., Berg, T., Kralovics, R., Planyavsky, M., Bennett, K.L., Colinge, J., & Superti-Furga, G. (2011) Functional Dissection of the TBK1 Molecular Network Volker Thiel (ed.). *PLoS ONE*. [Online] 6 (9), e23971. Available from: doi:10.1371/journal.pone.0023971.

Gorbea, C., Makar, K.A., Pauschinger, M., Pratt, G., Bersola, J.L.F., Varela, J., David, R.M., Banks, L., Huang, C.-H., Li, H., Schultheiss, H.-P., Towbin, J.A., Vallejo, J.G., & Bowles, N.E. (2010) A Role for Toll-like Receptor 3 Variants in Host Susceptibility to Enteroviral Myocarditis and Dilated Cardiomyopathy. *Journal of Biological Chemistry*. [Online] 285 (30), 23208–23223. Available from: doi:10.1074/jbc.M109.047464.

Gu, L., Fullam, A., Brennan, R., & Schröder, M. (2013) Human DEAD box helicase 3 couples IκB kinase ε to interferon regulatory factor 3 activation. *Molecular and cellular biology*. [Online] 33 (10), 2004–2015. Available from: doi:10.1128/MCB.01603-12.

Guo, Y., Audry, M., Ciancanelli, M., Alsina, L., Azevedo, J., Herman, M., Anguiano, E., Sancho-Shimizu, V., Lorenzo, L., Pauwels, E., Philippe, P.B., Pérez de Diego, R., Cardon, A., Vogt, G., Picard, C., Andrianirina, Z.Z., Rozenberg, F., Lebon, P., Plancoulaine, S., Tardieu, M., Valérie Doireau, Jouanguy, E., Chaussabel, D., Geissmann, F., Abel, L., Casanova, J.-L., & Zhang, S.-Y. (2011) Herpes simplex virus encephalitis in a patient with complete TLR3 deficiency: TLR3 is otherwise redundant in protective immunity. *The Journal of Experimental Medicine*. [Online] 208 (10), 2083–2098. Available from:

doi:10.1084/jem.20101568.

Gutierrez, M.G., Master, S.S., Singh, S.B., Taylor, G.A., Colombo, M.I., & Deretic, V. (2004) Autophagy Is a Defense Mechanism Inhibiting BCG and Mycobacterium tuberculosis Survival in Infected Macrophages. *Cell*. [Online] 119 (6), 753–766. Available from: doi:10.1016/j.cell.2004.11.038.

Harashima, N., Inao, T., Imamura, R., Okano, S., Suda, T., & Harada, M. (2012) Roles of the PI3K/Akt pathway and autophagy in TLR3 signaling-induced apoptosis and growth arrest of human prostate cancer cells. *Cancer Immunology, Immunotherapy*. [Online] 61 (5), 667–676. Available from: doi:10.1007/s00262-011-1132-1.

He, B., Gross, M., & Roizman, B. (1997) The gamma(1)34.5 protein of herpes simplex virus 1 complexes with protein phosphatase 1alpha to dephosphorylate the alpha subunit of the eukaryotic translation initiation factor 2 and preclude the shutoff of protein synthesis by double-stranded RNA-activa. *Proceedings of the National Academy of Sciences of the United States of America*. 94 (3), 843–848.

Heo, J.-M., Ordureau, A., Paulo, J.A., Rinehart, J., & Harper, J.W. (2015) The PINK1-PARKIN Mitochondrial Ubiquitylation Pathway Drives a Program of OPTN/NDP52 Recruitment and TBK1 Activation to Promote Mitophagy. *Molecular Cell*. [Online] 60 (1), 7–20. Available from: doi:10.1016/j.molcel.2015.08.016.

Herman, M., Ciancanelli, M., Ou, Y.-H., Lorenzo, L., Klaudel-Dreszler, M., Pauwels, E., Sancho-Shimizu, V., Pérez de Diego, R., Abhyankar, A., Israelsson, E., Guo, Y., Cardon, A., Rozenberg, F., Lebon, P., Tardieu, M., Heropolitańska-Pliszka, E., Chaussabel, D., White, M.A., Abel, L., Zhang, S.-Y., & Casanova, J.-L. (2012) Heterozygous TBK1 mutations impair TLR3 immunity and underlie

herpes simplex encephalitis of childhood. *The Journal of Experimental Medicine*. [Online] 209 (9), 1567–1582. Available from: doi:10.1084/jem.20111316.

Homer, C.R., Richmond, A.L., Rebert, N.A., Achkar, J., & McDonald, C. (2010) ATG16L1 and NOD2 Interact in an Autophagy-Dependent Antibacterial Pathway Implicated in Crohn's Disease Pathogenesis. *Gastroenterology*. [Online] 139 (5), 1630–1641.e2. Available from: doi:10.1053/j.gastro.2010.07.006.

Horan, K.A., Hansen, K., Jakobsen, M.R., Holm, C.K., Søby, S., Unterholzner, L., Thompson, M., West, J.A., Iversen, M.B., Rasmussen, S.B., Ellermann-Eriksen, S., Kurt-Jones, E., Landolfo, S., Damania, B., Melchjorsen, J., Bowie, A.G., Fitzgerald, K.A., & Paludan, S.R. (2013) Proteasomal degradation of herpes simplex virus capsids in macrophages releases DNA to the cytosol for recognition by DNA sensors. *Journal of immunology (Baltimore, Md.: 1950)*. [Online] 190 (5), 2311–2319. Available from: doi:10.4049/jimmunol.1202749.

Ishii, K.J., Coban, C., Kato, H., Takahashi, K., Torii, Y., Takeshita, F., Ludwig, H., Sutter, G., Suzuki, K., Hemmi, H., Sato, S., Yamamoto, M., Uematsu, S., Kawai, T., Takeuchi, O., & Akira, S. (2006) A Toll-like receptor–independent antiviral response induced by double-stranded B-form DNA. *Nature Immunology*. [Online] 7 (1), 40–48. Available from: doi:10.1038/ni1282.

Ishikawa, H., Ma, Z., & Barber, G.N. (2009) STING regulates intracellular DNA-mediated, type I interferon-dependent innate immunity. *Nature*. [Online] 461 (7265), 788–792. Available from: doi:10.1038/nature08476.

Jacquemont, B. & Roizman, B. (1975) RNA synthesis in cells infected with herpes simplex virus. X. Properties of viral symmetric transcripts and of double-stranded RNA prepared from them. *Journal of virology*. [Online] 15 (4), 707–713. Available from: http://www.ncbi.nlm.nih.gov/pubmed/163916.

Jeong, J.-Y., Yim, H.-S., Ryu, J.-Y., Lee, H.S., Lee, J.-H., Seen, D.-S., & Kang, S.G. (2012) One-step sequence- and ligation-independent cloning as a rapid and versatile cloning method for functional genomics studies. *Applied and environmental microbiology*. [Online] 78 (15), 5440–5443. Available from: doi:10.1128/AEM.00844-12.

Jiang, P. & Mizushima, N. (2014) Autophagy and human diseases. *Cell Research*. [Online] 24 (1), 69–79. Available from: doi:10.1038/cr.2013.161.

Jiang, Y.-C., Feng, H., Lin, Y.-C., & Guo, X.-R. (2016) New strategies against drug resistance to herpes simplex virus. *International journal of oral science*. [Online] 8 (1), 1–6. Available from: doi:10.1038/ijos.2016.3.

Jounai, N., Kobiyama, K., Shiina, M., Ogata, K., Ishii, K.J., & Takeshita, F. (2011) NLRP4 negatively regulates autophagic processes through an association with beclin1. *Journal of immunology (Baltimore, Md. : 1950)*. [Online] 186 (3), 1646–1655. Available from: doi:10.4049/jimmunol.1001654.

Kalamvoki, M. & Deschamps, T. (2016) Extracellular vesicles during Herpes Simplex Virus type 1 infection: an inquire. *Virology Journal*. [Online] 13 (1), 63. Available from: doi:10.1186/s12985-016-0518-2.

Kalamvoki, M., Du, T., & Roizman, B. (2014) Cells infected with herpes simplex virus 1 export to uninfected cells exosomes containing STING, viral mRNAs, and microRNAs. *Proceedings of the National Academy of Sciences of the United States of America*. [Online] 111 (46), E4991-6. Available from: doi:10.1073/pnas.1419338111.

Kato, H., Sato, S., Yoneyama, M., Yamamoto, M., Uematsu, S., Matsui, K., Tsujimura, T., Takeda, K., Fujita, T., Takeuchi, O., & Akira, S. (2005) Cell Type-Specific Involvement of RIG-I in Antiviral Response. *Immunity*. [Online] 23 (1),

19–28. Available from: doi:10.1016/j.immuni.2005.04.010.

Kato, H., Takeuchi, O., Mikamo-Satoh, E., Hirai, R., Kawai, T., Matsushita, K., Hiiragi, A., Dermody, T.S., Fujita, T., & Akira, S. (2008) Length-dependent recognition of double-stranded ribonucleic acids by retinoic acid–inducible gene-I and melanoma differentiation–associated gene 5. *The Journal of Experimental Medicine*. [Online] 205 (7), 1601–1610. Available from: doi:10.1084/jem.20080091.

Katzenell, S. & Leib, D.A. (2016) Herpes Simplex Virus and Interferon Signaling Induce Novel Autophagic Clusters in Sensory Neurons R. M. Longnecker (ed.). *Journal of Virology*. [Online] 90 (9), 4706–4719. Available from: doi:10.1128/JVI.02908-15.

Kawase, K., Allingham, R.R., Meguro, A., Mizuki, N., Roos, B., Solivan-Timpe, F.M., Robin, A.L., Ritch, R., & Fingert, J.H. (2012) Confirmation of TBK1 duplication in normal tension glaucoma. *Experimental eye research*. [Online] 96 (1), 178–180. Available from: doi:10.1016/j.exer.2011.12.021.

Kent, J.R., Kang, W., Miller, C.G., & Fraser, N.W. (2003) Herpes Simplex Virus Latency-Associated Transcript Gene Function. *Journal of Neurovirology*. [Online] 9 (3), 285–290. Available from: doi:10.1080/13550280390200994.

Kim, Y.-M., Brinkmann, M.M., Paquet, M.-E., & Ploegh, H.L. (2008) UNC93B1 delivers nucleotide-sensing toll-like receptors to endolysosomes. *Nature*. 452 (7184), 234–238.

Kirkin, V., Lamark, T., Sou, Y.-S., Bjørkøy, G., Nunn, J.L., Bruun, J.-A., Shvets, E., McEwan, D.G., Clausen, T.H., Wild, P., Bilusic, I., Theurillat, J.-P., Øvervatn, A., Ishii, T., Elazar, Z., Komatsu, M., Dikic, I., & Johansen, T. (2009) A Role for NBR1 in Autophagosomal Degradation of Ubiquitinated Substrates. *Molecular*

Cell. [Online] 33 (4), 505–516. Available from: doi:10.1016/j.molcel.2009.01.020.

Kishore, N., Huynh, Q.K., Mathialagan, S., Hall, T., Rouw, S., Creely, D., Lange, G., Caroll, J., Reitz, B., Donnelly, A., Boddupalli, H., Combs, R.G., Kretzmer, K., & Tripp, C.S. (2002) IKK-i and TBK-1 are enzymatically distinct from the homologous enzyme IKK-2: comparative analysis of recombinant human IKK-i, TBK-1, and IKK-2. *The Journal of biological chemistry*. [Online] 277 (16), 13840–13847. Available from: doi:10.1074/jbc.M110474200.

Klionsky, D.J., Abdelmohsen, K., Abe, A., Abedin, M.J., Abeliovich, H., …, Zois, C. E., Zoladek, T., Zong, W. X., Zorzano, A. & H., Zughaier, S.M. (2016) Guidelines for the use and interpretation of assays for monitoring autophagy (3rd edition). *Autophagy*. 12 (1), 1–222.

Ko, J.H., Yoon, S.-O., Lee, H.J., & Oh, J.Y. (2017) Rapamycin regulates macrophage activation by inhibiting NLRP3 inflammasome-p38 MAPK-NFκB pathways in autophagy- and p62-dependent manners. *Oncotarget*. [Online] 8 (25), 40817–40831. Available from: doi:10.18632/oncotarget.17256.

Kollias, C.M., Huneke, R.B., Wigdahl, B., & Jennings, S.R. (2015) Animal models of herpes simplex virus immunity and pathogenesis. *Journal of NeuroVirology*. [Online] 21 (1), 8–23. Available from: doi:10.1007/s13365-014-0302-2.

Komatsu, M., Waguri, S., Chiba, T., Murata, S., Iwata, J., Tanida, I., Ueno, T., Koike, M., Uchiyama, Y., Kominami, E., & Tanaka, K. (2006) Loss of autophagy in the central nervous system causes neurodegeneration in mice. *Nature*. [Online] 441 (7095), 880–884. Available from: doi:10.1038/nature04723.

Komine, O. & Yamanaka, K. (2015) Neuroinflammation in motor neuron disease. *Nagoya journal of medical science*. 77 (4), 537–549.

Kondo, Y., Kanzawa, T., Sawaya, R., & Kondo, S. (2005) The role of autophagy in

cancer development and response to therapy. *Nature Reviews Cancer*. [Online] 5 (9), 726–734. Available from: doi:10.1038/nrc1692.

Korac, J., Schaeffer, V., Kovacevic, I., Clement, A.M., Jungblut, B., Behl, C., Terzic, J., & Dikic, I. (2013) Ubiquitin-independent function of optineurin in autophagic clearance of protein aggregates. *Journal of Cell Science*. [Online] 126 (2), 580–592. Available from: doi:10.1242/jcs.114926.

Kukhanova, M.K., Korovina, A.N., & Kochetkov, S.N. (2014) Human herpes simplex virus: Life cycle and development of inhibitors. *Biochemistry (Moscow)*. 79 (13), 1635–1652.

Lafaille, F.G., Pessach, I.M., Zhang, S.-Y., Ciancanelli, M.J., Herman, M., Abhyankar, A., Ying, S.-W., Keros, S., Goldstein, P.A., Mostoslavsky, G., Ordovas-Montanes, J., Jouanguy, E., Plancoulaine, S., Tu, E., Elkabetz, Y., Al-Muhsen, S., Tardieu, M., Schlaeger, T.M., Daley, G.Q., Abel, L., Casanova, J.-L., Studer, L., & Notarangelo, L.D. (2012) Impaired intrinsic immunity to HSV-1 in human iPSC-derived TLR3-deficient CNS cells. *Nature*. [Online] 491 (7426), 769–773. Available from: doi:10.1038/nature11583.

Larabi, A., Devos, J.M., Ng, S.-L., Nanao, M.H., Round, A., Maniatis, T., & Panne, D. (2013) Crystal Structure and Mechanism of Activation of TANK-Binding Kinase 1. *Cell Reports*. [Online] 3 (3), 734–746. Available from: doi:10.1016/j.celrep.2013.01.034.

Lazarou, M., Sliter, D.A., Kane, L.A., Sarraf, S.A., Wang, C., Burman, J.L., Sideris, D.P., Fogel, A.I., & Youle, R.J. (2015) The ubiquitin kinase PINK1 recruits autophagy receptors to induce mitophagy. *Nature*. [Online] 524 (7565), 309–314. Available from: doi:10.1038/nature14893.

Lee, H.K., Lund, J.M., Ramanathan, B., Mizushima, N., & Iwasaki, A. (2007)

Autophagy-Dependent Viral Recognition by Plasmacytoid Dendritic Cells. *Science*. [Online] 315 (5817), 1398–1401. Available from: doi:10.1126/science.1136880.

Lee, H.K., Mattei, L.M., Steinberg, B.E., Alberts, P., Lee, Y.H., Chervonsky, A., Mizushima, N., Grinstein, S., & Iwasaki, A. (2010) In vivo requirement for Atg5 in antigen presentation by dendritic cells. *Immunity*. [Online] 32 (2), 227–239. Available from: doi:10.1016/j.immuni.2009.12.006.

Leib, D.A., Alexander, D.E., Cox, D., Yin, J., & Ferguson, T.A. (2009) Interaction of ICP34.5 with Beclin 1 modulates herpes simplex virus type 1 pathogenesis through control of CD4+ T-cell responses. *Journal of virology*. [Online] 83 (23), 12164–12171. Available from: doi:10.1128/JVI.01676-09.

Leib, D.A., Machalek, M.A., Williams, B.R.G., Silverman, R.H., & Virgin, H.W. (2000) Specific phenotypic restoration of an attenuated virus by knockout of a host resistance gene. *Proceedings of the National Academy of Sciences*. [Online] 97 (11), 6097–6101. Available from: doi:10.1073/pnas.100415697.

Lerner, C., Bitto, A., Pulliam, D., Nacarelli, T., Konigsberg, M., Van Remmen, H., Torres, C., & Sell, C. (2013) Reduced mammalian target of rapamycin activity facilitates mitochondrial retrograde signaling and increases life span in normal human fibroblasts. *Aging Cell*. [Online] 12 (6), 966–977. Available from: doi:10.1111/acel.12122.

Leuzinger, H., Ziegler, U., Schraner, E.M., Fraefel, C., Glauser, D.L., Heid, I., Ackermann, M., Mueller, M., & Wild, P. (2005) Herpes simplex virus 1 envelopment follows two diverse pathways. *Journal of virology*. [Online] 79 (20), 13047–13059. Available from: doi:10.1128/JVI.79.20.13047-13059.2005.

Levine, B., Mizushima, N., & Virgin, H.W. (2011) Autophagy in immunity and

inflammation. *Nature*. [Online] 469 (7330), 323–335. Available from: doi:10.1038/nature09782.

Li, J., Li, J., Miyahira, A., Sun, J., Liu, Y., Cheng, G., & Liang, H. (2012) Crystal structure of the ubiquitin-like domain of human TBK1. *Protein & cell*. [Online] 3 (5), 383–391. Available from: doi:10.1007/s13238-012-2929-1.

Li, X.-D., Wu, J., Gao, D., Wang, H., Sun, L., & Chen, Z.J. (2013) Pivotal Roles of cGAS-cGAMP Signaling in Antiviral Defense and Immune Adjuvant Effects. *Science*. [Online] 341 (6152), 1390–1394. Available from: doi:10.1126/science.1244040.

Li, X.L., Boyanapalli, M., Weihua, X., Kalvakolanu, D. V, & Hassel, B.A. (1998) Induction of interferon synthesis and activation of interferon-stimulated genes by liposomal transfection reagents. *Journal of interferon & cytokine research : the official journal of the International Society for Interferon and Cytokine Research*. [Online] 18 (11), 947–952. Available from: doi:10.1089/jir.1998.18.947.

Liang, X.H., Kleeman, L.K., Jiang, H.H., Gordon, G., Goldman, J.E., Berry, G., Herman, B., & Levine, B. (1998) Protection against fatal Sindbis virus encephalitis by beclin, a novel Bcl-2-interacting protein. *Journal of virology*. 72 (11), 8586–8596.

Lim, H.K., Seppanen, M., Hautala, T., Ciancanelli, M.J., Itan, Y., Lafaille, F.G., Dell, W., Lorenzo, L., Byun, M., Pauwels, E., Ronnelid, Y., Cai, X., Boucherit, S., Jouanguy, E., Paetau, A., Lebon, P., Rozenberg, F., Tardieu, M., Abel, L., Yildiran, A., Vergison, A., Roivainen, R., Etzioni, A., Tienari, P.J., Casanova, J.-L., & Zhang, S.-Y. (2014) TLR3 deficiency in herpes simplex encephalitis: High allelic heterogeneity and recurrence risk. *Neurology*. [Online] 83 (21), 1888–1897. Available from: doi:10.1212/WNL.0000000000000999.

Lomen-Hoerth, C., Anderson, T., & Miller, B. (2002) The overlap of amyotrophic lateral sclerosis and frontotemporal dementia. *Neurology*. 59 (7), 1077–1079.

Loo, Y.-M. & Gale, M. (2011) Immune Signaling by RIG-I-like Receptors. *Immunity*. [Online] 34 (5), 680–692. Available from: doi:10.1016/j.immuni.2011.05.003.

Looker, K.J., Magaret, A.S., May, M.T., Turner, K.M.E., Vickerman, P., Gottlieb, S.L., & Newman, L.M. (2015) Global and Regional Estimates of Prevalent and Incident Herpes Simplex Virus Type 1 Infections in 2012 Neal A. DeLuca (ed.). *PLOS ONE*. [Online] 10 (10), e0140765. Available from: doi:10.1371/journal.pone.0140765.

Lopez-Herrera, G., Tampella, G., Pan-Hammarström, Q., Herholz, P., Trujillo-Vargas, C.M., Phadwal, K., Simon, A.K., Moutschen, M., Etzioni, A., Mory, A., Srugo, I., Melamed, D., Hultenby, K., Liu, C., Baronio, M., Vitali, M., Philippet, P., Dideberg, V., Aghamohammadi, A., Rezaei, N., Enright, V., Du, L., Salzer, U., Eibel, H., Pfeifer, D., Veelken, H., Stauss, H., Lougaris, V., Plebani, A., Gertz, E.M., Schäffer, A.A., Hammarström, L., & Grimbacher, B. (2012) Deleterious Mutations in LRBA Are Associated with a Syndrome of Immune Deficiency and Autoimmunity. *The American Journal of Human Genetics*. [Online] 90 (6), 986–1001. Available from: doi:10.1016/j.ajhg.2012.04.015.

Lussignol, M., Queval, C., Bernet-Camard, M.-F., Cotte-Laffitte, J., Beau, I., Codogno, P., & Esclatine, A. (2013) The herpes simplex virus 1 Us11 protein inhibits autophagy through its interaction with the protein kinase PKR. *Journal of virology*. [Online] 87 (2), 859–871. Available from: doi:10.1128/JVI.01158-12.

Ma, Y., Jin, H., Valyi-Nagy, T., Cao, Y., Yan, Z., & He, B. (2012) Inhibition of TANK binding kinase 1 by herpes simplex virus 1 facilitates productive infection. *Journal of virology*. [Online] 86 (4), 2188–2196. Available from:

doi:10.1128/JVI.05376-11.

Matsumoto, G., Shimogori, T., Hattori, N., & Nukina, N. (2015) TBK1 controls autophagosomal engulfment of polyubiquitinated mitochondria through p62/SQSTM1 phosphorylation. *Human Molecular Genetics*. [Online] 24 (15), 4429–4442. Available from: doi:10.1093/hmg/ddv179.

Matsumoto, G., Wada, K., Okuno, M., Kurosawa, M., & Nukina, N. (2011) Serine 403 phosphorylation of p62/SQSTM1 regulates selective autophagic clearance of ubiquitinated proteins. *Molecular cell*. [Online] 44 (2), 279–289. Available from: doi:10.1016/j.molcel.2011.07.039.

McFarlane, S., Aitken, J., Sutherland, J.S., Nicholl, M.J., Preston, V.G., & Preston, C.M. (2011) Early induction of autophagy in human fibroblasts after infection with human cytomegalovirus or herpes simplex virus 1. *Journal of virology*. [Online] 85 (9), 4212–4221. Available from: doi:10.1128/JVI.02435-10.

McLean, J.E., Wudzinska, A., Datan, E., Quaglino, D., & Zakeri, Z. (2011) Flavivirus NS4A-induced autophagy protects cells against death and enhances virus replication. *The Journal of biological chemistry*. [Online] 286 (25), 22147–22159. Available from: doi:10.1074/jbc.M110.192500.

Mizushima, N., Yoshimori, T., & Levine, B. (2010) Methods in mammalian autophagy research. *Cell*. [Online] 140 (3), 313–326. Available from: doi:10.1016/j.cell.2010.01.028.

Mizushima, N., Yoshimori, T., & Ohsumi, Y. (2011) The Role of Atg Proteins in Autophagosome Formation. *Annual Review of Cell and Developmental Biology*. [Online] 27 (1), 107–132. Available from: doi:10.1146/annurev-cellbio-092910-154005.

Moore, A.S. & Holzbaur, E.L.F. (2016) Dynamic recruitment and activation of ALS-

associated TBK1 with its target optineurin are required for efficient mitophagy. *Proceedings of the National Academy of Sciences of the United States of America*. [Online] 113 (24), E3349-58. Available from: doi:10.1073/pnas.1523810113.

Moreau, K., Luo, S., & Rubinsztein, D.C. (2010) Cytoprotective roles for autophagy. *Current opinion in cell biology*. [Online] 22 (2), 206–211. Available from: doi:10.1016/j.ceb.2009.12.002.

Mortensen, M., Ferguson, D.J.P., Edelmann, M., Kessler, B., Morten, K.J., Komatsu, M., & Simon, A.K. (2010) Loss of autophagy in erythroid cells leads to defective removal of mitochondria and severe anemia in vivo. *Proceedings of the National Academy of Sciences*. [Online] 107 (2), 832–837. Available from: doi:10.1073/pnas.0913170107.

Morton, S., Hesson, L., Peggie, M., & Cohen, P. (2008) Enhanced binding of TBK1 by an optineurin mutant that causes a familial form of primary open angle glaucoma. *FEBS Letters*. [Online] 582 (6), 997–1002. Available from: doi:10.1016/j.febslet.2008.02.047.

Mostowy, S., Sancho-Shimizu, V., Hamon, M.A., Simeone, R., Brosch, R., Johansen, T., & Cossart, P. (2011) p62 and NDP52 Proteins Target Intracytosolic Shigella and Listeria to Different Autophagy Pathways. *Journal of Biological Chemistry*. [Online] 286 (30), 26987–26995. Available from: doi:10.1074/jbc.M111.223610.

von Muhlinen, N., Akutsu, M., Ravenhill, B.J., Foeglein, Á., Bloor, S., Rutherford, T.J., Freund, S.M.V., Komander, D., & Randow, F. (2012) LC3C, Bound Selectively by a Noncanonical LIR Motif in NDP52, Is Required for Antibacterial Autophagy. *Molecular Cell*. [Online] 48 (3), 329–342. Available from:

doi:10.1016/j.molcel.2012.08.024.

Münz, C. (2010) Antigen processing via autophagy—not only for MHC class II presentation anymore? *Current Opinion in Immunology*. [Online] 22 (1), 89–93. Available from: doi:10.1016/j.coi.2010.01.016.

Nedjic, J., Aichinger, M., Emmerich, J., Mizushima, N., & Klein, L. (2008) Autophagy in thymic epithelium shapes the T-cell repertoire and is essential for tolerance. *Nature*. [Online] 455 (7211), 396–400. Available from: doi:10.1038/nature07208.

Newman, A.C., Scholefield, C.L., Kemp, A.J., Newman, M.C., & Mciver, E.G. (2012) TBK1 Kinase Addiction in Lung Cancer Cells Is Mediated via Autophagy of Tax1bp1/Ndp52 and Non-Canonical NF-kB Signalling. *PLoS ONE*. [Online] 7 (11), 50672. Available from: doi:10.1371/journal.pone.0050672.

O'Connell, D. & Liang, C. (2016) Autophagy interaction with herpes simplex virus type-1 infection. *Autophagy*. 12 (3), 451–459.

Orvedahl, A., Alexander, D., Tallóczy, Z., Sun, Q., Wei, Y., Zhang, W., Burns, D., Leib, D.A., & Levine, B. (2007) HSV-1 ICP34.5 Confers Neurovirulence by Targeting the Beclin 1 Autophagy Protein. *Cell Host & Microbe*. [Online] 1 (1), 23–35. Available from: doi:10.1016/j.chom.2006.12.001.

Orvedahl, A., MacPherson, S., Sumpter, R., Tallóczy, Z., Zou, Z., & Levine, B. (2010) Autophagy Protects against Sindbis Virus Infection of the Central Nervous System. *Cell Host & Microbe*. [Online] 7 (2), 115–127. Available from: doi:10.1016/J.CHOM.2010.01.007.

Paludan, C., Schmid, D., Landthaler, M., Vockerodt, M., Kube, D., Tuschl, T., & Münz, C. (2005) Endogenous MHC Class II Processing of a Viral Nuclear Antigen After Autophagy. *Science*. [Online] 307 (5709), 593–596. Available from: doi:10.1126/science.1104904.

Paz, S., Sun, Q., Nakhaei, P., Romieu-Mourez, R., Goubau, D., Julkunen, I., Lin, R., & Hiscott, J. (2006) Induction of IRF-3 and IRF-7 phosphorylation following activation of the RIG-I pathway. *Cellular and molecular biology (Noisy-le-Grand, France)*. 52 (1), 17–28.

Pérez de Diego, R., Sancho-Shimizu, V., Lorenzo, L., Puel, A., Plancoulaine, S., Picard, C., Herman, M., Cardon, A., Durandy, A., Bustamante, J., Vallabhapurapu, S., Bravo, J., Warnatz, K., Chaix, Y., Cascarrigny, F., Lebon, P., Rozenberg, F., Karin, M., Tardieu, M., Al-Muhsen, S., Jouanguy, E., Zhang, S.-Y., Abel, L., & Casanova, J.-L. (2010) Human TRAF3 Adaptor Molecule Deficiency Leads to Impaired Toll-like Receptor 3 Response and Susceptibility to Herpes Simplex Encephalitis. *Immunity*. [Online] 33 (3), 400–411. Available from: doi:10.1016/j.immuni.2010.08.014.

Peters, O.M., Ghasemi, M., & Brown, R.H. (2015) Emerging mechanisms of molecular pathology in ALS. *Journal of Clinical Investigation*. [Online] 125 (5), 1767–1779. Available from: doi:10.1172/JCI71601.

Pilli, M., Arko-Mensah, J., Ponpuak, M., Roberts, E., Master, S., Mandell, M.A., Dupont, N., Ornatowski, W., Jiang, S., Bradfute, S.B., Bruun, J.-A., Hansen, T.E., Johansen, T., & Deretic, V. (2012) TBK-1 Promotes Autophagy-Mediated Antimicrobial Defense by Controlling Autophagosome Maturation. *Immunity*. [Online] 37 (2), 223–234. Available from: doi:10.1016/j.immuni.2012.04.015.

Poppers, J., Mulvey, M., Khoo, D., & Mohr, I. (2000) Inhibition of PKR activation by the proline-rich RNA binding domain of the herpes simplex virus type 1 Us11 protein. *Journal of virology*. [Online] 74 (23), 11215–11221. Available from: doi:10.1128/JVI.74.23.11215-11221.2000.

Pottier, C., Bieniek, K.F., Finch, N., van de Vorst, M., Baker, M., Perkersen, R.,

Brown, P., Ravenscroft, T., van Blitterswijk, M., Nicholson, A.M., DeTure, M., Knopman, D.S., Josephs, K.A., Parisi, J.E., Petersen, R.C., Boylan, K.B., Boeve, B.F., Graff-Radford, N.R., Veltman, J.A., Gilissen, C., Murray, M.E., Dickson, D.W., & Rademakers, R. (2015) Whole-genome sequencing reveals important role for TBK1 and OPTN mutations in frontotemporal lobar degeneration without motor neuron disease. *Acta Neuropathologica*. [Online] 130 (1), 77–92. Available from: doi:10.1007/s00401-015-1436-x.

Pozzi, L., Valenza, F., Mosca, L., Dal Mas, A., Domi, T., Romano, A., Tarlarini, C., Falzone, Y.M., Tremolizzo, L., Sorarù, G., Cerri, F., Ferraro, P.M., Basaia, S., Agosta, F., Fazio, R., Comola, M., Comi, G., Ferrari, M., Quattrini, A., Lunetta, C., Penco, S., Bonanomi, D., Carrera, P., & Riva, N. (2017) TBK1 mutations in Italian patients with amyotrophic lateral sclerosis: genetic and functional characterisation. *Journal of neurology, neurosurgery, and psychiatry*. [Online] 88 (10), 869–875. Available from: doi:10.1136/jnnp-2017-316174.

Prichard, M.N., Kern, E.R., Hartline, C.B., Lanier, E.R., & Quenelle, D.C. (2011) CMX001 Potentiates the Efficacy of Acyclovir in Herpes Simplex Virus Infections. *Antimicrobial Agents and Chemotherapy*. [Online] 55 (10), 4728–4734. Available from: doi:10.1128/AAC.00545-11.

Puri, C., Renna, M., Bento, C.F., Moreau, K., & Rubinsztein, D.C. (2013) Diverse Autophagosome Membrane Sources Coalesce in Recycling Endosomes. *Cell*. [Online] 154 (6), 1285–1299. Available from: doi:10.1016/j.cell.2013.08.044.

Quigley, H.A. (2011) Glaucoma. *The Lancet*. [Online] 377 (9774), 1367–1377. Available from: doi:10.1016/S0140-6736(10)61423-7.

Radtke, A.L., Delbridge, L.M., Balachandran, S., Barber, G.N., & O'Riordan, M.X.D. (2007) TBK1 Protects Vacuolar Integrity during Intracellular Bacterial Infection.

PLoS Pathogens. [Online] 3 (3), e29. Available from: doi:10.1371/journal.ppat.0030029.

Radtke, K., English, L., Rondeau, C., Leib, D., Lippé, R., & Desjardins, M. (2013) Inhibition of the host translation shutoff response by herpes simplex virus 1 triggers nuclear envelope-derived autophagy. *Journal of virology*. [Online] 87 (7), 3990–3997. Available from: doi:10.1128/JVI.02974-12.

Rasmussen, S.B., Horan, K.A., Holm, C.K., Stranks, A.J., Mettenleiter, T.C., Simon, A.K., Jensen, S.B., Rixon, F.J., He, B., & Paludan, S.R. (2011) Activation of Autophagy by α-Herpesviruses in Myeloid Cells Is Mediated by Cytoplasmic Viral DNA through a Mechanism Dependent on Stimulator of IFN Genes. *The Journal of Immunology*. [Online] 187 (10), 5268–5276. Available from: doi:10.4049/jimmunol.1100949.

Ravikumar, B., Berger, Z., Vacher, C., O'Kane, C.J., & Rubinsztein, D.C. (2006) Rapamycin pre-treatment protects against apoptosis. *Human Molecular Genetics*. [Online] 15 (7), 1209–1216. Available from: doi:10.1093/hmg/ddl036.

Reinert, L.S., Lopušná, K., Winther, H., Sun, C., Thomsen, M.K., Nandakumar, R., Mogensen, T.H., Meyer, M., Vægter, C., Nyengaard, J.R., Fitzgerald, K.A., & Paludan, S.R. (2016) Sensing of HSV-1 by the cGAS–STING pathway in microglia orchestrates antiviral defence in the CNS. *Nature Communications*. [Online] 7, 13348. Available from: doi:10.1038/ncomms13348.

Richter, B., Sliter, D.A., Herhaus, L., Stolz, A., Wang, C., Beli, P., Zaffagnini, G., Wild, P., Martens, S., Wagner, S.A., Youle, R.J., & Dikic, I. (2016) Phosphorylation of OPTN by TBK1 enhances its binding to Ub chains and promotes selective autophagy of damaged mitochondria. *Proceedings of the National Academy of Sciences*. [Online] 113 (15), 4039–4044. Available from:

doi:10.1073/pnas.1523926113.

Ritch, R., Darbro, B., Menon, G., Khanna, C.L., Solivan-Timpe, F., Roos, B.R., Sarfarzi, M., Kawase, K., Yamamoto, T., Robin, A.L., Lotery, A.J., & Fingert, J.H. (2014) TBK1 gene duplication and normal-tension glaucoma. *JAMA ophthalmology*. [Online] 132 (5), 544–548. Available from: doi:10.1001/jamaophthalmol.2014.104.

Rodolfo, C., Campello, S., & Cecconi, F. (2017) Mitophagy in neurodegenerative diseases. *Neurochemistry International*. [Online] Available from: doi:10.1016/J.NEUINT.2017.08.004.

Rubinsztein, D.C., Mariño, G., & Kroemer, G. (2011) Autophagy and aging. *Cell*. [Online] 146 (5), 682–695. Available from: doi:10.1016/j.cell.2011.07.030.

Sabah, M., Mulcahy, J., & Zeman, A. (2012) Herpes simplex encephalitis. *BMJ (Clinical research ed.)*. [Online] 344, e3166. Available from: doi:10.1136/BMJ.E3166.

Saitoh, T., Fujita, N., Hayashi, T., Takahara, K., Satoh, T., Lee, H., Matsunaga, K., Kageyama, S., Omori, H., Noda, T., Yamamoto, N., Kawai, T., Ishii, K., Takeuchi, O., Yoshimori, T., & Akira, S. (2009) Atg9a controls dsDNA-driven dynamic translocation of STING and the innate immune response. *Proceedings of the National Academy of Sciences of the United States of America*. [Online] 106 (49), 20842–20846. Available from: doi:10.1073/pnas.0911267106.

Sancho-Shimizu, V., Perez de Diego, R., Jouanguy, E., Zhang, S.-Y., & Casanova, J.-L. (2011a) Inborn errors of anti-viral interferon immunity in humans. *Current opinion in virology*. [Online] 1 (6), 487–496. Available from: doi:10.1016/j.coviro.2011.10.016.

Sancho-Shimizu, V., Pérez de Diego, R., Lorenzo, L., Halwani, R., Alangari, A.,

Israelsson, E., Fabrega, S., Cardon, A., Maluenda, J., Tatematsu, M., Mahvelati, F., Herman, M., Ciancanelli, M., Guo, Y., AlSum, Z., Alkhamis, N., Al-Makadma, A.S., Ghadiri, A., Boucherit, S., Plancoulaine, S., Picard, C., Rozenberg, F., Tardieu, M., Lebon, P., Jouanguy, E., Rezaei, N., Seya, T., Matsumoto, M., Chaussabel, D., Puel, A., Zhang, S.-Y., Abel, L., Al-Muhsen, S., & Casanova, J.-L. (2011b) Herpes simplex encephalitis in children with autosomal recessive and dominant TRIF deficiency. *Journal of Clinical Investigation*. [Online] 121 (12), 4889–4902. Available from: doi:10.1172/JCI59259.

Sancho-Shimizu, V., Zhang, S.-Y., Abel, L., Tardieu, M., Rozenberg, F., Jouanguy, E., & Casanova, J.-L. (2007) Genetic susceptibility to herpes simplex virus 1 encephalitis in mice and humans. *Current Opinion in Allergy and Clinical Immunology*. [Online] 7 (6), 495–505. Available from: doi:10.1097/ACI.0b013e3282f151d2.

Sarkar, S., Davies, J.E., Huang, Z., Tunnacliffe, A., & Rubinsztein, D.C. (2007) Trehalose, a Novel mTOR-independent Autophagy Enhancer, Accelerates the Clearance of Mutant Huntingtin and α-Synuclein. *Journal of Biological Chemistry*. [Online] 282 (8), 5641–5652. Available from: doi:10.1074/jbc.M609532200.

Schmeisser, H., Bekisz, J., & Zoon, K.C. (2014) New Function of Type I IFN: Induction of Autophagy. *Journal of Interferon & Cytokine Research*. [Online] 34 (2), 71–78. Available from: doi:10.1089/jir.2013.0128.

Schmeisser, H., Fey, S.B., Horowitz, J., Fischer, E.R., Balinsky, C.A., Miyake, K., Bekisz, J., Snow, A.L., & Zoon, K.C. (2013) Type I interferons induce autophagy in certain human cancer cell lines. *Autophagy*. [Online] 9 (5), 683–696. Available from: doi:10.4161/auto.23921.

Schneider, C.A., Rasband, W.S., & Eliceiri, K.W. (2012) NIH Image to ImageJ: 25 years of image analysis. *Nature methods*. [Online] 9 (7), 671–675. Available from: http://www.ncbi.nlm.nih.gov/pubmed/22930834.

Sen, G.C. & Peters, G.A. (2007) Viral Stress-Inducible Genes. In: *Advances in virus research*. [Online]. pp. 233–263. Available from: doi:10.1016/S0065-3527(07)70006-4.

Sharma, S., TenOever, B.R., Grandvaux, N., Zhou, G.-P., Lin, R., & Hiscott, J. (2003) Triggering the Interferon Antiviral Response Through an IKK-Related Pathway. *Science*. [Online] 300 (5622), 1148–1151. Available from: doi:10.1126/science.1081315.

Shaw, P.J. (2005) Molecular and cellular pathways of neurodegeneration in motor neurone disease. *Journal of neurology, neurosurgery, and psychiatry*. [Online] 76 (8), 1046–1057. Available from: doi:10.1136/jnnp.2004.048652.

Shi, C.-S. & Kehrl, J.H. (2008) MyD88 and Trif Target Beclin 1 to Trigger Autophagy in Macrophages. *Journal of Biological Chemistry*. [Online] 283 (48), 33175–33182. Available from: doi:10.1074/jbc.M804478200.

Smith, G. (2012) Herpesvirus Transport to the Nervous System and Back Again. *Annual Review of Microbiology*. [Online] 66 (1), 153–176. Available from: doi:10.1146/annurev-micro-092611-150051.

Smith, J.D. & de Harven, E. (1978) Herpes simplex virus and human cytomegalovirus replication in WI-38 cells. III. Cytochemical localization of lysosomal enzymes in infected cells. *Journal of virology*. 26 (1), 102–109.

Smith, M.G., Lennette, E.H., & Reames, H.R. (1941) Isolation of the virus of herpes simplex and the demonstration of intranuclear inclusions in a case of acute encephalitis. *The American journal of pathology*. [Online] 17 (1), 55–68.1.

Available from: http://www.ncbi.nlm.nih.gov/pubmed/19970544 [Accessed: 1 August 2018].

Soulat, D., Bürckstümmer, T., Westermayer, S., Goncalves, A., Bauch, A., Stefanovic, A., Hantschel, O., Bennett, K.L., Decker, T., & Superti-Furga, G. (2008) The DEAD-box helicase DDX3X is a critical component of the TANK-binding kinase 1-dependent innate immune response. *The EMBO journal*. [Online] 27 (15), 2135–2146. Available from: doi:10.1038/emboj.2008.126.

Sparrer, K.M.J., Gableske, S., Zurenski, M.A., Parker, Z.M., Full, F., Baumgart, G.J., Kato, J., Pacheco-Rodriguez, G., Liang, C., Pornillos, O., Moss, J., Vaughan, M., & Gack, M.U. (2017) TRIM23 mediates virus-induced autophagy via activation of TBK1. *Nature Microbiology*. [Online] 2 (11), 1543–1557. Available from: doi:10.1038/s41564-017-0017-2.

Stolz, A., Ernst, A., & Dikic, I. (2014) Cargo recognition and trafficking in selective autophagy. *Nature Cell Biology*. [Online] 16 (6), 495–501. Available from: doi:10.1038/ncb2979.

Sun, L., Wu, J., Du, F., Chen, X., & Chen, Z.J. (2013) Cyclic GMP-AMP Synthase Is a Cytosolic DNA Sensor That Activates the Type I Interferon Pathway. *Science*. [Online] 339 (6121), 786–791. Available from: doi:10.1126/science.1232458.

Tallóczy, Z., Jiang, W., Virgin, H.W., Leib, D.A., Scheuner, D., Kaufman, R.J., Eskelinen, E.-L., & Levine, B. (2002) Regulation of starvation- and virus-induced autophagy by the eIF2alpha kinase signaling pathway. *Proceedings of the National Academy of Sciences of the United States of America*. [Online] 99 (1), 190–195. Available from: doi:10.1073/pnas.012485299.

Tallóczy, Z., Virgin, H.W., & Levine, B. (2006) PKR-dependent autophagic degradation of herpes simplex virus type 1. *Autophagy*. [Online] 2 (1), 24–29.

Available from: http://www.ncbi.nlm.nih.gov/pubmed/16874088.

Tanaka, Y. & Chen, Z.J. (2012) STING Specifies IRF3 Phosphorylation by TBK1 in the Cytosolic DNA Signaling Pathway. *Science Signaling*. [Online] 5 (214), ra20-ra20. Available from: doi:10.1126/scisignal.2002521.

Thomas, P. & Smart, T.G. (2005) HEK293 cell line: A vehicle for the expression of recombinant proteins. *Journal of Pharmacological and Toxicological Methods*. [Online] 51 (3), 187–200. Available from: doi:10.1016/j.vascn.2004.08.014.

Thurston, T.L., Boyle, K.B., Allen, M., Ravenhill, B.J., Karpiyevich, M., Bloor, S., Kaul, A., Noad, J., Foeglein, A., Matthews, S.A., Komander, D., Bycroft, M., & Randow, F. (2016) Recruitment of TBK1 to cytosol-invading Salmonella induces WIPI2-dependent antibacterial autophagy. *The EMBO journal*. [Online] 35 (16), 1779–1792. Available from: doi:10.15252/embj.201694491.

Thurston, T.L.M., Ryzhakov, G., Bloor, S., von Muhlinen, N., & Randow, F. (2009) The TBK1 adaptor and autophagy receptor NDP52 restricts the proliferation of ubiquitin-coated bacteria. *Nature Immunology*. [Online] 10 (11), 1215–1221. Available from: doi:10.1038/ni.1800.

Tooze, S.A. & Yoshimori, T. (2010) The origin of the autophagosomal membrane. *Nature Cell Biology*. [Online] 12 (9), 831–835. Available from: doi:10.1038/ncb0910-831.

Tormo, D., Chęcińska, A., Alonso-Curbelo, D., Pérez-Guijarro, E., Cañón, E., Riveiro-Falkenbach, E., Calvo, T.G., Larribere, L., Megías, D., Mulero, F., Piris, M.A., Dash, R., Barral, P.M., Rodríguez-Peralto, J.L., Ortiz-Romero, P., Tüting, T., Fisher, P.B., & Soengas, M.S. (2009) Targeted Activation of Innate Immunity for Therapeutic Induction of Autophagy and Apoptosis in Melanoma Cells. *Cancer Cell*. [Online] 16 (2), 103–114. Available from:

doi:10.1016/j.ccr.2009.07.004.

Travassos, L.H., Carneiro, L.A.M., Ramjeet, M., Hussey, S., Kim, Y.-G., Magalhães, J.G., Yuan, L., Soares, F., Chea, E., Le Bourhis, L., Boneca, I.G., Allaoui, A., Jones, N.L., Nuñez, G., Girardin, S.E., & Philpott, D.J. (2010) Nod1 and Nod2 direct autophagy by recruiting ATG16L1 to the plasma membrane at the site of bacterial entry. *Nature Immunology*. [Online] 11 (1), 55–62. Available from: doi:10.1038/ni.1823.

Tu, D., Zhu, Z., Zhou, A.Y., Yun, C., Lee, K.-E., Toms, A. V, Li, Y., Dunn, G.P., Chan, E., Thai, T., Yang, S., Ficarro, S.B., Marto, J.A., Jeon, H., Hahn, W.C., Barbie, D.A., & Eck, M.J. (2013) Structure and ubiquitination-dependent activation of TANK-binding kinase 1. *Cell reports*. [Online] 3 (3), 747–758. Available from: doi:10.1016/j.celrep.2013.01.033.

Uhlén, M., Fagerberg, L., Hallström, B.M., Lindskog, C., Oksvold, P., Mardinoglu, A., Sivertsson, Å., Kampf, C., Sjöstedt, E., Asplund, A., Olsson, I., Edlund, K., Lundberg, E., Navani, S., Szigyarto, C.A.-K., Odeberg, J., Djureinovic, D., Takanen, J.O., Hober, S., Alm, T., Edqvist, P.-H., Berling, H., Tegel, H., Mulder, J., Rockberg, J., Nilsson, P., Schwenk, J.M., Hamsten, M., von Feilitzen, K., Forsberg, M., Persson, L., Johansson, F., Zwahlen, M., von Heijne, G., Nielsen, J., & Pontén, F. (2015) Proteomics. Tissue-based map of the human proteome. *Science (New York, N.Y.)*. [Online] 347 (6220), 1260419. Available from: doi:10.1126/science.1260419.

Unterholzner, L., Keating, S.E., Baran, M., Horan, K.A., Jensen, S.B., Sharma, S., Sirois, C.M., Jin, T., Latz, E., Xiao, T.S., Fitzgerald, K.A., Paludan, S.R., & Bowie, A.G. (2010) IFI16 is an innate immune sensor for intracellular DNA. *Nature Immunology*. [Online] 11 (11), 997–1004. Available from:

doi:10.1038/ni.1932.

Valadi, H., Ekström, K., Bossios, A., Sjöstrand, M., Lee, J.J., & Lötvall, J.O. (2007) Exosome-mediated transfer of mRNAs and microRNAs is a novel mechanism of genetic exchange between cells. *Nature Cell Biology*. [Online] 9 (6), 654–659. Available from: doi:10.1038/ncb1596.

Verpooten, D., Ma, Y., Hou, S., Yan, Z., & He, B. (2009) Control of TANK-binding Kinase 1-mediated Signaling by the γ 1 34.5 Protein of Herpes Simplex Virus 1. *Journal of Biological Chemistry*. [Online] 284 (2), 1097–1105. Available from: doi:10.1074/jbc.M805905200.

Virgin, H.W. & Levine, B. (2009) Autophagy genes in immunity. *Nature Immunology*. [Online] 10 (5), 461–470. Available from: doi:10.1038/ni.1726.

Wang, J.P., Bowen, G.N., Zhou, S., Cerny, A., Zacharia, A., Knipe, D.M., Finberg, R.W., & Kurt-Jones, E.A. (2012) Role of Specific Innate Immune Responses in Herpes Simplex Virus Infection of the Central Nervous System. *Journal of Virology*. [Online] 86 (4), 2273–2281. Available from: doi:10.1128/JVI.06010-11.

Wang, X., Majumdar, T., Kessler, P., Ozhegov, E., Zhang, Y., Chattopadhyay, S., Barik, S., & Sen, G.C. (2016) STING Requires the Adaptor TRIF to Trigger Innate Immune Responses to Microbial Infection. *Cell Host & Microbe*. [Online] 20 (3), 329–341. Available from: doi:10.1016/j.chom.2016.08.002.

Watson, R.O., Bell, S.L., MacDuff, D.A., Kimmey, J.M., Diner, E.J., Olivas, J., Vance, R.E., Stallings, C.L., Virgin, H.W., & Cox, J.S. (2015) The Cytosolic Sensor cGAS Detects Mycobacterium tuberculosis DNA to Induce Type I Interferons and Activate Autophagy. *Cell Host & Microbe*. [Online] 17 (6), 811–819. Available from: doi:10.1016/j.chom.2015.05.004.

Watson, R.O., Manzanillo, P.S., & Cox, J.S. (2012) Extracellular M. tuberculosis

DNA Targets Bacteria for Autophagy by Activating the Host DNA-Sensing Pathway. *Cell*. [Online] 150 (4), 803–815. Available from: doi:10.1016/j.cell.2012.06.040.

Whitehead, K.A., Dahlman, J.E., Langer, R.S., & Anderson, D.G. (2011) Silencing or Stimulation? siRNA Delivery and the Immune System. *Annual Review of Chemical and Biomolecular Engineering*. 2 (1), 77–96.

Whitley, R.J. & Gnann, J.W. (2002) Viral encephalitis: Familiar infections and emerging pathogens. *Lancet*. [Online] 359 (9305), 507–514. Available from: doi:10.1016/S0140-6736(02)07681-X.

Whitley, R.J. & Kimberlin, D.W. (2005) Herpes simplex: Encephalitis children and adolescents. *Seminars in Pediatric Infectious Diseases*. [Online]. 16 (1 SPEC.ISS.) pp.17–23. Available from: doi:10.1053/j.spid.2004.09.007.

Whitley, R.J. & Roizman, B. (2001) Herpes simplex virus infections. *The Lancet*. [Online] 357 (9267), 1513–1518. Available from: doi:10.1016/S0140-6736(00)04638-9.

Wild, P., Farhan, H., McEwan, D.G., Wagner, S., Rogov, V. V., Brady, N.R., Richter, B., Korac, J., Waidmann, O., Choudhary, C., Dotsch, V., Bumann, D., & Dikic, I. (2011) Phosphorylation of the Autophagy Receptor Optineurin Restricts Salmonella Growth. *Science*. [Online] 333 (6039), 228–233. Available from: doi:10.1126/science.1205405.

Wu, B. & Guo, W. (2015) The Exocyst at a Glance. *Journal of Cell Science*. [Online] 128 (16), 2957–2964. Available from: doi:10.1242/jcs.156398.

Xie, Z.-G., Xie, Y., & Dong, Q.-R. (2013) Inhibition of the mammalian target of rapamycin leads to autophagy activation and cell death of MG63 osteosarcoma cells. *Oncology letters*. [Online] 6 (5), 1465–1469. Available from:

doi:10.3892/ol.2013.1531.

Xu, Y., Jagannath, C., Liu, X.-D., Sharafkhaneh, A., Kolodziejska, K.E., & Eissa, N.T. (2007) Toll-like Receptor 4 Is a Sensor for Autophagy Associated with Innate Immunity. *Immunity*. [Online] 27 (1), 135–144. Available from: doi:10.1016/j.immuni.2007.05.022.

Yamamoto, M., Sato, S., Hemmi, H., Hoshino, K., Kaisho, T., Sanjo, H., Takeuchi, O., Sugiyama, M., Okabe, M., Takeda, K., & Akira, S. (2003) Role of Adaptor TRIF in the MyD88-Independent Toll-Like Receptor Signaling Pathway. *Science*. [Online] 301 (5633), 640–643. Available from: doi:10.1126/science.1087262.

Yordy, B., Iijima, N., Huttner, A., Leib, D., & Iwasaki, A. (2012) A Neuron-Specific Role for Autophagy in Antiviral Defense against Herpes Simplex Virus. *Cell Host & Microbe*. [Online] 12 (3), 334–345. Available from: doi:10.1016/j.chom.2012.07.013.

Yordy, B. & Iwasaki, A. (2013) Cell type-dependent requirement of autophagy in HSV-1 antiviral defense. *Autophagy*. [Online] 9 (2), 236–238. Available from: doi:10.4161/auto.22506.

Zatloukal, K., Stumptner, C., Fuchsbichler, A., Heid, H., Schnoelzer, M., Kenner, L., Kleinert, R., Prinz, M., Aguzzi, A., & Denk, H. (2002) p62 Is a Common Component of Cytoplasmic Inclusions in Protein Aggregation Diseases. *The American Journal of Pathology*. [Online] 160 (1), 255–263. Available from: doi:10.1016/S0002-9440(10)64369-6.

Zhan, Z., Xie, X., Cao, H., Zhou, X., Zhang, X.D., Fan, H., & Liu, Z. (2014) Autophagy facilitates TLR4- and TLR3-triggered migration and invasion of lung cancer cells through the promotion of TRAF6 ubiquitination. *Autophagy*. [Online] 10 (2), 257–268. Available from: doi:10.4161/auto.27162.

Zhang, D., Su, C., & Zheng, C. (2016) Herpes Simplex Virus 1 Serine Protease VP24 Blocks the DNA-Sensing Signal Pathway by Abrogating Activation of Interferon Regulatory Factor 3. *Journal of Virology*. [Online] 90 (12), 5824–5829. Available from: doi:10.1128/JVI.00186-16.

Zhang, S.-Y., Herman, M., Ciancanelli, M.J., Pérez de Diego, R., Sancho-Shimizu, V., Abel, L., & Casanova, J.-L. (2013) TLR3 immunity to infection in mice and humans. *Current Opinion in Immunology*. [Online] 25 (1), 19–33. Available from: doi:10.1016/J.COI.2012.11.001.

Zhang, S.-Y., Jouanguy, E., Ugolini, S., Smahi, A., Elain, G., Romero, P., Segal, D., Sancho-Shimizu, V., Lorenzo, L., Puel, A., Picard, C., Chapgier, A., Plancoulaine, S., Titeux, M., Cognet, C., von Bernuth, H., Ku, C.-L., Casrouge, A., Zhang, X.-X., Barreiro, L., Leonard, J., Hamilton, C., Lebon, P., Heron, B., Vallee, L., Quintana-Murci, L., Hovnanian, A., Rozenberg, F., Vivier, E., Geissmann, F., Tardieu, M., Abel, L., & Casanova, J.-L. (2007) TLR3 Deficiency in Patients with Herpes Simplex Encephalitis. *Science*. [Online] 317 (5844), 1522–1527. Available from: doi:10.1126/science.1139522.

Zhong, B., Yang, Y., Li, S., Wang, Y.-Y., Li, Y., Diao, F., Lei, C., He, X., Zhang, L., Tien, P., & Shu, H.-B. (2008) The Adaptor Protein MITA Links Virus-Sensing Receptors to IRF3 Transcription Factor Activation. *Immunity*. [Online] 29 (4), 538–550. Available from: doi:10.1016/j.immuni.2008.09.003.

Zhou, A., Li, S., Khan, F.A., & Zhang, S. (2016) Autophagy postpones apoptotic cell death in PRRSV infection through Bad-Beclin1 interaction. *Virulence*. [Online] 7 (2), 98–109. Available from: doi:10.1080/21505594.2015.1131381.

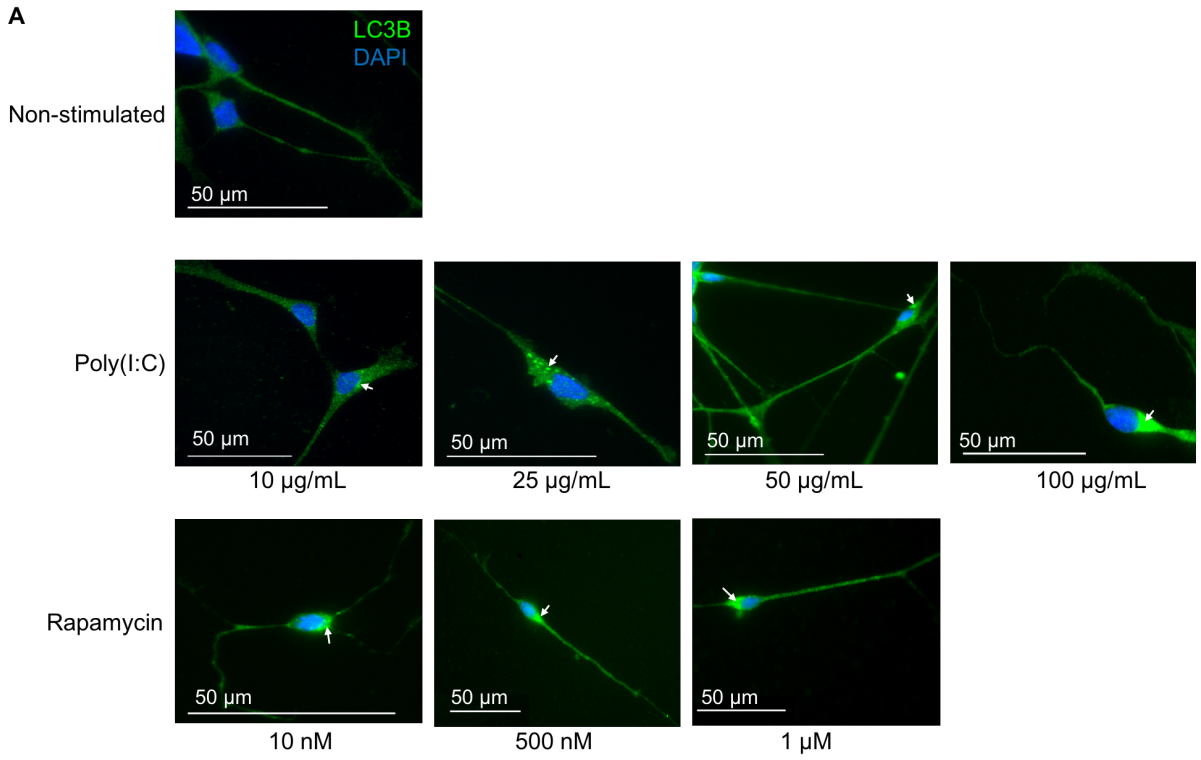
Zhou, R., Yazdi, A.S., Menu, P., & Tschopp, J. (2011) A role for mitochondria in NLRP3 inflammasome activation. *Nature*. [Online] 469 (7329), 221–225.

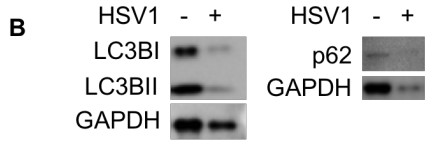
Available from: doi:10.1038/nature09663.

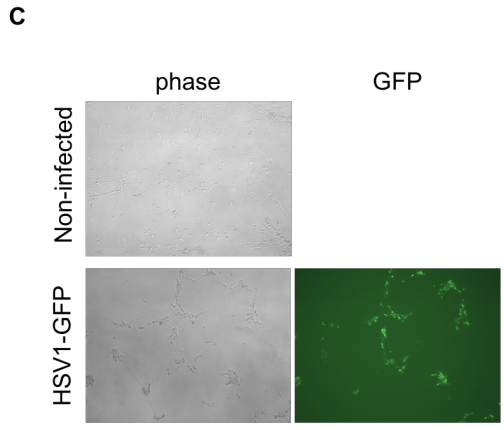
Zhou, X., Cheng, F., & Zhang, H. (2015) Emerging View of Autophagy in Systemic Lupus Erythematosus. *International Reviews of Immunology*. [Online] 34 (3), 280–292. Available from: doi:10.3109/08830185.2013.879711.

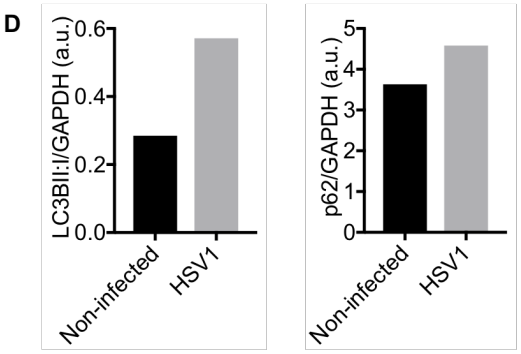
Appendix

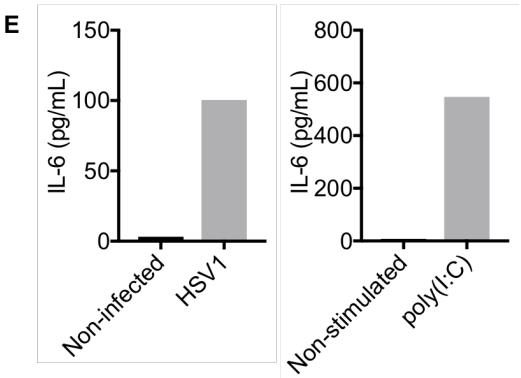
Appendix 1











Appendix 1. Optimisation of autophagy assays on neurons derived from NS cells. NS cells were cultured in differentiation medium for 7 days to reach pure population of cortical neurons. Neurons were subsequently maintained for another 7 days before performing the experiments. **(A)** Neurons were stimulated with indicated concentrations of poly(I:C) or rapamycin for 24 hours, before being fixed and stained for endogenous LC3B protein (green). Nuclei were stained with DAPI (blue). White arrows indicate the presence of LC3B puncta. Scale bar represents 50 μm. **(B)** Neurons were infected with HSV1 (MOI 1) for 24 hours before lysates were harvested and immunoblotted for LC3B and p62 protein expression. GAPDH was used as a loading control **(C)** Replication of HSV1-GFP (MOI 1) was visualised 24 h.p.i. **(D)** Immunoblots from (A) were subjected to densitrometric analysis **(E)** IL-6 secretion in culture supernatants of neurons infected with HSV1 (MOI 1) or stimulated with 25 μg/mL of poly(I:C) for 24 hours was quantified. Representative mages and data are derived from one experiment (n = 1). a.u., arbitrary unit.